

Aus dem Institut für Molekulare Onkologie,
Direktor: Prof. Dr. Thorsten Stiewe
des Fachbereichs Medizin der Philipps-Universität Marburg

Exploring mutant p53 targeting strategies for cancer therapy

Inaugural-Dissertation
zur Erlangung des Doktorgrades der Naturwissenschaften
dem Fachbereich Medizin der Philipps-Universität Marburg
vorgelegt von

Boris Klimovich

aus Sankt Petersburg

Marburg, 2019

Angenommen vom Fachbereich Medizin der Philipps-Universität
Marburg am: 13.01.2020

Gedruckt mit Genehmigung des Fachbereichs.

Dekan: Prof. Dr. Helmut Schäfer

Referent: PD Dr. Oleg Timofeev

Korreferent: Prof. Dr. Uta-Maria Bauer

In loving memory of my father

Table of contents

Summary	II
Zusammenfassung	III
1. Introduction.....	1
1.1 p53 is a major tumor suppressor	1
1.2 p53 target genes	1
1.3 Non-transcriptional functions of p53	2
1.4 p53 regulation: Mdm2-p53 feedback loop, ARF.....	3
1.5 <i>TP53</i> mutations: not all mutants are equal.....	3
1.6 p53 as a therapy target.....	5
2. Loss of p53 function at late stages of tumorigenesis confers ARF-dependent vulnerability to p53 reactivation therapy.....	7
2.1 Introduction	7
2.2 Summary and discussion	8
2.3 Contribution statement	10
3. Inactivation of Mdm2 restores apoptosis proficiency of cooperativity mutant p53 <i>in vivo</i>	11
3.1 Introduction	11
3.2 Summary and discussion	12
3.3 Contribution statement	13
4. Residual apoptotic activity of a tumorigenic p53 mutant improves cancer therapy responses.....	14
4.1 Introduction	14
4.2 Summary and discussion	14
4.3 Contribution statement	18
5. Summary and perspectives	19
5.1 p53 reactivation therapy is effective in tumors with late-stage p53 inactivation.....	19
5.2 Partial loss-of-function p53 mutants are actionable therapy targets	20
6. Publication bibliography	24
7. Appendix	I
Lists of abbreviations.....	I
Curriculum Vitae.....	II
List of publications.....	III
List of academic teachers.....	IV
Acknowledgments	V
Ehrenwörtliche Erklärung	VI
Publications.....	VII

Summary

TP53 is an essential tumor suppressor gene. It is inactivated in 50% of tumors, most frequently by missense mutations that result in the expression of a mutant p53 protein (mutp53). Mutp53 loses the ability to activate tumor-suppressive target genes and acquires pro-tumorigenic gain-of-function properties.

An emerging strategy for treatment of cancers with missense p53 mutations is pharmacological restoration of wild-type p53 activity. Initial evidence that p53 reactivation leads to tumor regression was obtained in mouse models where p53 loss was the initiating event. Many patient tumors, however, develop in the presence of wild-type p53 and inactivate it only at later stages of evolution. To bypass p53-dependent tumor suppression such tumors acquire alterations in the p53 pathway that, in principle, could render p53 reactivation inefficient. To test this, we have modeled late-stage p53 inactivation in mice. Surprisingly restoration of p53 in such late-inactivated tumors resulted in widespread apoptosis and superior survival of the animals. ARF gene alterations were identified as a cause of primary or acquired resistance that could be overcome by Mdm2 inhibitors. Together this study provided proof of concept that p53 reactivation is an effective therapy option for tumors with late-stage p53 inactivation and identified ARF as a predictive biomarker.

Among the many different missense mutations, cooperativity mutations represent a mechanistically unique class that often results in a partial loss-of-function (pLOF). As pLOF is a characteristic of many non-hotspot p53 mutations, we have tested if residual functions of two distinct p53 cooperativity mutants (p53E177R “RR” and p53R178E “EE”) may be exploited to induce cell death. Using embryonic development as a model, we have shown that Mdm2-deficiency results in constitutive stabilization of p53 cooperativity mutants and triggers massive apoptosis and embryonic lethality. This indicated that the apoptosis deficiency, characteristic for p53 pLOF mutants, can be rescued by inhibition of Mdm2. Studies of p53 cooperativity mutant mice confirmed that stabilization of mutp53 by pharmacological or constitutive Mdm2 inhibition lowers the apoptotic threshold, sensitizes tumor cells to the pro-apoptotic activity of DNA damaging drugs, and generates a survival benefit under chemotherapy. This was even seen for the DNA binding-deficient cooperativity mutant EE, pointing at a critical role of non-transcriptional apoptotic functions in the context of chemotherapy. In parallel, p53EE was found to be incapable of suppressing tumor development, highlighting a differential role of p53’s non-transcriptional apoptotic functions in tumor suppression and cancer therapy. Collectively, our investigation of two cooperativity mutants suggests that non-hot-spot p53 variants retain residual wild-type activities, that can be harnessed for cancer therapy.

Zusammenfassung

TP53 ist ein essentielles Tumorsuppressorgen, welches in über 50% aller Tumore inaktiv vorliegt. Häufig geschieht dies durch sogenannte Missense-Mutationen, welche zur Expression eines mutierten p53 Proteins führen. Mutp53 verliert zwar die Fähigkeit tumorsuppressive Zielgene zu aktivieren, gewinnt aber neue, pro-tumorale Eigenschaften hinzu.

Ein neu aufkommender Therapieansatz um Tumorpatienten mit einer Missense p53 Mutation zu behandeln, ist die pharmakologische Reaktivierung der p53-Wildtyp Funktion. Erste Anhaltspunkte, dass eine p53 Reaktivierung zu einer Tumorregression führen kann, wurden in Mausmodellen beobachtet, bei denen ein Verlust der p53 Funktion das auslösende Ereignis der Tumorentstehung darstellt. Im Gegensatz dazu entwickeln sich Tumore in Patienten oftmals in Gegenwart von Wildtyp p53 und dessen Inaktivierung stellt einen späten Schritt in der Tumorevolution dar. Um tumorsuppressive Funktionen von p53 in solchen Tumoren zu umgehen, ist vorstellbar, dass diese Tumore Alterationen im p53 Signalweg erwerben, die eine Ineffizienz späterer p53 Reaktivierung induzieren. Um diese Annahme zu testen, haben wir eine späte p53 Inaktivierung in Maustumoren untersucht. Überraschenderweise konnten wir zeigen, dass eine Reaktivierung von p53 in diesen spät inaktivierenden Maustumoren zum Auftreten massiver Apoptose und zu einer erhöhten Überlebensrate der Tiere führte. Alterationen des Arf Gens wurden hierbei als Ursache primärer oder akquirierter Resistenz identifiziert, welche jedoch durch Mdm2-Inhibitoren überkommen werden konnten. Zusammenfassend belegt unsere Studie ein Konzept, in dem die Reaktivierung von p53 auch in Tumoren mit einem späten Verlust der p53 Funktion eine effektive Therapie darstellt. Zudem haben wir in diesem Zusammenhang Arf als Biomarker identifizieren können.

P53 Kooperativitätsmutanten stellen eine aus mechanistischer Sicht einzigartige Klasse innerhalb des Spektrums von p53 Missense Mutationen dar und resultieren in einem teilweisen Verlust der Funktion von p53 (sogenannte pLOF Mutanten). Typischerweise handelt es sich bei vielen non-hotspot Mutanten ebenfalls um pLOF Mutationen. In unserem Projekt haben wir die Fragestellung untersucht, ob sich die residuale Funktion zweier solcher Mutanten (p53E177R "RR" und p53R178E "EE") nutzen lässt um Apoptose von Tumorzellen zu induzieren. Als Modell haben wir dabei die embryonale Mausentwicklung gewählt. Dabei führte eine Defizienz von Mdm2 zu einer konstitutiven Stabilisierung der p53 Kooperativitätsmutanten, was mit massiver Apoptoseinduktion und embryonaler Lethalität einherging. Das Ergebnis impliziert, dass eine für p53 pLOF typische Apoptosedefizienz durch gleichzeitige Hemmung von Mdm2 überwunden werden kann. So zeigen Studien mit Mäusen, die eine p53 Kooperativitätsmutante

Zusammenfassung

tragen, dass eine Stabilisierung von Mutp53, herbeigeführt durch pharmakologische oder konstitutive Hemmung von Mdm2, die Apoptoseschwelle herabsetzt. Tumorzellen werden so gegenüber DNA schädigenden Agenzien sensitiviert, was mit einem verbesserten Überleben der Tiere unter Chemotherapie einhergeht. Diese Beobachtung kann sogar für die DNA-bindungsdefiziente p53 Mutante "EE" gemacht werden, was auf eine nicht transkriptionelle apoptotische Funktion von p53 im Zusammenhang mit Chemotherapie hinweist. Parallel haben wir gezeigt, dass diese "EE" Mutante die Tumorentstehung per se nicht verhindern konnte. Somit scheinen nicht- transkriptionelle Eigenschaften von p53 eine differentielle Funktion bei Tumorentstehung versus Therapie zu spielen. Zusammenfassend zeigt unsere Studie an zwei kooperativitätsdefizienten p53 Mutanten, dass diese mit residualen tumorsuppressiven Funktionen ausgestattet sind, die für die Effizienz einer Chemotherapie ausgenutzt werden können.

1. Introduction

1.1 p53 is a major tumor suppressor

Cancer development involves two types of events: activation of oncogenes and inactivation of tumor suppressors (Weinberg 2014). Interference with activated oncogenic pathways is exploited by many anticancer drugs (e.g. BRAF, BCR-ABL, and EGFR inhibitors) (Luo et al. 2009). Tumor suppressors are frequently deleted, truncated or silenced so that restoration of their functions turned out to be challenging (Guo et al. 2014). *TP53* is recognized as an essential tumor suppressor gene because it is mutated in about 50% of tumors (Ahmed et al. 2010; Leroy et al. 2014; Donehower et al. 2019). Its product is a transcription factor that binds to DNA in response to various intrinsic or extrinsic cues: DNA damage, replicative stress, changes in metabolic and oxidative state, activation of oncogenic signaling pathways and regulates the activity of hundreds of genes by direct activation of transcription or indirect repression (Engeland 2018; Sullivan et al. 2018; Fischer 2017; Brady and Attardi 2010). p53 prevents spreading of damaged and genetically altered cells by inhibiting proliferation and activating irreversible cell cycle arrest (senescence) or cell death. Under conditions of moderate stress, p53 evokes pro-survival programs aimed to repair damage, preserve genomic integrity and return cells into proliferation (Levine 1997; Sullivan et al. 2018; Kaiser and Attardi 2018).

1.2 p53 target genes

p53 regulates transcription of a massive network of target genes. Besides bona fide targets which are activated by binding of p53 to their promoters, many genes are induced indirectly (Fischer 2017; Andrysiak et al. 2017; Tonelli et al. 2017). Additionally, p53 indirectly suppresses numerous genes via the p21-DREAM pathway (Engeland 2018). Genes activated upon moderate stress (*CDKN1A*, *CCNG1*, *GADD45*) promote pro-survival programs protecting cells from killing: temporary cell cycle arrest, DNA repair, activation of anti-oxidative mechanisms (Gordon et al. 2018; Biegging and Attardi 2012). Transactivation of pro-apoptotic genes (e.g. *BBC 3* (Puma), *BAX*, *PMAIP*, *CASP3*, *P53AIP1*) results in permeabilization of outer mitochondrial membrane (MOMP), cytochrome *c* release, activation of caspases and apoptosis (Haupt et al. 2003; Riley et al. 2008). Other cell death mechanisms, such as necrosis and ferroptosis can also be triggered in a p53-dependent manner (Dixon et al. 2012; Le Jiang et al. 2015; Vaseva et al. 2012).

An appropriate stress response requires tight control of p53's functions which is attained by complex post-translational modifications of the protein that, in turn, determine its stability, intracellular localization, and interaction with other factors (Gu and Zhu 2012). Another regulatory mechanism relies on the diversity of promoter sequences of pro-survival and pro-apoptotic genes. Pro-survival genes usually contain high-affinity p53

binding sites, which are readily and tightly bound by p53. Promoters of some important pro-apoptotic genes (*BAX*, *CASP1*, *p53AIP1*) contain low-affinity binding sites and can be bound only after overcoming a higher threshold level of p53 (Schlereth et al. 2010b; Schlereth et al. 2013). Thus, p53 concentration in the cell determines the spectrum of active target genes and defines cell fate: if p53 levels are below a particular threshold, cells undergo growth arrest; above the threshold apoptosis is induced (Kracikova et al. 2013).

Our group and others have established that an important property determining the binding spectrum and outcome of p53 activation is DNA binding cooperativity (Schlereth et al. 2010a; Dehner et al. 2005). p53 binds to DNA in a cooperative manner: binding of monomers to DNA strongly promotes formation of tetramers. Tetramer formation is supported by protein-protein interactions (Weinberg et al. 2004). Interactions between the H1 helices of the DNA-binding domains are crucial for cooperative DNA binding. Mutations influencing cooperativity weaken binding with DNA and reduce p53-mediated tumor suppression (Schlereth et al. 2013; Schlereth et al. 2010a; Timofeev et al. 2013).

1.3 Non-transcriptional functions of p53

Although p53 primarily works as a transcription factor, p53 can also promote MOMP and cytochrome c release from isolated mitochondria, indicating that transactivation may be dispensable for apoptosis (Chipuk et al. 2004; Mihara et al. 2003). In recent years, several mechanisms of transcription-independent (cytoplasmic) activities of p53 have been discovered. In stressed cells, p53 sequesters anti-apoptotic proteins Bcl-xL and Bcl-2, thereby liberating pro-apoptotic tBid and Bax proteins from inhibition (Arima et al. 2005; Moll et al. 2006; Tomita et al. 2006). Moreover, p53 interacts with Bak on the mitochondrial membrane, disrupting its complex with inhibitory Mcl-1 and promoting Bak oligomerization and MOMP (Mihara et al. 2003; Leu et al. 2004). Finally, p53 directly induces a conformational change and oligomerization of Bax at the mitochondria via a “hit-and-run” mechanism (Chipuk et al. 2004).

Both transcription-dependent and independent activities of p53 result in MOMP and apoptosis. Therefore, investigation of cytoplasmic functions requires models that separate them from nuclear activities. *In vitro* this was achieved by examining purified mitochondria, treatment of cells with inhibitors of nuclear export and transcription or by fusing p53 with signals for mitochondrial localization (Marchenko et al. 2000; Chipuk et al. 2004). Mouse models of transcriptionally-inactive p53 utilized overexpression of p53 fusions with transmembrane domains of Bcl-xL or Bcl-2 to enforce its mitochondrial localization (Talos et al. 2005; Palacios and Moll 2006). However, it remains unclear how relevant such cytoplasmic functions are in an organismal context and whether naturally-occurring p53 mutants possess some of these activities. Therefore, novel more physiological animal models separating cytoplasmic and nuclear p53 functions would be of great value.

1.4 p53 regulation: Mdm2-p53 feedback loop, ARF

In unstressed cells, p53 transcription and translation proceed constantly, but protein activity is inhibited by Mdm2 and Mdmx proteins (Marine and Jochemsen 2004). The E3-ubiquitin-ligase Mdm2 ubiquitinates p53 thereby stimulating its nuclear export and proteasomal degradation (Haupt et al. 1997; Sane and Rezvani 2017; Tollini et al. 2014; Boehme and Blattner 2009). Additionally, Mdm2 and Mdmx bind to the transactivation domain of p53 and inhibit target gene activation (Kussie et al. 1996; Shan et al. 2012). The importance of Mdm2 as the main negative regulator of p53 is substantiated by the fact, that Mdm2-knockout mice die in utero at 3.5-5.5 days post coitum (dpc) due to excessive p53 activation (Jones et al. 1995; Luna et al. 1995). The Mdm2 encoding gene *MDM2* is itself a p53 target gene. Elevated levels of p53, therefore, induce Mdm2 expression, which promotes p53 degradation (Wu et al. 1993). This negative feedback loop limits the duration of p53 accumulation after stress and protects cells from eventual killing. Mdm2-dependent degradation of p53 can be blocked by stress-induced mechanisms: DNA damage activates ATM/ATR-CHK2 kinases that phosphorylate p53 and Mdm2 leading to disruption of p53-Mdm2 binding (Kruse and Gu 2009).

The p53-Mdm2 feedback loop is essential for monitoring hyperproliferative signaling to safeguard cells from malignant transformation by activated oncogenes like Myc or Ras. Aberrant mitogenic signals lead to p53 activation via the ARF tumor suppressor. ARF protein (p14ARF in humans, p19Arf in mouse) is encoded by an alternative reading frame of the *CDKN2A* gene (Pomerantz et al. 1998). ARF sequesters Mdm2 in the nucleolus and inhibits p53 ubiquitination (Zhang et al. 1998; Pomerantz et al. 1998; Kamijo et al. 1998). Alterations in the *CDKN2A/p14ARF* gene are common in tumors with wild-type p53 (Mina et al. 2017; Zhang et al. 2018) underlining ARF's importance for p53-mediated tumor suppression.

1.5 TP53 mutations: not all mutants are equal

Tumor suppressor genes are usually inactivated by deletions or truncating mutations leading to irreversible loss of protein expression (Levine et al. 2008).

The unique feature of *TP53* is that it is most frequently disabled by missense mutations and that the mutant p53 protein (mutp53) is retained by cancer cells, opening opportunities for using it as a target for therapy – for example, by restoration of its functions (Muller and Vousden 2013; Donehower et al. 2019). Most frequently, mutations hit the central DNA binding domain (DBD) of p53 (Petitjean et al. 2007). Among more than 2000 annotated mutations, 8 so-called hot-spot mutations (R175H, G245S, R248W, R273C, R273H, R282W, R248Q, and R249S) are found in nearly 30% of human tumors (Baugh et al. 2018). The high frequency of hot-spot mutations prompted their extensive studies. The remaining 70% of tumors with p53 mutations harbor non-hotspot variants. Initially, all

mutations in p53 were considered to have a similar functional impact, but accumulating evidence suggests that p53 mutations represent a broad spectrum, or “rainbow” of mutations with different degrees of functional impairment (Sabapathy and Lane 2017; Manfredi 2019).

It is well documented, that hot-spot mutations completely abrogate the transactivating activity of p53 (Kato et al. 2003; Jia et al. 1997; Olive et al. 2004; Lee et al. 2012). However, comprehensive profiling of non-hot-spot p53 mutants has shown, that some of them keep the ability to transactivate certain sets of target genes, being, therefore, partial loss-of-function (partial-LOF) mutants (Kato et al. 2003; Campomenosi et al. 2001; Menendez et al. 2006; Jordan et al. 2010). For example, Jordan et al. identified 21 breast cancer-derived mutants, capable of activating p53 response elements in reporter assays. Similar results were obtained in our group for mutations causing hereditary cancer predisposition (Li-Fraumeni syndrome) (Schlereth et al. 2010a; Ludwig et al. 1996). Whether residual transactivating activities of partial-LOF mutants can be augmented and exploited for cancer therapy is unknown and deserves further investigation.

In addition, some p53 mutants (for example R175H, R273H, R248Q, R248W, and others), besides losing tumor-suppressive activities, can actively promote malignant growth (Muller and Vousden 2014; Kim and Lozano 2018). Mutation of a single *TP53* allele is sufficient to compromise normal functions of the second wild-type *TP53* allele via a dominant-negative effect (DN-effect) (Vries et al. 2002; Boettcher et al. 2019; Srivastava et al. 1993). Mechanistically, mutp53 forms non-functional heterotetramers with wild type protein and stimulates its unfolding and aggregation (Ano Bom et al. 2012; Milner and Medcalf 1991; Milner et al. 1991). Although the DN-effect has been repeatedly demonstrated in an experimental settings (Boettcher et al. 2019; Giacomelli et al. 2018; Hegi et al. 2000), the relevance of this phenomenon for cancer patients is still unclear. Analysis of p53 pathway alteration in hundreds of tumor samples from the TCGA dataset has shown, that both copies of *TP53* are inactivated in 90% of tumors, implying that the DN-effect is insufficient to completely suppress the remaining *TP53* wild-type allele (Donehower et al. 2019).

Besides the DN-effect, mutp53 can stimulate tumor growth via neomorphic oncogenic functions (gain-of-function, GOF) (Schulz-Heddergott and Moll 2018). Murine tumors expressing hot-spot p53 mutants are more aggressive and prone to metastasize as compared to p53-null tumors (Hanel et al. 2013; Lang et al. 2004; Loizou et al. 2019; Olive et al. 2004). Mutp53 has been shown to support invasion (Adorno et al. 2009; Muller et al. 2013; Vogiatzi et al. 2016), increase migration (Dong et al. 2013; Vaughan et al. 2012), promote metastasis (Basu et al. 2018; Morton et al. 2010; Vogiatzi et al. 2016), induce drug resistance (Blandino et al. 1999; Buganim et al. 2006; Do et al. 2012; Hientz et al. 2017) and exert other pro-tumorigenic effects (Zhou et al. 2019; Muller and Vousden 2014; Oren and Rotter 2010). Mutp53 can participate in aberrant interactions with transcription

factors and repressors followed by transcriptional dysregulation of non-canonical target genes (Chin et al. 1992; Frazier et al. 1998; Lee et al. 2000; Ludes-Meyers et al. 1996; Quante et al. 2012; Freed-Pastor et al. 2012). Moreover, mutp53 also interacts with other cellular proteins (e.g. PML, TopBP1, Pin1) to exert non-transcriptional activities (Freed-Pastor and Prives 2012).

A hallmark of mutp53 and prerequisite for gain-of-function is its constitutive stabilization in cancer cells (Terzian et al. 2008). Importantly, when mutant protein was introduced into normal non-transformed cells it was not accumulated emphasizing that mutp53 stability is not the inherent property of the protein, but is rather a product of a specific cellular environment (Frum and Grossman 2014; Terzian et al. 2008). One mechanism of mutp53 stabilization involves chaperones: Hsp70 and Hsp90 which protect p53 from degradation by the ubiquitin ligases Mdm2 and CHIP (Blagosklonny et al. 1996; Li et al. 2011b; Whitesell et al. 1998). It was demonstrated, that genetic inactivation of mutp53 impaired tumor growth and prolonged survival of tumor-bearing mice (Weissmueller et al. 2014; Alexandrova et al. 2015). This suggested that accumulated mutp53 creates an oncogene-like addiction and provided a rationale for the development of mutp53-destabilizing therapies.

1.6 p53 as a therapy target

Targeting of p53 gained lots of attention in recent years. Therapeutic strategies are divided into two categories: (1) targeting wild-type p53 and (2) targeting mutant p53.

Targeting wild-type p53: Mdm2 inhibitors

50% of tumors retain wild-type p53 but constantly degrade it (Donehower et al. 2019). The pivotal role of Mdm2 in degradation of wild-type p53 prompted the development of Mdm2 inhibitors. The prototypical compound Nutlin-3a blocks the p53-binding pocket of Mdm2 and induces p53 stabilization, activation of target genes and apoptosis (Tisato et al. 2017; Vassilev et al. 2004). Two Nutlin derivatives, RG7112 and RG7388, are being tested in clinical trials as a single agent or in combination with chemotherapy in patients with hematological malignancies, breast cancer and other tumor types (Andreeff et al. 2016; Khurana and Shafer 2019; Ray-Coquard et al. 2012; Tovar et al. 2013). Several other compounds disrupting the p53-Mdm2 interaction (e.g. MI-77301, AMG232, HDM201) have also entered clinical trials (Tisato et al. 2017).

Therapy of tumors with p53 mutations with Mdm2 inhibitors is considered useless, even though clinical activity was documented in 2 patients with *TP53* mutations in a Phase I trial of RG7112 (Andreeff et al. 2016).

Targeting mutant p53

It is well documented that experimental re-expression of wild-type p53 in mutp53 or p53-null tumors results in tumor stagnation or regression (Wang et al. 2011; Larsson et al. 2018; Feldser et al. 2010; Junttila et al. 2010; Ventura et al. 2007). Moreover, as already

mentioned, elimination of mutp53 disrupts the oncogene-like addiction and leads to improved survival in several animal models (Weissmueller et al. 2014; Alexandrova et al. 2015; Vogiatzi et al. 2016; Schulz-Heddergott et al. 2018). These observations encouraged development of several strategies for targeting mutp53.

Structural mutations in the p53 DNA binding domain result in protein unfolding and impaired DNA binding. Accordingly, one therapeutic strategy relies on the refolding of denatured mutant p53 into its native conformation, thereby restoring wild-type-like properties. Theoretically, this can be accomplished with ligands that preferentially bind to the correctly folded protein and shift the equilibrium between unfolded and natively folded isoforms in favor of the latter (Bullock and Fersht 2001). This, in turn, promotes accumulation of correctly folded mutant protein and at least partial rescue of DNA binding. A first compound capable of refolding several p53 mutants and impairing xenograft tumor growth was CP-31398 (Foster et al. 1999). Further efforts led to the development of the most advanced p53-reactivating compound to date, PRIMA-1. PRIMA-1 is a quinuclidine that binds to cysteine residues of mutp53 and stabilizes the natively-folded polypeptide (Lambert et al. 2009). APR-246, a methylated pro-drug analog of PRIMA-1, is currently tested in clinical trials (Blandino and Di Agostino 2018).

The other therapeutic approach targets the tumor addiction to mutant p53 by abrogating its constitutive stabilization. As mutp53 is strongly accumulated in tumors due to Hsp90-dependent stabilization, targeting Hsp90-machinery either with Hsp90 inhibitors (17-AAG or ganetespib) or HDAC6 inhibitor (vorinostat) induces proteasomal degradation of mutp53 and apoptosis in human cancer cells and improves survival of mice with tumors carrying R172H and R248Q mutations (Alexandrova et al. 2015; Alexandrova et al. 2017; Li et al. 2011a). Patients with p53 GOF mutants may likely benefit from mutp53-destabilizing therapy. However, considering that GOF was documented for only a relatively small number of mutants so far, the potential utility of this approach for patients with other mutations remains unclear.

In summary, alterations in the *TP53* gene generate an immense diversity of functionally distinct mutant proteins. Each of them can be characterized by several parameters: the degree of function loss, the degree of DN-effect and degree of gain-of-function. Determining these properties for each mutant may help to find the optimal therapeutic strategy for a cancer patient using mutp53-reactivating or degrading compounds, Mdm2 inhibitors or a combination of several drug classes. Unfortunately, most of the non-hotspot p53 mutants are only poorly characterized, so that extensive investigation of non-hot-spot mutants is important to advance personalized cancer treatments.

2. Loss of p53 function at late stages of tumorigenesis confers ARF-dependent vulnerability to p53 reactivation therapy

Boris Klimovich*, Samet Mutlu*, Jean Schneikert, Sabrina Elmshäuser, Maria Klimovich, Andrea Nist, Marco Mernberger, Oleg Timofeev*, and Thorsten Stiewe*

* both authors contributed equally to this manuscript

PNAS, 2019 Oct 14. PubMed ID: 31611375

2.1 Introduction

Reactivation of mutant p53 is an emerging therapeutic approach with proven efficacy in genetic mouse models (Xue et al. 2007; Ventura et al. 2007; Junttila et al. 2010; Feldser et al. 2010). A major limitation of these studies is that they utilized tumors that have developed in a p53-null background, where p53 loss was the initiating event. Although typical in animal models, such a situation is rare in cancer patients. Loss of p53 is obviously the initiating genetic lesion in individuals with Li-Fraumeni syndrome that carry germline *TP53* mutations (Malkin et al. 1990). Driver mutations in *TP53* are also typical for high-grade serous ovarian carcinomas and a few other cancer types (Ahmed et al. 2010; Kuhn et al. 2012). However, in the vast majority of cancer types, p53 mutations happen later during tumor evolution (Rivlin et al. 2011). In the well-recognized model of colorectal tumorigenesis, *TP53* mutations are among the latest genetic alterations, which drive the progression of benign adenomas towards aggressive carcinomas (Fearon and Vogelstein 1990). Subclonal p53 mutations often expand in tumors relapsing after therapy, further suggesting that p53 mutations are rather late events in cancer progression (Amin et al. 2016; Prochazka et al. 2019; Rossi et al. 2014).

Tumors retaining wild-type p53 need to bypass tumor-suppressive mechanisms by the acquisition of additional alterations. For example, disruption of the tumor surveillance by mutation or deletion of *CDKN2A/p14ARF* allows tumors to sustain high levels of oncogenic signaling without p53 activation (Mina et al. 2017; Sherr 1998). The importance of *CDKN2A* inactivation for disabling the p53 network is underlined by the mutual exclusivity of *TP53* and *CDKN2A* mutations (Zhang et al. 2018). This trend is recapitulated in the Eμ-Myc mouse, a model of Burkitt lymphoma: tumors expressing wild-type p53 frequently lose expression of *Cdkn2a/p19Arf* (homolog of human p14ARF) and, conversely, *p19Arf* deletion prevents p53-loss (Eischen et al. 1999). Importantly, ARF was proven to be indispensable for effective p53 reactivation in mouse models driven by p53-loss (Feldser et al. 2010; Junttila et al. 2010). Thus, if a tumor with wild-type p53 has blunted the p53 response by inactivation of upstream or downstream pathways and has later acquired a p53 mutation, the reactivation of p53 in such a tumor is expected to be futile. In other

words, there is a possibility, that p53-reactivating therapy might be effective only in tumors, where p53-loss was the initiating lesion, and useless for cancers with late p53-loss. Therefore, it was of considerable interest to investigate, if tumors, which have developed in the presence of wild-type p53 and inactivated it at a late stage of their evolution, are sensitive to p53 reactivation.

Important drawbacks of p53-reactivating drugs are their prominent off-target effects, raising considerable doubt that their mechanism of action operates through mutp53 repair. For example, APR-246 (PRIMA-1^{MET}) was shown to deplete the cellular glutathione pool, induce increased production of reactive oxygen species (ROS) and kill tumor cells independently of p53 status (Liu et al. 2017; Teoh et al. 2016; Tessoulin et al. 2014; Yoshikawa et al. 2016). Moreover, conflicting data regarding APR-246 effects on mutp53 level, mutp53 refolding, DNA binding and restoration of transactivating activity were reported (Perdrix et al. 2017).

Since presently no compound is known that specifically repairs mutp53 without any off-target effects, genetic models of p53 reactivation are of great value. In our study, instead of using p53-reactivating compounds, we took advantage of the well-established genetic model: the p53ER^{TAM} mouse (Christophorou et al. 2005; Martins et al. 2006). In this model, p53 is fused with a modified ligand-binding domain of the estrogen receptor so that p53 activity can be precisely regulated by the administration of the synthetic estrogen analog tamoxifen (TAM). In the absence of TAM, p53 is inactive and accumulates in the cell similar to p53 loss-of-function mutants. Addition of TAM leads to activation of p53 allowing to model sequential p53 loss and theoretically reactivation.

2.2 Summary and discussion

To model inactivation of p53 at late stages of tumorigenesis, we have established E μ -Myc lymphomas by injecting hematopoietic stem cells from *E μ -Myc;Trp53ER^{TAM/TAM}* embryos into recipient mice fed with tamoxifen-supplemented chow (Fig. 1A). Lymphomas that developed in the transplanted animals (designated as p53ER^{TAM}-ON) were indistinguishable from p53^{+/+} tumors and displayed down-regulated expression of p19Arf as characteristic for p53^{+/+} lymphomas (Fig. 1A, C, D). To model p53 inactivation, p53ER^{TAM}-ON lymphomas were retransplanted into normally-fed recipients, giving rise to p53ER^{TAM}-late-OFF lymphomas (Fig. 2A). p53ER^{TAM}-late-OFF lymphomas were further retransplanted into cohorts of mice and p53 reactivating therapy was modeled by intraperitoneal administration of TAM. Surprisingly, reactivation of p53 in p53ER^{TAM}-late-OFF lymphomas resulted in improved survival or even complete cure of mice (Fig. 2C-F) with strong induction of p53 target genes and apoptosis (Fig. 2G, H).

The superior response of p53ER^{TAM}-late-OFF lymphomas to p53 reactivation was unexpected given the down-regulated ARF expression in p53ER^{TAM}-ON lymphomas (Fig.

1C, D). As ARF inhibits Mdm2-mediated ubiquitination of p53, its loss induces p53 degradation, which explains the frequent loss of *Cdkn2a/p19Arf* in p53-wild-type lymphomas (Schmitt et al. 1999). Moreover, ARF was shown to be essential for effective p53 reactivation in mouse tumors driven by loss of p53 (Feldser et al. 2010; Juntila et al. 2010). Strikingly, examination of p53^{ER^{TAM}}-ON lymphoma samples before and after TAM removal revealed, that upon p53 inactivation ARF expression is quickly re-established (Fig. 3A-D). ARF expression was lost in tumors relapsing after TAM-therapy, demonstrating that all ARF-proficient cells were killed by reactivation (Fig. 3E, F). To further support the relevance of ARF for p53 restoration therapy, we have generated p53^{ER^{TAM}}-late-OFF lymphoma cell lines. These cells responded to TAM with strong apoptosis and induction of p53 target genes, phenocopying our *in vivo* experiments (Fig. 4A-E). Prolonged treatment of these cells with a low dose of tamoxifen selected TAM-resistant subpopulations which carried an ARF gene deletion (Fig. 4 F, G; Fig.S3). Furthermore, shRNA-mediated knockdown of ARF in p53^{ER^{TAM}}-late-OFF cell line conferred TAM resistance (Fig. 4 I, J). Resistant cells could be resensitized to TAM by the Mdm2 inhibitor Nutlin, which mimics the action of ARF. (Fig. 4H).

This provides evidence that during development of p53^{ER^{TAM}}-ON lymphomas ARF expression is down-regulated, allowing cells to sustain strong oncogenic Myc-signaling, avoid killing by p53, and progress to aggressive tumors even in the presence of wild-type p53. Upon late p53 inactivation, ARF is re-expressed and confers vulnerability to p53 restoration. *CDKN2A/p14ARF* is commonly inactivated in p53 wild-type tumors either by irreversible genetic alterations or by more or less reversible epigenetic modifications such as promoter methylation (Robertson and Jones 1998) or Polycomb group (PcG) protein-mediated repression (Zeng et al. 2011). We found no evidence of ARF locus deletions in our primary p53^{ER^{TAM}}-ON lymphomas (Fig.S3), as well as no consistent ARF-promoter methylation (Fig.S4). However, we have detected significantly increased levels of PcG protein-mediated histone modifications (H3K27me3 and H2AK119Ub) at the ARF locus in p53^{ER^{TAM}}-ON lymphomas (Supplementary Fig.S5), suggesting that PcG-mediated ARF repression may be responsible for the reversible defect in the Myc-ARF-Mdm2-p53 axis of p53 wild-type lymphomas.

To test if our findings also apply to human cancer cells, we have chosen colorectal cancer cell lines (HCT116 and RKO) and engineered them to express TAM-switchable p53 by targeting the ER^{TAM}-domain into the endogenous *TP53* locus using CRISPR-mediated homologous recombination. Notably, in both cell lines p14ARF expression is undetectable. In HCT116 cells one *CDKN2A* allele is methylated and the other is mutated; in RKO cells both alleles are methylated (Burri et al. 2001; Esteller et al. 2000). Although we have successfully targeted the *TP53* locus in both cell lines, converting their p53 to p53^{ER^{TAM}}

(Fig. 5A, B), and cultivated gene-edited cells for at least 20 passages in the absence of TAM, we have detected no decrease in viability upon addition of TAM and no ARF re-expression (Fig. 5 B-D). Confirming the lack of ARF as a reason for failed p53-reactivation response, introduction of exogenous ARF protein, or mimicking of ARF function with Mdm2-inhibitors strongly decreased the proliferation of these cells (Fig. 5F-H).

Our study provides evidence that tumors, which originate as p53-wild-type, can quickly become addicted to p53-loss and become vulnerable to p53 reactivation. The prerequisite for successful reactivation is that the p53 network is disabled not by downstream mutations (e.g. mutations of genes of the apoptotic pathway), but rather by inactivation of upstream effectors, such as ARF. The p53 network consists of hundreds of target genes, and multiple animal studies showed, that loss of one particular target gene, or even loss of the most of transactivating capacity, are not sufficient to completely disable p53-driven tumor suppression (Valente et al. 2013; Valente et al. 2016; Li et al. 2012; Timofeev et al. 2019). Therefore, inactivation of a single upstream effector like ARF is seemingly a more efficient way to bypass tumor suppression checkpoints. If this ARF inactivation is reversible as in our lymphoma model, it is conceivable, that p53-reactivating therapy is effective. If ARF is inactivated by deletion or poorly reversible silencing, p53-reactivating therapy alone might be ineffective, because oncogenic signaling cannot be sufficiently translated into p53 stabilization. However, therapy efficiency may be achieved in combination with Mdm2 inhibitors that stabilize p53 protein, mimicking the effect of ARF. We, therefore, conclude that p53 reactivating therapy is effective irrespective of whether p53-loss was the tumor-initiating event or not. Furthermore, our findings identify ARF expression and mutant p53 stabilization as potential biomarkers predicting sensitivity to p53-restoration therapy.

2.3 Contribution statement

In this project I have made the following contribution:

- - establishment of the animal model by optimizing retroviral infections of hematopoietic stem cells and optimizing *in vivo* treatment protocols (Fig.1A, Fig. 2A).
- ARF and p53 Western blots of primary lymphomas (Fig.S1).
- performed *in vivo* experiments presented in Fig. 2F-H and Fig.3C, D
- established lymphoma cell lines and performed all *in vitro* experiments with them (Fig.4)
- established and performed mapping of *Cdkn2a* deletion and ChIP assays (Fig. S3, S5).
- performed all experiments with human cell lines (Fig. 5 and Fig.S6)
- performed microscopy
- prepared and analyzed most of the data for the publication
- participated in assembling figures and writing the manuscript

3. Inactivation of Mdm2 restores apoptosis proficiency of cooperativity mutant p53 *in vivo*

Boris Klimovich, Thorsten Stiewe and Oleg Timofeev

Accepted for publication in *Cell Cycle* 15 October 2019

3.1 Introduction

Hot-spot mutations in *TP53* completely disable wild-type p53 functions and confer additional pro-tumorigenic activities to mutp53 (Freed-Pastor and Prives 2012). Non-hotspot p53 mutations are found in 70% of mutp53 tumors and are poorly characterized. Several studies suggest, that many non-hotspot p53 variants are partial loss-of-function (partial-LOF) mutants that possess residual transcriptional activity (Kato et al. 2003; Kotler et al. 2018; Campomenosi et al. 2001; Jordan et al. 2010; Resnick and Inga 2003). For example, p53^{R172P}, the murine ortholog of the human tumor-derived p53^{R175P} mutant, can induce cell cycle arrest, but not apoptosis *in vivo* (Liu et al. 2004). Retention of some p53 wild-type functions by p53 partial-LOF mutants may result in vulnerabilities that open new therapeutic windows. In addition, partial-LOF mutants are valuable experimental tools and numerous mouse models, mostly expressing non-naturally occurring mutants, have been used to dissect the complex nature of p53-mediated tumor suppression (Kenzelmann Broz and Attardi 2010; Li et al. 2012; Kaiser and Attardi 2018).

In general, p53 mutants fall into two large classes. “Structural” mutations such as R175H and R249S destabilize the DBD of p53 and lead to protein denaturation. “Contact” mutations affect residues that directly contact DNA (e.g. R273, R278), thereby abrogating DNA binding (Olivier et al. 2010). Our group and others have recently characterized a separate class of p53 “cooperativity” mutations, that neither lead to protein unfolding, nor affect DNA-contacting residues. These mutations are located in the H1 helix of the p53 DNA binding domain and affect residues E180 and R181. In the p53 tetramer these amino acids form salt bridges between adjacent subunits which stabilize the p53-DNA complex (Dehner et al. 2005; Schlereth et al. 2010a). Cooperativity mutations result in an altered degree of p53 binding to DNA and frequently demonstrate a partial-LOF phenotype. For example, E180R mutant can induce cell cycle arrest, but not apoptosis in human cells (Schlereth et al. 2010a). Cooperativity mutations account for approximately 34,000 cancer cases yearly (Leroy et al. 2014) warranting further investigations into their clinical relevance.

A mouse strain carrying the p53^{E177R} mutation (p53RR, corresponding to human E180R) was characterized in our group (Timofeev et al. 2013). Tumor suppression in these mice is intermediate between wild-type and p53-knockout animals, confirming the partial-LOF nature of this mutant.

Genetic deletion of *Mdm2* in mice with wild-type p53 leads to early embryonic lethality due to apoptosis. Concomitant deletion of *Trp53* completely rescues normal development (Jones et al. 1995; Luna et al. 1995). Partial rescue of embryonic development by *Bax* deletion, but not *Cdkn1a/p21*, implies that apoptosis is the main p53-dependent pathway responsible for embryonic lethality (Chavez-Reyes et al. 2003). Mouse models of hot-spot mutations R172H and R246S and the partial-LOF mutant R172P also rescue embryonic development of *Mdm2-null* mice (Abbas et al. 2010). Conversely, a hypomorphic p53^{neo} allele, which retains less than 20% of wild-type transactivation activity, fails to rescue lethality of *Mdm2*-knockout embryos (Wang et al. 2011), showing that embryonic development is very sensitive tool to detect p53 mutants with residual functionality. Using this model, we have tested if the apoptosis-deficient partial-LOF mutant p53RR can exert residual lethal activities.

3.2 Summary and discussion

We have crossed heterozygous *Mdm2*^{Δ7-9} mice, containing a deletion of *Mdm2* exons 7-9, with *Trp53*^{RR/RR} mice to obtain double heterozygous progeny. Intercrossing of *Mdm2*^{+/Δ7-9}; *Trp53*^{+/RR} animals revealed a strong deviation in distribution of genotypes of newborns from the Mendelian ratio: in particular, no double homozygous (DH) *Mdm2*^{Δ7-9/Δ7-9}; *Trp53*^{RR/RR} pups were recovered (Fig. 1A), clearly indicating embryonic lethality of DH embryos. We have isolated embryos at various developmental stages and observed that p53RR significantly prolonged the embryonic development. Unlike p53 wild-type embryos, which die at 3.5-5.5 dpc, DH embryos looked normal until 7.5-8.5 dpc (Fig. 2A). After 9 dpc, all embryos exhibited severe growth retardation and failed neural tube closure which led to embryonic death (Fig. 2C-F). Immunostaining of abnormal DH embryos revealed strong accumulation of p53 (Fig. 3A, B). Although p53RR can activate *Cdkn1a/p21*-dependent cell cycle arrest (Timofeev et al. 2013), staining for the proliferation marker PCNA displayed no difference between DH and normal embryos, suggesting that impaired development is not a consequence of a p21-mediated block of proliferation (Fig. 2C, D). In line with this, genetic co-ablation of *Cdkn1a* did not prolong embryonic development or mitigate the observed developmental defects (Fig. 3), further suggesting that p21-mediated cell cycle arrest and p21-DREAM-dependent gene repression are not causes of embryonic lethality. Surprisingly, all examined abnormal DH embryos were strongly positive for the apoptosis markers cleaved caspase 3 (CC3) and TUNEL. Importantly, we have detected clear signs of apoptosis already in 9 dpc DH embryos, which were abnormal but still alive and intact arguing that the observed apoptosis is a cause rather than consequences of embryonic lethality (Supp. Fig. 1 A, C, F). This finding was unexpected because p53RR has been shown deficient for binding promoters of pro-apoptotic genes and activation of apoptosis in response to various stimuli (Timofeev et al. 2013; Schlereth

et al. 2010a; Schlereth et al. 2013). Therefore, we have analyzed if apoptosis in DH embryos is accompanied by expression of pro-apoptotic genes. Besides activation of known non-apoptotic p53RR target genes (*Cdkn1a*, *Ccng1*, *Aldh4a*, *Gls2*, and *Sesn2*), we also detected substantial induction of the typical pro-apoptotic genes *Bbc3* (Puma) and *Bax* (Fig. 5A). To explore the role of Mdm2 deficiency for apoptosis induction by p53RR, we treated p53^{RR/RR} mouse embryonic fibroblasts (MEFs) with a combination of doxorubicin and Mdm2 inhibitor Nutlin. As expected and previously shown, treatment of p53^{RR/RR} MEFs with any of the two compounds alone did not induce cell death (Fig. 5C). However, combined treatment of p53^{RR/RR} MEFs induced pronounced apoptosis associated with activation of pro-apoptotic target genes (Fig. 5B, C).

Taken together, our experiments revealed that massive accumulation of partial-LOF mutant p53RR due to genetic or pharmacological ablation of Mdm2 can partially compensate for a defect in cooperative DNA binding and restore apoptotic proficiency. We anticipate that stabilization of p53RR compensates apoptotic defect by mass action: the more protein resides in the cell, the higher is the probability that the low-affinity promoters of pro-apoptotic genes become bound and activated.

In contrast to hot-spot p53 mutations which commonly lead to severely impaired transactivation and distorted interactions with other proteins, many non-hot-spot mutants are capable of transactivating small sets of target genes, suggesting that they keep native-like conformation and preserve some natural protein-protein interactions (Menendez et al. 2006; Resnick and Inga 2003). Our data imply that residual transactivating activities of such mutants could be boosted to enhance tumor cell killing with, for example, Mdm2 inhibitors.

3.3 Contribution statement

In this project I have made the following contribution:

- planned and performed breeding of animals
- performed all experiments with embryos, including embedding, sectioning, and microscopy, as well as IHC quantification
- prepared data and microphotographs
- participated in assembling figures and writing the manuscript

4. Residual apoptotic activity of a tumorigenic p53 mutant improves cancer therapy responses

Timofeev O, Klimovich B, Schneikert J, Wanzel M, Pavlakis E, Noll J, Mutlu S, Elmshäuser S, Nist A, Mernberger M, Lamp B, Wenig U, Brobeil A, Gattenlöhner S, Köhler K, Stiewe T.

EMBO Journal 2019 Sep 4 PubMed ID: 31483066

Commentary by James Manfredi: “p53 defies convention again: a p53 mutant that has lost tumor suppression but still can kill”, EMBO Journal 2019 (PMID: 31553097)

4.1 Introduction

In Klimovich et al. (Cell cycle, in press) we have demonstrated that the apoptosis-deficient cooperativity mutant p53RR (human E180R, murine E177R) exhibits unexpected lethal activity upon genetic or pharmacological depletion of Mdm2. Excessive stabilization of p53RR partially compensates for transactivation defect and leads to induction of pro-apoptotic genes.

Our group has described another cooperativity mutation, p53EE (human R181E, murine R178E) with completely abolished DNA binding (Schlereth et al. 2010a). Despite being entirely transcriptionally inactive, p53EE is natively folded, suggesting that some of its protein-protein interactions may be preserved (Dehner et al. 2005). To test if the transactivation-deficient p53 mutant possesses residual tumor-suppressive activity, we have generated a mouse with the *Trp53*^{R178E} germline mutation and characterized the tumor susceptibility of these animals.

4.2 Summary and discussion

Confirming our earlier data for human p53EE (Schlereth et al. 2013), murine p53EE was unable to bind promoters of target genes and induce their transcription upon treatment with Nutlin or doxorubicin (Fig. 1A). Consequently, p53EE failed to induce typical stress-response programs. Apoptosis and cell cycle arrest were undetectable in p53^{EE/EE}-MEFs in response to treatment with doxorubicin or Nutlin and cells failed to undergo senescence upon expression of oncogenic Ras (Fig. 2A-C, Fig. EV2A, B). Thymus and spleen of adult p53^{EE/EE} mice showed no apoptosis or blocked proliferation in response to gamma-irradiation, similar to p53-knockout mice. Thus, p53EE is indistinguishable from the p53-null allele in multiple cell types. However, prolonged passaging of p53^{EE/EE}-MEFs resulted in a declined proliferation rate when compared to p53-null cells (Fig. EV3A). Moreover, p53EE cells demonstrated positive β -galactosidase staining – a characteristic sign of

senescence (Fig. EV3B). Western blotting revealed additional stabilization of the p53EE mutant protein in late-passage cells (Fig. EV3C), which was not accompanied by induction of p53 target genes (Fig. EV3D). Senescence in primary MEF cultures is commonly caused by oxidative stress (Liguori et al. 2018). Passaging of p53EE MEFs in hypoxic conditions rescued them from senescence implying a causal role of ROS (Fig. EV3H). To confirm the role of p53EE in senescence, we established isogenic p53EE MEF cell lines with CRISPR-Cas9-induced knockout of p53, which completely rescued cells from oxidative stress-induced senescence (Fig. EV3E).

The senescent phenotype of MEFs gave a first hint that p53EE, despite being transcriptionally dead, possesses some residual anti-proliferative activities. To further elaborate this possibility, we investigated if p53EE rescues embryonic lethality of *Mdm2*-knockout embryos, as we previously did for the p53RR mutant. Surprisingly, no newborn pups with the *Mdm2*^{Δ7-9/Δ7-9};*Trp53*^{EE/EE} genotype were recovered from matings, clearly indicating embryonic lethality (Fig. 3A). Double homozygous pups (*Mdm2*^{Δ7-9/Δ7-9};*Trp53*^{-/-}) from control matings of *Mdm2*^{+Δ7-9};*Trp53*^{+/-} mice were born at the expected ratio (Fig. 3B). Strikingly, p53EE embryos were phenotypically indistinguishable from p53RR embryos (see previous report). They were developing normally until 8 dpc and displayed severe growth retardation and failed neural tube closure after 9 dpc (Fig. 3C). p53EE protein was strongly accumulated in embryos and this was accompanied by high levels of apoptosis (Fig. 3E). Thus, similar to p53RR, the cooperativity mutant p53EE also revealed residual lethal activities upon *Mdm2* deletion.

To investigate if lethal activities of p53EE could be pharmacologically engaged upon stabilization in the absence of Mdm2, we ectopically expressed p53EE in *Mdm2*^{Δ7-9/Δ7-9};*Trp53*^{-/-} MEFs and treated them with doxorubicin. *Mdm2*^{Δ7-9/Δ7-9};*Trp53*^{-/-} MEFs were highly resistant to treatment, whereas induction of p53EE expression led to strongly increased levels of apoptosis (Fig. 4A). Importantly, and in contrast to what we had observed in p53RR cells, no induction of pro-apoptotic target genes was evident under treatment, implying that the lethal activity of p53EE is transcription-independent (Fig. 4B). Pharmacological inhibition of Mdm2 with Nutlin had a similar effect on E1A-immortalized p53^{EE/EE} MEFs and strongly impaired cell growth under combined treatment with doxorubicin (Fig. 4C-D). In line with transcription-independent pro-apoptotic effects of wild-type p53 at the mitochondria (Chipuk et al. 2004; Mihara et al. 2003), we observed mitochondrial localization for p53EE (Fig. 4I) suggesting that transcription-independent apoptosis can be activated by p53EE due to increased mitochondrial localization.

To investigate whether p53EE can induce cell death also in human cancer cells, we have overexpressed human p53^{R181E} in p53-null H1299 cells. Treatment of H1299-p53^{R181E} cells with doxorubicin resulted in remarkably strong apoptosis, which was further enhanced by Nutlin (Fig. 5A, C). Just as in murine cells, apoptosis in human cells was accompanied by

mitochondrial localization of p53EE (Fig. 5E, F) without evidence for transcriptional activation of p53 target genes (Fig. 5D).

Next, we investigated the role of the residual pro-apoptotic activity of the p53EE mutant in suppression of carcinogenesis. First, we aged cohorts of p53EE mice and revealed no difference in survival of *Trp53*^{-/-} and *Trp53*^{EE/EE} animals (Fig. 6A), indicating lack of protection from spontaneous tumorigenesis. To test if p53EE can counteract enforced expression of oncogenes, we crossed *Trp53*^{+/-}, *Trp53*^{+/+} and *Trp53*^{+/EE} animals with *Eμ-Myc* mice, which develop B-cell lymphomas. *Eμ-Myc;Trp53*^{+/-} and *Eμ-Myc;Trp53*^{+/EE} animals succumbed to lymphoma equally rapid compared to *Eμ-Myc;Trp53*^{+/+} mice (Fig. 6D), pointing at an inability of p53EE to prevent Myc-induced transformation. Finally, we established an acute myeloid leukemia (AML) model by injecting mice with hematopoietic stem cells (HSC) transduced with AML1-Eto9a and NRas^{G12D} oncogenes (Zuber et al. 2009). Mice transplanted with p53^{-/-} and p53^{EE/EE} HSC both developed leukemias with short latency (median survival 49 and 34 days respectively), significantly earlier than animals injected with p53^{+/+} HSC (95 days) (Fig. 6E). Taken together, these data indicated that p53EE is unable to protect animals from carcinogenesis.

Since p53EE lacks tumor-suppressive potential despite strong p53EE protein expression in tumors, we speculated that the transcription-independent pro-apoptotic activities of p53EE observed *in vitro* are spared from selection pressure and preserved in tumors. To test this possibility, we established cell lines from p53-wild-type, p53-null, and p53^{EE} *Eμ-Myc* lymphomas and treated them with the cyclophosphamide analog mafosfamide (MAF) *in vitro*. As expected, p53^{+/+} cells were rapidly killed by MAF, whereas p53-null lymphomas were highly resistant to treatment (Fig. 7A). Knockdown of p53EE rescued p53^{EE}-cells from MAF cytotoxicity, confirming that killing was mediated by the p53EE mutant (Fig. 7B). Moreover, chemotherapy of mice carrying p53^{EE} lymphomas resulted in exceptionally good response rates and disease control as compared to p53-null lymphomas (Fig. 7D-F). To further corroborate this finding, we tested responses to combined chemotherapy with cytarabine and doxorubicin in the AML model. Animals transplanted with p53-wild-type leukemia cells showed robust response, significantly prolonged survival and a 20% complete cure rate. p53^{-/-} leukemias cells rapidly progressed under chemotherapy, which provided little to no survival benefit. Importantly, animals carrying p53EE-leukemias responded to therapy and demonstrated significantly improved survival (Fig. 7G, H).

Our results obtained from multiple *in vitro* and *in vivo* models reveal remarkable properties of the p53EE mutant. On one hand, it is completely deficient for transactivation which is believed to be indispensable for tumor suppression (Brady et al. 2011; Jiang et al. 2011). In line with this, we were unable to detect any tumor-suppressive activities of p53EE in spontaneous and two oncogene-driven animal tumor models. On the other hand, lethality of *Mdm2*^{Δ7-9/Δ7-9}; *Trp53*^{EE/EE} embryos clearly revealed cytotoxic activity of p53EE upon

excessive stabilization driven by Mdm2 loss. In support of this finding, we observed massive induction of apoptosis by DNA-damage and ROS-induced stress upon genetic or pharmacological ablation of the Mdm2-p53EE interaction. p53EE-mediated apoptosis was not accompanied by detectable target gene activation. Transcription-independent ability of p53 to induce apoptosis via interactions with anti-apoptotic proteins Bcl-2 and Bcl-xL (Mihara et al. 2003) and pro-apoptotic Bax (Leu et al. 2004; Chipuk et al. 2004) is well documented. In line with this, p53EE was accumulated on mitochondria and interacted with Bcl-2 family members (Fig. 5F).

We have translated our *in vitro* findings into two preclinical cancer models and documented the superior response of p53EE-expressing tumors to chemotherapy. These data suggest that missense mutations of p53 do not necessarily result in poor chemotherapy response. Of note, p53EE mutation does not naturally occur in human cancers. While hot-spot mutations are known to disrupt both transcription-dependent and independent activities of p53 due to denaturation (Mihara et al. 2003), there is a reasonable possibility, that selected non-hotspot mutants retain some of the native interactions and can elicit transcription-independent apoptosis, as does p53EE. Supporting such a possibility, the tumor-derived cooperativity mutant p53^{R181L} was able to induce apoptosis in H1299 cells upon treatment with doxorubicin or its combination with Nutlin (Fig. 5H, I).

Our findings from this and previous report (see above) imply that apoptotic defects in two cooperativity mutants p53^{E177R} and p53^{R178E} can be compensated by genetic or pharmacological depletion of Mdm2. Interestingly, lethal activities, unleashed by these two mutant proteins rely on distinct mechanisms. Apoptosis activated by p53^{R178E} is transcription-independent, whereas cell death induced by p53^{E177R} is accompanied by activation of pro-apoptotic target genes. We conclude that the apoptosis defect in the two partial-LOF non-hotspot mutants is not absolute and context-dependent. It is therefore conceivable that cell death pathways can be re-engaged by these and potentially many other p53 mutants.

As noted before, one of the emerging strategies for the treatment of mutp53-expressing tumors relies on its degradation (Sabapathy and Lane 2017). Our findings imply that this approach may be suitable for mutants with strong GOF effects but may be counterproductive for mutants which retain residual pro-apoptotic activities. Indeed, we revealed no GOF activities of p53EE in animal models but convincingly demonstrated that p53EE-driven apoptosis strongly depends on mutant stabilization (Fig. 4H). Therefore, inducing degradation of p53EE or similar mutants may result in an impaired chemotherapy response.

Our data advocate the need of comprehensive investigation of non-hot-spot p53 mutations in order to improve clinical decision making based on p53 status.

4.3 Contribution statement

In this project I have made the following contribution:

- AML model: established protocols for HSC isolation and infection, optimized irradiation and bioimaging protocols, performed AML therapy experiments, optimized chemotherapy regime, planned and performed all animal experiments with this model, collected samples and performed analysis (Fig 6E; Fig 7 G, H)
- participated in animal experiments with E μ -Myc lymphoma model (Fig 7D, E)
- planned and performed all experiments with respect to embryonic lethality in *Mdm2*-knockout mice
- established lymphoma cell lines and performed *in vitro* experiments with them (Fig.7A, B)
- established cell lines with ectopic overexpression of p53EE (MEFs and H1299) and performed experiments with them (Fig. 5A-C, Fig. 4A, B)
- performed CRISPR-mediated knockout of p53 in MEFs and proliferation assays with these cells (Fig. EV3E)
- analyzed and prepared data for figures
- participated in manuscript writing

5. Summary and perspectives

5.1 p53 reactivation therapy is effective in tumors with late-stage p53 inactivation

In the current work, we have explored various aspects of the problem of targeting of mutp53 for cancer therapy. Over the past several decades, significant progress in understanding of mutant p53 biology has been made (Levine and Oren 2009; Freed-Pastor and Prives 2012). However, translation of these findings into clinical practice is hampered by challenges with pharmacological targeting of mutp53 (Levine 2019). Considerable research efforts have led to the development of several promising strategies. Clinical trials with p53-reactivating drug APR 246 are underway: 9 phase 1-3 clinical trials with APR 246 are currently listed at clinicaltrials.gov (Perdrix et al. 2017). Mutp53-degradation therapy with Hsp90 inhibitors has also reached clinical investigation (Ray-Coquard et al. 2019).

An important obstacle for further clinical development is the lack of predictors for clinical benefit of any of these therapies. Effective restoration of the wild-type functions in mutant p53 with drugs like APR 246 requires the integrity of the downstream effector pathways. If mutation in p53 is the initiating event in cancer development, downstream pathways stay unaffected and may be engaged by reactivated p53. Many tumors inactivate p53 at the late stages of malignant growth. In such conditions, additional alterations inactivating p53-mediated pathways are strongly supported by selection. Reactivation of p53 in tumors with multiple alterations downstream or upstream of p53 may be worthless. It is therefore plausible, that only tumors where p53-loss was the initiating driver lesion may be sensitive to p53-reactivating therapy.

In our first report, we have explored if p53-reactivating therapy is effective in tumors, which arise in the presence of active p53 (Klimovich et al. 2019). Using the refined genetic mouse model of p53 reactivation, we discovered that inactivation of p53 in established aggressive tumors leads to fast acquisition of addiction to p53-loss and, consequently, makes cancer cells vulnerable to p53 restoration. Mechanistically, effective p53 reactivation in our model relies on ARF, which is reversibly inactivated during tumor development and is quickly re-expressed after p53 loss. The paramount importance of the ARF-Mdm2-p53 axis in cancer suggests that our findings may be applicable to a broader range of human tumors. As noted above, genetic alteration in any single gene of the p53 network is insufficient to completely disable tumor suppression. On the contrary, inactivation of the single upstream effector ARF allows to bypass tumor surveillance. In our experiments, temporary silencing of ARF by PcG-mediated histone modifications was quickly reversed after p53 inactivation. PcG-mediated repression of *CDKN2A* locus has been shown in human tumor cells (Jacobs et al. 1999; Kia et al. 2008; Li et al. 2011c; Zeng et al. 2011; Bracken et al. 2007) and primary tumors (Meseure et al. 2016; Yap et al. 2010). It is reported, that inhibitors of the

polycomb repressive complex 2 (PRC2) component EZH2 can induce ARF derepression (Marchesi and Bagella 2016; Sun et al. 2016). Thus, EZH2 inhibitors can theoretically boost p53-reactivation responses. PRIMA-1 indeed showed strong synergy with the EZH2 inhibitor DZNep in p53-mutant thyroid cancer cell lines (Cui et al. 2014).

But *CDKN2A/p14ARF* is also frequently inactivated by promoter methylation (Burri et al. 2001). In both colorectal cell lines used in our study, *CDKN2A* is disabled by this mechanism. p53 loss in these cells did not lead to ARF re-expression and therefore p53 reactivation was inefficient. The same is expected for tumors with ARF promoter methylation. However, re-expression of the silenced *CDKN2A* locus under treatment with demethylating agents or their combination with HDAC inhibitors has been documented (Badal et al. 2008; Esteller et al. 2000; Coombes et al. 2003; Cameron et al. 1999). Thus, even if the ARF promoter is methylated, tumors may, in principle, be resensitized to p53 reactivating therapy by demethylating drugs. In case that *CDKN2A/p14ARF* is irreversibly silenced or disabled by mutation, Mdm2 inhibitors may be used to mimic ARF functions as shown in our experiments (Izetti et al. 2014; Liu et al. 2013).

Our data provide proof-of-principle that p53 reactivation is a feasible therapeutic approach for a broad spectrum of tumors with p53 mutations, independently of the timing of p53-loss.

5.2 Partial loss-of-function p53 mutants are actionable therapy targets

Missense mutations in *TP53* generate a “rainbow” of >2000 mutants. Growing evidence suggests, that p53 mutants are unequal. Some non-hot-spot mutants are partial-LOF and therefore may make tumors susceptible to distinct therapeutic modalities. Recently described cooperativity mutants frequently demonstrate a partial-LOF. We, therefore, took advantage of two distinct cooperativity mutations to explore their residual tumor-suppressive activities. Our experiments revealed that both mutants (p53RR and p53EE) induce massive apoptosis under conditions of genetic or pharmacological Mdm2 inactivation, indicating that the apoptosis defect typical for partial-LOF mutants may be rescued by Mdm2 inhibition.

The ability of p53 to induce apoptosis depends on several factors: p53 protein levels in the cell, the duration of elevated p53 expression and intrinsic apoptotic sensitivity of the cell (apoptotic threshold) (Kracikova et al. 2013; Purvis et al. 2012; Le Pen et al. 2016). In our experiments, Mdm2 inhibition resulted in prolonged elevation of mutant p53 levels and lowering of the apoptotic threshold. Interestingly, apoptosis induced by the two cooperativity mutants relies on distinct mechanisms. Stabilization of p53RR partially restores binding to promoters of pro-apoptotic genes whereas accumulation of p53EE leads to increased mitochondrial localization, interaction with Bcl-2 family members and transcription-independent apoptosis. It is tempting to speculate that both transcription-dependent and independent mechanisms may be engaged by partial-LOF mutants upon

Summary and perspectives

excessive stabilization. Transcription-independent pro-apoptotic activity exerted by p53EE mutant is of particular interest. Although cytoplasmic apoptogenic role of p53 has been extensively documented *in vitro*, its importance for tumor suppression *in vivo* is rather elusive. Two reports have demonstrated, that targeting of p53 to mitochondria by overexpressing p53 fused to transmembrane domains of Bcl2 and Bcl-xL induced apoptosis in Eμ-Myc lymphomas *in vivo* (Talos et al. 2005; Palacios and Moll 2006). However, substantial drawbacks of the existing models for p53's extra-nuclear activities are non-physiological expression levels and enforced localization of the protein. Moreover, these models do not clarify whether cytoplasmic activities can counteract primary tumor development. p53EE demonstrates normal subcellular localization, trafficking, and stress response kinetics, and has expression levels similar to mutants from naturally-occurring tumors (Timofeev et al., 2019, Fig. 4I, EV4). Therefore the p53EE (*Trp53^{R178E}*) mouse represents a valuable expansion of the toolbox of p53 mutations, as pointed out by James Manfredi in his „News and Views” column in EMBO Journal (Fig. 1) (Manfredi 2019). This model allowed us to investigate extra-nuclear functions of p53 in a physiological *in vivo* context that was unachievable before. We provide evidence, that p53EE does not delay onset of spontaneous and oncogene-driven tumors, which strongly suggests that transactivation is indispensable for tumor suppression. Importantly, this finding further implies that cytoplasmic proapoptotic mechanisms are ineffective in tumor suppression, therefore remain unaffected during tumor development and result in actionable vulnerabilities associated with p53 non-hot-spot mutants.

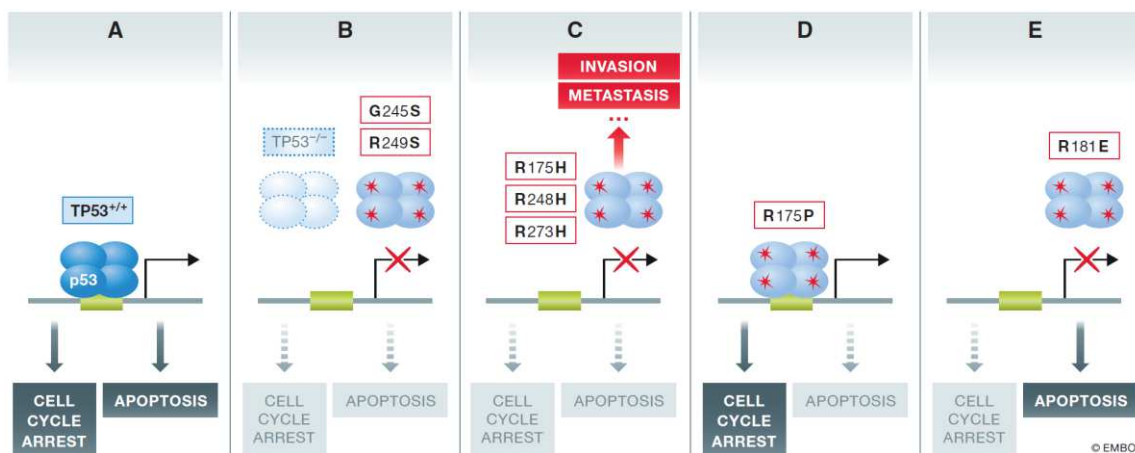


Figure 1. (A) – wild-type p53 mediates a full set of responses, mainly via transactivation of target genes. Hot-spot mutation completely inactivate tumor-suppressive functions (B) and acquire neomorphic oncogenic functions (C). Certain non-hot-spot mutants selectively retain some activities, being partial-LOF (D). Our results expand the complexity of the paradigm: p53^{R181E} completely lacks transactivating ability, but retain strong non-transcriptional apoptotic activity, being a valuable model for extra-nuclear functions of p53 (E) (from Manfredi, 2019).

Summary and perspectives

Our data call for focusing on such vulnerabilities during development of mutp53 targeting strategies. Unfortunately, most screening efforts aim to identify compounds restoring the transactivating functions of mutp53. Studies of p53RR and other cooperativity mutants have demonstrated, that p53 with partially impaired DNA interactions preferentially binds to the promoters of pro-survival genes (*CDKN1A*, *CCNG1* etc.) (Schlereth et al. 2013). Therefore, incomplete recovery of transactivation by suboptimal p53-reactivating compounds will result in preferential induction of cell cycle arrest and senescence but not apoptosis. Although therapy-induced senescence is shown to effectively promote tumor clearance under chemotherapy (Kahlem et al. 2004), multiple studies have demonstrated, that senescence may also lead to cancer cell reprogramming, formation of a pro-tumorigenic microenvironment and consecutive tumor relapse (Dökümcü and Farahani 2019; Lee and Schmitt 2019; Schosserer et al. 2017; Milanovic et al. 2017). From this perspective, compounds which specifically reactivate transcription-independent proapoptotic activities of p53 mutants might have considerable therapeutic advantages.

Mdm2 inhibitors were designed for tumors with wild-type p53 and are generally deemed useless for treatment of mutp53-tumors. This consideration is supported by the fact, that acquisition of p53 mutations or upregulation of Mdm2 and Bcl-xL are known mechanisms of resistance to Mdm2 inhibitors (Cinatl et al. 2014; Chapeau et al. 2017). We have demonstrated that Mdm2 inhibitors unleash the apoptotic potential of cooperativity mutants, advocating the use of Mdm2 inhibitors together with other drugs. Synergy of Mdm2 inhibitors with many approved drugs (e.g. cytostatics, kinase inhibitors, HDAC inhibitors) has already been demonstrated for p53 wild-type cells (Hoe et al. 2014). Whether some of these combinations can also improve killing of mutp53-expressing tumors remains to be determined. Manipulating the apoptotic threshold of cancer cells with BH3 mimetics could potentially improve their apoptotic response induced by partial-LOF mutants even further (Montero and Letai 2018). Importantly, clinical activity was documented in 2 patients with *TP53* mutations in Phase I trial of RG 7112 (Andreeff et al. 2016), indicating that certain p53 mutants may indeed respond to Mdm2 inhibitors.

A potential danger of treating mutp53-tumors with Mdm2 inhibitors is that the treatment may boost oncogenic GOF activities due to additional mutant stabilization. How many non-hot-spot mutants possess GOF properties is currently unknown. Our experiments clearly demonstrate a lack of any pro-tumorigenic GOF activity for p53EE: tumor spectra and survival in p53^{EE/EE} mice was very similar to p53^{-/-} and no increase in metastasis frequency was observed (Timofeev et al., 2019, Fig 6A; Appendix Tables S1 and S2). It is plausible, that GOF effects are less widespread than generally assumed and confined to small sets of hot-spot mutations only. In line, a recent report failed to identify GOF properties for any of the hot-spot mutants in AML cells *in vivo*, suggesting that GOF effects are mutant- and context-specific (Boettcher et al. 2019).

Summary and perspectives

The observation that some tumors exhibit an addiction to GOF activities of mutp53 provided a rationale for the development of p53-degradation therapy with Hsp90 inhibitors (Alexandrova et al. 2015; Ray-Coquard et al. 2019). Since GOF activity is not a universal trait of mutp53, therapeutic agents triggering p53 degradation may be effective only against a small subset of tumors. In case of mutants analogous to p53EE and p53RR, administration of such compounds together with chemotherapy would even be detrimental, because the chemotherapy response relies on a strongly stabilized mutant.

Improvement of clinical decision making based on p53 mutation status requires extensive characterization of the p53 “mutome” in respect of LOF, GOF and DN-properties. For this purpose, the sensitivity of tumor cells harboring hundreds of different mutants to multiple treatments and drug combinations in various contexts needs to be assessed. Recent advances in next-generation sequencing made it possible to phenotypically profile thousands of p53 mutants in parallel (Kotler et al. 2018; Giacomelli et al. 2018; Boettcher et al. 2019). In these studies, p53 mutants were assayed for their ability to inhibit growth either under normal culture conditions or under Nutlin treatment. The R181E mutant was present in one of the three datasets and classified as “common cancer missense” (phenotype scores R181E=0,98; R175H=1,025 wt=0,036, PHANTM algorithm) even though our extensive analysis clearly identified residual wild-type activities for this mutant (Giacomelli et al. 2018). It can be anticipated that R181E is not the only mutant with residual cytotoxic activity that high-throughput screens have overlooked. We propose that existing screening protocols must be optimized to identify partial-LOF variants with higher precision.

Collectively, our data encourage to expand the development of p53-targeting strategies beyond current frameworks taking into account mutant p53 functional heterogeneity for personalized precision medicine.

6. Publication bibliography

Abbas, Hussein A.; MacCio, Daniela R.; Coskun, Suleyman; Jackson, James G.; Hazen, Amy L.; Sills, Tiffany M. et al. (2010): Mdm2 Is Required for Survival of Hematopoietic Stem Cells/Progenitors via Dampening of ROS-Induced p53 Activity. In *Cell Stem Cell*. DOI: 10.1016/j.stem.2010.09.013.

Adorno, Maddalena; Cordenonsi, Michelangelo; Montagner, Marco; Dupont, Sirio; Wong, Christine; Hann, Byron et al. (2009): A Mutant-p53/Smad complex opposes p63 to empower TGFbeta-induced metastasis. In *10974172* 137 (1), pp. 87–98. DOI: 10.1016/j.cell.2009.01.039.

Ahmed, Ahmed Ashour; Etemadmoghadam, Dariush; Temple, Jillian; Lynch, Andy G.; Riad, Mohamed; Sharma, Raghwa et al. (2010): Driver mutations in TP53 are ubiquitous in high grade serous carcinoma of the ovary. In *The Journal of pathology* 221 (1), pp. 49–56. DOI: 10.1002/path.2696.

Alexandrova, E. M.; Yallowitz, A. R.; Li, D.; Xu, S.; Schulz, R.; Proia, D. A. et al. (2015): Improving survival by exploiting tumour dependence on stabilized mutant p53 for treatment. In *Nature* 523 (7560), pp. 352–356. DOI: 10.1038/nature14430.

Alexandrova, Evguenia M.; Xu, Sulan; Moll, Ute M. (2017): Ganetespib synergizes with cyclophosphamide to improve survival of mice with autochthonous tumors in a mutant p53-dependent manner. In *Cell Death & Disease* 8 (3), e2683. DOI: 10.1038/cddis.2017.108.

Amin, Nisar A.; Seymour, Erlene; Saiya-Cork, Kamlai; Parkin, Brian; Shedden, Kerby; Malek, Sami N. (2016): A Quantitative Analysis of Subclonal and Clonal Gene Mutations before and after Therapy in Chronic Lymphocytic Leukemia. In *Clinical cancer research : an official journal of the American Association for Cancer Research* 22 (17), pp. 4525–4535. DOI: 10.1158/1078-0432.CCR-15-3103.

Andreeff, Michael; Kelly, Kevin R.; Yee, Karen; Assouline, Sarit; Strair, Roger; Popplewell, Leslie et al. (2016): Results of the Phase I Trial of RG7112, a Small-Molecule MDM2 Antagonist in Leukemia. In *Clinical cancer research : an official journal of the American Association for Cancer Research* 22 (4), pp. 868–876. DOI: 10.1158/1078-0432.CCR-15-0481.

Andrysik, Zdenek; Galbraith, Matthew D.; Guarnieri, Anna L.; Zaccara, Sara; Sullivan, Kelly D.; Pandey, Ahwan et al. (2017): Identification of a core TP53 transcriptional program with highly distributed tumor suppressive activity. In *Genome Research* 27 (10), pp. 1645–1657. DOI: 10.1101/gr.220533.117.

Ano Bom, Ana P. D.; Rangel, Luciana P.; Costa, Danielly C. F.; Oliveira, Guilherme A. P. de; Sanches, Daniel; Braga, Carolina A. et al. (2012): Mutant p53 aggregates into prion-like amyloid oligomers and fibrils: implications for cancer. In *The Journal of Biological Chemistry* 287 (33), pp. 28152–28162. DOI: 10.1074/jbc.M112.340638.

Arima, Yoshimi; Nitta, Masayuki; Kuninaka, Shinji; Zhang, Dongwei; Fujiwara, Toshiyoshi; Taya, Yoichi et al. (2005): Transcriptional blockade induces p53-dependent apoptosis associated with translocation of p53 to mitochondria. In *The Journal of Biological Chemistry* 280 (19), pp. 19166–19176. DOI: 10.1074/jbc.M410691200.

Badal, Vinay; Menendez, Sergio; Coomber, David; Lane, David P. (2008): Regulation of the p14ARF promoter by DNA methylation. In *Cell cycle (Georgetown, Tex.)* 7 (1), pp. 112–119. DOI: 10.4161/cc.7.1.5137.

- Basu, Subhasree; Gnanapradeepan, Keerthana; Barnoud, Thibaut; Kung, Che-Pei; Tavecchio, Michele; Scott, Jeremy et al. (2018): Mutant p53 controls tumor metabolism and metastasis by regulating PGC-1 α . In *Genes & development* 32 (3-4), pp. 230–243. DOI: 10.1101/gad.309062.117.
- Baugh, Evan H.; Ke, Hua; Levine, Arnold J.; Bonneau, Richard A.; Chan, Chang S. (2018): Why are there hotspot mutations in the TP53 gene in human cancers? In *14765403* 25 (1), pp. 154–160. DOI: 10.1038/cdd.2017.180.
- Biegging, Kathryn T.; Attardi, Laura D. (2012): Deconstructing p53 transcriptional networks in tumor suppression. In *Trends in cell biology* 22 (2), pp. 97–106. DOI: 10.1016/j.tcb.2011.10.006.
- Blagosklonny, M. V.; Toretsky, J.; Bohlen, S.; Neckers, L. (1996): Mutant conformation of p53 translated in vitro or in vivo requires functional HSP90. In *Proceedings of the National Academy of Sciences of the United States of America* 93 (16), pp. 8379–8383. DOI: 10.1073/pnas.93.16.8379.
- Blandino, G.; Levine, A. J.; Oren, M. (1999): Mutant p53 gain of function: differential effects of different p53 mutants on resistance of cultured cells to chemotherapy. In *Oncogene* 18 (2), pp. 477–485.
- Blandino, Giovanni; Di Agostino, Silvia (2018): New therapeutic strategies to treat human cancers expressing mutant p53 proteins. In *Journal of Experimental & Clinical Cancer Research : CR* 37 (1), p. 30. DOI: 10.1186/s13046-018-0705-7.
- Boehme, Karen A.; Blattner, Christine (2009): Regulation of p53--insights into a complex process. In *Critical reviews in biochemistry and molecular biology* 44 (6), pp. 367–392. DOI: 10.3109/10409230903401507.
- Boettcher, Steffen; Miller, Peter G.; Sharma, Rohan; McConkey, Marie; Leventhal, Matthew; Krivtsov, Andrei V. et al. (2019): A dominant-negative effect drives selection of TP53 missense mutations in myeloid malignancies. In *Science (New York, N.Y.)* 365 (6453), pp. 599–604. DOI: 10.1126/science.aax3649.
- Bracken, Adrian P.; Kleine-Kohlbrecher, Daniela; Dietrich, Nikolaj; Pasini, Diego; Gargiulo, Gaetano; Beekman, Chantal et al. (2007): The Polycomb group proteins bind throughout the INK4A-ARF locus and are disassociated in senescent cells. In *Genes & development* 21 (5), pp. 525–530. DOI: 10.1101/gad.415507.
- Brady, Colleen a.; Attardi, Laura D. (2010): P53 At a Glance. In *Journal of cell science* 123 (Pt 15), pp. 2527–2532. DOI: 10.1242/jcs.064501.
- Brady, Colleen a.; Jiang, Dadi; Mello, Stephano S.; Johnson, Thomas M.; Jarvis, Lesley A.; Kozak, Margaret M. et al. (2011): Distinct p53 Transcriptional Programs Dictate Acute DNA Damage Responses and Tumor Suppression. In *Cell* 145 (4), pp. 571–583. DOI: 10.1016/j.cell.2011.03.035.
- Buganim, Yosef; Kalo, Eyal; Brosh, Ran; Besserglick, Hila; Nachmany, Ido; Rais, Yoach et al. (2006): Mutant p53 protects cells from 12-O-tetradecanoylphorbol-13-acetate-induced death by attenuating activating transcription factor 3 induction. In *Cancer Res* 66 (22), pp. 10750–10759. DOI: 10.1158/0008-5472.CAN-06-0916.
- Bullock, A. N.; Fersht, A. R. (2001): Rescuing the function of mutant p53. In *Nature reviews. Cancer* 1 (1), pp. 68–76. DOI: 10.1038/35094077.
- Burri, N.; Shaw, P.; Bouzourene, H.; Sordat, I.; Sordat, B.; Gillet, M. et al. (2001): Methylation silencing and mutations of the p14ARF and p16INK4a genes in colon cancer. In *Laboratory investigation; a journal of technical methods and pathology* 81 (2), pp. 217–229.

- Cameron, E. E.; Bachman, K. E.; Myöhänen, S.; Herman, J. G.; Baylin, S. B. (1999): Synergy of demethylation and histone deacetylase inhibition in the re-expression of genes silenced in cancer. In *Nature genetics* 21 (1), pp. 103–107. DOI: 10.1038/5047.
- Campomenosi, P.; Monti, P.; Aprile, A.; Abbondandolo, A.; Frebourg, T.; Gold, B. et al. (2001): p53 mutants can often transactivate promoters containing a p21 but not Bax or PIG3 responsive elements. In *Oncogene* 20 (27), pp. 3573–3579. DOI: 10.1038/sj.onc.1204468.
- Chapeau, Emilie A.; Gembarska, Agnieszka; Durand, Eric Y.; Mandon, Emeline; Estadieu, Claire; Romanet, Vincent et al. (2017): Resistance mechanisms to TP53-MDM2 inhibition identified by in vivo piggyBac transposon mutagenesis screen in an Arf^{-/-} mouse model. In *Proceedings of the National Academy of Sciences of the United States of America* 114 (12), pp. 3151–3156. DOI: 10.1073/pnas.1620262114.
- Chavez-Reyes, Arturo; Parant, John M.; Amelse, Lisa L.; Montes De Oca Luna, Roberto; Korsmeyer, Stanley J.; Lozano, Guillermina (2003): Switching Mechanisms of Cell Death in mdm2- and mdm4-null Mice by Deletion of p53 Downstream Targets. In *Cancer research*.
- Chin, K. V.; Ueda, K.; Pastan, I.; Gottesman, M. M. (1992): Modulation of activity of the promoter of the human MDR1 gene by Ras and p53. In *Science* 255 (5043), pp. 459–462. DOI: 10.1126/science.1346476.
- Chipuk, Jerry E.; Kuwana, Tomomi; Bouchier-Hayes, Lisa; Droin, Nathalie M.; Newmeyer, Donald D.; Schuler, Martin; Green, Douglas R. (2004): Direct activation of Bax by p53 mediates mitochondrial membrane permeabilization and apoptosis. In *Science (New York, N.Y.)* 303 (5660), pp. 1010–1014. DOI: 10.1126/science.1092734.
- Christophorou, Maria A.; Martin-Zanca, Dionisio; Soucek, Laura; Lawlor, Elizabeth R.; Brown-Swigart, Lamorna; Verschuren, Emmy W.; Evan, Gerard I. (2005): Temporal dissection of p53 function in vitro and in vivo. In *Nature genetics* 37 (7), pp. 718–726. DOI: 10.1038/ng1572.
- Cinatl, Jindrich; Speidel, Daniel; Hardcastle, Ian; Michaelis, Martin (2014): Resistance acquisition to MDM2 inhibitors. In *Biochemical Society transactions* 42 (4), pp. 752–757. DOI: 10.1042/BST20140035.
- Coombes, Madelene M.; Briggs, Katrina L.; Bone, James R.; Clayman, Gary L.; El-Naggar, Adel K.; Dent, Sharon Y. R. (2003): Resetting the histone code at CDKN2A in HNSCC by inhibition of DNA methylation. In *Oncogene* 22 (55), pp. 8902–8911. DOI: 10.1038/sj.onc.1207050.
- Cui, Bo; Yang, Qi; Guan, Haixia; Shi, Bingyin; Hou, Peng; Ji, Meiju (2014): PRIMA-1, a mutant p53 reactivator, restores the sensitivity of TP53 mutant-type thyroid cancer cells to the histone methylation inhibitor 3-Deazaneplanocin A. In *The Journal of clinical endocrinology and metabolism* 99 (6), E962-70. DOI: 10.1210/jc.2013-3147.
- Dehner, Alexander; Klein, Christian; Hansen, Silke; Müller, Lin; Buchner, Johannes; Schwaiger, Manfred; Kessler, Horst (2005): Cooperative binding of p53 to DNA: regulation by protein-protein interactions through a double salt bridge. In *Angewandte Chemie (International ed. in English)* 44 (33), pp. 5247–5251. DOI: 10.1002/anie.200501887.
- Dixon, Scott J.; Lemberg, Kathryn M.; Lamprecht, Michael R.; Skouta, Rachid; Zaitsev, Eleina M.; Gleason, Caroline E. et al. (2012): Ferroptosis: an iron-dependent form of nonapoptotic cell death. In *10974172* 149 (5), pp. 1060–1072. DOI: 10.1016/j.cell.2012.03.042.
- Do, Phi M.; Varanasi, Lakshman; Fan, Songqing; Li, Chunyang; Kubacka, Iwona; Newman, Virginia et al. (2012): Mutant p53 cooperates with ETS2 to promote etoposide resistance. In *Genes & development* 26 (8), pp. 830–845. DOI: 10.1101/gad.181685.111.

- Dökümcü, Kağan; Farahani, Ramin M. (2019): Evolution of Resistance in Cancer: A Cell Cycle Perspective. In *Frontiers in Oncology* 9, p. 376. DOI: 10.3389/fonc.2019.00376.
- Donehower, Lawrence A.; Soussi, Thierry; Korkut, Anil; Liu, Yuexin; Schultz, Andre; Cardenas, Maria et al. (2019): Integrated Analysis of TP53 Gene and Pathway Alterations in The Cancer Genome Atlas. In *Cell reports* 28 (5), 1370-1384.e5. DOI: 10.1016/j.celrep.2019.07.001.
- Dong, P.; Karaayvaz, M.; Jia, N.; Kaneuchi, M.; Hamada, J.; Watari, H. et al. (2013): Mutant p53 gain-of-function induces epithelial-mesenchymal transition through modulation of the miR-130b-ZEB1 axis. In *Oncogene* 32 (27), pp. 3286–3295. DOI: 10.1038/onc.2012.334.
- Eischen, C. M.; Weber, J. D.; Roussel, M. F.; Sherr, C. J.; Cleveland, J. L. (1999): Disruption of the ARF-Mdm2-p53 tumor suppressor pathway in Myc-induced lymphomagenesis. In *Genes & development* 13 (20), pp. 2658–2669. DOI: 10.1101/gad.13.20.2658.
- Engeland, Kurt (2018): Cell cycle arrest through indirect transcriptional repression by p53: I have a DREAM. In *14765403* 25 (1), pp. 114–132. DOI: 10.1038/cdd.2017.172.
- Esteller, M.; Tortola, S.; Toyota, M.; Capella, G.; Peinado, M. A.; Baylin, S. B.; Herman, J. G. (2000): Hypermethylation-associated inactivation of p14(ARF) is independent of p16(INK4a) methylation and p53 mutational status. In *Cancer Res* 60 (1), pp. 129–133.
- Fearon, E. R.; Vogelstein, B. (1990): A genetic model for colorectal tumorigenesis. In *Cell* 61 (5), pp. 759–767. DOI: 10.1016/0092-8674(90)90186-i.
- Feldser, David M.; Kostova, Kamena K.; Winslow, Monte M.; Taylor, Sarah E.; Cashman, Chris; Whittaker, Charles A. et al. (2010): Stage-specific sensitivity to p53 restoration during lung cancer progression. In *Nature* 468 (7323), pp. 572–575. DOI: 10.1038/nature09535.
- Fischer, M. (2017): Census and evaluation of p53 target genes. In *Oncogene*.
- Foster, B. A.; Coffey, H. A.; Morin, M. J.; Rastinejad, F. (1999): Pharmacological rescue of mutant p53 conformation and function. In *Science* 286 (5449), pp. 2507–2510. DOI: 10.1126/science.286.5449.2507.
- Frazier, M. W.; He, X.; Wang, J.; Gu, Z.; Cleveland, J. L.; Zambetti, G. P. (1998): Activation of c-myc gene expression by tumor-derived p53 mutants requires a discrete C-terminal domain. In *Molecular and cellular biology* 18 (7), pp. 3735–3743. DOI: 10.1128/mcb.18.7.3735.
- Freed-Pastor, William A.; Mizuno, Hideaki; Zhao, Xi; Langerød, Anita; Moon, Sung-Hwan; Rodriguez-Barrueco, Ruth et al. (2012): Mutant p53 disrupts mammary tissue architecture via the mevalonate pathway. In *10974172* 148 (1-2), pp. 244–258. DOI: 10.1016/j.cell.2011.12.017.
- Freed-Pastor, William A.; Prives, Carol (2012): Mutant p53: one name, many proteins. In *Genes & development* 26 (12), pp. 1268–1286. DOI: 10.1101/gad.190678.112.
- Frum, Rebecca A.; Grossman, Steven R. (2014): Mechanisms of mutant p53 stabilization in cancer. In *Sub-cellular biochemistry* 85, pp. 187–197. DOI: 10.1007/978-94-017-9211-0_10.
- Giacomelli, Andrew O.; Yang, Xiaoping; Lintner, Robert E.; McFarland, James M.; Duby, Marc; Kim, Jaegil et al. (2018): Mutational processes shape the landscape of TP53 mutations in human cancer. In *Nature genetics* 50 (10), pp. 1381–1387. DOI: 10.1038/s41588-018-0204-y.
- Gordon, Erlinda M.; Ravicz, Joshua R.; Liu, Seiya; Chawla, Sant P.; Hall, Frederick L. (2018): Cell cycle checkpoint control: The cyclin G1/Mdm2/p53 axis emerges as a strategic target for broad-spectrum cancer gene therapy - A review of molecular mechanisms for oncologists. In *Molecular and clinical oncology* 9 (2), pp. 115–134. DOI: 10.3892/mco.2018.1657.

- Gu, Bo; Zhu, Wei-Guo (2012): Surf the post-translational modification network of p53 regulation. In *International journal of biological sciences* 8 (5), pp. 672–684. DOI: 10.7150/ijbs.4283.
- Guo, Xuning Emily; Ngo, Bryan; Modrek, Aram Sandaldjian; Lee, Wen-Hwa (2014): Targeting tumor suppressor networks for cancer therapeutics. In *Current drug targets* 15 (1), pp. 2–16. DOI: 10.2174/1389450114666140106095151.
- Hanel, W.; Marchenko, N.; Xu, S.; Yu, S. Xiaofeng; Weng, W.; Moll, U. (2013): Two hot spot mutant p53 mouse models display differential gain of function in tumorigenesis. In *14765403* 20 (7), pp. 898–909. DOI: 10.1038/cdd.2013.17.
- Haupt, Susan; Berger, Michael; Goldberg, Zehavit; Haupt, Ygal (2003): Apoptosis - the p53 network. In *Journal of cell science* 116 (Pt 20), pp. 4077–4085. DOI: 10.1242/jcs.00739.
- Haupt, Y.; Maya, R.; Kazaz, A.; Oren, M. (1997): Mdm2 promotes the rapid degradation of p53. In *Nature* 387 (6630), pp. 296–299. DOI: 10.1038/387296a0.
- Hegi, M. E.; Klein, M. A.; Ruedi, D.; Chène, P.; Hamou, M. F.; Aguzzi, A. (2000): p53 transdominance but no gain of function in mouse brain tumor model. In *Cancer Res* 60 (11), pp. 3019–3024.
- Hientz, Karin; Mohr, André; Bhakta-Guha, Dipita; Efferth, Thomas (2017): The role of p53 in cancer drug resistance and targeted chemotherapy. In *Oncotarget* 8 (5), pp. 8921–8946. DOI: 10.18632/oncotarget.13475.
- Hoe, Khoo Kian; Verma, Chandra S.; Lane, David P. (2014): Drugging the p53 pathway: understanding the route to clinical efficacy. In *Nature reviews. Drug discovery* 13 (3), pp. 217–236. DOI: 10.1038/nrd4236.
- Izetti, Patricia; Hautefeuille, Agnes; Abujamra, Ana Lucia; Farias, Caroline Brunetto de; Giacomazzi, Juliana; Alemar, Bárbara et al. (2014): PRIMA-1, a mutant p53 reactivator, induces apoptosis and enhances chemotherapeutic cytotoxicity in pancreatic cancer cell lines. In *Investigational new drugs* 32 (5), pp. 783–794. DOI: 10.1007/s10637-014-0090-9.
- Jacobs, J. J.; Kieboom, K.; Marino, S.; DePinho, R. A.; van Lohuizen, M. (1999): The oncogene and Polycomb-group gene bmi-1 regulates cell proliferation and senescence through the ink4a locus. In *Nature* 397 (6715), pp. 164–168. DOI: 10.1038/16476.
- Jia, L. Q.; Osada, M.; Ishioka, C.; Gamo, M.; Ikawa, S.; Suzuki, T. et al. (1997): Screening the p53 status of human cell lines using a yeast functional assay. In *Molecular carcinogenesis* 19 (4), pp. 243–253.
- Jiang, Dadi; Brady, Colleen a.; Johnson, Thomas M.; Lee, Eunice Y.; Park, Eunice J.; Scott, Matthew P.; Attardi, Laura D. (2011): Full p53 transcriptional activation potential is dispensable for tumor suppression in diverse lineages. In *Proceedings of the National Academy of Sciences of the United States of America* 108 (41), pp. 17123–17128. DOI: 10.1073/pnas.1111245108.
- Jones, S. N.; Roe, A. E.; Donehower, L. A.; Bradley, A. (1995): Rescue of embryonic lethality in Mdm2-deficient mice by absence of p53. In *Nature* 378 (6553), pp. 206–208. DOI: 10.1038/378206a0.
- Jordan, Jennifer J.; Inga, Alberto; Conway, Kathleen; Edmiston, Sharon; Carey, Lisa A.; Wu, Lin; Resnick, Michael A. (2010): Altered-function p53 missense mutations identified in breast cancers can have subtle effects on transactivation. In *Molecular cancer research : MCR* 8 (5), pp. 701–716. DOI: 10.1158/1541-7786.MCR-09-0442.

- Junttila, Melissa R.; Karnezis, Anthony N.; Garcia, Daniel; Madriles, Francesc; Kortlever, Roderik M.; Rostker, Fanya et al. (2010): Selective activation of p53-mediated tumour suppression in high-grade tumours. In *Nature* 468 (7323), pp. 567–571. DOI: 10.1038/nature09526.
- Kahlem, Pascal; Dörken, Bernd; Schmitt, Clemens A. (2004): Cellular senescence in cancer treatment: friend or foe? In *The Journal of clinical investigation* 113 (2), pp. 169–174. DOI: 10.1172/JCI20784.
- Kaiser, Alyssa M.; Attardi, Laura D. (2018): Deconstructing networks of p53-mediated tumor suppression in vivo. In *14765403* 25 (1), pp. 93–103. DOI: 10.1038/cdd.2017.171.
- Kamijo, T.; Weber, J. D.; Zambetti, G.; Zindy, F.; Roussel, M. F.; Sherr, C. J. (1998): Functional and physical interactions of the ARF tumor suppressor with p53 and Mdm2. In *Proceedings of the National Academy of Sciences of the United States of America* 95 (14), pp. 8292–8297. DOI: 10.1073/pnas.95.14.8292.
- Kato, Shunsuke; Han, Shuang-Yin; Liu, Wen; Otsuka, Kazunori; Shibata, Hiroyuki; Kanamaru, Ryunosuke; Ishioka, Chikashi (2003): Understanding the function-structure and function-mutation relationships of p53 tumor suppressor protein by high-resolution missense mutation analysis. In *Proceedings of the National Academy of Sciences of the United States of America* 100 (14), pp. 8424–8429. DOI: 10.1073/pnas.1431692100.
- Kenzelmann Broz, Daniela; Attardi, Laura D. (2010): In vivo analysis of p53 tumor suppressor function using genetically engineered mouse models. In *Carcinogenesis* 31 (8), pp. 1311–1318. DOI: 10.1093/carcin/bgp331.
- Khurana, Arushi; Shafer, Danielle A. (2019): MDM2 antagonists as a novel treatment option for acute myeloid leukemia: perspectives on the therapeutic potential of idasanutlin (RG7388). In *OncoTargets and therapy* 12, pp. 2903–2910. DOI: 10.2147/OTT.S172315.
- Kia, Sima Kheradmand; Gorski, Marcin M.; Giannakopoulos, Stavros; Verrijzer, C. Peter (2008): SWI/SNF mediates polycomb eviction and epigenetic reprogramming of the INK4b-ARF-INK4a locus. In *Molecular and cellular biology* 28 (10), pp. 3457–3464. DOI: 10.1128/MCB.02019-07.
- Kim, Michael P.; Lozano, Guillermina (2018): Mutant p53 partners in crime. In *14765403* 25 (1), pp. 161–168. DOI: 10.1038/cdd.2017.185.
- Klimovich, Boris; Mutlu, Samet; Schneikert, Jean; Elmshäuser, Sabrina; Klimovich, Maria; Nist, Andrea et al. (2019): Loss of p53 function at late stages of tumorigenesis confers ARF-dependent vulnerability to p53 reactivation therapy. In *Proceedings of the National Academy of Sciences of the United States of America*. DOI: 10.1073/pnas.1910255116.
- Kotler, Eran; Shani, Odem; Goldfeld, Guy; Lotan-Pompan, Maya; Tarcic, Ohad; Gershoni, Anat et al. (2018): A Systematic p53 Mutation Library Links Differential Functional Impact to Cancer Mutation Pattern and Evolutionary Conservation. In *Molecular Cell* 71 (1), 178-190.e8. DOI: 10.1016/j.molcel.2018.06.012.
- Kracikova, M.; Akiri, G.; George, A.; Sachidanandam, R.; Aaronson, S. A. (2013): A threshold mechanism mediates p53 cell fate decision between growth arrest and apoptosis. In *14765403* 20 (4), pp. 576–588. DOI: 10.1038/cdd.2012.155.
- Kruse, Jan-Philipp; Gu, Wei (2009): Modes of p53 regulation. In *Cell* 137 (4), pp. 609–622. DOI: 10.1016/j.cell.2009.04.050.
- Kuhn, Elisabetta; Kurman, Robert J.; Vang, Russell; Sehdev, Ann Smith; Han, Guangming; Soslow, Robert et al. (2012): TP53 mutations in serous tubal intraepithelial carcinoma and concurrent

- pelvic high-grade serous carcinoma--evidence supporting the clonal relationship of the two lesions. In *The Journal of pathology* 226 (3), pp. 421–426. DOI: 10.1002/path.3023.
- Kussie, P. H.; Gorina, S.; Marechal, V.; Elenbaas, B.; Moreau, J.; Levine, A. J.; Pavletich, N. P. (1996): Structure of the MDM2 oncoprotein bound to the p53 tumor suppressor transactivation domain. In *Science* 274 (5289), pp. 948–953. DOI: 10.1126/science.274.5289.948.
- Lambert, Jeremy M. R.; Gorzov, Petr; Veprintsev, Dimitry B.; Söderqvist, Maja; Segerbäck, Dan; Bergman, Jan et al. (2009): PRIMA-1 reactivates mutant p53 by covalent binding to the core domain. In *Cancer Cell* 15 (5), pp. 376–388. DOI: 10.1016/j.ccr.2009.03.003.
- Lang, Gene A.; Iwakuma, Tomoo; Suh, Young-Ah; Liu, Geng; Rao, V. Ashutosh; Parant, John M. et al. (2004): Gain of function of a p53 hot spot mutation in a mouse model of Li-Fraumeni syndrome. In *Cell* 119 (6), pp. 861–872. DOI: 10.1016/j.cell.2004.11.006.
- Larsson, Connie A.; Moyer, Sydney M.; Liu, Bin; Michel, Keith A.; Pant, Vinod; Yang, Peirong et al. (2018): Synergistic and additive effect of retinoic acid in circumventing resistance to p53 restoration. In *Proceedings of the National Academy of Sciences of the United States of America* 115 (9), pp. 2198–2203. DOI: 10.1073/pnas.1719001115.
- Le Jiang; Kon, Ning; Li, Tongyuan; Wang, Shang-Jui; Su, Tao; Hibshoosh, Hanina et al. (2015): Ferroptosis as a p53-mediated activity during tumour suppression. In *Nature* 520 (7545), pp. 57–62. DOI: 10.1038/nature14344.
- Le Pen, J.; Maillet, L.; Sarosiek, K.; Vuillier, C.; Gautier, F.; Montessuit, S. et al. (2016): Constitutive p53 heightens mitochondrial apoptotic priming and favors cell death induction by BH3 mimetic inhibitors of BCL-xL. In *Cell Death & Disease* 7, e2083. DOI: 10.1038/cddis.2015.400.
- Lee, Ming Kei; Teoh, Wei Wei; Phang, Beng Hooi; Tong, Wei Min; Wang, Zhao Qi; Sabapathy, Kanaga (2012): Cell-type, dose, and mutation-type specificity dictate mutant p53 functions in vivo. In *Cancer Cell* 22 (6), pp. 751–764. DOI: 10.1016/j.ccr.2012.10.022.
- Lee, Soyoung; Schmitt, Clemens A. (2019): The dynamic nature of senescence in cancer. In *Nature Cell Biology* 21 (1), pp. 94–101. DOI: 10.1038/s41556-018-0249-2.
- Lee, Y. I.; Lee, S.; Das, G. C.; Park, U. S.; Park, S. M. (2000): Activation of the insulin-like growth factor II transcription by aflatoxin B1 induced p53 mutant 249 is caused by activation of transcription complexes; implications for a gain-of-function during the formation of hepatocellular carcinoma. In *Oncogene* 19 (33), pp. 3717–3726. DOI: 10.1038/sj.onc.1203694.
- Leroy, Bernard; Anderson, Martha; Soussi, Thierry (2014): TP53 mutations in human cancer: database reassessment and prospects for the next decade. In *Human mutation* 35 (6), pp. 672–688. DOI: 10.1002/humu.22552.
- Leu, J. I-Ju; Dumont, Patrick; Hafey, Michael; Murphy, Maureen E.; George, Donna L. (2004): Mitochondrial p53 activates Bak and causes disruption of a Bak-Mcl1 complex. In *Nature Cell Biology* 6 (5), pp. 443–450. DOI: 10.1038/ncb1123.
- Levine, Arnold J. (1997): p53, the Cellular Gatekeeper for Growth and Division. In *Cell* 88 (3), pp. 323–331. DOI: 10.1016/S0092-8674(00)81871-1.
- Levine, Arnold J. (2019): Targeting Therapies for the p53 Protein in Cancer Treatments. In *Annu. Rev. Cancer Biol.* 3 (1), pp. 21–34. DOI: 10.1146/annurev-cancerbio-030518-055455.
- Levine, Arnold J.; Hu, Wenwei; Feng, Zhaohui (2008): Tumor Suppressor Genes. In : *The Molecular Basis of Cancer*: Elsevier, pp. 31–38.

- Levine, Arnold J.; Oren, Moshe (2009): The first 30 years of p53: growing ever more complex. In *Nature reviews. Cancer* 9 (10), pp. 749–758. DOI: 10.1038/nrc2723.
- Li, D.; Marchenko, N. D.; Moll, U. M. (2011a): SAHA shows preferential cytotoxicity in mutant p53 cancer cells by destabilizing mutant p53 through inhibition of the HDAC6-Hsp90 chaperone axis. In *14765403* 18 (12), pp. 1904–1913. DOI: 10.1038/cdd.2011.71.
- Li, Dun; Marchenko, Natalia D.; Schulz, Ramona; Fischer, Victoria; Velasco-Hernandez, Talia; Talos, Flaminia; Moll, Ute M. (2011b): Functional inactivation of endogenous MDM2 and CHIP by HSP90 causes aberrant stabilization of mutant p53 in human cancer cells. In *Molecular cancer research : MCR* 9 (5), pp. 577–588. DOI: 10.1158/1541-7786.MCR-10-0534.
- Li, Tongyuan; Kon, Ning; Le Jiang; Tan, Minjia; Ludwig, Thomas; Zhao, Yingming et al. (2012): Tumor Suppression in the Absence of p53-Mediated Cell-Cycle Arrest, Apoptosis, and Senescence. In *Cell* 149 (6), pp. 1269–1283. DOI: 10.1016/j.cell.2012.04.026.
- Li, Xiangzhi; Isono, Kyo-Ichi; Yamada, Daisuke; Endo, Takaho A.; Endoh, Mitsuhiro; Shinga, Jun et al. (2011c): Mammalian polycomb-like Pcl2/Mtf2 is a novel regulatory component of PRC2 that can differentially modulate polycomb activity both at the Hox gene cluster and at Cdkn2a genes. In *Molecular and cellular biology* 31 (2), pp. 351–364. DOI: 10.1128/MCB.00259-10.
- Liguori, Ilaria; Russo, Gennaro; Curcio, Francesco; Bulli, Giulia; Aran, Luisa; Della-Morte, David et al. (2018): Oxidative stress, aging, and diseases. In *Clinical interventions in aging* 13, pp. 757–772. DOI: 10.2147/CIA.S158513.
- Liu, David S.; Duong, Cuong P.; Haupt, Sue; Montgomery, Karen G.; House, Colin M.; Azar, Walid J. et al. (2017): Inhibiting the system xC-/glutathione axis selectively targets cancers with mutant-p53 accumulation. In *Nature Communications* 8, p. 14844. DOI: 10.1038/ncomms14844.
- Liu, Geng; Parant, John M.; Lang, Gene; Chau, Patty; Chavez-Reyes, Arturo; El-Naggar, Adel K. et al. (2004): Chromosome stability, in the absence of apoptosis, is critical for suppression of tumorigenesis in Trp53 mutant mice. In *Nature genetics* 36 (1), pp. 63–68. DOI: 10.1038/ng1282.
- Liu, Xiangrui; Wilcken, Rainer; Joerger, Andreas C.; Chuckowree, Irina S.; Amin, Jahangir; Spencer, John; Fersht, Alan R. (2013): Small molecule induced reactivation of mutant p53 in cancer cells. In *Nucleic acids research* 41 (12), pp. 6034–6044. DOI: 10.1093/nar/gkt305.
- Loizou, Evangelia; Banito, Ana; Livshits, Geulah; Ho, Yu-Jui; Koche, Richard P.; Sánchez-Rivera, Francisco J. et al. (2019): A Gain-of-Function p53-Mutant Oncogene Promotes Cell Fate Plasticity and Myeloid Leukemia through the Pluripotency Factor FOXH1. In *Cancer discovery* 9 (7), pp. 962–979. DOI: 10.1158/2159-8290.CD-18-1391.
- Ludes-Meyers, J. H.; Subler, M. A.; Shivakumar, C. V.; Munoz, R. M.; Jiang, P.; Bigger, J. E. et al. (1996): Transcriptional activation of the human epidermal growth factor receptor promoter by human p53. In *Molecular and cellular biology* 16 (11), pp. 6009–6019. DOI: 10.1128/mcb.16.11.6009.
- Ludwig, R. L.; Bates, S.; Vousden, K. H. (1996): Differential activation of target cellular promoters by p53 mutants with impaired apoptotic function. In *Molecular and cellular biology* 16 (9), pp. 4952–4960. DOI: 10.1128/mcb.16.9.4952.
- Luna, R. de OcaM; Wagner, D. S.; Lozano, G. (1995): Rescue of early embryonic lethality in mdm2-deficient mice by deletion of p53. In *Nature*.
- Luo, Ji; Solimini, Nicole L.; Elledge, Stephen J. (2009): Principles of Cancer Therapy: Oncogene and Non-oncogene Addiction. In *Cell* 136 (5), pp. 823–837. DOI: 10.1016/j.cell.2009.02.024.

- Malkin, D.; Li, F. P.; Strong, L. C.; Fraumeni, J. F.; Nelson, C. E.; Kim, D. H. et al. (1990): Germ line p53 mutations in a familial syndrome of breast cancer, sarcomas, and other neoplasms. In *Science* 250 (4985), pp. 1233–1238. DOI: 10.1126/science.1978757.
- Manfredi, James J. (2019): p53 defies convention again: a p53 mutant that has lost tumor suppression but still can kill. In *The EMBO journal*, e103322. DOI: 10.15252/embj.2019103322.
- Marchenko, N. D.; Zaika, A.; Moll, U. M. (2000): Death signal-induced localization of p53 protein to mitochondria. A potential role in apoptotic signaling. In *The Journal of Biological Chemistry* 275 (21), pp. 16202–16212. DOI: 10.1074/jbc.275.21.16202.
- Marchesi, Irene; Bagella, Luigi (2016): Targeting Enhancer of Zeste Homolog 2 as a promising strategy for cancer treatment. In *World journal of clinical oncology* 7 (2), pp. 135–148. DOI: 10.5306/wjco.v7.i2.135.
- Marine, Jean Christophe; Jochemsen, Aart G. (2004): Mdmx and Mdm2: Brothers in arms? In *15384101*.
- Martins, Carla P.; Brown-Swigart, Lamorna; Evan, Gerard I. (2006): Modeling the therapeutic efficacy of p53 restoration in tumors. In *Cell* 127 (7), pp. 1323–1334. DOI: 10.1016/j.cell.2006.12.007.
- Menendez, Daniel; Inga, Alberto; Resnick, Michael A. (2006): The biological impact of the human master regulator p53 can be altered by mutations that change the spectrum and expression of its target genes. In *Molecular and cellular biology* 26 (6), pp. 2297–2308. DOI: 10.1128/MCB.26.6.2297-2308.2006.
- Meseure, Didier; Vacher, Sophie; Alsibai, Kinan Drak; Nicolas, Andre; Chemlali, Walid; Caly, Martial et al. (2016): Expression of ANRIL-Polycomb Complexes-CDKN2A/B/ARF Genes in Breast Tumors: Identification of a Two-Gene (EZH2/CBX7) Signature with Independent Prognostic Value. In *Molecular cancer research : MCR* 14 (7), pp. 623–633. DOI: 10.1158/1541-7786.MCR-15-0418.
- Mihara, Motohiro; Erster, Susan; Zaika, Alexander; Petrenko, Oleksi; Chittenden, Thomas; Pancoska, Petr; Moll, Ute M. (2003): p53 has a direct apoptogenic role at the mitochondria. In *Molecular Cell* 11 (3), pp. 577–590. DOI: 10.1016/s1097-2765(03)00050-9.
- Milanovic, Maja; Fan, Dorothy N. Y.; Belenki, Dimitri; Däbritz, J. Henry M.; Zhao, Zhen; Yu, Yong et al. (2017): Senescence-associated reprogramming promotes cancer stemness. In *Nature*. DOI: 10.1038/nature25167.
- Milner, J.; Medcalf, E. A. (1991): Cotranslation of activated mutant p53 with wild type drives the wild-type p53 protein into the mutant conformation. In *Cell* 65 (5), pp. 765–774. DOI: 10.1016/0092-8674(91)90384-b.
- Milner, J.; Medcalf, E. A.; Cook, A. C. (1991): Tumor suppressor p53: analysis of wild-type and mutant p53 complexes. In *Molecular and cellular biology* 11 (1), pp. 12–19. DOI: 10.1128/mcb.11.1.12.
- Mina, Marco; Raynaud, Franck; Tavernari, Daniele; Battistello, Elena; Sungalee, Stephanie; Saghafinia, Sadegh et al. (2017): Conditional Selection of Genomic Alterations Dictates Cancer Evolution and Oncogenic Dependencies. In *Cancer Cell* 32 (2), 155-168.e6. DOI: 10.1016/j.ccell.2017.06.010.
- Moll, U. M.; Marchenko, N.; Zhang, X-K (2006): p53 and Nur77/TR3 - transcription factors that directly target mitochondria for cell death induction. In *Oncogene* 25 (34), pp. 4725–4743. DOI: 10.1038/sj.onc.1209601.

- Montero, Joan; Letai, Antony (2018): Why do BCL-2 inhibitors work and where should we use them in the clinic? In *14765403* 25 (1), pp. 56–64. DOI: 10.1038/cdd.2017.183;
- Morton, Jennifer P.; Timpson, Paul; Karim, Saadia A.; Ridgway, Rachel A.; Athineos, Dimitris; Doyle, Brendan et al. (2010): Mutant p53 drives metastasis and overcomes growth arrest/senescence in pancreatic cancer. In *Proceedings of the National Academy of Sciences of the United States of America* 107 (1), pp. 246–251. DOI: 10.1073/pnas.0908428107.
- Muller, P. A. J.; Trinidad, A. G.; Timpson, P.; Morton, J. P.; Zanivan, S.; van den Berghe, P. V. E. et al. (2013): Mutant p53 enhances MET trafficking and signalling to drive cell scattering and invasion. In *Oncogene* 32 (10), pp. 1252–1265. DOI: 10.1038/onc.2012.148.
- Muller, Patricia a. J.; Vousden, Karen H. (2013): p53 mutations in cancer. In *Nature Cell Biology* 15 (1), pp. 2–8. DOI: 10.1038/ncb2641.
- Muller, Patricia a. J.; Vousden, Karen H. (2014): Mutant p53 in cancer: new functions and therapeutic opportunities. In *Cancer Cell* 25 (3), pp. 304–317. DOI: 10.1016/j.ccr.2014.01.021.
- Olive, Kenneth P.; Tuveson, David A.; Ruhe, Zachary C.; Yin, Bob; Willis, Nicholas A.; Bronson, Roderick T. et al. (2004): Mutant p53 gain of function in two mouse models of Li-Fraumeni syndrome. In *Cell* 119 (6), pp. 847–860. DOI: 10.1016/j.cell.2004.11.004.
- Olivier, Magali; Hollstein, Monica; Hainaut, Pierre (2010): TP53 mutations in human cancers: origins, consequences, and clinical use. In *Cold Spring Harbor perspectives in biology* 2 (1), a001008. DOI: 10.1101/cshperspect.a001008.
- Oren, Moshe; Rotter, Varda (2010): Mutant p53 gain-of-function in cancer. In *Cold Spring Harbor perspectives in biology* 2 (2), a001107. DOI: 10.1101/cshperspect.a001107.
- Palacios, G.; Moll, U. M. (2006): Mitochondrially targeted wild-type p53 suppresses growth of mutant p53 lymphomas in vivo. In *Oncogene* 25 (45), pp. 6133–6139. DOI: 10.1038/sj.onc.1209641.
- Perdrix, Anne; Najem, Ahmad; Saussez, Sven; Awada, Ahmad; Journe, Fabrice; Ghanem, Ghanem; Krayem, Mohammad (2017): PRIMA-1 and PRIMA-1Met (APR-246): From Mutant/Wild Type p53 Reactivation to Unexpected Mechanisms Underlying Their Potent Anti-Tumor Effect in Combinatorial Therapies. In *Cancers* 9 (12). DOI: 10.3390/cancers9120172.
- Petitjean, Audrey; Mathe, Ewy; Kato, Shunsuke; Ishioka, Chikashi; Tavtigian, Sean V.; Hainaut, Pierre; Olivier, Magali (2007): Impact of mutant p53 functional properties on TP53 mutation patterns and tumor phenotype: lessons from recent developments in the IARC TP53 database. In *Human mutation* 28 (6), pp. 622–629. DOI: 10.1002/humu.20495.
- Pomerantz, J.; Schreiber-Agus, N.; Liégeois, N. J.; Silverman, A.; Alland, L.; Chin, L. et al. (1998): The Ink4a tumor suppressor gene product, p19Arf, interacts with MDM2 and neutralizes MDM2's inhibition of p53. In *Cell* 92 (6), pp. 713–723. DOI: 10.1016/s0092-8674(00)81400-2.
- Prochazka, Katharina T.; Pregartner, Gudrun; Rücker, Frank G.; Heitzer, Ellen; Pabst, Gabriel; Wölfler, Albert et al. (2019): Clinical implications of subclonal TP53 mutations in acute myeloid leukemia. In *Haematologica* 104 (3), pp. 516–523. DOI: 10.3324/haematol.2018.205013.
- Purvis, Jeremy E.; Karhohs, Kyle W.; Mock, Caroline; Batchelor, Eric; Loewer, Alexander; Lahav, Galit (2012): p53 dynamics control cell fate. In *Science (New York, N.Y.)* 336 (6087), pp. 1440–1444. DOI: 10.1126/science.1218351.
- Quante, Timo; Otto, Benjamin; Brázdová, Marie; Kejnovská, Iva; Deppert, Wolfgang; Tolstonog, Genrich V. (2012): Mutant p53 is a transcriptional co-factor that binds to G-rich regulatory

- regions of active genes and generates transcriptional plasticity. In *Cell cycle (Georgetown, Tex.)* 11 (17), pp. 3290–3303. DOI: 10.4161/cc.21646.
- Ray-Coquard, Isabelle; Blay, Jean-Yves; Italiano, Antoine; Le Cesne, Axel; Penel, Nicolas; Zhi, Jianguo et al. (2012): Effect of the MDM2 antagonist RG7112 on the P53 pathway in patients with MDM2-amplified, well-differentiated or dedifferentiated liposarcoma: an exploratory proof-of-mechanism study. In *The Lancet. Oncology* 13 (11), pp. 1133–1140. DOI: 10.1016/S1470-2045(12)70474-6.
- Ray-Coquard, Isabelle; Braicu, Ioana; Berger, Regina; Mahner, Sven; Sehouli, Jalid; Pujade-Lauraine, Eric et al. (2019): Part I of GANNET53: A European Multicenter Phase I/II Trial of the Hsp90 Inhibitor Ganetespib Combined With Weekly Paclitaxel in Women With High-Grade, Platinum-Resistant Epithelial Ovarian Cancer-A Study of the GANNET53 Consortium. In *Frontiers in Oncology* 9, p. 832. DOI: 10.3389/fonc.2019.00832.
- Resnick, Michael A.; Inga, Alberto (2003): Functional mutants of the sequence-specific transcription factor p53 and implications for master genes of diversity. In *Proceedings of the National Academy of Sciences of the United States of America* 100 (17), pp. 9934–9939. DOI: 10.1073/pnas.1633803100.
- Riley, Todd; Sontag, Eduardo; Chen, Patricia; Levine, Arnold (2008): Transcriptional control of human p53-regulated genes. In *Nature reviews. Molecular cell biology* 9 (5), pp. 402–412. DOI: 10.1038/nrm2395.
- Rivlin, Noa; Brosh, Ran; Oren, Moshe; Rotter, Varda (2011): Mutations in the p53 Tumor Suppressor Gene: Important Milestones at the Various Steps of Tumorigenesis. In *Genes & cancer* 2 (4), pp. 466–474. DOI: 10.1177/1947601911408889.
- Robertson, K. D.; Jones, P. A. (1998): The human ARF cell cycle regulatory gene promoter is a CpG island which can be silenced by DNA methylation and down-regulated by wild-type p53. In *Molecular and cellular biology* 18 (11), pp. 6457–6473. DOI: 10.1128/mcb.18.11.6457.
- Rossi, Davide; Khiabani, Hossein; Spina, Valeria; Ciardullo, Carmela; Brusca, Alessio; Famà, Rosella et al. (2014): Clinical impact of small TP53 mutated subclones in chronic lymphocytic leukemia. In *Blood* 123 (14), pp. 2139–2147. DOI: 10.1182/blood-2013-11-539726.
- Sabapathy, Kanaga; Lane, David P. (2017): Therapeutic targeting of p53: all mutants are equal, but some mutants are more equal than others. In *Nature reviews Clinical oncology*. DOI: 10.1038/nrclinonc.2017.151.
- Sane, Sanam; Rezvani, Khosrow (2017): Essential Roles of E3 Ubiquitin Ligases in p53 Regulation. In *International Journal of Molecular Sciences* 18 (2). DOI: 10.3390/ijms18020442.
- Schlereth, Katharina; Beinoraviciute-Kellner, Rasa; Zeitlinger, Marie K.; Bretz, Anne C.; Sauer, Markus; Charles, Joël P. et al. (2010a): DNA binding cooperativity of p53 modulates the decision between cell-cycle arrest and apoptosis. In *Molecular Cell* 38 (3), pp. 356–368. DOI: 10.1016/j.molcel.2010.02.037.
- Schlereth, Katharina; Charles, Joël P.; Bretz, Anne C.; Stiewe, Thorsten (2010b): Life or death: p53-induced apoptosis requires DNA binding cooperativity. In *Cell cycle (Georgetown, Tex.)* 9 (20), pp. 4068–4076. DOI: 10.4161/cc.9.20.13595.
- Schlereth, Katharina; Heyl, Charlotte; Krampitz, Anna-maria; Mernberger, Marco; Finkernagel, Florian; Scharfe, Maren et al. (2013): Characterization of the p53 Cistrome – DNA Binding Cooperativity Dissects p53's Tumor Suppressor Functions. In *PLoS Genetics* 9 (8). DOI: 10.1371/journal.pgen.1003726.

- Schmitt, Clemens A.; McCurrach, Mila E.; Stanchina, Elisa de; Wallace-Brodeur, Rachel R.; Lowe, Scott W. (1999): INK4a/ARF mutations accelerate lymphomagenesis and promote chemoresistance by disabling p53. In *Genes & development* 13 (20), pp. 2670–2677.
- Schosserer, Markus; Grillari, Johannes; Breitenbach, Michael (2017): The Dual Role of Cellular Senescence in Developing Tumors and Their Response to Cancer Therapy. In *Frontiers in Oncology* 7, p. 278. DOI: 10.3389/fonc.2017.00278.
- Schulz-Heddergott, Ramona; Moll, Ute M. (2018): Gain-of-Function (GOF) Mutant p53 as Actionable Therapeutic Target. In *Cancers* 10 (6). DOI: 10.3390/cancers10060188.
- Schulz-Heddergott, Ramona; Stark, Nadine; Edmunds, Shelley J.; Li, Jinyu; Conradi, Lena-Christin; Bohnenberger, Hanibal et al. (2018): Therapeutic Ablation of Gain-of-Function Mutant p53 in Colorectal Cancer Inhibits Stat3-Mediated Tumor Growth and Invasion. In *Cancer Cell* 34 (2), 298–314.e7. DOI: 10.1016/j.ccell.2018.07.004.
- Shan, Bing; Li, Da-Wei; Brüscheweiler-Li, Lei; Brüscheweiler, Rafael (2012): Competitive binding between dynamic p53 transactivation subdomains to human MDM2 protein: implications for regulating the p53-MDM2/MDMX interaction. In *The Journal of Biological Chemistry* 287 (36), pp. 30376–30384. DOI: 10.1074/jbc.M112.369793.
- Sherr, C. J. (1998): Tumor surveillance via the ARF-p53 pathway. In *Genes & development* 12 (19), pp. 2984–2991. DOI: 10.1101/gad.12.19.2984.
- Srivastava, S.; Wang, S.; Tong, Y. A.; Hao, Z. M.; Chang, E. H. (1993): Dominant negative effect of a germ-line mutant p53: a step fostering tumorigenesis. In *Cancer Res* 53 (19), pp. 4452–4455.
- Sullivan, Kelly D.; Galbraith, Matthew D.; Andrysiak, Zdenek; Espinosa, Joaquin M. (2018): Mechanisms of transcriptional regulation by p53. In *14765403* 25 (1), pp. 133–143. DOI: 10.1038/cdd.2017.174.
- Sun, Yang; Jin, Long; Liu, Jia-Hua; Sui, Yu-Xia; Han, Li-Li; Shen, Xiao-Li (2016): Interfering EZH2 Expression Reverses the Cisplatin Resistance in Human Ovarian Cancer by Inhibiting Autophagy. In *Cancer biotherapy & radiopharmaceuticals* 31 (7), pp. 246–252. DOI: 10.1089/cbr.2016.2034.
- Talos, Flaminia; Petrenko, Oleksi; Mena, Patricio; Moll, Ute M. (2005): Mitochondrially targeted p53 has tumor suppressor activities in vivo. In *Cancer Res* 65 (21), pp. 9971–9981. DOI: 10.1158/0008-5472.CAN-05-1084.
- Teoh, Phaik Ju; Bi, Chonglei; Sintosebastian, Chirackal; Tay, Liang Seah; Fonseca, Rafael; Chng, Wee Joo (2016): PRIMA-1 targets the vulnerability of multiple myeloma of deregulated protein homeostasis through the perturbation of ER stress via p73 demethylation. In *Oncotarget* 7 (38), pp. 61806–61819. DOI: 10.18632/oncotarget.11241.
- Terzian, Tamara; Suh, Young-Ah; Iwakuma, Tomoo; Post, Sean M.; Neumann, Manja; Lang, Gene A. et al. (2008): The inherent instability of mutant p53 is alleviated by Mdm2 or p16INK4a loss. In *Genes & development* 22 (10), pp. 1337–1344. DOI: 10.1101/gad.1662908.
- Tessoulin, Benoît; Descamps, Géraldine; Moreau, Philippe; Maïga, Sophie; Lodé, Laurence; Godon, Catherine et al. (2014): PRIMA-1Met induces myeloma cell death independent of p53 by impairing the GSH/ROS balance. In *Blood* 124 (10), pp. 1626–1636. DOI: 10.1182/blood-2014-01-548800.
- Timofeev, Oleg; Klimovich, Boris; Schneikert, Jean; Wanzel, Michael; Pavlakis, Evangelos; Noll, Julia et al. (2019): Residual apoptotic activity of a tumorigenic p53 mutant improves cancer therapy responses. In *The EMBO journal*, e102096. DOI: 10.15252/embj.2019102096.

- Timofeev, Oleg; Schlereth, Katharina; Wanzel, Michael; Braun, Attila; Nieswandt, Bernhard; Pagenstecher, Axel et al. (2013): p53 DNA binding cooperativity is essential for apoptosis and tumor suppression in vivo. In *Cell reports* 3 (5), pp. 1512–1525. DOI: 10.1016/j.celrep.2013.04.008.
- Tisato, Veronica; Voltan, Rebecca; Gonelli, Arianna; Secchiero, Paola; Zauli, Giorgio (2017): MDM2/X inhibitors under clinical evaluation: perspectives for the management of hematological malignancies and pediatric cancer. In *Journal of hematology & oncology* 10 (1), p. 133. DOI: 10.1186/s13045-017-0500-5.
- Tollini, Laura A.; Jin, Aiwen; Park, Jikyoung; Zhang, Yanping (2014): Regulation of p53 by Mdm2 E3 ligase function is dispensable in embryogenesis and development, but essential in response to DNA damage. In *Cancer Cell* 26 (2), pp. 235–247. DOI: 10.1016/j.ccr.2014.06.006.
- Tomita, York; Marchenko, Natasha; Erster, Susan; Nemajerova, Alice; Dehner, Alexander; Klein, Christian et al. (2006): WT p53, but not tumor-derived mutants, bind to Bcl2 via the DNA binding domain and induce mitochondrial permeabilization. In *The Journal of Biological Chemistry* 281 (13), pp. 8600–8606. DOI: 10.1074/jbc.M507611200.
- Tonelli, C.; Morelli, M. J.; Sabò, A.; Verrecchia, A.; Rotta, L.; Capra, T. et al. (2017): Genome-wide analysis of p53-regulated transcription in Myc-driven lymphomas. In *Oncogene*. DOI: 10.1038/onc.2016.443.
- Tovar, Christian; Graves, Bradford; Packman, Kathryn; Filipovic, Zoran; Higgins, Brian; Xia, Mingxuan et al. (2013): MDM2 small-molecule antagonist RG7112 activates p53 signaling and regresses human tumors in preclinical cancer models. In *Cancer research* 73 (8), pp. 2587–2597. DOI: 10.1158/0008-5472.CAN-12-2807.
- Valente, L. J.; Grabow, S.; Vandenberg, C. J.; Strasser, A.; Janic, A. (2016): Combined loss of PUMA and p21 accelerates c-MYC-driven lymphoma development considerably less than loss of one allele of p53. In *Oncogene*. DOI: 10.1038/onc.2015.457.
- Valente, Liz J.; Gray, Daniel H. D.; Michalak, Ewa M.; Pinon-Hofbauer, Josefina; Egle, Alex; Scott, Clare L. et al. (2013): p53 Efficiently Suppresses Tumor Development in the Complete Absence of Its Cell-Cycle Inhibitory and Proapoptotic Effectors p21, Puma, and Noxa. In *Cell reports*. DOI: 10.1016/j.celrep.2013.04.012.
- Vaseva, Angelina V.; Marchenko, Natalie D.; Ji, Kyungmin; Tsirka, Stella E.; Holzmann, Sonja; Moll, Ute M. (2012): p53 opens the mitochondrial permeability transition pore to trigger necrosis. In *10974172* 149 (7), pp. 1536–1548. DOI: 10.1016/j.cell.2012.05.014.
- Vassilev, Lyubomir T.; Vu, Binh T.; Graves, Bradford; Carvajal, Daisy; Podlaski, Frank; Filipovic, Zoran et al. (2004): In vivo activation of the p53 pathway by small-molecule antagonists of MDM2. In *Science (New York, N.Y.)* 303 (5659), pp. 844–848. DOI: 10.1126/science.1092472.
- Vaughan, Catherine A.; Singh, Shilpa; Windle, Brad; Sankala, Heidi M.; Graves, Paul R.; Andrew Yeudall, W. et al. (2012): p53 mutants induce transcription of NF- κ B2 in H1299 cells through CBP and STAT binding on the NF- κ B2 promoter and gain of function activity. In *Archives of biochemistry and biophysics* 518 (1), pp. 79–88. DOI: 10.1016/j.abb.2011.12.006.
- Ventura, Andrea; Kirsch, David G.; McLaughlin, Margaret E.; Tuveson, David A.; Grimm, Jan; Lintault, Laura et al. (2007): Restoration of p53 function leads to tumour regression in vivo. In *Nature* 445 (7128), pp. 661–665. DOI: 10.1038/nature05541.
- Vogiatzi, Fotini; Brandt, Dominique T.; Schneikert, Jean; Fuchs, Jeannette; Grikscheit, Katharina; Wanzel, Michael et al. (2016): Mutant p53 promotes tumor progression and metastasis by the

- endoplasmic reticulum UDPase ENTPD5. In *Proceedings of the National Academy of Sciences of the United States of America* 113 (52), E8433–E8442. DOI: 10.1073/pnas.1612711114.
- Vries, Annemieke de; Flores, Elsa R.; Miranda, Barbara; Hsieh, Harn-Mei; van Oostrom, Conny Th M.; Sage, Julien; Jacks, Tyler (2002): Targeted point mutations of p53 lead to dominant-negative inhibition of wild-type p53 function. In *Proceedings of the National Academy of Sciences of the United States of America* 99 (5), pp. 2948–2953. DOI: 10.1073/pnas.052713099.
- Wang, Yongxing; Suh, Young-Ah; Fuller, Maren Y.; Jackson, James G.; Xiong, Shunbin; Terzian, Tamara et al. (2011): Restoring expression of wild-type p53 suppresses tumor growth but does not cause tumor regression in mice with a p53 missense mutation. In *The Journal of clinical investigation* 121 (3), pp. 893–904. DOI: 10.1172/JCI44504.
- Weinberg, Richard L.; Veprintsev, Dmitry B.; Fersht, Alan R. (2004): Cooperative binding of tetrameric p53 to DNA. In *Journal of molecular biology* 341 (5), pp. 1145–1159. DOI: 10.1016/j.jmb.2004.06.071.
- Weinberg, Robert a. (2014): *The biology of cancer*. Second edition. New York: Garland Science Taylor & Francis Group.
- Weissmueller, Susann; Manchado, Eusebio; Saborowski, Michael; Morris, John P.; Wagenblast, Elvin; Davis, Carrie A. et al. (2014): Mutant p53 drives pancreatic cancer metastasis through cell-autonomous PDGF receptor β signaling. In *10974172* 157 (2), pp. 382–394. DOI: 10.1016/j.cell.2014.01.066.
- Whitesell, L.; Sutphin, P. D.; Pulcini, E. J.; Martinez, J. D.; Cook, P. H. (1998): The physical association of multiple molecular chaperone proteins with mutant p53 is altered by geldanamycin, an hsp90-binding agent. In *Molecular and cellular biology* 18 (3), pp. 1517–1524. DOI: 10.1128/mcb.18.3.1517.
- Wu, X.; Bayle, J. H.; Olson, D.; Levine, A. J. (1993): The p53-mdm-2 autoregulatory feedback loop. In *Genes & development* 7 (7A), pp. 1126–1132. DOI: 10.1101/gad.7.7a.1126.
- Xue, Wen; Zender, Lars; Miething, Cornelius; Dickins, Ross A.; Hernando, Eva; Krizhanovsky, Valery et al. (2007): Senescence and tumour clearance is triggered by p53 restoration in murine liver carcinomas. In *Nature* 445 (7128), pp. 656–660. DOI: 10.1038/nature05529.
- Yap, Kyoko L.; Li, Side; Muñoz-Cabello, Ana M.; Raguz, Selina; Zeng, Lei; Mujtaba, Shiraz et al. (2010): Molecular interplay of the noncoding RNA ANRIL and methylated histone H3 lysine 27 by polycomb CBX7 in transcriptional silencing of INK4a. In *Molecular Cell* 38 (5), pp. 662–674. DOI: 10.1016/j.molcel.2010.03.021.
- Yoshikawa, Nobuhisa; Kajiyama, Hiroaki; Nakamura, Kae; Utsumi, Fumi; Niimi, Kaoru; Mitsui, Hiroko et al. (2016): PRIMA-1MET induces apoptosis through accumulation of intracellular reactive oxygen species irrespective of p53 status and chemo-sensitivity in epithelial ovarian cancer cells. In *Oncology reports* 35 (5), pp. 2543–2552. DOI: 10.3892/or.2016.4653.
- Zeng, Yaxue; Kotake, Yojiro; Pei, Xin Hai; Smith, Matthew D.; Xiong, Yue (2011): p53 binds to and is required for the repression of Arf tumor suppressor by HDAC and polycomb. In *Cancer research*. DOI: 10.1158/0008-5472.CAN-10-3483.
- Zhang, Y.; Xiong, Y.; Yarbrough, W. G. (1998): ARF promotes MDM2 degradation and stabilizes p53: ARF-INK4a locus deletion impairs both the Rb and p53 tumor suppression pathways. In *Cell* 92 (6), pp. 725–734. DOI: 10.1016/s0092-8674(00)81401-4.

References

Zhang, Ying; Dube, Collin; Gibert, Myron; Cruickshanks, Nichola; Wang, Baomin; Coughlan, Maeve et al. (2018): The p53 Pathway in Glioblastoma. In *Cancers* 10 (9). DOI: 10.3390/cancers10090297.

Zhou, Xiang; Hao, Qian; Lu, Hua (2019): Mutant p53 in cancer therapy-the barrier or the path. In *Journal of Molecular Cell Biology* 11 (4), pp. 293–305. DOI: 10.1093/jmcb/mjy072.

Zuber, Johannes; Radtke, Ina; Pardee, Timothy S.; Zhao, Zhen; Rappaport, Amy R.; Luo, Weijun et al. (2009): Mouse models of human AML accurately predict chemotherapy response. In *Genes & development* 23 (7), pp. 877–889. DOI: 10.1101/gad.1771409.

7. Appendix**Lists of abbreviations**

ARF	Alternative reading frame
ATR	Ataxia Telangiectasia And Rad3-Related Protein
BAX	BCL2-Associated X Protein
BBC3/PUMA	BCL2 Binding Component 3
CC3	Cleaved caspase 3
CDKN1A/CDKN2A	Cyclin-Dependent Kinase Inhibitor 1A (p21) / 2A (p14ARF/p16)
CRISPR	Clustered Regularly Interspaced Short Palindromic Repeats
DN-effect	Dominant-negative effect
GOF	Gain-of-function
Hsp70	Heat Shock Protein 70 kDa
Hsp90	Heat Shock Protein 90 kDa
LOF	Loss-of-function
Mdm2	Mouse double minute 2 homolog
MEFs	Mouse embryonic fibroblasts
MOMP	Mitochondrial outer membrane permeabilization
mRNA	messenger RNA
Mutp53	Mutant p53
NOXA/PMAIP1	Phorbol-12-Myristate-13-Acetate-Induced Protein 1
PTEN	Phosphatase And Tensin Homolog
qPCR	quantitative polymerase chain reaction
shRNA	short hairpin RNA
TUNEL	Terminal deoxynucleotidyl transferase dUTP nick end labeling

Curriculum Vitae

removed for final print

List of publications

Klimovich B, Stiewe T, Timofeev O. Inactivation of Mdm2 restores apoptosis proficiency of cooperativity mutant p53 in vivo. *Cell Cycle*. Accepted for publication 15 October 2019

Klimovich B, Mutlu S, Schneikert J, Elmshäuser S, Klimovich M, Nist A, Mernberger M, Timofeev O, Stiewe T. **Loss of p53 function at late stages of tumorigenesis confers ARF-dependent vulnerability to p53 reactivation therapy**. *Proc Natl Acad Sci USA* (PNAS). 2019, Oct 14. PMID: 31611375

Timofeev O, **Klimovich B**, Schneikert J, Wanzel M, Pavlakis E, Noll J, Mutlu S, Elmshäuser S, Nist A, Mernberger M, Lamp B, Wenig U, Brobeil A, Gattenlöhner S, Köhler K, Stiewe T. **Residual apoptotic activity of a tumorigenic p53 mutant improves cancer therapy responses**. *EMBO J*. 2019 Sep 4. PMID: 31483066.

Michurina T, Kerzhner M, **Klimovich B**. **Development and characterization of three novel monoclonal antibodies against CA-125**. *Monoclon Antib Immunodiagn Immunother*. 2014, 33(5):319-24. PMID:25357999.

Sommer F., Awazu S., Anton-Erxleben F., Jiang D., Klimovich A., **Klimovich B.**, Samoilovich M., Satou Y., Krüss M., Gelhaus C., Kürn U., Bosch T. Khalturin K. **Blood system formation in the urochordate *Ciona intestinalis* requires the variable receptor vCRL1**. *Mol Biol Evol.*, 2012, 29 (10), 3081-3092. PMID:22513285.

Griazeva I, Samoilovich M, **Klimovich B**, Pavlova M, Vartanian N, Kirienko A, Klimovich V. **[Monoclonal antibodies against human secretory component: epitope specificity and utility for immunoanalysis]**. *Zh Mikrobiol Epidemiol Immunobiol*. 2010 Jul-Aug;(4):54-59. PMID:20795387.

Samoilovich M, Gryazeva I, **Klimovich B**, Artemyeva A, Ibragimova D, Pisareva M, Klimovich V. **[Monoclonal antibodies against J chain of polymeric immunoglobulins]**. *Russ J Immunol*. 2008, 2(11): 398–404.

Klimovich V, Samoïlovich M, **Klimovich B**. *J Evolutionary Biochemistry and Physiology*. **Problem of J-chain of immunoglobulins**. 2008 Mar-Apr;44(2):151-66. PMID: 18669274.

List of academic teachers

My academic teachers at the Philipps University Marburg were Messrs Stiewe and Timofeev

My academic teachers at the St.-Petersburg State University were Mmes and Messrs Baskakov, Evtushenko, Gorbushin, Granovich, Khaitov, Kharazova, Klimovich, Kruglikov, Kuznetsov, Polevshikov, Rodionov, Samoilovich, Sergovskaya, Shyam, Simbirtsev, Sinitzina, Tishenko

Acknowledgments

First, I would like to thank my supervisors Prof. Dr. Thorsten Stiewe and PD Dr. Oleg Timofeev for giving me an opportunity to work in the group, for their careful guidance, advice, support and fruitful discussions through all these years.

I am especially grateful to my first co-author and friend Samet Mutlu for fruitful collaboration and his support during preparation of the publication, as well as for many extracurricular hours spent together.

I would like to thank my colleagues from the Stiewe lab for their excellent technical support and scientific advice during my work, and for creating warm and motivating environment:

Siggi Bischofsberger and Johanna Graß for their exceptional help in performing immunohistochemistry. Dr. Andrea Nist, Dr. Marco Mernberger, Geli Filmer and Alexandra Schneider for performing NG-sequencing and data analysis. Dr. Sabrina Elmshäuser for her extremely important and carefully executed job on preparing research proposals and supporting my animal experiments. Björn Geißert, Anjela Mühling and Antje Grzeschiczek for their critical contribution into animal experiments and for keeping the lab running. Nasti, Julia, Avanee, Pierre, Michelle, Pascal, Anna Bo, Lucas, Konstantin for making the lab a very pleasant place to work in. Laura Guth for being my best master student and for her dedicated and careful work on my projects. Jean Schneikert for helping me with CHIP experiments.

I would like to thank other members of the University for their help:

Guido Schemken, Dieter Schäfer and other employees of the Animal Facility for their excellent care on experimental animals. Dr. Andrea Arenz and other members of the irradiation core facility for helping with setting up irradiation experiments. Gavin Giel for his excellent help with FACS. Dr. Ying Wang for sharing plasmids and troubleshooting of the virus production protocol, other members of AG Burchert for occasional help. Prof. Dr. Geregana Dobрева (University of Heidelberg) and Dr. Kathrin Roth for helping with microscopy.

I am very grateful to former members of AG Stiewe: Anne, Martina, Jöel, Jeanie for supporting me during my first years in the lab.

I am especially thankful to my colleagues from the lab who became my friends and with whom I have spent most delightful hours both inside and outside of the lab: Oleg, Tini, Michael, Siggi, Samet, Berni, Anna, Niklas, thank you for all.

I am very grateful to my talented German teachers: Annette, Clara, Maria, and Larisa: you made my life much easier.

I want to thank my friends Maria, Frank, Vasili, and Anna who made these years in Marburg pleasant and interesting. I am very grateful to Sergey Kuznetsov for very valuable long-distance support and friendship during past 15 years which made my career path much easier.

Finally, I owe my deepest gratitude to my family and especially to my dear wife Maria: without your everyday support, care and inspiration nothing would have been possible.

Ehrenwörtliche Erklärung

Ich erkläre ehrenwörtlich, dass ich die dem Fachbereich Medizin Marburg zur Promotionsprüfung eingereichte Arbeit mit dem Titel „Exploring mutant p53 targeting strategies for cancer therapy“ im Institut für Molekulare Onkologie unter Leitung von PD Dr. Oleg Timofeev ohne sonstige Hilfe selbst durchgeführt und bei der Abfassung der Arbeit keine anderen als die in der Dissertation aufgeführten Hilfsmittel benutzt habe. Ich habe bisher an keinem in- oder ausländischen Medizinischen Fachbereich ein Gesuch um Zulassung zur Promotion eingereicht, noch die vorliegende oder eine andere Arbeit als Dissertation vorgelegt.

Ich versichere, dass ich sämtliche wörtlichen oder sinngemäßen Übernahmen und Zitate kenntlich gemacht habe.

Mit dem Einsatz von Software zur Erkennung von Plagiaten bin ich einverstanden.

Vorliegende Arbeit wurde in folgenden Publikationsorganen veröffentlicht:

Klimovich B, Stiewe T, Timofeev O. Inactivation of Mdm2 restores apoptosis proficiency of cooperativity mutant p53 in vivo. *Cell Cycle*. Accepted for publication 15 October 2019

Klimovich B, Mutlu S, Schneikert J, Elmshäuser S, Klimovich M, Nist A, Mernberger M, Timofeev O, Stiewe T. Loss of p53 function at late stages of tumorigenesis confers ARF-dependent vulnerability to p53 reactivation therapy. *Proc Natl Acad Sci USA (PNAS)*. 2019, Oct 14. PMID: 31611375

Timofeev O, Klimovich B, Schneikert J, Wanzel M, Pavlakis E, Noll J, Mutlu S, Elmshäuser S, Nist A, Mernberger M, Lamp B, Wenig U, Brobeil A, Gattenlöhner S, Köhler K, Stiewe T. Residual apoptotic activity of a tumorigenic p53 mutant improves cancer therapy responses. *EMBO J*. 2019 Sep 4. PMID: 31483066.

Ort, Datum, Unterschrift Doktorandin/Doktorand

Die Hinweise zur Erkennung von Plagiaten habe ich zur Kenntnis genommen.

Ort, Datum, Unterschrift Referentin/Referent

Publications



Loss of p53 function at late stages of tumorigenesis confers ARF-dependent vulnerability to p53 reactivation therapy

Boris Klimovich^{a,1}, Samet Mutlu^{a,1}, Jean Schneikert^a, Sabrina Elmshäuser^a, Maria Klimovich^a, Andrea Nist^b, Marco Mernberger^a, Oleg Timofeev^{a,2}, and Thorsten Stiewe^{a,b,2,3}

^aInstitute of Molecular Oncology, Member of the German Center for Lung Research, Philipps University Marburg, 35043 Marburg, Germany; and ^bGenomics Core Facility, Philipps University Marburg, 35043 Marburg, Germany

Edited by Carol Prives, Columbia University, New York, NY, and approved September 20, 2019 (received for review June 14, 2019)

Cancer development is driven by activated oncogenes and loss of tumor suppressors. While oncogene inhibitors have entered routine clinical practice, tumor suppressor reactivation therapy remains to be established. For the most frequently inactivated tumor suppressor p53, genetic mouse models have demonstrated regression of p53-null tumors upon p53 reactivation. While this was shown in tumor models driven by p53 loss as the initiating lesion, many human tumors initially develop in the presence of wild-type p53, acquire aberrations in the p53 pathway to bypass p53-mediated tumor suppression, and inactivate p53 itself only at later stages during metastatic progression or therapy. To explore the efficacy of p53 reactivation in this scenario, we used a reversibly switchable p53 (p53ER^{TAM}) mouse allele to generate Eμ-Myc-driven lymphomas in the presence of active p53 and, after full lymphoma establishment, switched off p53 to model late-stage p53 inactivation. Although these lymphomas had evolved in the presence of active p53, later loss and subsequent p53 reactivation surprisingly activated p53 target genes triggering massive apoptosis, tumor regression, and long-term cure of the majority of animals. Mechanistically, the reactivation response was dependent on Cdkn2a/p19Arf, which is commonly silenced in p53 wild-type lymphomas, but became reexpressed upon late-stage p53 inactivation. Likewise, human p53 wild-type tumor cells with CRISPR-engineered switchable p53ER^{TAM} alleles responded to p53 reactivation when CDKN2A/p14ARF function was restored or mimicked with Mdm2 inhibitors. Together, these experiments provide genetic proof of concept that tumors can respond, in an ARF-dependent manner, to p53 reactivation even if p53 inactivation has occurred late during tumor evolution.

p53 | tumor suppressor gene | reactivation therapy | Mdm2 | Arf

Cell fusion experiments in the 1960s showed that fusion of normal cells with tumor cells results in a nonmalignant phenotype (1). This not only provided the experimental evidence for the existence of tumor suppressor genes, but also suggested restoration of tumor suppressors as a tumor therapy. Today, stimulated by the clinical success of oncogene-targeted drugs, there is a regained interest in therapeutic targeting of defective tumor suppressors, in particular the most frequently mutated tumor suppressor p53.

The tumorigenic potential of p53 mutations correlates with the loss of p53's physiological function as a DNA binding transcription factor (loss of function, LOF) (2, 3). In addition, a subset of p53 missense mutations is known to confer neomorphic activities that promote tumor progression and therapy resistance (gain of function, GOF) (4, 5). Strategies aimed at repairing the LOF are technically challenging, but promise to be a universal therapy approach for a broad spectrum of cancer patients. The best-known compound for reactivating mutant p53 (mutp53) is PRIMA-1 which, in the form of PRIMA-1^{MET}/APR-246, is currently evaluated in clinical trials up to phase III (6). Other compounds aim at reactivating specific p53 missense mutants (7, 8) or nonsense mutants by promoting transcriptional readthrough (9). A major

concern with all small molecule approaches are off-target effects, which have been documented broadly for mutp53-reactivating compounds, questioning whether observed therapeutic responses are caused by off-target activities rather than mutp53 reactivation (5, 10, 11).

As there is currently no sufficiently specific compound available to reactivate a p53 LOF mutant to a fully functional wild type, genetically defined models for reactivation therapy have proven essential to establish proof-of-principle evidence for mutp53 as a suitable target for therapeutic reactivation. For example, mutp53 reactivation was modeled by fusing the ligand binding domain of a modified estrogen receptor to the C terminus of p53 (p53ER^{TAM}), thereby rendering p53 switchable at the protein activity level with tamoxifen (TAM) (12, 13). In the absence of tamoxifen (TAM), p53ER^{TAM} is inactive (OFF state) and accumulates similarly to cancer-derived p53 mutants (12). TAM switches p53ER^{TAM} to the ON state, resulting in p53 target gene activation (12). TAM treatment thereby models therapy of p53-mutated tumor cells with p53-reactivating small molecule compounds (12–14). Lymphomas that developed in Eμ-Myc transgenic p53ER^{TAM} mice in the absence of tamoxifen, i.e., in the p53 OFF state, rapidly regressed upon activation of p53ER^{TAM} with tamoxifen. Together with other

Significance

Mouse studies demonstrating regression of p53-null tumors following reinstatement of functional p53 have fueled the development of p53 reactivating drugs. However, successful p53 reactivation responses have only been formally demonstrated in tumor models where p53 inactivation served as the initiating event. Our study provides the first proof-of-principle evidence that p53 inactivation at late stages of tumorigenesis can also generate a vulnerability to p53 reactivation. However, this is dependent on intact ARF function highlighting ARF as a potential biomarker for p53 reactivation responses in tumors with late-stage p53 inactivation. It furthermore suggests the use of Mdm2 inhibitors as ARF mimetics for sensitizing ARF-deficient tumors to p53-reactivating drugs.

Author contributions: B.K., O.T., and T.S. designed research; B.K., S.M., J.S., S.E., M.K., and A.N. performed research; B.K., S.M., M.M., O.T., and T.S. analyzed data; B.K. and T.S. wrote the paper; S.E. planned and supervised animal experiments; A.N. performed next generation sequencing; and O.T. planned and supervised animal experiments.

The authors declare no competing interest.

This article is a PNAS Direct Submission.

This open access article is distributed under [Creative Commons Attribution-NonCommercial-NoDerivatives License 4.0 \(CC BY-NC-ND\)](https://creativecommons.org/licenses/by-nc-nd/4.0/).

¹B.K. and S.M. contributed equally to this work.

²O.T. and T.S. contributed equally to this work.

³To whom correspondence may be addressed. Email: stiewe@uni-marburg.de.

This article contains supporting information online at www.pnas.org/lookup/suppl/doi:10.1073/pnas.1910255116/-DCSupplemental.

First published October 14, 2019.

studies in independent mouse models (15–18), this firmly established the therapeutic potential of p53 reactivation and provided critical support for further research into the development of mutp53-reactivating drugs.

An important caveat to these experiments is their focus on tumors that have developed in a p53-compromised background where p53 loss served as an initiating driver of tumorigenesis (13, 15–18). p53 mutations are certainly driver mutations in Li-Fraumeni syndrome patients, who suffer from hereditary cancer susceptibility because of germline p53 mutations (19), and in certain sporadic cancer types such as high-grade serous ovarian cancer where p53 mutations are found already in the earliest premalignant cells (20). In other cancer entities, the timing of p53 mutations during tumor evolution is highly variable and often occurs only at later stages of tumor development (21, 22). For example, according to the prevailing multistep progression model for colorectal cancer, p53 mutations occur only late at the adenoma-to-carcinoma transition (23). Furthermore, recent tumor genome sequencing studies identified widespread subclonal p53 mutations in p53 wild-type tumors that expand during metastatic progression or therapy relapse, implicating them as a cause of therapy failure (21, 24–26). It is therefore of considerable clinical interest to explore whether tumors that have initially evolved in the presence of wild-type p53—but inactivated p53 at later stages of tumorigenesis—are similarly dependent on persistent p53 loss as tumors originating from a p53-compromised precursor cell.

This question is far from trivial as p53 wild-type tumors usually acquire aberrations in the p53 pathway. For example, TCGA tumors without p53 mutations are significantly enriched for copy-number deletions affecting the *CDKN2A* alternative reading frame (ARF) encoding the p14ARF protein (27). This observation on cancer patients is experimentally well recapitulated by the Eμ-Myc lymphoma model in mice: p53 wild-type lymphomas frequently lack expression of the murine *CDKN2A/p14ARF* homolog *Cdkn2a/p19Arf* and, vice versa, enforced *Cdkn2a/p19Arf* loss protects from p53 inactivation (28, 29). Importantly, several mouse models identified *Cdkn2a/p19Arf* to be essential for tumor regression upon p53 reactivation (13, 17, 18). If a p53 wild-type tumor cell with inactive p14ARF/p19Arf (in short ARF) acquires a secondary p53 mutation at a late stage of tumorigenesis, p53 reactivation would therefore be expected to be ineffective. In other words, p53 reactivation as a therapeutic strategy would only be effective if the p53 mutation has been the initiating driver lesion, but not in cases where the p53 mutation has occurred at later stages of tumor evolution on the background of other p53 pathway aberrations.

To explore whether tumors with late stage p53 inactivation respond to p53 reactivation, we genetically modeled late-stage p53 inactivation and therapeutic reactivation in mice and human tumor cells using the reversibly switchable p53ER^{TAM} (12). Our results confirm that ARF alterations prevent a p53ER^{TAM} reactivation response in tumor cells with late-stage p53ER^{TAM} inactivation as predicted. However, we also observed that Myc-driven lymphomas with active p53ER^{TAM} down-regulated ARF, but restore ARF expression upon p53ER^{TAM} inactivation and thereby become susceptible to p53ER^{TAM} reactivation. ARF expression in tumors with late stage p53 mutations could therefore serve as a potential biomarker for predicting p53 reactivation responses and Mdm2 inhibitors could be exploited as ARF mimetics to sensitize ARF-deficient p53-mutated tumor cells to p53 reactivation.

Results

Generation of Tamoxifen-Switchable p53ER^{TAM} Lymphomas. The p53ER^{TAM} knockin mouse provides a unique opportunity to reversibly switch p53 at the protein activity level with TAM (12). To engineer lymphomas with early or late p53 inactivation, hematopoietic stem cells were obtained from the liver of Eμ-Myc; *Trp53ER^{TAM/TAM}* embryos at embryonic day 13.5 (E13.5), transduced with luciferase for monitoring lymphomagenesis and

transplanted into lethally irradiated recipient mice. Transplanted mice were fed either normal or TAM-supplemented chow, giving rise to Eμ-Myc lymphomas with inactive (early OFF) or active (p53 ON) p53ER^{TAM}, respectively (Fig. 1A). Comparative gene expression profiling of Eμ-Myc; *Trp53^{+/+}* (p53^{+/+}) and Eμ-Myc; *Trp53^{-/-}* (p53^{-/-}) lymphomas identified ARF to be the most differentially expressed gene (Fig. 1B). Early-OFF lymphomas expressed equally high ARF mRNA and protein levels as p53^{-/-} lymphomas (Fig. 1C and D). In contrast, ARF was undetectable in both p53-ON and p53^{+/+} lymphomas, indicating that in the presence of TAM p53ER^{TAM} lymphomas bypass p53-mediated tumor suppression just like p53^{+/+} lymphomas via ARF inactivation (Fig. 1C and D and *SI Appendix, Fig. S1A*). Of note, p53ER^{TAM} protein was almost undetectable in p53-ON lymphomas, but strongly expressed in early-OFF lymphomas (Fig. 1D and *SI Appendix, Fig. S1A*), reminiscent of the stabilization of mutant p53 proteins in human cancer tissues (4).

Late-Stage p53 Inactivation and Reactivation Therapy. To model late-stage p53 inactivation, p53-ON Eμ-Myc lymphomas from moribund TAM-fed mice were transplanted into normally fed

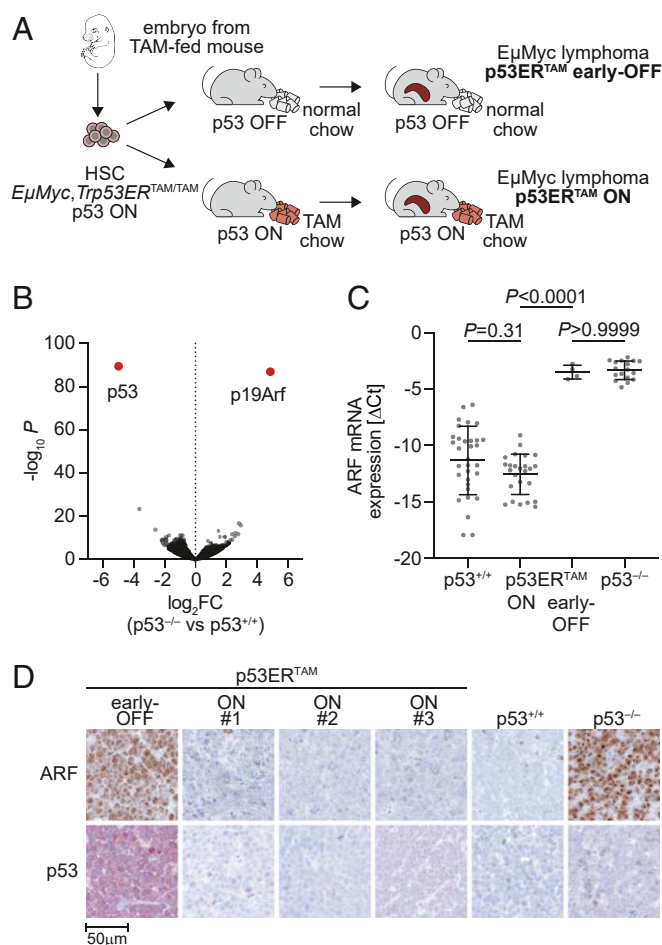


Fig. 1. Generation of Eμ-Myc;p53ER^{TAM} lymphomas with active p53. (A) Scheme illustrating the experimental outline. HSC, hematopoietic stem cells from fetal liver. (B) Volcano plot depicting fold change in gene expression ($\log_2 FC$) and significance ($-\log_{10} P$) for Eμ-Myc;p53^{+/+} and Eμ-Myc;p53^{-/-} lymphomas ($n = 4$ each). (C) ARF mRNA expression of lymphomas with indicated p53 genotype and activity status. Expression of individual lymphomas is shown normalized to β -actin as ΔCt (mean \pm SD, 1-way ANOVA with Tukey's multiple comparisons test). (D) Immunostaining of ARF and p53 (CM5) for lymphomas with indicated p53 genotype and activity status.

recipients, switching p53ER^{TAM} to the OFF state and thereby generating lymphomas with late-stage p53 inactivation (late OFF) (Fig. 2A). Survival of mice with late-OFF lymphomas was significantly shorter than for p53-ON lymphomas and similar to early-OFF lymphomas (Fig. 2B), indicating that late-stage p53 inactivation can render Eμ-Myc lymphomas more aggressive.

To explore whether late-OFF tumors respond to p53 reactivation, p53-ON Eμ-Myc lymphomas were retransplanted into cohorts of normal-fed mice and monitored by bioluminescence imaging (BLI). When the animals showed first signs of disease in BLI, they were treated for 1 wk with daily injections of TAM to switch p53ER^{TAM} to the ON state as a model for treatment with a p53 reactivating drug. Already 2 d after initiation of treatment, stagnation of lymphoma growth was detectable (Fig. 2C). Photon flux as a surrogate marker of lymphoma burden progressively decreased over the following days (Fig. 2C and D). When TAM was administered to animals that showed full-blown lymphoma, the treatment more than doubled median survival (vehicle: 4 d, TAM: 9.5 d, $P < 0.0001$, Fig. 2E) similar to what has been reported for lymphomas that had evolved in the absence of active p53 (13). We observed equivalent reactivation responses for late-OFF lymphomas generated from 3 independent primary p53-ON lymphomas (SI Appendix, Fig. S24). p53^{-/-} lymphomas failed to profit from TAM treatment (SI Appendix, Fig. S2B), confirming that the TAM effect in late-OFF lymphomas is p53 mediated and therefore on target. When mice were treated already 4 d after transplantation, TAM even cured the majority (80%) of animals (Fig. 2F). In contrast, control mice that received oil injections rapidly progressed and reached a median survival of just 18 d following transplantation (Fig. 2F). TAM-treated late-OFF lymphomas showed induction of canonical p53 target genes peaking at 3 h

(Fig. 2G) and massive and progressive apoptosis over 3 to 7 h following TAM injection (Fig. 2H). In parallel, p53ER^{TAM} protein levels decreased, consistent with the lower half-life of active p53 (Fig. 2H). We conclude, that late-OFF Eμ-Myc lymphomas, which have developed in the presence of active p53ER^{TAM} and were later switched to a p53-inactive state, regress when p53ER^{TAM} is reactivated, indicating that they have rapidly become addicted to p53 inactivation.

Late-OFF Lymphomas Reactivate p19ARF. Regression of late-OFF lymphomas upon TAM treatment was rather unexpected, considering that Eμ-Myc lymphomas, which have originated in the presence of active p53, commonly blunt p53-mediated tumor suppression by losing ARF expression (Fig. 1B) (28, 29). As ARF is induced by oncogenes such as Myc and stabilizes p53 by inhibiting Mdm2-mediated ubiquitination (30), ARF loss promotes p53 degradation and enables tumor cells to survive and expand in the presence of wild-type p53 despite high oncogenic signaling flux. Intriguingly, although p53ER^{TAM} and ARF were expressed at low levels in p53-ON lymphomas, late-OFF lymphomas showed ARF up-regulation at the protein and mRNA level along with p53ER^{TAM} accumulation (Fig. 3A and B and SI Appendix, Fig. S1B). In fact, ARF up-regulation and p53ER^{TAM} stabilization were evident in p53-ON lymphomas already 3 d after TAM withdrawal and increased further within the next days (Fig. 3C and D). Consistent with an absence of ARF gene deletions or promoter methylation (SI Appendix, Figs. S3 and S4), this indicated that the defect in the Myc-ARF-Mdm2-p53 pathway of p53-ON Eμ-Myc lymphomas is reversible, which allows tumor cells to rapidly rewire the signaling network and reengage this pathway as soon as p53ER^{TAM} is inactivated by TAM withdrawal.

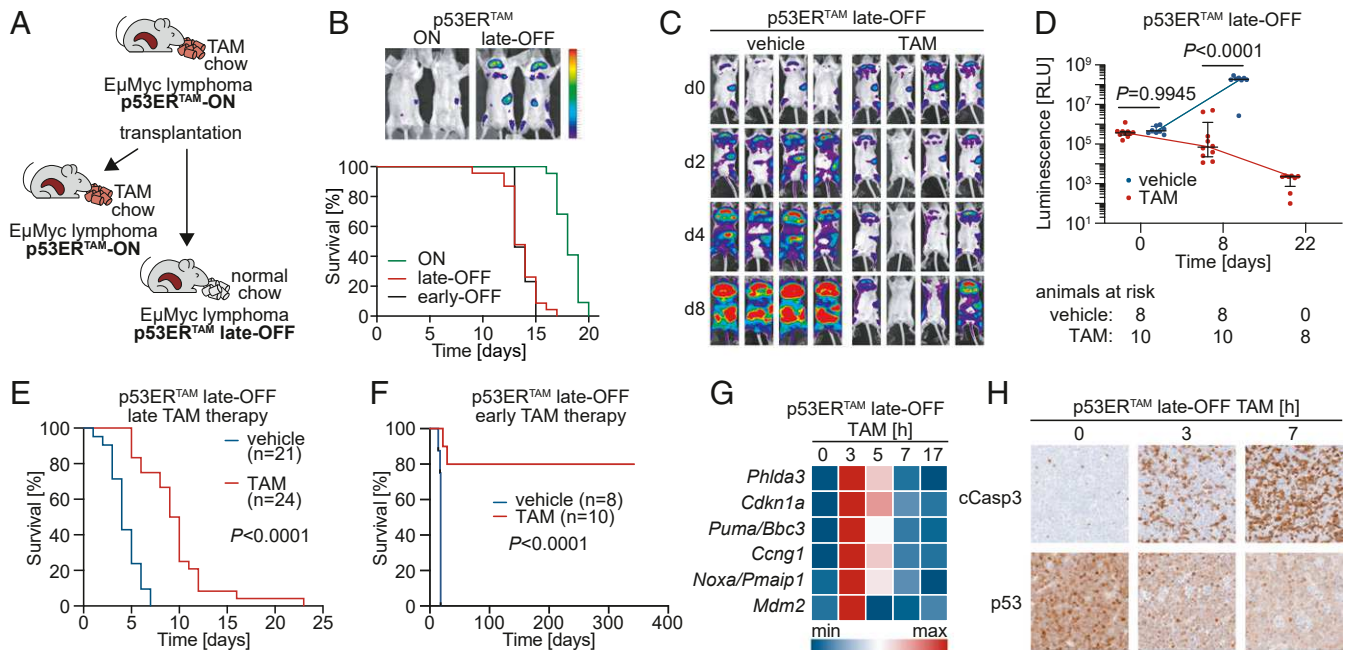


Fig. 2. Tumor regression following p53 reactivation in late-OFF Eμ-Myc lymphomas. (A) Scheme depicting generation of late-OFF lymphomas by transplantation of p53-ON lymphomas into normal chow-fed mice. (B, Top) Bioluminescence images of representative p53-ON and late-OFF lymphoma mice at day 9. (B, Bottom) Kaplan-Meier survival plots for mice with p53-ON ($n = 22$), late-OFF ($n = 23$), and early-OFF ($n = 13$) Eμ-Myc lymphomas. Median survival: ON, 18 d; early OFF, 13 d; and late OFF, 13 d. Log-rank test: ON vs. late OFF $P < 0.0001$; ON vs. early OFF $P < 0.0001$; late OFF vs. early OFF $P = 0.9043$. (C) Bioluminescence images of representative mice with late-OFF lymphomas treated with either TAM or vehicle. (D) Quantification of whole-body bioluminescence. Shown is the photon flux for individual mice and the mean \pm SD for both cohorts at indicated time points. Multiple t test corrected with the Holm-Sidak method. (E and F) Kaplan-Meier survival plots for mice with late-OFF Eμ-Myc lymphomas treated as indicated. Treatment started when mice showed full-blown lymphoma (E) or 4 d after transplantation (F). Shown is time after start of treatment. (G) p53 target gene expression in late-OFF lymphomas at indicated time points after TAM administration was quantified by RTqPCR and depicted as a heatmap of the row-wise min-max scaled mean mRNA expression ($n = 3$). (H) Immunostaining of late-OFF lymphomas for cleaved caspase-3 and p53 (CM5) at indicated time points after TAM administration.

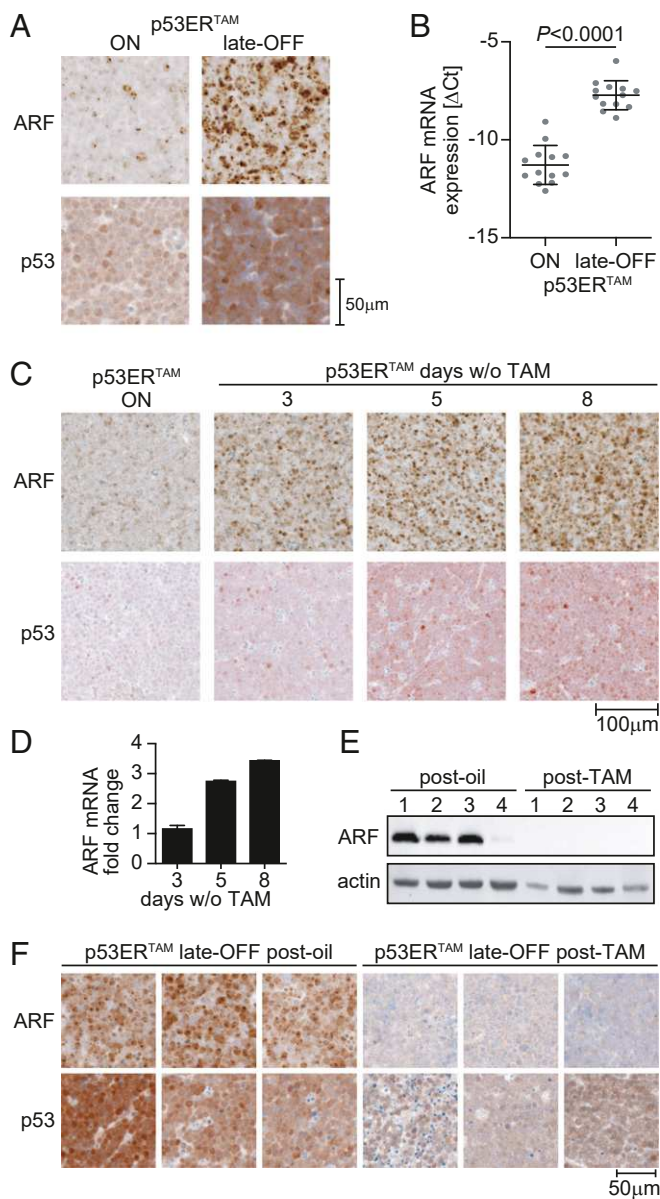


Fig. 3. Late-OFF lymphomas reactivate p19ARF. (A) Immunostaining of p53-ON and late-OFF lymphomas for ARF and p53 (CM5). Images are representative of more than 10 animals of each group. (B) ARF mRNA expression normalized to β -actin shown as Δ Ct (mean \pm SD, 2-sided unpaired *t* test). (C and D) ARF and p53 protein (CM5) (C) and ARF mRNA levels (D) were analyzed in p53-ON lymphomas before ($n = 4$) and at indicated time points after tamoxifen withdrawal ($n = 2$). (E and F) p53 late-OFF lymphomas from mice that had relapsed after therapy were analyzed for ARF and p53 (CM5) expression by (E) Western blot and (F) immunohistochemistry. Late-OFF lymphomas from vehicle-treated mice are shown for comparison. Images are representative of multiple samples from 3 mice of each treatment group.

Mechanistically, wild-type p53 is known to repress the p19ARF promoter by recruitment of Polycomb group (PcG) proteins as part of a negative regulatory feedback loop (31), that has also been described for human p14ARF (32). In line with disruption of negative feedback upon loss of p53, we observed significantly reduced PcG protein-mediated histone modifications at the ARF gene locus of late-OFF versus p53-ON E μ -Myc lymphomas as an explanation for the observed increase in ARF mRNA levels and consequent stabilization of p53ER^{TAM} (SI Appendix, Fig. S5).

p19Arf Loss Causes Resistance to p53 Reactivation. These observations suggested that the reengagement of the Myc-ARF-Mdm2-p53 pathway in late-OFF E μ -Myc lymphomas is responsible for the therapeutic effect of acute p53ER^{TAM} reactivation. In support of this, late-OFF lymphomas that had relapsed after TAM treatment displayed loss of ARF expression along with reduced p53ER^{TAM} levels (Fig. 3 E and F). To formally test the role of ARF for the reactivation response, a late-OFF lymphoma was explanted in culture where the cells responded to TAM treatment with loss of viability (Fig. 4A), induction of apoptosis (Fig. 4B–D), and transactivation of bona fide p53 target genes similar to p53^{+/+} lymphoma cells under chemotherapy (Fig. 4E). The few late-OFF lymphoma cells that survived TAM treatment in vitro could be expanded and yielded reactivation/TAM-resistant late-OFF lymphoma cell populations. Similar to late-OFF lymphomas that have relapsed in vivo (Fig. 3 E and F), TAM-resistant lymphoma cell cultures showed significantly reduced ARF expression at the mRNA and protein levels (Fig. 4 F and G). Genetic analysis revealed a deletion in the ARF gene locus comprising exons 2 and 3 that was not detectable before TAM treatment (SI Appendix, Fig. S3B). As all TAM-resistant cultures contained the same deletion, we concluded that an ARF-deleted subclone was present in the original lymphoma and selected under TAM treatment. This illustrates that a genetic, nonreversible loss of ARF results in resistance to p53ER^{TAM} reactivation. Moreover, when we “repaired” the ARF-Mdm2-p53 pathway in TAM-resistant cells using the Mdm2 inhibitor Nutlin-3a to mimic the Mdm2-inhibitory function of ARF, sensitivity to TAM was restored (Fig. 4H), formally proving that ARF loss was responsible for resistance to TAM-induced p53ER^{TAM} reactivation.

To further validate the role of ARF for the reactivation response, we experimentally reduced ARF expression in late-OFF E μ -Myc lymphoma cells by RNA interference. Tet-inducible ARF knockdown blunted the induction of p53 target genes by TAM (Fig. 4I) and conferred a survival advantage resulting in the rapid overgrowth of ARF-depleted (dsRed-positive) cells under TAM treatment (Fig. 4J). In contrast, late-OFF lymphoma cells expressing a control shRNA were completely killed by TAM. Together, this further attests to the critical role of a functional ARF-Mdm2-p53 signaling pathway for a successful therapeutic reactivation response of late-stage p53-inactivated (late OFF) E μ -Myc lymphomas.

p14ARF-Dependent p53 Reactivation Response in Human p53ER^{TAM} Tumor Cells. To explore p53 reactivation in human tumor cells with late-stage p53 inactivation, we chose colorectal cancer as a model where, according to the well-accepted multistep progression model, p53 inactivation is most frequently a late event (23). HCT116 and RKO cells are colorectal adenocarcinoma cells that have retained wild-type *TP53*. Similar to most other *TP53* wild-type cell lines, both lack p14ARF expression. In HCT116 cells, one ARF allele is mutated, the other is epigenetically silenced by promoter methylation (33); in RKO cells both alleles are methylated (34). To reversibly inactivate the endogenous *TP53* gene in these cell lines, we inserted the tamoxifen-responsive ER^{TAM} cDNA into *TP53* exon 11 using CRISPR/Cas9-induced homology-directed repair (Fig. 5A). Successful targeting was confirmed for single-cell clones by sequencing genomic DNA (Fig. 5A) and detection of the p53ER^{TAM} fusion protein instead of the wild-type p53 in Western blots (Fig. 5B). As single cells were clonally expanded in the absence of TAM, the HCT116_p53ER^{TAM} and RKO_p53ER^{TAM} cell lines had undergone at least 20 population doublings in the p53-OFF state. Nevertheless, different from late-OFF lymphomas, HCT116/RKO_p53ER^{TAM} cells showed comparably low p53 protein levels as the parental cell lines and the epigenetically silenced ARF alleles were not reexpressed (Fig. 5B). Of note, mimicking the Mdm2-inhibitory function of ARF with Nutlin-3a strongly stabilized p53ER^{TAM} in both cell lines

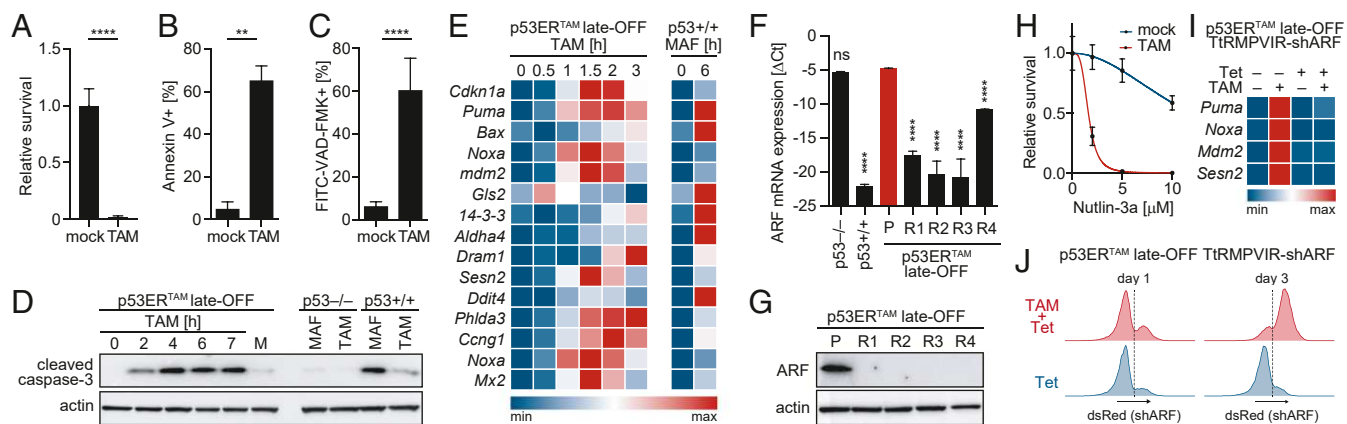


Fig. 4. p19ARF loss causes resistance to p53 reactivation in vitro. (A) Survival of late-OFF lymphoma cells treated for 24 h with 4-OHT (TAM) relative to mock ($n = 4$). (B and C) Percentage of (B) Annexin V-positive ($n = 3$) or (C) active caspase-positive cells treated for 5 h with 4-OHT (TAM). (D) Western blot for cleaved caspase-3 (Asp175) of μ -Myc lymphoma cells with indicated p53 status treated with 4-OHT (TAM) or 3 μ g/mL mafosfamide (MAF). (E) Expression of p53 target genes measured by RTqPCR in late-OFF lymphoma cells treated with 4-OHT (TAM) compared to μ -Myc;p53^{+/+} lymphoma cells treated with 3 μ g/mL MAF. Depicted is the row-wise min-max scaled mean mRNA expression ($n = 3$). (F) ARF mRNA expression normalized to β -actin shown as Δ Ct for late-OFF lymphoma cell lines: parental (P) and TAM-resistant (R1–R4). μ -Myc;p53^{-/-} and μ -Myc;p53^{+/+} lymphoma cells are shown for comparison. One-way ANOVA with Tukey’s multiple comparisons test. (G) Western blot of parental and TAM-resistant late-OFF lymphoma cells. (H) Nutlin-3a overcomes TAM resistance of late-OFF lymphoma cells. Shown is survival following 24-h treatment with Nutlin-3a \pm TAM relative to untreated. (I and J) Late-OFF lymphoma cells were transduced with a construct for Tet-inducible coexpression of ARF-shRNA and dsRed. (I) Expression of p53 target genes measured by RTqPCR following treatment with Tet and TAM as indicated. Depicted is the row-wise min-max scaled mean mRNA expression ($n = 3$). (J) Flow cytometry of dsRed expression following 1 to 3 d of treatment with Tet \pm TAM. All graphs show mean \pm SD and 2-sided, unpaired t tests unless indicated otherwise. ** $P < 0.01$, **** $P < 0.0001$; ns, not significant.

(SI Appendix, Fig. S6A), supporting that the low p53ER^{TAM} expression level is caused by lack of ARF-mediated Mdm2 inhibition. Consistent with the critical role of p53ER^{TAM} accumulation for the reactivation response of late-OFF lymphomas, TAM failed to inhibit proliferation of HCT116/RKO_p53ER^{TAM} (Fig. 5 C and D). Confirming the lack of ARF as a cause, Tet-inducible reexpression of ARF or treatment with different Mdm2 inhibitors (Fig. 5 E–H and SI Appendix, Fig. S6 B–F) sensitized HCT116/RKO_p53ER^{TAM} cells to TAM. Together these results from human colorectal cancer cells confirm the data obtained on murine

μ -Myc lymphomas and reinforce the conclusion that a therapeutic reactivation response of tumors with a late-acquired loss of p53 function will depend on ARF status.

Discussion

In light of the regained interest in therapeutic p53 reactivation, our findings provide proof of principle that tumor cells which have evolved in the presence of nonmutated active p53 can rapidly adapt and become addicted to p53 inactivation. Reinstatement of functional p53 could therefore be an effective approach even if

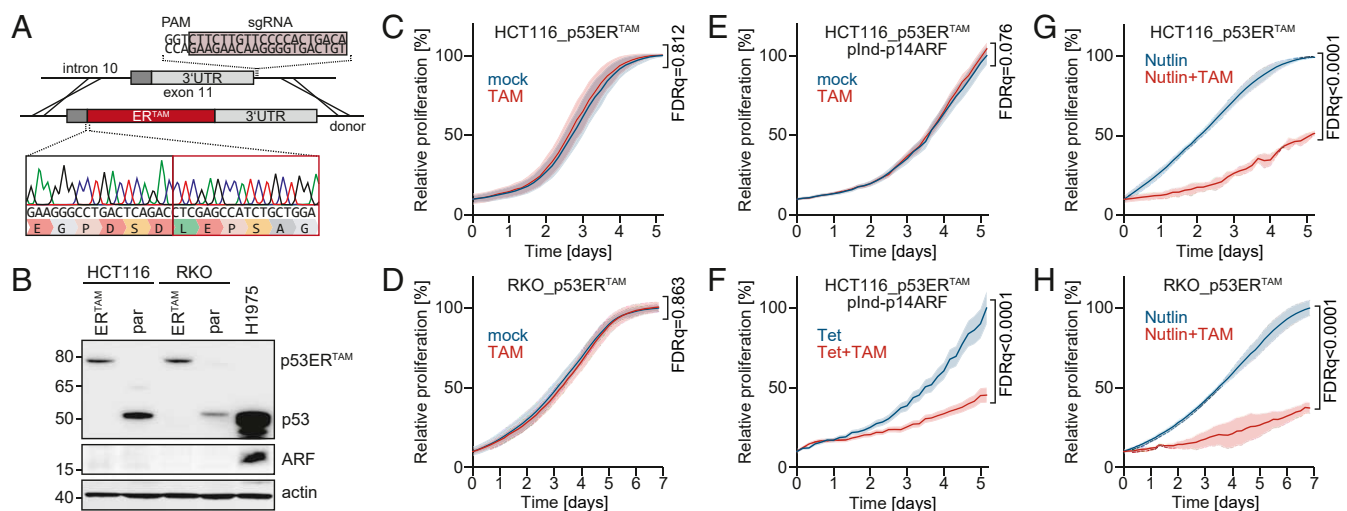


Fig. 5. p14ARF-dependent p53 reactivation response in human p53ER^{TAM} tumor cells. (A) Scheme for CRISPR/Cas9-mediated insertion of ER^{TAM} domain into the TP53 gene of human p53 wild-type tumor cells. (Bottom) Validation of correct insertion by Sanger sequencing. (B) Western blot of parental and p53ER^{TAM}-edited HCT116 and RKO cells for ARF and p53 (DO1). H1975 cells with endogenous p53^{R273H} mutation are shown for comparison. (C and D) Proliferation of p53ER^{TAM}-edited cells in response to TAM. (E and F) Proliferation of HCT116_p53ERTAM cells with Tet-inducible expression of ARF in response to TAM in the absence (E) and presence (F) of Tet. (G and H) Proliferation of p53ER^{TAM}-edited cells treated with Nutlin-3a \pm TAM. (C–H) In all graphs, day 0 is the start of TAM treatment. All proliferation curves were normalized to the confluence of non-TAM-treated reference cells at the end of the time course and shown as mean \pm SD. Statistical significance was assessed with multiple 2-sided t tests in combination with false discovery rates (FDRs). Reported are FDR q-values for relative proliferation at the end of the observation period.

inactivation of p53 is not the initiating driver lesion and has occurred late during tumorigenesis. This was not expected as it is generally believed that p53 wild-type tumors are enriched for p53 pathway alterations that bypass p53-mediated tumor suppression and would similarly blunt a p53 reactivation response. In principle, such aberrations can hit p53 downstream effectors. However, the tumor suppressor response of p53 is highly pleiotropic (35). No single or compound mouse knockout of specific p53 target genes has recapitulated the dramatic tumor predisposition that characterizes p53-null mice (36). Even p53 mutants deprived of most of their transactivation function can retain remarkably potent tumor suppressor activity (36–38). It is therefore unlikely that mutations affecting single arms of the p53 response undermine a p53 reactivation response. Alterations in upstream effectors such as ARF, on the other hand, could be more critical and it has been shown previously for tumors, which have developed in a p53-compromised background, that successful p53 reactivation is dependent on oncogene-driven up-regulation of p19Arf and that p53-null tumors with ARF deletions or insufficient oncogenic signaling are resistant to p53 restoration (17, 18). In line with this, our study also demonstrates that a successful reactivation response depends on ARF expression. Based on the results in the p53ER^{TAM} model, it can be speculated that a p53 loss-of-function mutant might not be sufficiently stabilized if ARF is deleted, mutated, or irreversibly silenced and that Mdm2 inhibitors could serve as ARF mimics to boost the effect of mutant p53 reactivating drugs in this scenario. Consistent with this concept, it was shown that Mdm2 inhibitors synergistically enhance the activity of small-molecule stabilizers of conformationally unstable p53 mutants and readthrough-promoting

drugs for p53 nonsense mutants (39, 40). For p53 reactivation to be therapeutically effective, it therefore does not seem to be critical whether p53 was inactivated at the onset of malignant transformation or at later stages, as long as strong oncogenic signals are present and transmitted via ARF to stabilize p53. ARF expression along with stabilization of mutant p53 should therefore be considered as potential biomarkers for tumors susceptible to p53 reactivation approaches.

Materials and Methods

p53ER^{TAM} late-OFF lymphoma cells, mimicking late-stage p53 inactivation, were generated from Eμ-Myc;p53ER^{TAM/TAM} [B6.Cg-Tg(lghMyc)22Bri/JThst; B6;129Sv-Trp53^{tm1Gev}/JThst] fetal liver cells. For p53 reactivation experiments, cohorts of B6-albino mice were transplanted with late-OFF lymphoma cells, treated for 7 d with daily i.p. injections of tamoxifen (100 μL of 10 mg/mL solution in corn oil) or vehicle and monitored by BLI. A detailed description of the materials and methods used in this study is provided in *SI Appendix*. All animal experiments were performed according to the German Animal Welfare Act and approved by the Regional Board of Giessen.

ACKNOWLEDGMENTS. This work was supported by research grants from the Deutsche Forschungsgemeinschaft (TI 1028/2-1 to O.T., TRR81 TPA10 to T.S.), Deutsche José Carreras Leukämie Stiftung (09 R/2018 to O.T. and T.S.), German Center for Lung Research (DZL) to T.S., Deutsche Krebshilfe (70112623 to T.S.), and von Behring-Röntgen Stiftung (65-0004, 66-LV06 to T.S.). We thank Gerard Evan for kindly providing the p53ER^{TAM} mouse strain and the members of the T.S. laboratory for helpful discussion and advice. We acknowledge Sigrid Bischofsberger, Antje Grzeschiczek, Björn Geißert, and Angela Mühlhng for technical assistance and the Irradiation Core Facility for providing access to the X-RAD 320iX platform.

- Harris, O. J., Miller, G., Klein, P., Worst, T., Tachibana, Suppression of malignancy by cell fusion. *Nature* **223**, 363–368 (1969).
- Kato et al., Understanding the function-structure and function-mutation relationships of p53 tumor suppressor protein by high-resolution missense mutation analysis. *Proc. Natl. Acad. Sci. U.S.A.* **100**, 8424–8429 (2003).
- Kotler et al., A systematic p53 mutation library links differential functional impact to cancer mutation pattern and evolutionary conservation. *Mol. Cell* **71**, 178–190.e8 (2018).
- P. A. Muller, K. H. Vousden, Mutant p53 in cancer: New functions and therapeutic opportunities. *Cancer Cell* **25**, 304–317 (2014).
- A. C. Joerger, A. R. Fersht, The p53 pathway: Origins, inactivation in cancer, and emerging therapeutic approaches. *Annu. Rev. Biochem.* **85**, 375–404 (2016).
- V. J. N. Bykov, S. E. Eriksson, J. Bianchi, K. G. Wiman, Targeting mutant p53 for efficient cancer therapy. *Nat. Rev. Cancer* **18**, 89–102 (2018).
- X. Yu, A. Vazquez, A. J. Levine, D. R. Carpizo, Allele-specific p53 mutant reactivation. *Cancer Cell* **21**, 614–625 (2012).
- A. C. Joerger et al., Exploiting transient protein states for the design of small-molecule stabilizers of mutant p53. *Structure* **23**, 2246–2255 (2015).
- C. Floquet, J. Deforges, J. P. Rousset, L. Bidou, Rescue of non-sense mutated p53 tumor suppressor gene by aminoglycosides. *Nucleic Acids Res.* **39**, 3350–3362 (2011).
- X. Peng et al., APR-246/PRIMA-1^{MET} inhibits thioredoxin reductase 1 and converts the enzyme to a dedicated NADPH oxidase. *Cell Death Dis.* **8**, e2751 (2017).
- D. S. Liu et al., Inhibiting the system x_c⁻/glutathione axis selectively targets cancers with mutant-p53 accumulation. *Nat. Commun.* **8**, 14844 (2017).
- M. A. Christophorou et al., Temporal dissection of p53 function in vitro and in vivo. *Nat. Genet.* **37**, 718–726 (2005).
- C. P. Martins, L. Brown-Swigart, G. I. Evan, Modeling the therapeutic efficacy of p53 restoration in tumors. *Cell* **127**, 1323–1334 (2006).
- N. E. Sharpless, R. A. DePinho, Cancer biology: Gone but not forgotten. *Nature* **445**, 606–607 (2007).
- W. Xue et al., Senescence and tumour clearance is triggered by p53 restoration in murine liver carcinomas. *Nature* **445**, 656–660 (2007).
- A. Ventura et al., Restoration of p53 function leads to tumour regression in vivo. *Nature* **445**, 661–665 (2007).
- M. R. Junttila et al., Selective activation of p53-mediated tumour suppression in high-grade tumours. *Nature* **468**, 567–571 (2010).
- D. M. Feldser et al., Stage-specific sensitivity to p53 restoration during lung cancer progression. *Nature* **468**, 572–575 (2010).
- D. Malkin et al., Germ line p53 mutations in a familial syndrome of breast cancer, sarcomas, and other neoplasms. *Science* **250**, 1233–1238 (1990).
- E. Kuhn et al., TP53 mutations in serous tubal intraepithelial carcinoma and concurrent pelvic high-grade serous carcinoma—Evidence supporting the clonal relationship of the two lesions. *J. Pathol.* **226**, 421–426 (2012).
- M. Gerlinger et al., Cancer: Evolution within a lifetime. *Annu. Rev. Genet.* **48**, 215–236 (2014).
- N. Rivlin, R. Brosh, M. Oren, V. Rotter, Mutations in the p53 tumor suppressor gene: Important milestones at the various steps of tumorigenesis. *Genes Cancer* **2**, 466–474 (2011).
- E. R. Fearon, B. Vogelstein, A genetic model for colorectal tumorigenesis. *Cell* **61**, 759–767 (1990).
- M. K. Hong et al., Tracking the origins and drivers of subclonal metastatic expansion in prostate cancer. *Nat. Commun.* **6**, 6605 (2015).
- N. A. Amin et al., A quantitative analysis of subclonal and clonal gene mutations before and after therapy in chronic lymphocytic leukemia. *Clin. Cancer Res.* **22**, 4525–4535 (2016).
- D. Rossi et al., Clinical impact of small TP53 mutated subclones in chronic lymphocytic leukemia. *Blood* **123**, 2139–2147 (2014).
- M. Mina et al., Conditional selection of genomic alterations dictates cancer evolution and oncogenic dependencies. *Cancer Cell* **32**, 155–168.e6 (2017).
- C. A. Schmitt, M. E. McCurrach, E. de Stanchina, R. R. Wallace-Brodeur, S. W. Lowe, INK4a/ARF mutations accelerate lymphomagenesis and promote chemoresistance by disabling p53. *Genes Dev.* **13**, 2670–2677 (1999).
- C. M. Eischen, J. D. Weber, M. F. Roussel, C. J. Sherr, J. L. Cleveland, Disruption of the ARF-Mdm2-p53 tumor suppressor pathway in Myc-induced lymphomagenesis. *Genes Dev.* **13**, 2658–2669 (1999).
- F. Zindy et al., Myc signaling via the ARF tumor suppressor regulates p53-dependent apoptosis and immortalization. *Genes Dev.* **12**, 2424–2433 (1998).
- Y. Zeng, Y. Kotake, X. H. Pei, M. D. Smith, Y. Xiong, p53 binds to and is required for the repression of Arf tumor suppressor by HDAC and polycomb. *Cancer Res.* **71**, 2781–2792 (2011).
- F. J. Stott et al., The alternative product from the human CDKN2A locus, p14(ARF), participates in a regulatory feedback loop with p53 and MDM2. *EMBO J.* **17**, 5001–5014 (1998).
- N. Burri et al., Methylation silencing and mutations of the p14ARF and p16INK4a genes in colon cancer. *Lab. Invest.* **81**, 217–229 (2001).
- M. Esteller et al., Hypermethylation-associated inactivation of p14(ARF) is independent of p16(INK4a) methylation and p53 mutational status. *Cancer Res.* **60**, 129–133 (2000).
- E. R. Kasthuber, S. W. Lowe, Putting p53 in context. *Cell* **170**, 1062–1078 (2017).
- K. T. Biegling, L. D. Attardi, Deconstructing p53 transcriptional networks in tumor suppression. *Trends Cell Biol.* **22**, 97–106 (2012).
- C. A. Brady et al., Distinct p53 transcriptional programs dictate acute DNA-damage responses and tumor suppression. *Cell* **145**, 571–583 (2011).
- T. Li et al., Tumor suppression in the absence of p53-mediated cell-cycle arrest, apoptosis, and senescence. *Cell* **149**, 1269–1283 (2012).
- M. Zhang et al., Synergistic rescue of nonsense mutant tumor suppressor p53 by combination treatment with aminoglycosides and Mdm2 inhibitors. *Front. Oncol.* **7**, 323 (2018).
- X. Liu et al., Small molecule induced reactivation of mutant p53 in cancer cells. *Nucleic Acids Res.* **41**, 6034–6044 (2013).

RESEARCH PAPER



Inactivation of Mdm2 restores apoptosis proficiency of cooperativity mutant p53 in vivo

Boris Klimovich, Thorsten Stiewe ^{*}, and Oleg Timofeev^{*}

Institute of Molecular Oncology, Member of the German Center for Lung Research (DZL), Philipps-University, Marburg, Germany

ABSTRACT

TP53 mutations are found in 50% of all cancers and mutated *TP53* status is considered poor for treatment. However, some *TP53* mutations exhibit only partial loss-of-function (LOF), meaning they retain residual transcriptional and non-transcriptional activities that are potentially beneficial for therapy. Earlier we have characterized a knock-in mouse model for the partial LOF mutant *Trp53*^{E177R} (p53RR). Reduced DNA binding cooperativity of this mutant led to the loss of p53-dependent apoptosis, while p53 functions in cell cycle control, senescence, metabolism, and antioxidant defense remained intact. Concomitantly, tumor suppression was evident but strongly compromised compared to wild-type mice. Here we used the *Trp53*^{E177R} mouse as a model to investigate whether residual functions of mutant p53 can be engaged to induce cell death, which is considered the most desirable outcome of tumor therapy. We made use of *Mdm2* knock-out in developing embryos as a sensitive tool for detecting remaining p53 activities. Genetic ablation of *Mdm2* led to embryonic lethality in *Trp53*^{E177R/E177R} homozygotes at days 9.5–11.5. This effect was not rescued by concomitant p21-knockout, indicating its independence of p21-mediated cell cycle arrest. Instead, immunohistochemical analysis showed widespread apoptosis in tissues of defective embryos accompanied by persistent accumulation of p53RR protein. This led to partial restoration of the mutant's proficiency in transcriptional induction of the pro-apoptotic genes *Bbc3* (Puma) and *Bax*. These data indicate that increased quantity can compensate for qualitative defects of p53 mutants and suggest that Mdm2-targeting (potentially in combination with other drugs) might be effective against cells bearing p53 partial LOF mutants.

ARTICLE HISTORY

Received 29 July 2019
Revised 8 October 2019
Accepted 14 October 2019

KEYWORDS

Mutant p53; Mdm2; apoptosis


Introduction

Among all tumor suppressor genes, *TP53* is the most recognized one. Also known as the “guardian of the genome” [1], it is activated upon DNA damage and other stresses and drives a plethora of cellular programs, ranging from temporary cell cycle arrest to apoptosis that either ensure repair and survival of damaged cells or promote their elimination – depending on the cell type, damage level and intensity of stress signal [2]. Loss of p53 activity makes cells vulnerable to malignant transformation, therefore a partial or complete inactivation of the p53-dependent network takes place in virtually all human cancers. Approximately 50% of tumors retain wild-type p53 but manage to blunt its functions by blocking up- or downstream pathways involved in p53-mediated responses; in another half of cancer cases p53 itself is hit by

mutations [3]. Unlike other tumor suppressor genes, p53 is only rarely affected by nonsense or frame-shift mutations – more than 70% of all genetic alterations found in *TP53* are missense mutations and most of them are located in the DNA-binding domain (DBD) [4]. The majority of such mutations result in functional inactivation of p53. Some codons are hit with an extraordinary frequency, like the positions R175, G245, R248, R249, R273, and R282 – so-called “hotspot” mutations [5]. Together they represent approximately 30% of all missense *TP53* mutations found in tumors, but the frequency for each of them does not exceed 6% [6]. For some hotspot mutations, oncogenic “gain of function” (GOF) properties have been demonstrated, as they convert p53 into an oncogene: instead of suppressing tumorigenesis, mutant protein enhances metastasis, promotes genomic instability and supports survival

CONTACT Oleg Timofeev  timofeev@staff.uni-marburg.de

^{*}These authors contributed equally to this work.

 Supplemental data of this article can be accessed here.

© 2019 Informa UK Limited, trading as Taylor & Francis Group

of cancer cells under therapy [7]. However, the bulk of p53 mutants remains poorly characterized and the frequency of GOF variants is presently unclear. Nevertheless, several high-throughput screens demonstrated that the degree of functional inactivation and residual activities are very divergent between different mutants [8,9].

Missense mutations affecting the p53 DBD are typically classified as either DNA contact mutations affecting residues involved in binding DNA or structural mutations that thermodynamically destabilize the conformation of the DBD [10]. DNA binding cooperativity mutations represent a new third class of mutations that affect interactions between DBDs of four p53 monomers, bound to DNA. These interactions are maintained by ionic bonds between H1 helices located within the DBD, which are not involved in contact with DNA but play an essential role in stabilization of the p53-DNA complexes [11,12]. Double salt bridges established between two oppositely charged amino acids (Glu180 and Arg181 in human p53) provide the structural basis for DNA binding cooperativity, which determines the ability of p53 tetramers to recognize and bind specific DNA sequences, thus shaping p53's transcriptional activity [13–15]. In contrast to structural and DNA-contact mutations, cooperativity mutations that affect the critical R180 and E181 residues have no or little effect on the DBD structure itself [13]. Cooperativity mutations are detected in spontaneous tumors and in hereditary cancer (Li-Fraumeni syndrome) and can lead to selective apoptosis defects [15]. Despite not being mutational hot-spots, cooperativity mutations are estimated to account for 34,000 cancer cases per year world-wide [3]. Recently we have described mouse models for the p53 cooperativity mutations E177R and R178E (p53RR and p53EE, corresponding to human E180 and R181 codons) [16,17]. The R178E mutation abolishes cooperative interactions between p53 monomers and therefore renders p53 entirely deficient in DNA binding, recapitulating mutations that lead to a severe loss of function. In contrast, E177R substitution leads to a reduced interaction between H1 helices and results in a complete deficiency in p53-dependent activation of pro-apoptotic genes, whereas regulation of genes involved in the control of the cell cycle, oxidative defense and metabolism remains intact or only slightly affected [18]. Importantly, tumor-suppressive functions of p53RR

were dramatically impaired, making mice a suitable model for studying tumorigenic p53 mutations with partial loss of function.

Mdm2 and Mdm4 (MdmX) are major negative regulators of p53. These homologous proteins share C-terminal RING-finger domains that are necessary for the formation of Mdm2-Mdm4 heterodimers, but only Mdm2 possesses E3 ubiquitin ligase activity and can mono- and poly-ubiquitinate p53 protein thus controlling its intracellular localization and stability, respectively [19]. In addition, Mdm2 and Mdm4 can inhibit transcriptional activity of p53 via binding to its N-terminal transactivation domain [20]. In turn, Mdm2 transcription is regulated by p53, which represents a negative feedback loop mechanism that restrains p53 activity in normal cells [19]. Oncogenic stress mobilizes the ARF tumor suppressor protein which sequesters Mdm2 and thus leads to stabilization and activation of p53 [21]. When tumor cells retain wild-type p53, its level is usually kept low due to loss of ARF or overexpression of Mdm2, which provides a therapeutic window for using Mdm2 inhibitors in cancer treatment, aiming at the restoration of tumor-suppressive p53 functions in tumor cells. In the last two decades, multiple Mdm2 inhibitors were developed and tested in pre-clinical studies and early clinical trials [22]. Mutant p53 protein levels are typically high in tumor cells which indicates uncoupling from the ARF-Mdm2 regulatory circuit and suggests at least partial loss of p53's tumor-suppressive functions. Therefore, the use of Mdm2 inhibitors is considered unbeneficial for treatment of tumors with mutant p53. Instead, alternative methods such as restoration of native conformation, disaggregation or destabilization are being tested [23]. Although specific accumulation of p53 in cancer cells makes the mutant protein a tempting target for therapy, insufficient knowledge of vulnerabilities created by different mutants hampers the development of such approaches.

Genetic ablation of *Mdm2* in mice causes early embryonic lethality (3.5–5.5 dpc) due to massive apoptosis, whereas simultaneous disruption of the *Trp53* gene completely rescues the lethal phenotype [24–26]. Moreover, inactivation of the pro-apoptotic p53 target *Bax* prolongs the development of *Mdm2*-null embryos up to day 6.5 [24], but knock-out of the cell cycle regulator *Cdkn1a* (p21) had no rescue effect [27]. These data underscore p53-dependent

apoptosis as the primary lethal activity that must be inhibited by Mdm2 during embryogenesis. Importantly, typical p53 hotspot mutations R172H and R246S (corresponding to human R175H and R249S, respectively) and rare partial loss of function R172P (human R175P) mutant rescued embryonic lethality of Mdm2 knock-out mice [28,29]. In contrast, the hypomorphic p53^{neo} allele that retained only about 16% of wild-type *Trp53* gene expression did not [30], indicating that the *Mdm2* knock-out model can be used for identification of even subtle residual lethal activities of mutant p53. Here we used the *Trp53*^{E177R} (p53RR) mouse to test if Mdm2-targeting approaches can drive a therapy-relevant response in cells with partial LOF mutants that are defective for p53-dependent apoptosis.

Materials and methods

Animals

The *Trp53*^{LSL-RR} (p53LSL-RR) and *Trp53*^{RR} (p53RR) mice with conditional expression of *Trp53*^{E177R} mutant allele were described elsewhere [16]. For embryonic lethality studies, we used *Mdm2*^{Δ7-9} (129-Mdm2<tm1.2Mep>) mice that lack exons 7–9 [31]. These mice were obtained from the NCI Mouse Repository (Frederick, USA) and mated with *Trp53*^{LSL-RR/LSL-RR} (not expressing p53 and used as the p53 knock-out control, further indicated as *Trp53*^{-/-}) or *Trp53*^{RR/RR} homozygote animals to generate double heterozygous *Mdm2*^{Δ7-9};*Trp53*^{+ / RR} and *Mdm2*^{Δ7-9};*Trp53*^{+ / -} mice for intercrossing. The p21/*Cdkn1a* knock-out mice (129S2-Cdkn1a<tm1Tyj>) were obtained from the Jackson Laboratory. All mouse experiments were approved by the local authorities and performed in accordance with the German Animal Welfare Act (Deutsches Tierschutzgesetz).

Cell culture and apoptosis assay

Mouse embryonic fibroblasts were isolated at 13.5 dpc using standard protocols and kept at low oxygen conditions (5% O₂). MEF were immortalized using the E1A.12S adenoviral oncogene, infections and transfections were performed as described earlier [16]. Cells were cultured in DMEM (Gibco, Life Technologies) with 10% fetal calf serum (Sigma-Aldrich), supplemented with 100 U/ml

penicillin and 100 μg/ml streptomycin (both from Gibco, Life Technologies). E1A MEFs were treated with 400 ng/ml doxorubicin for 16 h and collected for RNA isolation.

Isolation of embryos and whole-mount immunostaining

Whole-mount PECAM-staining was performed as described [32] with modifications. All solutions were filtered through 0.45 μm filters. Embryos were isolated, deposited in 12 well plates, fixed for 1.5 h in cold 4% buffered formalin, washed 3 × 10 minutes in 0.1% Tween-20 in PBS (PBST). All steps were performed upon gentle agitation. Catalase was inactivated by incubation in 50 mM NaN₃ in PBST (20 min, RT). Endogenous peroxidase was blocked with 3% H₂O₂ + 50 mM NaN₃ in PBST (20 min, RT). After washing with PBST (3X10 min, RT) embryos were blocked in PBST supplemented with 10% normal goat serum (NGS) and 0.5% bovine serum albumin (BSA) for 1.5 h (RT). Embryos were incubated in anti-PECAM antibodies (MEC 13.3, BD Pharmingen, 553370, 1:300 in PBST, 1% NGS, 0.5% BSA) for 24–48 h (+4°C). Embryos were washed (PBST, 0.5% BSA, 6 × 1 h, RT) and incubated with secondary antibodies (donkey anti-rat HRP-conjugate (Rockland, 612-703-120) 1:500 in PBST, 1% NGS, 0.5% BSA overnight (+4°C). After washing with PBST, 0.5% BSA (6x30 min, RT) embryos were incubated in TBTI buffer (10 mM imidazole, 0.2% BSA in PBST) for 1 h at RT. All further steps were performed in the dark. Solution was replaced with DyLight-488-tyramide amplification solution (1:100 in TBTI + 0.0015% H₂O₂) for 2 h at RT. Embryos were washed with PBST overnight (+4°C). Embryos were cleared as described [33]. Briefly, embryos were incubated in 25% formamide + 10% PEG 8000 solution (1 h), and then in 50% formamide + 20% PEG 8000 (two times). Embryos were imaged with a Zeiss stereo microscope. Synthesis of tyramide conjugate was performed as follows: stock solution A (10 mg/ml DyLight-488-NHS ester (Thermo Fisher Scientific, 46402 in dimethylformamide (DMF) and solution B (10 mg/ml tyramine-HCl (Sigma Aldrich, T2879 in DMF supplemented with 7.2 M trimethylamine (Sigma Aldrich, T0886) were prepared. Then 100 μl of solution A was mixed

with 15.6 μ l of solution B and incubated for 2 h in the dark at RT. Afterward, 884 μ l of 100% ethanol was added to obtain a working tyramide amplification solution.

Immunohistochemistry

Embryos were fixed overnight in 4% buffered formalin, washed with PBS and stored until further processing in 70% ethanol. For embedding, embryos were sequentially treated as follows: 80% EtOH 5 min, 95% EtOH 2 \times 5 min, 100% EtOH 1 \times 5 min, 100% EtOH/Roticlear (Roth) 1:1 5 min, Roticlear – 5 min. Then embryos were incubated sequentially in 3 vessels with paraffin for 5 min (65°C) and embedded immediately after. 5 μ m thick sections were mounted to SuperFrost glass slides (Thermo Fischer Scientific) and processed as described earlier [16]. The following antibodies and dilutions were used: anti-p53 (NCL-p53-505, Leica Microsystems, 1:1000), anti-cleaved caspase-3 (#9661, Cell Signaling, 1:100), anti-PCNA (sc-56, clone PC10, Santa Cruz Biotech, 1:100), anti-mouse CD31/PECAM-1 (#553370, clone MEK 13.3, BD Pharmingen). Apoptosis was detected with the DeadEnd™ colorimetric TUNEL System (Promega).

IHC quantification

Staining intensity was quantified using Aperio ImageScope software and a positive pixel count algorithm v9. For each embryo at least 10 regions, covering in total > 50% of the whole section area were randomly selected from several sections at 10x magnification. 3 embryos of each genotype were quantified for every staining. The positivity index was calculated as the ratio of positive pixels over the total number of pixels in regions used for quantification. Statistical significance was assessed using ANOVA with Holm-Sidak multiple comparison test.

Cellular fractionation and western blotting

Nuclear and cytosolic fractions were prepared as follows: cells were collected and resuspended in 2–3 volumes of Buffer A (10 mM HEPES pH 7.9, 10 mM KCl, 0.1 mM EDTA, 0.1 mM EGTA, 1 mM

β -mercaptoethanol) supplemented with protease inhibitors, and incubated for 10 minutes on ice. Then 10% NP-40 was added to a final concentration of 0.25%. Cells were passed through a 27G needle 5–10 times, nuclei were pelleted by centrifugation (500xg, 10 min). The cytoplasmic fraction was collected and re-centrifuged for 10–15 minutes. Nuclear fractions were washed 3 times in 5–10 volumes of Buffer A and pelleted by centrifugation. Nuclei were lysed with 1–2 volumes of Buffer C (20 mM HEPES pH 7.9, 400 mM NaCl, 1 mM EDTA, 1 mM EGTA, 1 mM β -mercaptoethanol) and soluble fraction was collected by centrifugation (10000xg, 10 min). Mitochondrial fractions were isolated using Mitochondria Isolation Kit for Cultured Cells (Thermo Scientific) as described by the manufacturer. For Western Blotting 50 μ g of total protein were resolved on 4–12% NuPAGE polyacrylamide gels (Invitrogen). After wet transfer to Hybond-P nitrocellulose membrane (GE Healthcare) antigens were detected using the following antibodies: anti-p53 (NCL-p53-505, Leica Microsystems, 1:2000), anti-PCNA (PC10, #sc-56, 1:1000), anti-Bak (At8B4, Abcam, 1:250), anti-Tom20 (FL-145, #sc-11415, 1:100). Specific immunocomplexes were detected with secondary anti-mouse or anti-rabbit IgG-HRP (GE Healthcare, 1:5,000) and SuperSignal ECL kit (Thermo Fisher).

PCR and RTqPCR

Genotypes of mice, isolated embryos and embryonic tissues were identified by PCR using following primers: 5'TCTTTGTGAAGGAACCTTACT3'; 5'CATTCATCAGTTCATAGGTT3'; 5'CCCTGAGAAGAGCAAGGC3', 5'AACCAGATCAGGAGGGTCA C3' for genotyping of p53RR; 5'CGCCACCA GAAGAGAAACCT3'; 5'TGTCCCTATGTACCTG TCTCACT3'; 5'GTATTGGGCATGTGTTAGACT GG3'; 5'CCTGGATTTAATCTGCAGCACTC3' for genotyping of Mdm2; 5'ATCAGCAGCCTCTGTT CCAC3'; 5'GTCTAGCTCCGGCATTCTCG3'; 5'ACTCCATGTCTCCAGCCTCT3' for genotyping of p21. For PCR genotyping, tail tips or tissues were lysed overnight at 55°C in PBNB buffer (10 mM Tris-HCl pH 8.3, 50 mM KCl, 2.5 mM MgCl₂, 0.45% NP-40, 0.45% Tween-20) supplemented with 8 U/ml proteinase K (AppliChem). Proteinase was heat-inactivated at 95°C for 10 min. For reverse

transcription quantitative PCR (RTqPCR), RNA was isolated from cells or whole embryos using the RNeasy Mini kit (Qiagen) according to the manufacturer's protocols. Isolated embryos were controlled microscopically to ensure the absence of resorption and intactness of tissues. cDNA was synthesized from 0.5–1 μg of total RNA with the SuperScript VILO cDNA Synthesis Kit (Invitrogen). Gene expression was assessed on a LightCycler-480 (Roche) using the ABsolute QPCR SYBR Green Mix (Thermo Scientific). Data were analyzed with the $\Delta\Delta\text{Ct}$ method using β -actin as a reference gene for normalization. Sequences of primers used for RTqPCR were described earlier [16].

Flow cytometry

Flow cytometry analysis was performed on the Accuri C6 flow cytometer (BD Biosciences). For analysis of apoptosis Annexin V-APC (MabTag) kit was used according to the manufacturer's protocol. Cell viability was determined by staining of freshly collected cells with 0.2 $\mu\text{g}/\text{ml}$ propidium iodide (PI) in PBS in non-permeable conditions.

Results

P53RR does not rescue embryonic lethality caused by deletion of Mdm2

We used heterozygous mice with a deletion of exons 7–9 of the *Mdm2* locus (*Mdm2* ^{$\Delta 7-9$}) [31] which were bred with homozygous *Trp53*^{E177R/E177R} (RR) mice to generate double heterozygous *Mdm2* ^{$\Delta 7-9$} ; *Trp53*^{+/RR} animals. The double heterozygous progenies were viable and we used them for further breeding. When we genotyped newborn mice obtained from intercrossing of double heterozygous *Mdm2* ^{$\Delta 7-9$} ; *Trp53*^{+/RR} animals, we observed a clear deviation from the expected Mendelian distribution: notably, no double homozygous *Mdm2* ^{$\Delta 7-9/\Delta 7-9$} ; *Trp53*^{RR/RR} mice were born alive (Figure 1(a)). Similar results were obtained upon breeding of *Mdm2* ^{$\Delta 7-9$} ; *Trp53*^{RR/RR} animals to each other (Figure 1(c)), indicating that the double homozygous *Mdm2* ^{$\Delta 7-9/\Delta 7-9$} ; *Trp53*^{RR/RR} embryos die *in utero*. In

contrast, upon crossing of double heterozygous *Mdm2* ^{$\Delta 7-9$} ; *Trp53*^{+/-} mice used as the control, double homozygous offspring was obtained with a frequency only insignificantly deviating from the expected one (Figure 1(b)). This data clearly indicated that the cooperativity mutant p53RR, similar to wild-type p53 and different from other partially inactive or cancer-associated mutants such as R172P, R172H, and R246S, exhibits lethal activity in the absence of Mdm2.

Double homozygous mdm2 ^{$\Delta 7-9/\Delta 7-9$} ; Trp53^{RR/RR} embryos show severe developmental defects

We have previously demonstrated that p53RR is deficient for induction of apoptosis and transcriptional activation of apoptosis-related genes such as Puma, Noxa, and Bax [16] in response to DNA damage. We, therefore, expected survival of double homozygous *Mdm2* ^{$\Delta 7-9/\Delta 7-9$} ; *Trp53*^{RR/RR} embryos beyond the terms observed in p53 wild-type background (3.5–5.5 dpc). We started collecting embryos from 6.5 dpc and did not observe any abnormalities until day 7.5–8.5 (Figure 2(a) and not shown). Strikingly, at 9–9.5 dpc the majority of double homozygous embryos displayed severe developmental defects and after day 11 no normal embryos with this genotype were recovered (Figure 2(b,c), Suppl. Figure 1(a)). Also, no living double homozygous embryos were found at later developmental stages. At day 9 dpc (TS 14) pronounced defects in neural tube closure and formation of brain vesicles of *Mdm2* ^{$\Delta 7-9/\Delta 7-9$} ; *Trp53*^{RR/RR} embryos were evident (Suppl. Figure 1(a)), which became further aggravated at day 9.5–10.5 and were accompanied with growth retardation (Figure 2(c)). Hemizygous *Mdm2* ^{$\Delta 7-9/\Delta 7-9$} ; *Trp53*^{RR/-} embryos displayed the same morphological abnormalities (Suppl. Figure 1(b)). Notably, the double homozygous embryos that were found alive (heart beating) at day 10.5–11.5 looked pale and bloodless (Figure 2(c,d)). The yolk sac of those embryos had a clearly reduced number of large blood vessels and abnormal structure of the capillary network (Figure 2(e)). Similar defects were detected in whole-mount *Mdm2* ^{$\Delta 7-9/\Delta 7-9$} ; *Trp53*^{RR/RR} embryos stained with antibodies to the endothelial marker Pecam-1 (Figure 2(f)).

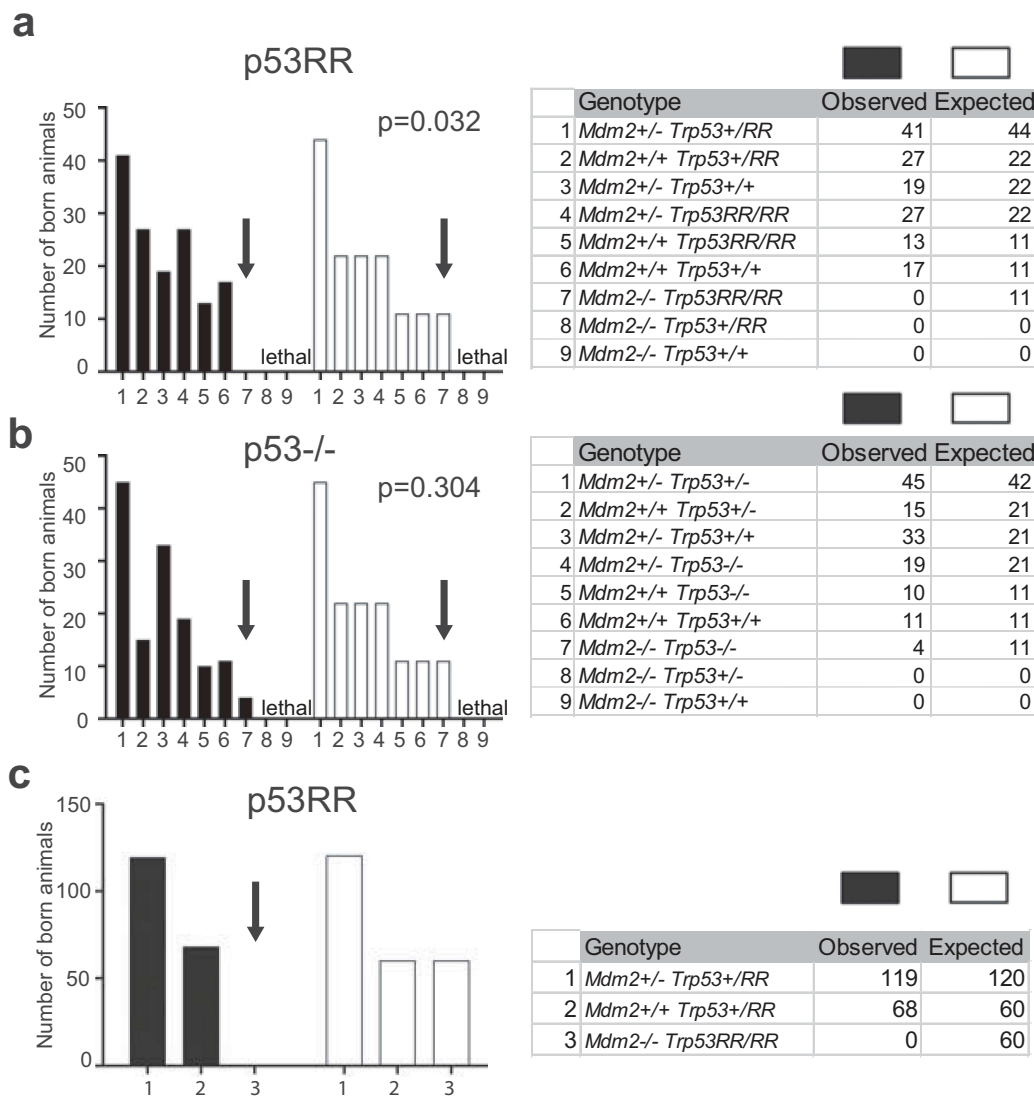


Figure 1. p53RR does not rescue embryonic lethality caused by deletion of *Mdm2*. (a) Observed and expected genotype distribution of newborn offspring from matings of *Mdm2*^{+/ Δ 7-9}; *Trp53*^{+/ Δ 7-9} mice (total number of pups $n = 144$; contingency test $P = 0.032$). (b) Observed and expected genotype distribution of newborn offspring from matings *Mdm2*^{+/ Δ 7-9}; *Trp53*^{+/-} mice (total number of pups $n = 137$; contingency test $P = 0.3044$). (c) Observed and expected genotype distribution of newborn offspring from matings *Mdm2*^{+/ Δ 7-9}; *Trp53*^{RR/RR} mice (total number of pups $n = 187$; contingency test $P < 0.0001$).

***Mdm2* ^{Δ 7-9/ Δ 7-9}; *Trp53*^{RR/RR} embryos die with signs of apoptosis**

To investigate the pathological phenotype of double heterozygous embryos in more detail, we used intact embryos with no signs of resorption for immunohistochemical staining. First, we analyzed p53 protein levels. As expected, in all analyzed samples collected at 9–10.5 dpc (TS 14–17) we observed a strong accumulation of p53RR protein, particularly in the neuroepithelium, limb buds, and somites, whereas in the cardiac tissues the p53 level was markedly lower (Figure 3(a,b) and Suppl. Figure 2(b)). The p53RR

protein retains the ability to induce expression of the *Cdkn1a* gene and therefore is proficient in mounting cell cycle arrest [16]. The abnormal phenotype of *Mdm2* ^{Δ 7-9/ Δ 7-9}; *Trp53*^{RR/RR} embryos was reminiscent of that published for *Mdm4* deficient mice which die at 7.5–10.5 dpc because of cessation of proliferation by p21-mediated cell cycle arrest [34]. We hypothesized that accumulation of p53RR may lead to high expression of p21 and loss of proliferative potential resulting in developmental aberrations and death of *Mdm2* ^{Δ 7-9/ Δ 7-9}; *Trp53*^{RR/RR} embryos. However, quantitative analysis of PCNA staining that is

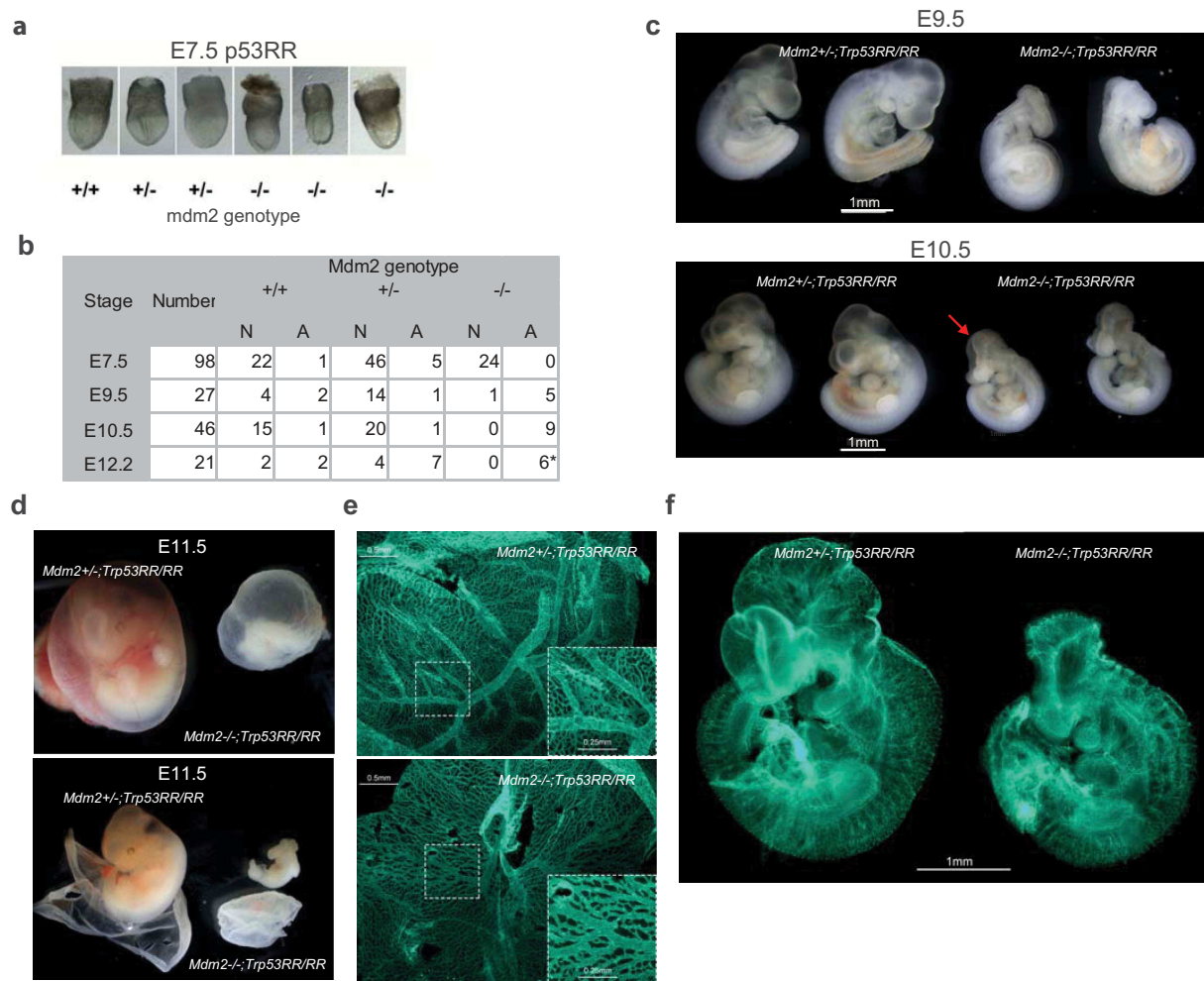


Figure 2. $Mdm2^{\Delta 7-9/\Delta 7-9}; Trp53^{RR/RR}$ embryos show severe developmental defects. (a) Representative images of E7.5 embryos demonstrating absence of developmental abnormalities in $Mdm2^{\Delta 7-9/\Delta 7-9}; Trp53^{RR/RR}$ embryos at this stage. (b) Phenotype analysis of $Trp53^{RR/RR}$ embryos with different $Mdm2$ genotypes reveals developmental defects in $Mdm2^{\Delta 7-9/\Delta 7-9}; Trp53^{RR/RR}$ embryos starting from E9.5. N – normal, A – abnormal morphology. Asterisk – embryos were partially resorbed. (c) Representative images of $Trp53^{RR/RR}$ embryos with hetero- and homozygous $Mdm2$ deletion at stages E9.5 (TS15, upper panel) and E10.5–11 (TS18, bottom panel) show progressive growth retardation, abnormal head morphology and neural tube closure defects (arrow) in $Mdm2^{\Delta 7-9/\Delta 7-9}; Trp53^{RR/RR}$ embryos. (d) Representative image of $Mdm2^{+/\Delta 7-9}$ and $Mdm2^{\Delta 7-9/\Delta 7-9}; Trp53^{RR/RR}$ embryos at stage E11.5, (TS19) with the intact (upper panel) and opened (bottom panel) embryonic envelope demonstrates a “bloodless” phenotype of the $Mdm2^{\Delta 7-9/\Delta 7-9}; Trp53^{RR/RR}$ embryos. (e) Representative picture of PECAM-1 (endothelial marker) staining in whole mount yolk sac samples shows a reduced number of large blood vessels and decreased branching of the capillary network (zoom-in) in homozygous $Mdm2^{\Delta 7-9/\Delta 7-9}; Trp53^{RR/RR}$ embryos (bottom panel). (f) Representative picture of Pecam-1 staining in whole mount embryos shows a reduced branching in blood vessel network and abnormal head morphology of homozygous $Mdm2^{\Delta 7-9/\Delta 7-9}; Trp53^{RR/RR}$ embryos.

commonly used as a marker for proliferating cells revealed no difference between normal $Mdm2^{+/\Delta 7-9}; Trp53^{RR/RR}$ and abnormal $Mdm2^{\Delta 7-9/\Delta 7-9}; Trp53^{RR/RR}$ embryos (Figure 3(c,d)). Abnormalities in development of embryonic vasculature can result in insufficient blood supply and acute ischemia, which in turn can lead to necrotic cell death. However, we have not seen typical microscopic signs of necrosis such as swelling of cells and membrane rupture in tissues of double homozygous embryos.

Instead we observed widespread apoptosis, especially in the neuroepithelial tissues, as suggested by chromatin condensation, nuclear DNA fragmentation (TUNEL) and caspase-3 cleavage (CC3), which started approximately at 9 dpc and progressively increased at later stages (Figure 3(e,g) and Suppl. Figure 2(c,f)). Importantly, tissues with weak staining for p53 protein also demonstrated low levels of apoptosis (Figure 3(a,e,g)), indicating that high levels of p53 protein may be responsible for apoptosis. This

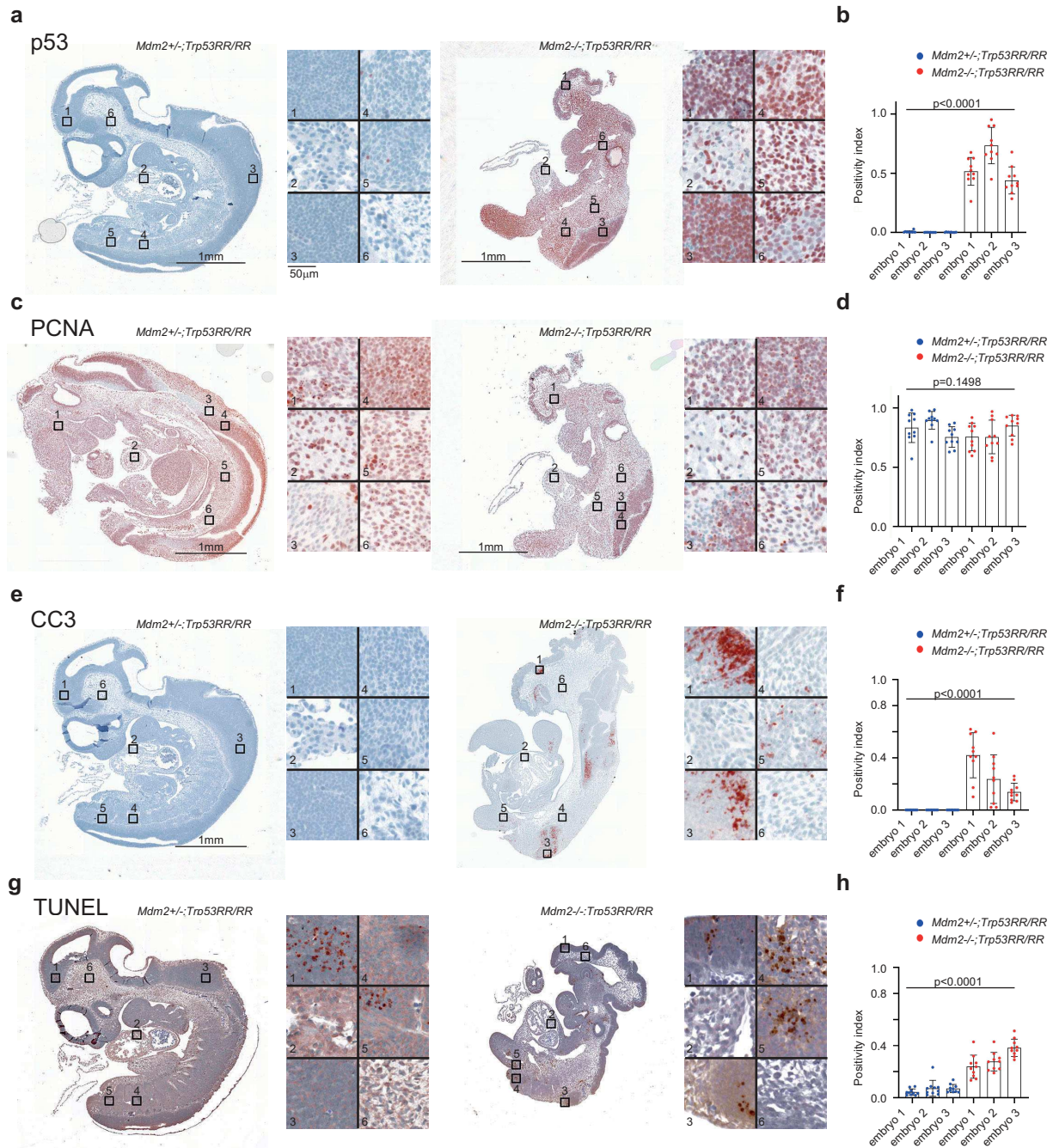


Figure 3. *Mdm2*^{Δ7-9/Δ7-9}; *Trp53*^{RR/RR} embryos die with signs of apoptosis. (a,b) Representative immunohistochemical (IHC) staining of *Mdm2*^{+/-}; *Trp53*^{RR/RR} and *Mdm2*^{-/-}; *Trp53*^{RR/RR} E10.5 embryos using anti-p53 antibodies. Right panel: different tissues shown at high magnification (1,3 – neuroepithelial, 2 – heart, 4,5 – somites, 6 – mesenchyme). Strong accumulation of p53 protein is evident in all tissues except the heart in *Mdm2*^{-/-}; *Trp53*^{RR/RR} samples. (b) – quantification of IHC staining in 3 embryos for each genotype, 10 random fields of view covering in total >50% of the section area, ANOVA test. (c,d) IHC staining of proliferating cells nuclear antigen (PCNA) in a serial section from the same samples as in (a). Right panel: different tissues shown at high magnification (1 – mesenchyme, 2 – heart, 3,4 – neuroepithelial, 5,6 – somites). (d) – quantification of PCNA staining, done as in (b), shows a slight reduction in PCNA levels in *Mdm2*^{-/-}; *Trp53*^{RR/RR} embryos, ANOVA test. (e,f) IHC staining of apoptosis marker cleaved caspase 3 (CC3) in a serial section from the same samples as in (a). Right panel: different tissues shown at high magnification (1,3 – neuroepithelial, 2 – heart, 4,5 – somites/limb bud, 6 – mesenchyme). Note apoptosis in neural tissues and limb bud of *Mdm2*^{-/-}; *Trp53*^{RR/RR} embryo. (f) – quantification of IHC staining in 3 embryos for each genotype, done as in (b), ANOVA test. (g,h) Terminal deoxynucleotidyl transferase (TdT) dUTP Nick-End Labeling (TUNEL) assay in a serial section from the same samples as in (a). Right panel shows the same sites as in (e). Note only a small foci of apoptosis in neural tissue of the normal *Mdm2*^{+/-}; *Trp53*^{RR/RR} embryo, whereas massive apoptosis is observed in multiple tissues of the abnormal double homozygous *Mdm2*^{-/-}; *Trp53*^{RR/RR} embryo. (h) – quantification of IHC staining, done as in (b), ANOVA test.

was entirely unexpected, given that all our previous experiments had demonstrated a complete loss of p53-dependent apoptosis in human and mouse p53RR cells that was explained by a defect of p53RR in binding and transactivating pro-apoptotic target genes [1,5,16]. To analyze this surprising finding in more detail, we examined different tissues at 9.5 and 10.5 dpc (magnification panels in Figure 3(a,e,g) and Suppl. Figure 2(c)) of intact embryos and quantified p53, TUNEL and CC3 staining at these stages. As shown in Figure 3(f,h) and Suppl. Figure 2(f), we consistently observed a strong accumulation of p53 and increase of apoptosis in $Mdm2^{\Delta7-9/\Delta7-9}; Trp53^{RR/RR}$ embryos. Moreover, we detected a direct correlation between p53 protein and apoptosis levels (Suppl. Figure 2d,e). Collectively, these data pointed to p53RR as the cause of cell death.

Genetic ablation of *Cdkn1a* does not provide even partial rescue of embryonic lethality

Apart from transactivating tumor-suppressive target genes, p53 also activates the p21-DREAM pathway and thereby indirectly represses dozens of genes involved in cell proliferation and survival, which might lead to developmental defects, embryonic death, and secondary apoptosis [35]. Importantly, p53RR retains the ability to induce p21 and therefore engages the p21-DREAM pathway for gene repression [18]. We reasoned that if embryonic lethality was caused by activation of the p53-p21-DREAM pathway, knock-out of p21/*Cdkn1a* should provide at least partial rescue of developmental defects. We, therefore, generated triple transgenic $Mdm2^{\Delta7-9/\Delta7-9}; Cdkn1a^{-/-}; Trp53^{RR/RR}$ mice and bred them to obtain triple-homozygous offspring. However, we detected no triple homozygotes upon genotyping of newborn pups obtained from such matings (Figure 4(a)). In fact, genetic inactivation of p21 did not provide even partial rescue of the lethal *Mdm2*-null phenotype – $Mdm2^{\Delta7-9/\Delta7-9}; Cdkn1a^{-/-}; Trp53^{RR/RR}$ embryos died at E9.5–10.5 dpc with the same morphological abnormalities as observed in $Mdm2^{\Delta7-9/\Delta7-9}; Trp53^{RR/RR}$ mice – developmental retardation, impaired blood supply, neural tube closure defects (Figure 4(b,c,d)). It suggested that the observed abnormal phenotype was caused primarily by a mechanism distinct from the lack of proliferation or p21-DREAM mediated gene repression.

Like $Mdm2^{\Delta7-9/\Delta7-9}; Trp53^{RR/RR}$ embryos, triple homozygous embryos expressed very high levels of p53 protein (Figure 4(e)). Moreover, also in $Mdm2^{\Delta7-9/\Delta7-9}; Cdkn1a^{-/-}; Trp53^{RR/RR}$ embryos we detected high levels of apoptosis in neuroepithelial tissues and somites as indicated by TUNEL assay, similar to double homozygous samples (compare Figures 4(f) and 3(g)). Although it is unclear, whether p53-induced apoptosis or developmental defects caused the embryonic lethality, these data show that the apoptosis defect of p53RR, previously reported for newborn and adult tissues following DNA damage [16], was rescued in embryonic cells by loss of Mdm2.

High levels of mutant p53RR protein can partially compensate for the cooperativity defect

The apoptosis deficiency of p53RR is caused by weakened interactions between p53 monomers that result in a compromised ability to bind promoters of many pro-apoptotic target genes [15,18,36]. To analyze expression of p53-dependent genes in embryos, we bred $Mdm2^{+/\Delta7-9}; Trp53^{RR/RR}$ mice and collected embryos at 10.5 dpc. All embryos were genotyped for *Mdm2* and used for isolation of RNA. As expected, quantitative PCR analysis of *Mdm2*-deficient embryos showed a strongly elevated expression of *Cdkn1a*, *Ccng1*, *Aldh4a*, *Gls2*, and *Sesn2* genes that have been demonstrated earlier as p53RR targets in human and mouse cells [16,18] (Figure 5(a), left panel). Surprisingly, we also detected significant upregulation of pro-apoptotic *Bbc3* (Puma) and *Bax* transcripts, which was comparable to activation levels observed in p53 wild-type MEFs after treatment with doxorubicin, used as a positive control (compare Figure 5(a), right panel and Figure 5(b)). This finding was unexpected because in our earlier experiments we did not detect any increase in expression of Puma or Bax in p53RR cells after irradiation or doxorubicin treatment [16]. The validity of our previous findings was confirmed by the lack of *Bbc3* and *Bax* induction in doxorubicin-treated p53RR MEFs (Figure 5(b)). Because of the very limited amount of embryonic tissues, we decided to use readily available mouse fibroblasts (MEFs) to further analyze the mechanisms of apoptosis triggered by p53RR. Recently, the combination of *Mdm2* inhibitor Nutlin-3a and doxorubicin was shown to evoke apoptotic activity, mediated by

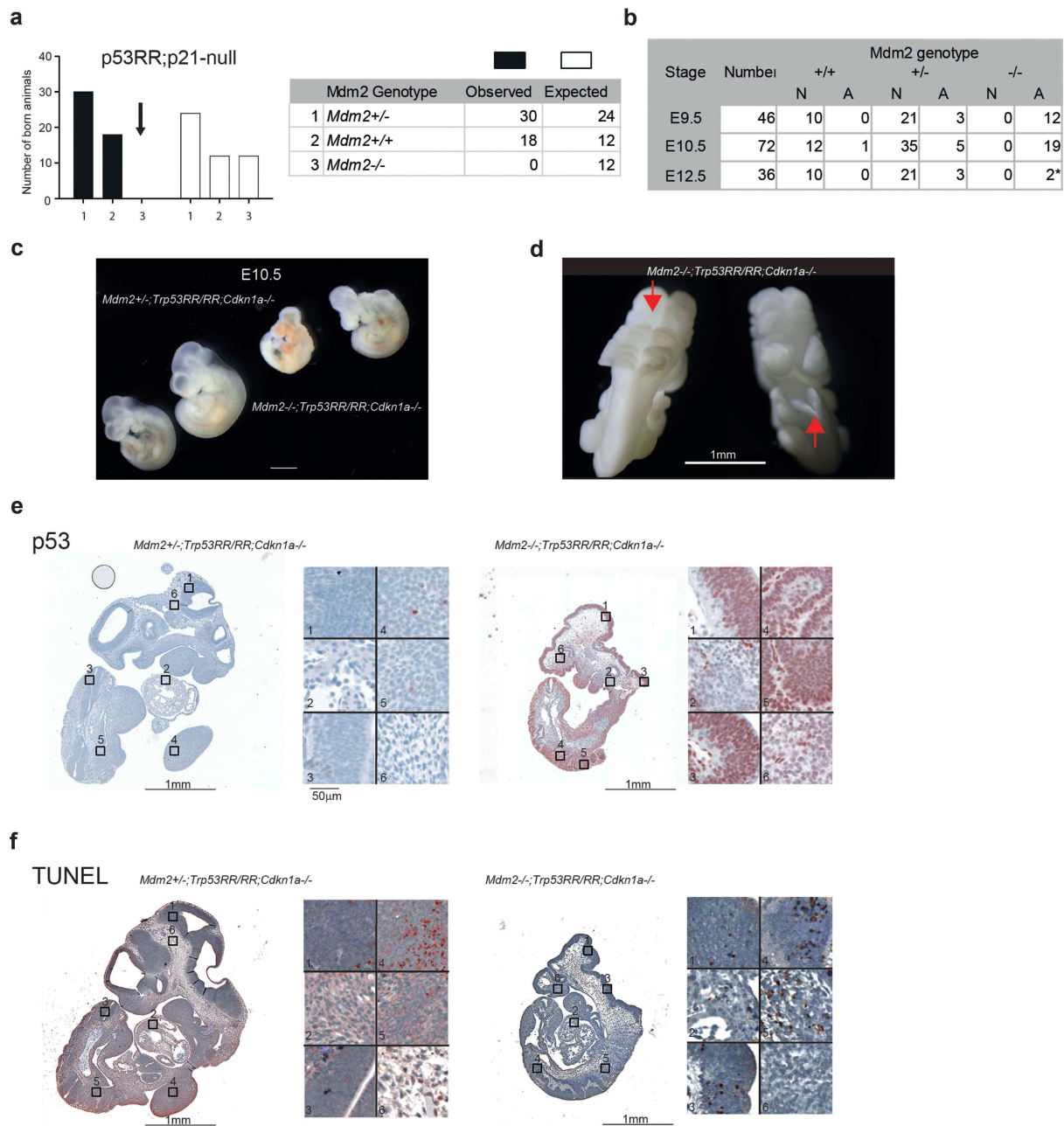


Figure 4. Genetic ablation of *Cdkn1a* fails to rescue embryonic lethality. (a) Observed and expected genotype distribution of newborn offspring from matings of *Mdm2*^{Δ7-9/Δ7-9};*Cdkn1a*^{-/-};*Trp53*^{RR/RR} mice (total number of pups $n = 48$; contingency test $P = 0.001$). (b) Phenotype analysis of *Cdkn1a*^{-/-};*Trp53*^{RR/RR} embryos with different *Mdm2* genotypes shows the onset of development defects at the same stage (E9.5 – E10.5) as in *Mdm2*^{Δ7-9/Δ7-9};*Trp53*^{RR/RR} embryos. N – normal, A – abnormal morphology. Asterisk – embryos were partially resorbed. (c) Representative images of *Cdkn1a*^{-/-};*Trp53*^{RR/RR} embryos with hetero- and homozygous *Mdm2* deletion at stage E10.5 (TS17-18) show same phenotypic abnormalities as in *Mdm2*^{Δ7-9/Δ7-9};*Trp53*^{RR/RR} embryos. (d) Representative image of an *Mdm2*^{Δ7-9/Δ7-9};*Cdkn1a*^{-/-};*Trp53*^{RR/RR} embryo shows neural tube closure defects (arrows) in cranial (left) and caudal (right) parts of the embryo. (e) Representative IHC staining of E10.5 embryos for p53 shows strong accumulation of p53 protein in *Mdm2*^{Δ7-9/Δ7-9};*Cdkn1a*^{-/-};*Trp53*^{RR/RR} samples. Right panel: different tissues shown at high magnification (1,3 – neuroepithelial, 2 – heart, 4,5 – somites/limb bud, 6 – mesenchyme). (f) TUNEL assay in a serial section from the same samples as in (E). Note the enhanced apoptosis in neuroepithelial tissues and somites of *Mdm2*^{Δ7-9/Δ7-9};*Cdkn1a*^{-/-};*Trp53*^{RR/RR} embryos.

direct mitochondrial functions, of the entirely DNA binding-deficient cooperativity mutant R178E [17]. To check if p53RR MEFs are sensitive to such a combination of drugs, we analyzed apoptosis and

overall cell death in treated cells using flow cytometry and found p53RR cells to be highly apoptotic in these conditions (Figure 5(c)), whereas treatment with Nutlin-3a or doxorubicin alone had no effect.

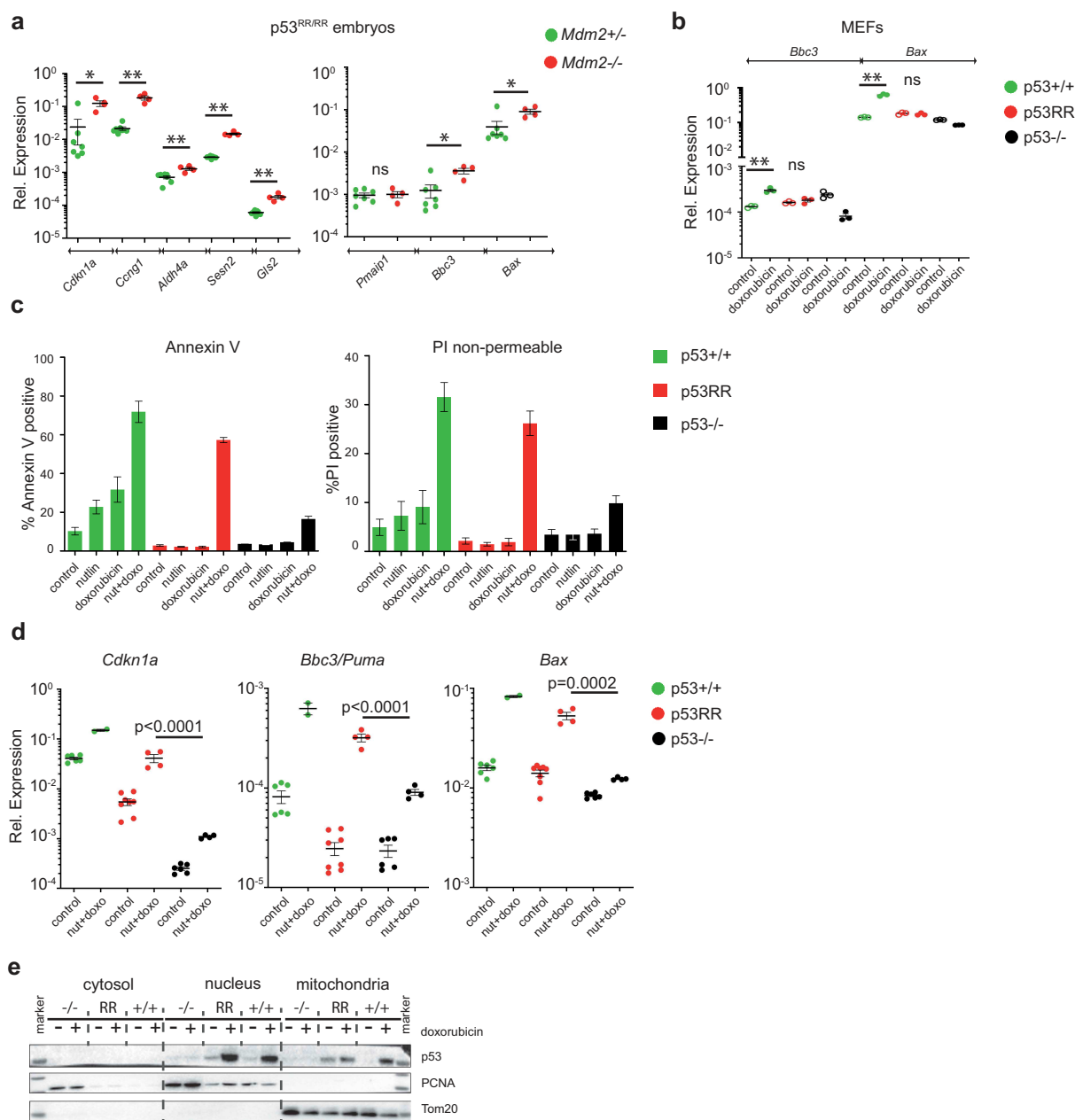


Figure 5. High levels of mutant p53RR protein can partially compensate for the cooperativity defect. (a) mRNA expression analysis (RTqPCR) of p53 target genes in *Trp53^{RR/RR}* embryos with indicated *Mdm2* genotypes. Shown are expression values normalized to β -actin, normal $n = 7$, abnormal $n = 4$. (b) RTqPCR analysis of the expression of pro-apoptotic p53 target genes *Bbc3* (*Puma*) and *Bax* in primary *Trp53^{+/+}*, *Trp53^{RR/RR}* and *Trp53^{-/-}* MEFs after 16 h treatment with 400 ng/ml doxorubicin. Shown are technical triplicates. In (a) and (b) * $P < 0.05$, ** $P < 0.01$, ns – not significant, error bars represent SD, two-tailed Mann Whitney test. (c) Quantification of apoptosis detected by flow cytometry with Annexin-V and non-permeable PI staining in *Trp53^{+/+}*, *Trp53^{RR/RR}* and *Trp53^{-/-}* E1A-immortalized MEFs upon 16 h treatment with 10 μ M Nutlin-3a, 400 ng/ml doxorubicin or a combination of both. (d) RTqPCR quantification of p53 target genes in E1A-MEFs from (c) upon treatment with Nutlin-3a and doxorubicin. Each dot indicates one biological replicate, ANOVA test. (e) Representative western blot of cytosolic, nuclear and mitochondrial fractions from primary MEFs (untreated and treated with 400 ng/ml doxorubicin), probed with anti-p53 antibodies. PCNA and Tom20 antibodies were used as fractionation controls.

Importantly, apoptosis was associated with transcriptional activation of proapoptotic target genes *Bbc3* and *Bax*, similarly as observed in *Mdm2 ^{$\Delta 7-9/\Delta 7-9$}* ; *Trp53^{RR/RR}* embryos (Figure 5(d)).

Of note, combination treatment also induced *Bbc3* and *Bax* in p53-null MEFs, but to significantly lesser extent (Figure 5(d)). It is possible that the apoptotic activity of p53RR mutant was also supported by

transcription-independent mechanisms because we detected p53RR protein in mitochondrial fractions (Figure 5(e)). Taken together, these data suggest that massive stabilization of p53RR protein – either due to complete genetic inactivation of Mdm2 or upon its pharmacological inhibition complemented with cytotoxic stress can partially compensate for the defect in DNA binding cooperativity and restore apoptotic proficiency of the mutant.

Discussion

Cooperativity mutations belong to a third and distinct class of p53 missense mutations affecting the DBD. They are found as sporadic cancer mutations and also as germ-line mutations giving rise to hereditary cancer susceptibility [15]. They are estimated to account for approximately 34,000 cancer cases per year world-wide [3]. In contrast to p53 “hotspot” mutations, cooperativity mutations commonly do not result in a complete loss of DNA binding but rather cause a partial loss of function. In particular, reduction in cooperative interactions between p53 monomers severely impairs the ability of p53RR to bind and transactivate pro-apoptotic target genes, whereas induction of cell cycle arrest and senescence along with other homeostatic p53 functions are only weakly affected [15,18,16]. Such a selective loss of p53-induced apoptosis has also been observed for many other non-hotspot p53 mutants [8,37–41], making p53 cooperativity mutants a valuable model to study the consequences of a partial loss of p53 activity for tumorigenesis or cancer therapy.

Here we report the surprising observation that the apoptosis deficiency of the cooperativity mutation p53RR was overcome by the loss of Mdm2. Although it is unclear whether the enhanced apoptosis is the main reason for embryonic lethality caused by p53RR, this genetic model demonstrated that a p53 mutant, deficient for apoptosis in other settings, can exert lethal activity. Recently, also using the *Mdm2* knock-out model, we have shown that another cooperativity mutant *Trp53*^{E177R} (p53EE) can induce embryonic lethality [17]. The *Trp53*^{E177R} (p53RR) and *Trp53*^{R178E} (p53EE) knock-in mice with cooperativity mutations have different phenotypes as the DNA binding and transcriptional activity of p53 is affected to a different degree: whereas p53EE is

fully deficient in DNA binding and devoid of direct transcriptional activity, p53RR is only partially compromised regarding DNA binding and transactivation resulting in a selective loss of transcription-dependent apoptosis. As a consequence, substantial differences between these mutants in p53-dependent response and tumor suppression were observed [16,17]. Interestingly, although both mutations strongly affect transactivation of p53-dependent apoptotic genes and render cells apoptosis-deficient, our data show that this deficiency is not absolute and can be compensated, yet by different mechanisms: while p53EE mutant induces apoptosis independently of regular transcriptional activity, p53RR seems to engage both mitochondrial and transcription-mediated pathways, as suggested by a restored ability to induce proapoptotic *Puma/Bbc3* and *Bax* expression. One reasonable explanation for this unexpected finding could be that in developing embryos an abnormal accumulation of p53RR triggered by the loss of Mdm2 can compensate for the cooperativity defect and in combination with endogenous stress signals mobilize accumulated p53 to transactivate pro-apoptotic targets. The ability of wild-type p53 to trigger apoptosis is known to be dependent on at least three factors: the expression level of p53, the duration of increased p53 expression and the intrinsic apoptotic sensitivity of cells, i.e. its apoptosis threshold [42–45]. Embryonic cells have an exceptionally low apoptosis threshold, explained at least in part by high levels of mitochondrial priming [46]. In the case of *Mdm2*^{Δ7–9/Δ7–9}; *Trp53*^{RR/RR} embryos, p53RR protein is massively and constitutively stabilized because of the lack of Mdm2 as the major negative regulator of p53. We speculate that the sustained high-level expression of p53RR restores binding to pro-apoptotic gene promoters by simple mass action: the more protein is available, the higher is its probability to bind DNA. The elevated expression of *Puma/Bbc3* and *Bax* in *Mdm2*^{Δ7–9/Δ7–9}; *Trp53*^{RR/RR} embryos and MEFs treated with Mdm2 inhibitor Nutlin-3a combined with doxorubicin also supports this hypothesis. We, therefore, assume that the combination of these factors in *Mdm2*-deficient embryos suffices to rescue the transcriptional apoptosis defect of p53RR cells.

Furthermore, p53 possesses transcription-independent cytotoxic activity [47]. Several studies have shown that p53 drives mitochondrial apoptosis

via direct interaction with Bcl2 family proteins: it inhibits anti-apoptotic members (Bcl2, BclxL, Mcl1) and activates pro-apoptotic Bak and Bax, leading to mitochondrial outer membrane permeabilization [48–50]. Interestingly, it has been reported that the Mdm2 inhibitor Nutlin-3a can enhance the non-transcriptional pro-apoptotic functions of p53 and treatment of chronic lymphocytic leukemia cells with nutlin induces a more robust non-transcriptional than transcription-dependent apoptotic response [51,52]. Thus, activation of non-transcriptional apoptosis by targeting Mdm2 may contribute to and support the lethal activity of p53 mutants with impaired transcriptional functions. Whereas hotspot mutations that severely affect the DNA-interaction interface or global structure of p53 were shown to reduce both transcriptional and non-transcriptional apoptosis [53], non-hotspot mutants may retain some of these functions. In support of this, the *Trp53*^{R178E} (p53EE) cooperativity mutant is capable of inducing mitochondrial apoptosis in the absence of target gene activation [17]. It is therefore conceivable also for p53RR that residual non-transcriptional cell death activities further contribute to the apoptosis observed in *Mdm2*^{Δ7–9/Δ7–9}; *Trp53*^{RR/RR} embryos and E1A MEFs treated with nutlin and doxorubicin. In line with this hypothesis we detected p53RR in mitochondrial fractions (Figure 5(e)).

It has been shown for wild-type p53 that the amount and dynamics of p53 protein accumulation determine the shape and outcome of the stress response [43–45,54,55]. Intriguingly, our results identify the well-established apoptosis deficiency of cooperativity mutants as a relative, context-dependent defect that, in principle, can be overcome by interventions which increase the level and duration of mutant p53 expression or lower the cell-intrinsic apoptosis threshold. It is tempting to speculate that the residual transcriptional activities described for numerous other p53 mutants could be boosted therapeutically, for example with Mdm2 inhibitors, to drive pro-apoptotic target gene expression beyond the apoptosis threshold. Such efforts might be supported with compounds such as BH3 mimetics which lower the apoptosis threshold. As many cancer-associated p53 mutants, even those with residual transcriptional activity, are highly accumulated in tumor cells, it might be possible to

identify proper stimuli to limit the apoptotic response to cancer cells while sparing normal cells.

Acknowledgments

Authors thank Sigrid Bischofsberger, Antje Grzeschiczek, Angela Mühling, Björn Geissert for technical assistance and Dr. Sabrina Elmshäuser and employees of the animal facility of Marburg University for help in mouse experiments. We acknowledge Dr. Deckelbaum and Julia Lerner (Regeneron Pharmaceuticals, NY, USA) for sharing a protocol of whole-mount PECAM staining and preparation of tyramide conjugates; we thank Dr. Gergana Dobreva (Heidelberg University) for help with microscopy.

Disclosure statement

No potential conflict of interest was reported by the authors.

Funding

This work was supported by the Deutsche Forschungsgemeinschaft [TRR81 A10, TI 1028/2-1]; Deutsche Krebshilfe [111250, 70112623, 111444]; José Carreras Leukämie-Stiftung [R13/08, R09/2018]; German Center for Lung Research (DZL).

ORCID

Thorsten Stiewe  <http://orcid.org/0000-0003-0134-7826>


References

- [1] Lane DP. 1992. Cancer p53 guardian of the genome. *Nature* 358 (6381):15–6.
- [2] Kasthuber ER, Lowe SW. Putting p53 in context. *Cell*. 2017;170:1062–1078.
- [3] Leroy B, Girard L, Hollestelle A, et al. Analysis of TP53 mutation status in human cancer cell lines: A reassessment. *Hum Mutat*. 2014;35(6):756–65.
- [4] Brosh R, Rotter V. When mutants gain new powers: news from the mutant p53 field. *Nat Rev Cancer* [Internet] 2009; 9:701–713.
- [5] Muller PAJ, Vousden KH. P53 mutations in cancer. *Nat Cell Biol*. [Internet] 2013; 15:2–8. Available from: <http://www.ncbi.nlm.nih.gov/pubmed/23263379>
- [6] Stiewe T, Haran TE. How mutations shape p53 interactions with the genome to promote tumorigenesis and drug resistance. *Drug Resist Updat*. 2018;38:27–43.
- [7] Muller PAJ, Vousden KH. Mutant p53 in cancer: new functions and therapeutic opportunities. *Cancer Cell*. 2014;25:304–317.

- [8] Shibata H, Kato S, Han S-Y, et al. Understanding the function–structure and function–mutation relationships of p53 tumor suppressor protein by high-resolution missense mutation analysis. *Proc Natl Acad Sci*. 2003;100(14):8424–8429.
- [9] Kotler E, Shani O, Goldfeld G, et al. A systematic p53 mutation library links differential functional impact to cancer mutation pattern and evolutionary conservation. *Mol Cell*. 2018;71:178–190.e8.
- [10] Joerger AC, Fersht AR. The p53 pathway: origins, inactivation in cancer, and emerging therapeutic approaches. *Annu Rev Biochem*. [Internet] 2016; 85:375–404. Available from: <http://www.annualreviews.org/doi/10.1146/annurev-biochem-060815-014710>
- [11] Kitayner M, Rozenberg H, Kessler N, et al. Structural basis of DNA recognition by p53 tetramers. *Mol Cell*. 2006;22:741–753.
- [12] Klein C, Planker E, Diercks T, et al. NMR spectroscopy reveals the solution dimerization interface of p53 core domains bound to their consensus DNA. *J Biol Chem*. 2001;276:49020–49027.
- [13] Dehner A, Klein C, Hansen S, et al. Cooperative binding of p53 to DNA: regulation by protein-protein interactions through a double salt bridge. *Angew Chemie - Int Ed*. 2005;44:5247–5251.
- [14] Kitayner M, Rozenberg H, Rohs R, et al. Diversity in DNA recognition by p53 revealed by crystal structures with Hoogsteen base pairs. *Nat Struct Mol Biol*. [Internet]. 2010;17:423–429.
- [15] Schlereth K, Beinoravičiute-Kellner R, Zeitlinger MK, et al. DNA binding cooperativity of p53 modulates the decision between cell-cycle arrest and apoptosis. *Mol Cell*. 2010;38:356–368.
- [16] Timofeev O, Schlereth K, Wanzel M, et al. P53 DNA binding cooperativity is essential for apoptosis and tumor suppression in vivo. *Cell Rep*. 2013;3:1512–1525.
- [17] Timofeev O, Klimovich B, Schneikert J, et al. Residual apoptotic activity of a tumorigenic p53 mutant improves cancer therapy responses. *Embo J*. 2019;38(20):e102096.
- [18] Schlereth K, Heyl C, Krampitz AM, et al. Characterization of the p53 cistrome - DNA binding cooperativity dissects p53's tumor suppressor functions. *PLoS Genet*. 2013;9:e1003726.
- [19] Marine J-C, Lozano G. Mdm2-mediated ubiquitylation: p53 and beyond. *Cell Death Differ*. [Internet]. 2010;17:93–102.
- [20] Marine JC, Francoz S, Maetens M, et al. Keeping p53 in check: essential and synergistic functions of Mdm2 and Mdm4. *Cell Death Differ*. [Internet] 2006; 13:927–934. Available from: <http://www.ncbi.nlm.nih.gov/pubmed/16543935>
- [21] Weber JD, Taylor LJ, Roussel MF, et al. Nucleolar Arf sequesters Mdm2 and activates p53. *Nat Cell Biol*. 1999;1:20–26.
- [22] Burgess A, Chia KM, Haupt S, et al. Clinical overview of MDM2/X-targeted therapies. *Front Oncol*. 2016;6:7.
- [23] Sabapathy K, Lane DP. Therapeutic targeting of p53: all mutants are equal, but some mutants are more equal than others. *Nat Rev Clin Oncol*. [Internet] 2017; Available from: <http://www.nature.com/doi/10.1038/nrclinonc.2017.151>
- [24] Chavez-Reyes A, Parant JM, Amelse LL, et al. Switching mechanisms of cell death in mdm2- and mdm4-null mice by deletion of p53 downstream targets. *Cancer Res*. 2003;63:8664–8669.
- [25] Jones SN, Roe AE, Donehower LA, et al. Rescue of embryonic lethality in Mdm2-deficient mice by absence of p53. *Nature*. 1995;378:206–208.
- [26] Montes de Oca Luna R, Wagner DS, Lozano G. Rescue of early embryonic lethality in mdm2-deficient mice by deletion of p53. *Nature*. 1995;378:203–206.
- [27] Oca Luna RM, De, Amelse LL, Chavez-Reyes A, et al. Deletion of p21 cannot substitute for p53 loss in rescue of mdm2 null lethality. *Nat Genet*. 1997;16(4):336–337.
- [28] Lee MK, Teoh WW, Phang BH, et al. Cell-type, dose, and mutation-type specificity dictate mutant p53 functions in vivo. *Cancer Cell*. [Internet]. 2012;22:751–764.
- [29] Abbas HA, MacCio DR, Coskun S, et al. Mdm2 is required for survival of hematopoietic stem cells/progenitors via dampening of ros-induced p53 activity. *Cell Stem Cell*. 2010;7:606–617.
- [30] Wang Y, Suh YA, Fuller MY, et al. Restoring expression of wild-type p53 suppresses tumor growth but does not cause tumor regression in mice with a p53 missense mutation. *J Clin Invest*. 2011;121:893–904.
- [31] Mendrysa SM, McElwee MK, Michalowski J, et al. Mdm2 is critical for inhibition of p53 during lymphopoiesis and the response to ionizing irradiation. *Mol Cell Biol*. 2003;23:462–472.
- [32] Lazarus A, Del-Moral PM, Ilovich O, et al. A perfusion-independent role of blood vessels in determining branching stereotypy of lung airways. *Development*. 2011;138:2359–2368.
- [33] Kuwajima T, Sitko AA, Bhansali P, et al. ClearT: a detergent- and solvent-free clearing method for neuronal and non-neuronal tissue. *Development*. 2013;140:1364–1368.
- [34] Migliorini D, Lazzarini, Denchi E, et al. Mdm4 (Mdmx) regulates p53-induced growth arrest and neuronal cell death during early embryonic mouse development. *Mol Cell Biol*. [Internet] 2002; 22:5527–5538. Available from: <http://www.ncbi.nlm.nih.gov/pubmed/12101245>
- [35] Engeland K. Cell cycle arrest through indirect transcriptional repression by p53: I have a DREAM. *Cell Death Differ*. 2018;25:114–132.
- [36] Schlereth K, Charles JP, Bretz AC, et al. Life or death: p53-induced apoptosis requires DNA binding cooperativity. *Cell Cycle*. 2010;9:4068–4076.
- [37] Rowan S, Ludwig RL, Haupt Y, et al. Specific loss of apoptotic but not cell-cycle arrest function in a human tumor derived p53 mutant. *Embo J*. 1996; 15(4):827–838.

- [38] Ludwig RL, Bates S, Vousden KH. Differential activation of target cellular promoters by p53 mutants with impaired apoptotic function. *Mol Cell Biol.* 1996;16:4952–4960.
- [39] Campomenosi P, Monti P, Aprile A, et al. P53 mutants can often transactivate promoters containing a p21 but not Bax or PIG3 responsive elements. *Oncogene.* 2001;20:3573–3579.
- [40] Jordan JJ, Inga A, Conway K, et al. Altered-function p53 missense mutations identified in breast cancers can have subtle effects on transactivation. *Mol Cancer Res.* 2010;8:701–716.
- [41] Menendez D, Inga A, Resnick MA. The biological impact of the human master regulator p53 can be altered by mutations that change the spectrum and expression of its target genes. *Mol Cell Biol.* 2006;26:2297–2308.
- [42] Le Pen J, Laurent M, Sarosiek K, et al. Constitutive p53 heightens mitochondrial apoptotic priming and favors cell death induction by BH3 mimetic inhibitors of BCL-xL. *Cell Death Dis.* [Internet] 2016 [cited 2016 Jun 24]; 7:e2083. Available from: <http://www.nature.com/doi/10.1038/cddis.2015.400>
- [43] Speidel D, Helmbold H, Deppert W. Dissection of transcriptional and non-transcriptional p53 activities in the response to genotoxic stress. *Oncogene.* [Internet] 2006; 25:940–953. Available from: <http://www.ncbi.nlm.nih.gov/pubmed/16247471>
- [44] Kracikova M, Akiri G, George A, et al. A threshold mechanism mediates p53 cell fate decision between growth arrest and apoptosis. *Cell Death Differ.* 2013; 20(4):576–588.
- [45] Purvis JE, Karhohs KW, Mock C, et al. p53 dynamics control cell fate. *Science.* 2012;336:1440–1444.
- [46] Sarosiek KA, Fraser C, Muthalagu N, et al. Developmental regulation of mitochondrial apoptosis by c-myc governs age- and tissue-specific sensitivity to cancer therapeutics. *Cancer Cell.* 2017;31:142–156.
- [47] Marchenko ND, Moll UM. Mitochondrial death functions of p53. *Mol Cell Oncol.* [Internet] 2014 [cited 2017 Dec 8]; 1:e955995. Available from: <https://www.tandfonline.com/doi/full/10.1080/23723548.2014.955995>
- [48] Marchenko ND, Zaika A, Moll UM. Death signal-induced localization of p53 protein to mitochondria. *J Biol Chem.* 2000;275(21):16202–16212.
- [49] Chipuk JE, Kuwana T, Bouchier-Hayes L, et al. Direct activation of Bax by p53~{m}ediates mitochondrial membrane permeabilization and apoptosis. *Science.* 2004;303:1010–1014.
- [50] Leu JIJ, Dumont P, Hafey M, et al. Mitochondrial p53 activates Bak and causes disruption of a Bak-Mcl1 complex. *Nat Cell Biol.* 2004;6:443–450.
- [51] Kojima K, Konopleva M, McQueen T, et al. Mdm2 inhibitor Nutlin-3a induces p53-mediated apoptosis by transcription-dependent and transcription-independent mechanisms and may overcome Atm-mediated resistance to fludarabine in chronic lymphocytic leukemia. *Blood.* 2006;108:993–1000.
- [52] Steele AJ, Prentice AG, Hoffbrand AV, et al. P53-mediated apoptosis of CLL cells: evidence for a transcription-independent mechanism. *Blood.* 2008;112:3827–3834.
- [53] Tomita Y, Marchenko N, Erster S, et al. WT p53, but not tumor-derived mutants, bind to Bcl2 via the DNA binding domain and induce mitochondrial permeabilization. *J Biol Chem.* [Internet] 2006 [cited 2018 Mar 13]; 281:8600–8606. Available from: <http://www.ncbi.nlm.nih.gov/pubmed/16443602>
- [54] Chen X, Ko LJ, Jayaraman L, et al. p53 levels, functional domains, and DNA damage determine the extent of the apoptotic response of tumor cells. *Genes Dev.* 1996;10:2438–2451.
- [55] Paek AL, Liu JC, Loewer A, et al. Cell-to-cell variation in p53 dynamics leads to fractional killing. *Cell.* 2016;165:631–642.

Residual apoptotic activity of a tumorigenic p53 mutant improves cancer therapy responses

Oleg Timofeev¹, Boris Klimovich¹, Jean Schneikert¹, Michael Wanzel^{1,2}, Evangelos Pavlakis¹, Julia Noll¹, Samet Mutlu¹, Sabrina Elmshäuser¹, Andrea Nist³, Marco Mernberger¹, Boris Lamp³, Ulrich Wenig⁴, Alexander Brobeil⁴, Stefan Gattenlöhner⁴, Kernt Köhler⁵ & Thorsten Stiewe^{1,2,3,*} 

Abstract

Engineered p53 mutant mice are valuable tools for delineating p53 functions in tumor suppression and cancer therapy. Here, we have introduced the R178E mutation into the *Trp53* gene of mice to specifically ablate the cooperative nature of p53 DNA binding. *Trp53*^{R178E} mice show no detectable target gene regulation and, at first sight, are largely indistinguishable from *Trp53*^{-/-} mice. Surprisingly, stabilization of p53^{R178E} in *Mdm2*^{-/-} mice nevertheless triggers extensive apoptosis, indicative of residual wild-type activities. Although this apoptotic activity suffices to trigger lethality of *Trp53*^{R178E};*Mdm2*^{-/-} embryos, it proves insufficient for suppression of spontaneous and oncogene-driven tumorigenesis. *Trp53*^{R178E} mice develop tumors indistinguishably from *Trp53*^{-/-} mice and tumors retain and even stabilize the p53^{R178E} protein, further attesting to the lack of significant tumor suppressor activity. However, *Trp53*^{R178E} tumors exhibit remarkably better chemotherapy responses than *Trp53*^{-/-} ones, resulting in enhanced eradication of p53-mutated tumor cells. Together, this provides genetic proof-of-principle evidence that a p53 mutant can be highly tumorigenic and yet retain apoptotic activity which provides a survival benefit in the context of cancer therapy.

Keywords apoptosis; Mdm2; mutant p53; p53; tumor suppression

Subject Categories Autophagy & Cell Death; Cancer; Molecular Biology of Disease

DOI 10.15252/emboj.2019102096 | Received 25 March 2019 | Revised 30 July 2019 | Accepted 5 August 2019

The EMBO Journal (2019) e102096

Introduction

The *TP53* gene, encoding the tumor-suppressive transcription factor p53, is mutated in about half of all human cancers. The presence of *TP53* mutations correlates in many cancer types with enhanced

metastasis and aggressiveness, reduced responses to chemotherapeutic drugs, and, thus, a poor prognosis (Robles *et al*, 2016; Sabapathy & Lane, 2018). More than 85% of all amino acid positions were found to be mutated in cancer patients, generating a “rainbow” of > 2,000 distinct missense variants (Sabapathy & Lane, 2018). Mutations cluster in the central DNA binding domain (DBD), suggesting that tumorigenesis selects against p53’s DNA binding function (Muller & Vousden, 2014; Stiewe & Haran, 2018). In support of this, mutant frequency was found to directly correlate with loss of transactivation function (Kato *et al*, 2003). However, *TP53* mutations show a remarkable preference for missense mutations, although DNA binding can be disrupted equally well by nonsense or frame-shift mutations. Furthermore, missense mutants are unstable in normal unstressed cells, but become constitutively stabilized in tumors by Hsp90 which protects mutant p53 from degradation by Mdm2 and CHIP (Terzian *et al*, 2008; Alexandrova *et al*, 2015). The preferential selection of missense mutants together with their excessive stabilization therefore points at additional mechanisms that promote tumor development beyond a mere loss of DNA binding activity: Missense mutants exhibit dominant-negative effects on remaining wild-type p53 and display neomorphic properties that—like an oncogene—actively drive tumor development to a metastatic and drug-resistant state (Freed-Pastor & Prives, 2012; Muller & Vousden, 2014; Kim & Lozano, 2018; Stiewe & Haran, 2018). Missense mutations therefore enhance tumor development and progression in three ways: the loss of wild-type-like DNA binding activity (loss of function, LOF), dominant-negative effects on wild-type p53, and the gain of new tumor-promoting oncogenic properties (gain of function, GOF) (Stiewe & Haran, 2018).

p53 missense mutants are broadly classified as either “structural” or “DNA contact” mutants (Bullock & Fersht, 2001). Structural mutants destabilize the inherently low stability of the DBD resulting in its denaturation at body temperature and therefore likely affect also those non-transcriptional functions which are mediated by the DBD through, for instance, protein–protein interactions. In contrast, DNA contact mutants affect single

¹ Institute of Molecular Oncology, Philipps-University, Marburg, Germany

² German Center for Lung Research (DZL), Universities of Giessen and Marburg Lung Center, Marburg, Germany

³ Genomics Core Facility, Philipps University, Marburg, Germany

⁴ Institute of Pathology, Justus Liebig University, Giessen, Germany

⁵ Institute of Veterinary Pathology, Justus Liebig University, Giessen, Germany

*Corresponding author. Tel: +49 6421 28 26280; E-mail: thorsten.stiewe@uni-marburg.de

DNA-interacting residues and retain an intact native fold (Bullock & Fersht, 2001). We and others have previously described a new class of non-structural mutations affecting the DBD surface residues E180 and R181 which form a reciprocal salt bridge between two adjacent p53 subunits in the tetrameric DNA-bound complex (Klein *et al*, 2001; Kitayner *et al*, 2010). This salt bridge is essential for p53 to bind DNA in a cooperative manner so that mutations at these sites are referred to as cooperativity mutations (Dehner *et al*, 2005; Schlereth *et al*, 2010a). Despite being no mutational hot-spots, cooperativity mutations at residues E180 and R181 are estimated to account for 34,000 cancer cases per year (Leroy *et al*, 2014). Importantly, distinct cooperativity mutations reduce p53 DNA binding to different extents without changing the overall DBD structure determined by NMR spectroscopy (Dehner *et al*, 2005). Of all mutations of the double salt bridge, the R181E mutant disrupts formation of the intermolecular salt bridge most effectively (Schlereth *et al*, 2010a). Although R181E retains a native fold, it is entirely DNA binding deficient as assessed by electrophoretic mobility shift assays and genome-wide chromatin immunoprecipitation analysis (Dehner *et al*, 2005; Schlereth *et al*, 2010a, 2013). In R181E, the double salt bridge residues 180 and 181 are both glutamic acid (E), so that we refer to this mutant in short as “EE”.

Mutations engineered into the mouse *Trp53* gene locus are valuable tools to delineate *in vivo* tumor suppressor functions in tumorigenesis and cancer therapy (Biegging *et al*, 2014; Mello & Attardi, 2018). Besides mutations derived from cancer patients, especially non-naturally occurring mutations of post-translational modification sites (Sluss *et al*, 2004; Slee *et al*, 2010; Li *et al*, 2012) or functional domains (Toledo *et al*, 2006; Brady *et al*, 2011; Hamard *et al*, 2013; Simeonova *et al*, 2013) have yielded substantial mechanistic insight into the pathways required for tumor suppression. To explore the relevance of DNA binding cooperativity for p53's anti-tumor activities, we therefore generated the “EE” mouse carrying the human R181E-equivalent R178E mutation at the endogenous *Trp53* gene locus. Cistrome and transcriptome analysis confirms the EE mutant as DNA binding deficient *in vivo*. Phenotype analysis demonstrates a knock-out-like appearance characterized by undetectable p53 target gene regulation and widespread, early-onset tumorigenesis, indicating that DNA binding cooperativity is essential for DNA binding and tumor suppression *in vivo*. Surprisingly, the EE mutation—different from the p53-knock-out—does not rescue the embryonic lethality of the *Mdm2* knock-out and triggers massive apoptotic cell death providing support for residual cytotoxic activities upon constitutive stabilization. An essential role of caspases, localization of EE to the mitochondria, and sensitization to mitochondrial outer membrane permeabilization point toward the intrinsic apoptosis pathway as the cause of cell death. Importantly, apoptosis was also triggered *in vitro* and *in vivo* by DNA-damaging chemotherapy of tumor cells expressing constitutively or pharmacologically stabilized EE. This translated into improved survival under chemotherapy. Similar results were obtained with the human R181L cooperativity mutant, which has been recurrently identified in cancer patients. Together, these findings highlight that mutant p53, in principle, can retain residual apoptotic activities that are insufficient to prevent tumorigenesis and not efficiently counter-selected during tumor evolution. Stabilization of such a p53 mutant in combination with chemotherapy is capable to trigger mutant p53-mediated

cytotoxicity resulting in improved anti-cancer responses and increased survival.

Results

p53EE is deficient for DNA binding and target gene activation

We previously showed that the DNA binding cooperativity mutant p53^{R181E} (EE) fails to bind p53 response elements *in vitro* and when exogenously expressed in p53-null cells (Schlereth *et al*, 2010a, 2013). To address how ablation of DNA binding cooperativity affects p53 functions *in vivo*, we generated a conditional knock-in mouse, carrying the R178E (EE) mutation in exon 5 of the endogenous mouse *Trp53* gene locus (Fig EV1A–D). DNA binding deficiency of the EE mutation in the context of the mouse p53 protein was confirmed by electrophoretic mobility shift assays using nuclear extracts of homozygous p53^{EE/EE} mouse embryonic fibroblasts (MEFs) and a high-affinity, consensus-like p53 response element (Fig EV1E). Next, DNA binding was assessed genome-wide by sequencing chromatin immunoprecipitated with a p53 antibody from MEFs under untreated conditions and following p53 stabilization with the Mdm2 inhibitor Nutlin-3a (Nutlin) (ChIP-seq, Fig 1A). We identified a total of 468 p53-specific peaks in Nutlin-treated p53^{+/+} MEFs (Figs 1A and EV1F). Validating the quality of the ChIP-seq, these peaks were strongly enriched for the p53 consensus motif at the peak center and significantly annotated with multiple Molecular Signatures Database (MSigDB) gene sets related to p53 function (Fig 1B and G). Only 3 peaks were identified in Nutlin-treated p53^{EE/EE} MEFs that were, however, also called in p53^{-/-} MEFs and therefore considered non-specific (Fig EV1F). Thus, the p53 binding pattern observed in p53^{EE/EE} MEFs was indistinguishable from p53^{-/-} MEFs, irrespective of Nutlin treatment, and therefore validated the p53EE mutant expressed from the endogenous *Trp53* gene locus to be DNA binding deficient in cells.

When global gene expression was profiled by RNA-seq, Nutlin exerted a significantly stronger effect on global gene expression in p53^{+/+} versus either p53^{EE/EE} or p53^{-/-} MEFs, while Nutlin effects on p53^{EE/EE} and p53^{-/-} cells showed no significant difference (Fig EV1H). Furthermore, we observed in p53^{+/+} but not in p53^{EE/EE} or p53-null MEFs a strong Nutlin-inducible expression of a p53 signature including both *bona fide* p53 pathway genes (MSigDB HALLMARKS_P53_PATHWAY) and non-canonical targets previously identified to be critical mediators of tumor suppression (Figs 1C and EV1I) (Brady *et al*, 2011). Gene set enrichment analysis (GSEA) showed a highly significant enrichment of a p53 target gene signature (MSigDB P53_DOWNSTREAM_PATHWAY) in p53^{+/+} cells compared to either p53^{EE/EE} or p53^{-/-} MEFs, but no enrichment in p53^{EE/EE} versus p53^{-/-} MEFs (Fig 1D). The same was observed for multiple other p53-related gene sets (Fig 1D). The lack of p53 target gene activation in p53^{EE/EE} MEFs was confirmed also under conditions of DNA damage induced with doxorubicin (Fig 1F). Western blots revealed increased p53 expression in p53^{EE/EE} versus p53^{+/+} MEFs, which was further augmented by Nutlin or doxorubicin—yet in the absence of detectable expression of the p53 targets p21 and Mdm2 (Fig 1G and H). We conclude from these data that the murine p53EE mutant lacks detectable sequence-specific DNA binding and p53 target gene activation.

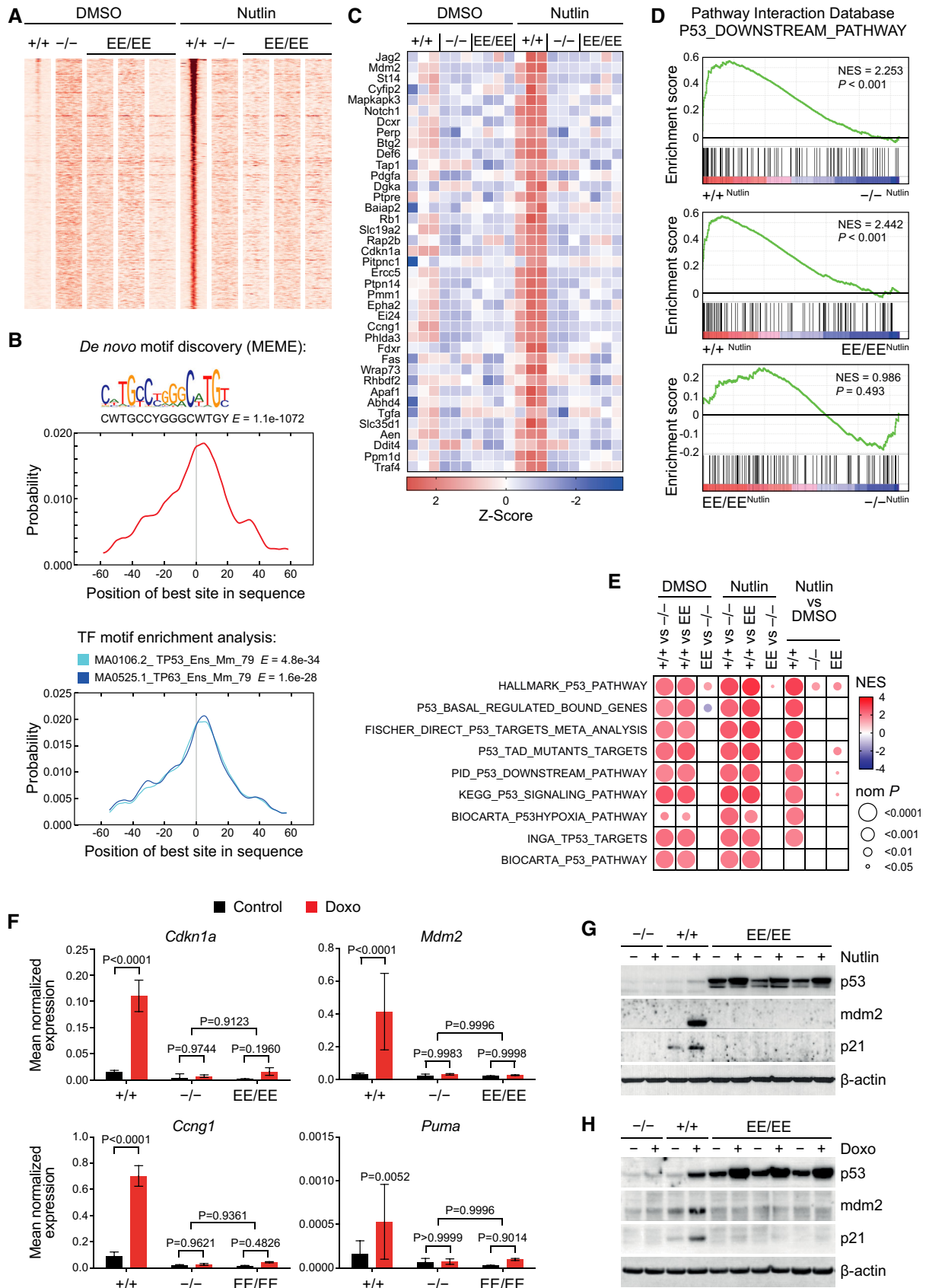


Figure 1.

Figure 1. p53EE is deficient for DNA binding and target gene activation.

- A p53 ChIP-seq in MEFs of the indicated genotype treated with or without 10 μ M Nutlin-3a (Nutlin) for 16 h. Shown are 2 kb regions surrounding the summit of the 468 p53 binding peaks called in Nutlin-treated p53^{+/+}, but not p53^{-/-} or p53^{EE/EE} MEFs. For p53^{EE/EE} MEFs, three independent replicates are shown.
- B *De novo* motif search using MEME-Chip was performed on the 468 p53 binding peaks (as in A). The best hit motif is reported with corresponding *E*-value and logo (upper part). Graphs depict a CentriMo enrichment analysis for the best MEME motif (middle) and for known transcription factor binding sites (bottom). The top two hits are shown with corresponding *E*-values.
- C RNA-seq was performed with MEFs of the indicated genotype untreated or treated with 10 μ M Nutlin for 16 h. Shown are all Nutlin-regulated genes from the MSigDB gene set HALLMARKS_P53_PATHWAY with a mean log₂FC \geq 1 in p53^{+/+} cells. Shown are the z-transformed RNA expression values (FPKM).
- D, E RNA-seq data were subjected to gene set enrichment analysis (GSEA). Shown are enrichment plots for the indicated set of p53 downstream genes in pairwise comparisons of Nutlin-treated MEFs with the indicated p53 genotypes. (E) Summary of GSEA results for p53-related gene sets. NES, normalized enrichment score; nom P, nominal P value.
- F Reverse transcription-quantitative PCR (RT-qPCR) analysis of p53 target genes in MEFs treated for 24 h with 1 μ g/ml doxorubicin (Doxo). Shown are expression values normalized to β -actin as mean \pm SD ($n = 6$). *P* values were calculated by 2-way ANOVA with Sidak's multiple comparisons test.
- G, H Western blots of protein lysates prepared from MEFs treated for 24 h with (G) 10 μ M Nutlin or (H) 0.4 μ g/ml Doxo.

p53EE fails to induce apoptosis, cell cycle arrest, and senescence

In response to various types of stress, wild-type p53 elicits cell cycle arrest and senescence mediated by transcriptional activation of target genes, such as *Cdkn1a/p21*. Consistent with the inability of p53EE to induce target genes, p53^{EE/EE} and p53-null MEFs comparably failed to undergo cell cycle arrest in response to doxorubicin-triggered DNA damage (Fig 2A) or to enter senescence upon enforced expression of oncogenic Ras (Fig EV2A) or *in vitro* passaging (Figs 2B and EV2B).

Besides cell cycle arrest, p53 is capable of inducing apoptotic cell death upon severe DNA damage. While immortalization with adenoviral E1A.12S strongly sensitized p53^{+/+} MEFs to apoptosis, E1A-expressing p53^{EE/EE} and p53-null MEFs remained refractory to apoptosis induction by genotoxic damage or Nutlin (Fig 2C). Likewise, p53^{EE/EE} thymocytes were as resistant as p53-null cells to apoptosis triggered by ionizing radiation, despite retaining the ability to undergo p53-independent apoptosis thereby excluding a general failure of the apoptosis machinery (Fig 2D). The apoptosis defect corresponded with a deficiency in transactivating not only *Cdkn1a/p21* but also the key pro-apoptotic target genes *Pmaip1/Noxa* and *Bbc3/Puma* (Fig 2E).

Of note, we have previously reported a similar but more selective apoptosis defect in p53RR mice carrying the E177R (RR) cooperativity mutation (Fig EV2C) (Timofeev *et al*, 2013). p53RR forms a p53WT-like salt bridge with p53EE which enables formation of stably DNA-bound and transcriptionally active p53EE/p53RR heterotetramers (Fig EV2C) (Dehner *et al*, 2005; Schlereth *et al*, 2010a, 2013). We therefore crossed p53^{EE/EE} mice to p53^{RR/RR} mice and obtained compound p53^{EE/RR} animals that launched an apoptotic DNA damage response like p53^{+/+} animals in thymocytes *ex vivo* (Fig EV2D) and upon whole-body irradiation *in vivo* (Fig EV2E). Rescue of the apoptosis deficiency of p53^{EE/EE} mice by the equally apoptosis-defective p53RR mutant proves that the p53EE loss-of-function phenotype is directly linked to the inability to form the salt bridge responsible for cooperative DNA binding and in turn further excludes global DBD misfolding or secondary local structural alterations at the DNA binding surface as an underlying cause.

Like p53WT and the hot-spot mutant p53R172H (Terzian *et al*, 2008), p53EE was undetectable *in vivo* by immunostaining in all tissues analyzed, but rapidly stabilized in response to whole-body ionizing radiation (Fig EV2F). This suggests that the elevated p53EE protein level observed in MEF cultures (Fig 1G and H) reflects a stabilization in response to unphysiological culture stress. p53 stabilization upon whole-body irradiation triggered waves of cell cycle

inhibition and apoptosis in intestinal crypts and other radiosensitive organs of p53^{+/+} animals (Figs 2F–I and EV2G and H). None of these effects were recorded in p53^{EE/EE} or p53-null mice (Figs 2F–I and EV2G and H), indicating a complete defect of p53EE regarding classical p53 effector functions *in vivo*.

Constitutive p53EE stabilization triggers**ROS-dependent senescence**

When passaging p53^{EE/EE} MEFs for longer time periods, we noted that—unlike p53^{-/-} MEFs—the proliferation rate of p53^{EE/EE} MEFs eventually declined and the cells started to express the senescence marker SA- β -galactosidase (Fig EV3A and B). This was accompanied by a progressive increase in p53EE protein levels, but without the increased expression in p53 target genes that was detectable in p53^{+/+} MEFs (Fig EV3C and D). Spontaneous (Fig EV3C) or CRISPR-enforced (Fig EV3E) deletion of p53EE caused senescence bypass resulting in immortalization. Senescent p53^{EE/EE} MEFs exhibited strongly elevated levels of mitochondrial ROS (Fig EV3F). Oxygen reduction from ambient to physiological levels promoted immortalization (Fig EV3G and H), implying ROS as the trigger of senescence in response to p53EE accumulation. However, there was no evidence for a p53WT-like inhibition of aerobic glycolysis (Warburg effect) and shift toward oxidative phosphorylation by p53EE which could explain an increased ROS production (Fig EV3I). Instead, we observed a somewhat reduced oxidative ATP production under basal conditions and significantly impaired spare respiratory capacity upon mitochondrial uncoupling, suggesting an inhibitory effect of p53EE on mitochondrial functions (Fig EV3J). In line, the mitochondrial DNA content of p53^{EE/EE} MEFs was significantly decreased, especially at late passages (Fig EV3J).

A common regulator of ROS defense, oxidative phosphorylation, and mitochondrial biogenesis is the transcription factor Nrf2 (nuclear respiratory factor 2) (Dinkova-Kostova & Abramov, 2015). Basal and ROS-triggered expression of anti-oxidative Nrf2 target genes was diminished in p53^{EE/EE} MEFs (Fig EV3K and L), strongly suggesting that p53EE inhibits Nrf2 activity similar as other p53 mutants (Walerych *et al*, 2016; Liu *et al*, 2017; Merkel *et al*, 2017). We therefore postulate that the Nrf2-inhibitory activity of p53EE sensitizes to ROS-induced senescence.

p53EE is unable to rescue the lethality of Mdm2-null mice

In light of the senescence induced by progressive accumulation of p53 upon long-term cultivation (Fig EV3), we further explored

whether p53EE exerts anti-proliferative or cytotoxic activities when constitutively stabilized by *Mdm2* knock-out. Genetic ablation of *Mdm2* in mice causes early embryonic lethality due to massive

apoptosis initiated as early as E3.5, whereas simultaneous disruption of the *Trp53* gene rescues the lethal phenotype (Jones et al, 1995; Montes de Oca Luna et al, 1995; Chavez-Reyes et al, 2003).

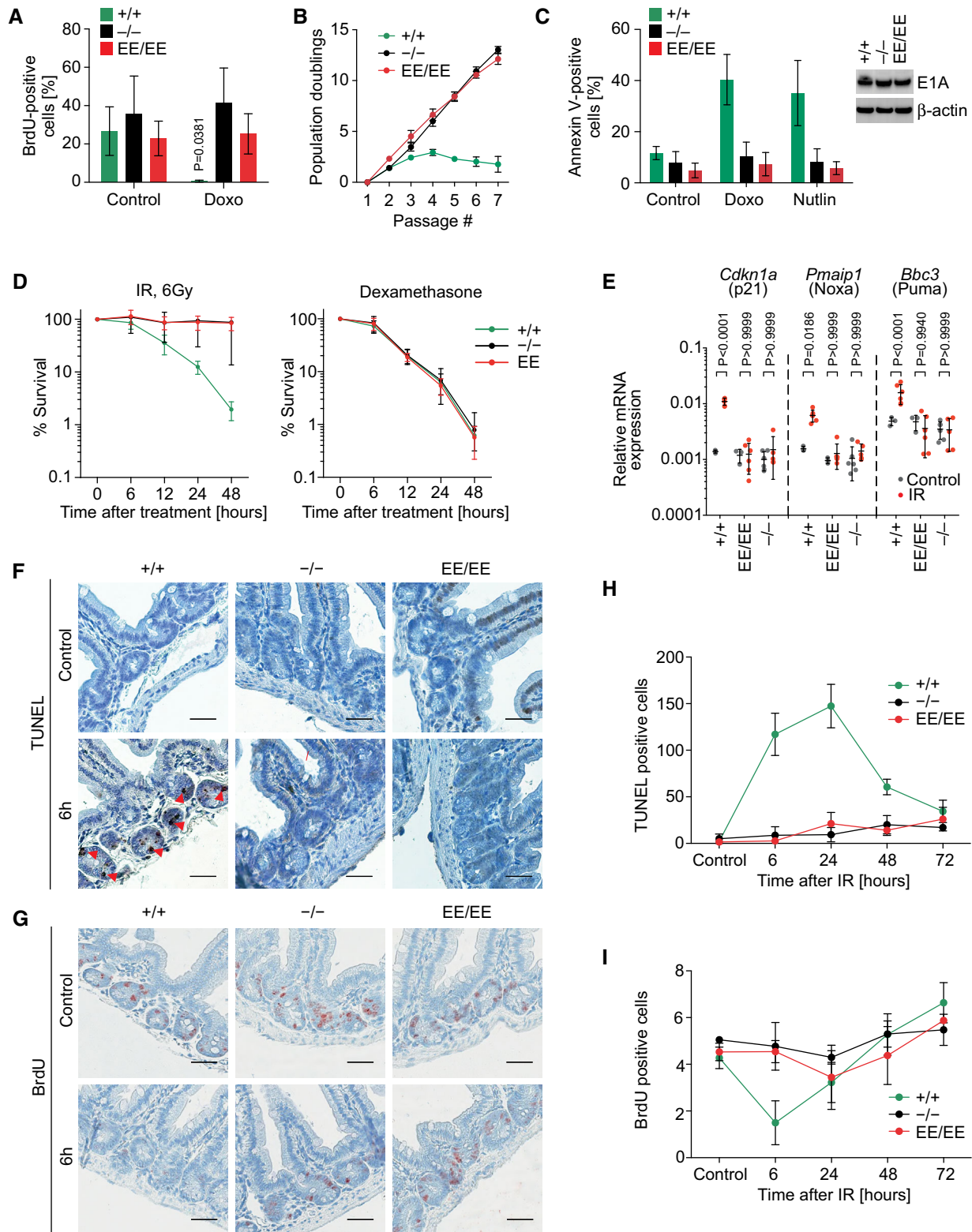


Figure 2.

Figure 2. p53EE fails to induce apoptosis, cell cycle arrest, and senescence.

- A Proliferation of primary MEFs. Cells were treated *o/n* with 0.2 $\mu\text{g/ml}$ doxorubicin (Doxo) and pulse-labeled with 32 μM 5-bromo-2-deoxyuridine (BrdU), fixed and processed for flow cytometry analysis. $n = 4$.
- B Long-term proliferation assay with primary MEFs of indicated genotypes. $+/+$ and $-/-$: $n = 3$; EE/EE: $n = 6$.
- C MEFs were immortalized with the adenoviral oncogene E1A.12S (E1A MEF) and treated with 0.4 $\mu\text{g/ml}$ Doxo for 17 h. Apoptosis (annexin V) was quantified by flow cytometry. $+/+$ and $-/-$: $n = 3$; EE/EE: $n = 6$. Western blots show expression of E1A and β -actin as loading control.
- D Primary thymocytes were irradiated *ex vivo* with 6 Gy or treated with 1 μM dexamethasone as a control for p53-independent apoptosis. Cell survival relative to untreated samples was analyzed using CellTiter-Glo assay (Promega). $n = 11$ for each time point and genotype.
- E mRNA expression analysis (RT-qPCR) of p53 target genes in thymocytes 6 h after 6 Gy irradiation. Shown are expression values normalized to β -actin.
- F–I Mice of indicated genotype were subjected to 6 Gy whole-body irradiation and pulse-labeled with 120 mg/kg BrdU 2 h before sacrifice at different time points. Small intestines were stained for (F) apoptosis (TUNEL) and (G) proliferation (BrdU); scale bars 50 μm . Red arrowheads highlight TUNEL-positive apoptotic cells. (H,I) Quantification for $n = 3$ mice/genotype (150 crypts/mouse).
- Data information: All data are shown as mean \pm SD. P values were calculated by 2-way ANOVA with Sidak's multiple comparisons test.

Embryonic lethality of *Mdm2* knock-out animals is also rescued by p53 missense mutations such as *Trp53*^{R246S} and *Trp53*^{R172H} that mimic human hot-spot mutants p53^{R249S} and p53^{R175H}, respectively (Lee *et al.*, 2012). Moreover, the apoptosis-deficient mutant p53^{R172P} also rescued *Mdm2*^{-/-} embryos, but the newborn mice showed severe developmental defects and died soon due to ROS-dependent hematopoietic failure (Abbas *et al.*, 2010). Surprisingly, we observed a clear deviation from the expected Mendelian distribution in intercrosses of double heterozygous *Trp53*^{+/-EE};*Mdm2*^{+/-} animals. Notably, no *Trp53*^{EE/EE};*Mdm2*^{-/-} pups were born alive, indicating that those embryos died *in utero* (Fig 3A). In contrast, upon breeding *Trp53*^{+/-};*Mdm2*^{+/-} mice as controls, viable double homozygous offspring was obtained as expected (Fig 3B). *Trp53*^{EE/EE};*Mdm2*^{-/-} embryos displayed severe developmental defects starting at days E9.5–10.5 (Fig 3C and D), and no living *Trp53*^{EE/EE};*Mdm2*^{-/-} embryos were recovered after day E12.5 (Fig 3D). Immunohistochemical analysis of tissue sections revealed strong accumulation of p53 protein in *Trp53*^{EE/EE};*Mdm2*^{-/-} embryos compared to *Trp53*^{EE/EE};*Mdm2*^{+/-} controls accompanied by high levels of apoptosis (Fig 3E). We conclude that *Trp53*^{EE/EE};*Mdm2*^{-/-} embryos survive approximately 1 week longer than *Trp53*^{+/+};*Mdm2*^{-/-} embryos which further underlines the functional defect of p53EE. Importantly, the failure of p53EE to completely rescue *Mdm2*-deficient embryos from lethality distinguishes p53EE from the p53 knock-out and reveals residual cytotoxic activities of p53EE with severe biological consequences *in vivo*.

However, the lethality of *Trp53*^{EE/EE};*Mdm2*^{-/-} embryos contrasted with the lack of any detectable cytotoxic activity of the *Mdm2* inhibitor Nutlin in p53^{EE/EE} MEFs (Fig 2C). Of note, Nutlin specifically disrupts the interaction between p53 and *Mdm2* leading to p53 stabilization, but does not inhibit many other *Mdm2* functions, such as its p53-independent metabolic role in ROS detoxification (Riscal *et al.*, 2016). As the p53EE-mediated senescence in late passage cultures was linked to both p53 accumulation and ROS (Fig EV3), we hypothesize that the lethality of *Trp53*^{EE/EE};*Mdm2*^{-/-} embryos also results from the combination of p53EE stabilization and increased ROS, which are both consequences of *Mdm2* ablation.

Pharmacological inhibition of *Mdm2* unleashes cytotoxic activities of p53EE

This prompted us to investigate whether accumulation of p53EE caused by loss of *Mdm2* sensitizes cells to doxorubicin whose cytotoxicity involves ROS- and DNA damage-dependent mechanisms

(Trachootham *et al.*, 2009; Huang *et al.*, 2011). Because of the embryonic lethality, we could not establish *Trp53*^{EE/EE};*Mdm2*^{-/-} MEFs and used *Trp53*^{-/-};*Mdm2*^{-/-} (DKO) MEFs ectopically expressing p53EE from a tetracycline-activated promoter instead (DKO-tetEE). As expected, in the absence of tetracycline the DKO-tetEE MEFs were as resistant to doxorubicin as the parental DKO cells but showed significantly elevated levels of apoptosis in response to doxorubicin treatment following induction of p53EE expression (Fig 4A). In compliance with the DNA binding deficiency of p53EE, this was not accompanied by transcriptional activation of key pro-apoptotic p53 target genes (Fig 4B).

Next, we tested whether pharmacological inhibition of *Mdm2* with Nutlin has a similar effect on E1A-MEFs with endogenous expression of p53EE. While Nutlin or doxorubicin alone had no or minimal effects on p53^{EE/EE} MEFs, combined treatment of p53^{EE/EE} cells with Nutlin and doxorubicin caused significant, p53-dependent reduction in proliferation and survival (Fig 4C and D). Similar cytotoxic activity was also observed when doxorubicin was combined with other *Mdm2* inhibitors (Fig 4E), excluding toxic off-target effects of Nutlin as an explanation. Cell death involved cleavage of Parp and caspase-3, but upregulation of p53 target genes was not detectable (Fig 4F and G).

The Hsp90 inhibitor ganetespib, which targets mutant p53 for proteasomal degradation, efficiently degraded p53EE in E1A-MEFs, highlighting a role for Hsp90 in p53EE stability (Fig 4H). p53EE degradation itself was not associated with apoptosis, indicating that E1A-MEFs are not dependent on p53EE. In line with the role of *Mdm2* for ganetespib-induced mutant p53 degradation (Li *et al.*, 2011), p53EE degradation by ganetespib was prevented when administered simultaneously with Nutlin (Fig 4H). Pre-treatment with ganetespib, however, led to p53EE degradation and efficiently counteracted the apoptosis induced by sequential treatment with Nutlin plus doxorubicin, thereby validating stabilized p53EE as the mediator (Fig 4H).

As wild-type p53 exerts direct, non-transcriptional, pro-apoptotic effects at the mitochondria (Mihara *et al.*, 2003; Chipuk *et al.*, 2004; Leu *et al.*, 2004; Le Pen *et al.*, 2016), we tested for mitochondrial localization of p53EE (Fig 4I). Remarkably, mitochondrial fractions of untreated p53^{EE/EE} MEFs contained p53 at levels similarly high as p53^{+/+} cells following doxorubicin treatment. The amount of mitochondrial p53EE increased even further under doxorubicin treatment. The increased amount of p53EE at the mitochondria could therefore provide a plausible explanation for the sensitivity of p53^{EE/EE} MEFs to apoptotic stimuli even in the absence of p53 target gene activation.

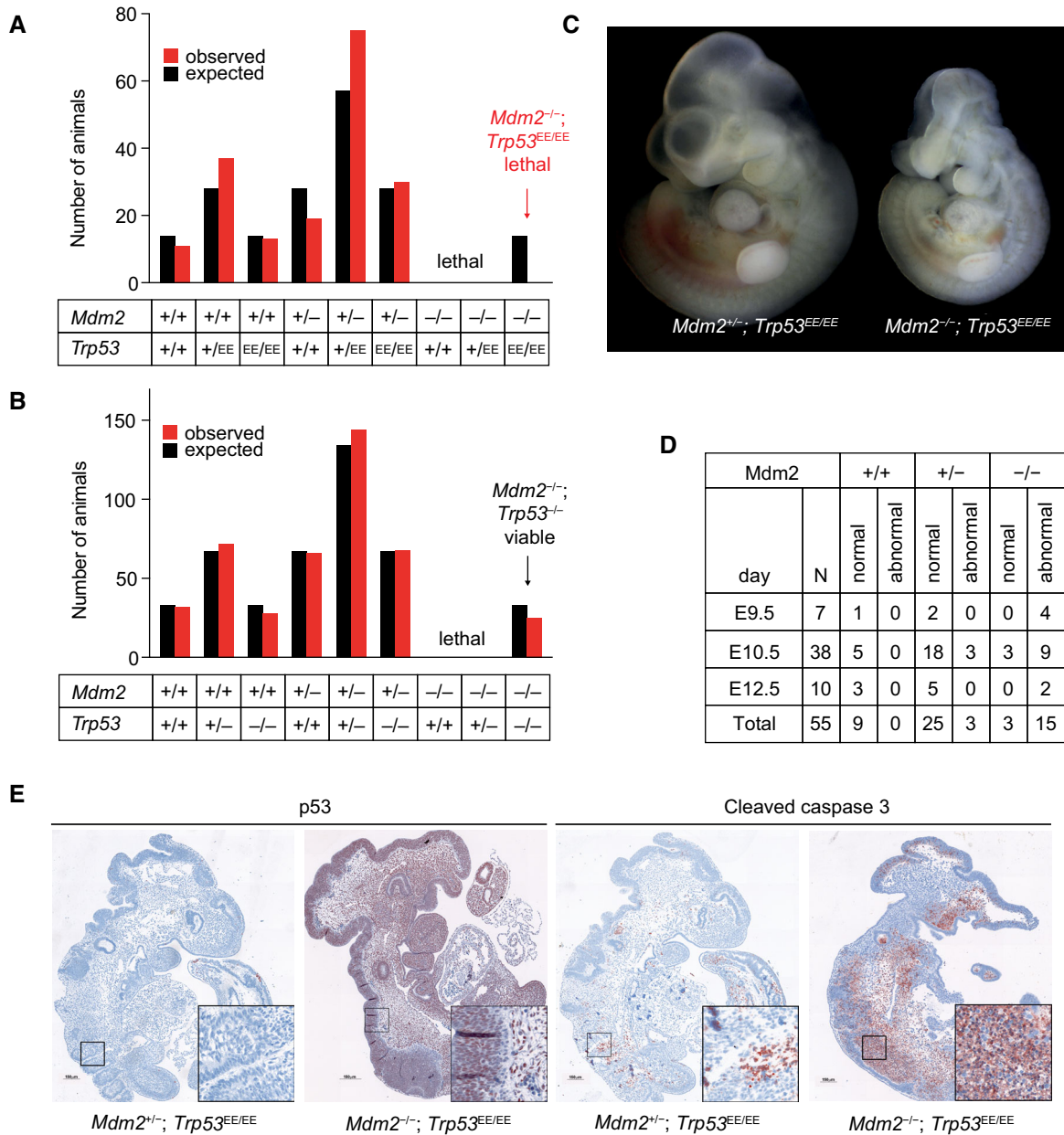


Figure 3. Lethality of p53EE embryos in the absence of Mdm2.

A Observed and expected genotype distribution of newborn offspring from mating *Mdm2*^{+/-}*Trp53*^{EE/+} mice (total number of pups *n* = 185; contingency test *P* = 0.0029).
 B Observed and expected genotype distribution of newborn offspring from mating *Mdm2*^{+/-}*Trp53*^{+/-} mice (total number of pups *n* = 435; contingency test *P* = 0.912).
 C Representative picture of an E9.5 *Mdm2*^{+/-}*Trp53*^{EE/EE} embryo (right) displays characteristic phenotypic abnormalities compared to an *Mdm2*^{+/-}*Trp53*^{EE/EE} embryo (left).
 D Phenotype analysis of *Trp53*^{EE/EE} embryos with different *Mdm2* genotypes reveals developmental defects in *Mdm2*^{-/-}*Trp53*^{EE/EE} embryos starting from E9.5.
 E IHC for p53 and cleaved caspase-3 shows strong accumulation of p53EE protein and massive apoptosis in *Mdm2*^{-/-}*Trp53*^{EE/EE} compared to *Mdm2*^{+/-}*Trp53*^{EE/EE} control embryos.

Residual apoptotic activities of mutant p53 in human cancer cells

To test whether p53EE is also capable of inducing apoptosis in human cancer cells, we generated a human p53-null H1299 lung cancer cell line with stable Tet-inducible expression of the human p53^{R181E} (p53EE) mutant. Overexpression of p53EE rendered H1299 cells, which express only barely detectable levels of Mdm2, sensitive

to doxorubicin, and addition of Nutlin further augmented this effect (Fig 5A). Cell death was inhibited by Q-VD-OPH, a blocker of caspase-dependent apoptosis, but not by the ferroptosis inhibitor ferrostatin as a control (Fig 5B). Annexin V staining revealed a p53-dependent increase in apoptotic cells under combined doxorubicin and Nutlin treatment, confirming the observed cell death as apoptotic (Fig 5C). p53EE-mediated apoptosis in H1299 cells occurred in

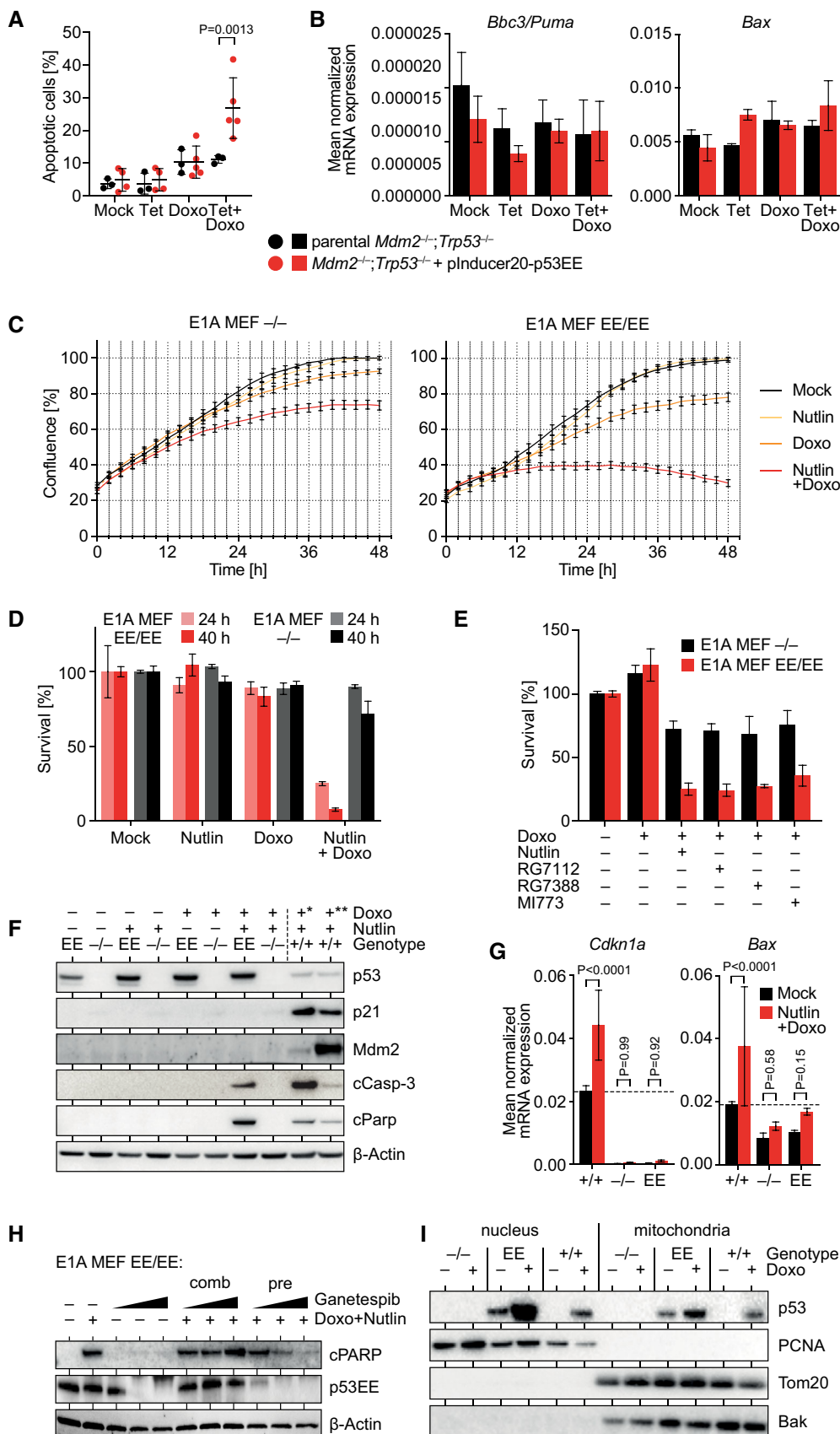


Figure 4.

Figure 4. Pharmacological inhibition of Mdm2 unleashes cytotoxic activities of p53EE.

- A *Mdm2*^{-/-}*Trp53*^{-/-} (double knock-out, DKO) MEFs were transduced with plnducer20-p53EE lentivirus to enable tetracycline (Tet)-inducible expression of mouse p53EE. Induction of p53EE sensitized cells to apoptosis induced by 24-h treatment with 1 μg/ml doxorubicin (Doxo) as detected by flow cytometry for annexin V.
- B mRNA expression of p53 target genes was measured in cells from (A) relative to β-actin by RT-qPCR following treatment with Tet ± 1 μg/ml Doxo. Expression of the pro-apoptotic p53 target genes *Bbc3* (Puma) and *Bax* is not significantly induced. *n* = 6.
- C Proliferation of MEFs with indicated genotypes was analyzed by live-cell imaging in the presence of 10 μM Nutlin-3a (Nutlin) and/or 0.05 μg/ml doxorubicin (Doxo). Shown is the median confluence ± SEM (*n* = 12).
- D, E Cell viability assays for MEFs with indicated genotypes treated with Mdm2 inhibitors ± 0.4 μg/ml Doxo. *n* = 3.
- F Western blot of E1A-MEFs with indicated genotypes treated with 10 μM Nutlin ± 0.4 μg/ml Doxo for 18 h reveals induction of apoptosis (cCasp-3, cleaved caspase-3; cParp, cleaved Parp) in double-treated p53^{EE/EE} MEFs in the absence of p53 target gene (p21, Mdm2) activation. *10 h 0.4 μg/ml Doxo; **10 h 0.2 μg/ml Doxo.
- G mRNA expression of p53 target genes was measured in E1A MEFs of indicated genotype relative to β-actin by RT-qPCR following combined treatment with 10 μM Nutlin and 1 μg/ml Doxo. *n* = 12.
- H Western blot of p53^{EE/EE} E1A-MEFs with indicated genotypes treated for 18 h with 10 μM Nutlin, 0.4 μg/ml Doxo, and 30–100–500 nM ganetespib as indicated. Comb, combined treatment with 3 drugs for 18 h. Pre, pre-treatment with ganetespib for 24 h followed by combined treatment with Nutlin and doxorubicin for 18 h.
- I Western blot of cellular fractions from unstressed and Doxo-treated MEFs of indicated genotype identifies p53EE protein in the mitochondrial fraction. PCNA and Tom20/Bak are shown as nuclear and mitochondrial marker proteins.

Data information: All data are shown as mean ± SD unless indicated otherwise. Significance was tested between the two cell lines or treatments. *P* values were calculated by 2-way ANOVA with Sidak's multiple comparisons test.

the absence of detectable p53 target gene activation (Fig 5D). Proximity ligation experiments demonstrated a specific co-localization of p53EE with the outer mitochondrial membrane protein Tom20 in untreated and, even more, in doxorubicin-treated cells (Fig 5E and F). p53EE co-localization was also observed with the Bcl-2 family members Bcl-xL, Bcl-2, and Bak (Fig 5F), which were previously shown to specifically interact with wild-type but not mutant p53 (Mihara *et al*, 2003; Leu *et al*, 2004; Pietsch *et al*, 2008). Mitochondrial activities of wild-type p53 “prime” mitochondria to mitochondrial depolarization by BH3 peptides (Montero *et al*, 2015; Le Pen *et al*, 2016). In support of a direct mitochondrial apoptotic priming activity, p53EE expression sensitized H1299 cells to mitochondrial depolarization by BID BH3 peptides (Fig 5G).

The apoptotic activity of p53EE raised the question of whether p53 mutants in cancer patients can also retain apoptotic activity. Although p53EE (R181E) is not found in cancer patients, various other cooperativity mutations have been recurrently identified as somatic cancer mutations and account for an estimated 34,000 new cancer cases each year (Leroy *et al*, 2014). R181 mutations were also reported as germline alterations associated with a family history of cancer, identifying them as *bona fide* driver mutations (Freboung *et al*, 1992; Leroy *et al*, 2014). In particular, R181L was among the first p53 cancer mutants reported to be specifically deficient for binding and activating pro-apoptotic target genes while retaining regulation of other genes such as *CDKN1A* and *MDM2* (Ludwig *et al*, 1996; Schlereth *et al*, 2010a). Consistently, R181L failed to induce apoptosis when overexpressed irrespective of Nutlin treatment (Fig 5H). However, R181L—like p53EE—effectively triggered apoptosis when combined with doxorubicin and Nutlin (Fig 5H). As with p53EE, apoptosis occurred without activation of the key pro-apoptotic p53 target gene *Puma* (Fig 5I). In contrast, the R175P mutant, which also lacks the ability to transactivate pro-apoptotic target genes but belongs to the class of structural mutations (Rowan *et al*, 1996; Liu *et al*, 2004), failed to trigger apoptosis in the presence of doxorubicin and Nutlin (Fig 5H). We conclude that, in principle, also cancer mutants can trigger apoptosis when stimulated sufficiently with Nutlin and doxorubicin in a manner depending on the identity of the individual mutant.

p53EE fails to suppress tumor development

To investigate the role of DNA binding cooperativity for tumor suppression, we aged cohorts of EE mutant mice. Surprisingly, despite evidence for residual apoptotic activity of p53EE (Figs 3–5), homozygous p53^{EE/EE} and hemizygous p53^{EE/-} mice developed tumors very rapidly resulting in a short median survival of 150 and 128 days, respectively (Fig 6A). This was not significantly different from p53^{-/-} animals. Heterozygous p53^{EE/+} showed an intermediate median survival of 519 days that was not significantly altered as compared to p53^{+/-} mice (Fig 6A). The lack of a difference in survival between p53^{EE/+} and p53^{+/-} mice, despite evidence for a dominant-negative activity of p53EE in overexpression studies (Schlereth *et al*, 2010a), is reminiscent of mice heterozygous for the hot-spot mutants R172H and R270H and consistent with the hypothesis that dominant-negative effects might require prior mutant p53 stabilization (Lang *et al*, 2004; Olive *et al*, 2004).

As previously reported for p53^{-/-} animals, the tumor spectra of p53^{EE/EE} and hemizygous p53^{EE/-} were dominated by thymic lymphoma (Fig 6B; Appendix Table S1). Additional tumor types were B-cell lymphomas, sarcomas, and testicular tumors (Appendix Table S1). The tumors of p53^{EE/+} were similar to those of p53^{+/-} mice and mostly non-thymic lymphomas, sarcomas, and several types of carcinoma (Fig 6B, Appendix Table S2).

Unlike what has been reported for the p53 hot-spot mutants R172H or R270H, we did not observe an increase in metastatic tumors in p53^{EE/EE} and p53^{EE/-} compared to p53^{-/-} and p53^{+/-} mice (Appendix Table S1), suggesting a lack of GOF properties of the EE mutant. For hot-spot mutants, constitutive stabilization was identified as a prerequisite for GOF effects (Terzian *et al*, 2008). Similar as described for tumors in R172H-mutant mice (Terzian *et al*, 2008), we noted varying levels of p53EE expression in spontaneous tumors arising in p53^{EE/EE} or p53^{EE/-} mice, with a high fraction (67%) of p53^{EE/EE} tumors exhibiting p53EE stabilization comparable to p53-mutated human cancer samples (Figs 6C and EV4 and EV5). This indicates that the absence of a pro-metastatic GOF cannot be explained by a lack of constitutive p53EE stabilization and suggests that p53EE, similar to p53 mutants like R246S or

G245S (Lee *et al*, 2012; Hanel *et al*, 2013), lacks the pro-metastatic GOF activity described for R172H and R270H (Olive *et al*, 2004).

To explore whether p53EE can counteract oncogene-induced tumorigenesis in a genetically more defined setting, we crossed p53EE animals with Eμ-Myc mice which serve as a

well-characterized model of Burkitt-like B-cell lymphoma (Adams *et al*, 1985). Loss of p53 is known to strongly accelerate lymphoma development in this model (Schmitt *et al*, 1999). We observed that Eμ-Myc;p53^{EE/+} mice survived markedly shorter than Eμ-Myc;p53^{+/+} but not significantly longer than Eμ-Myc;p53^{+/-} mice

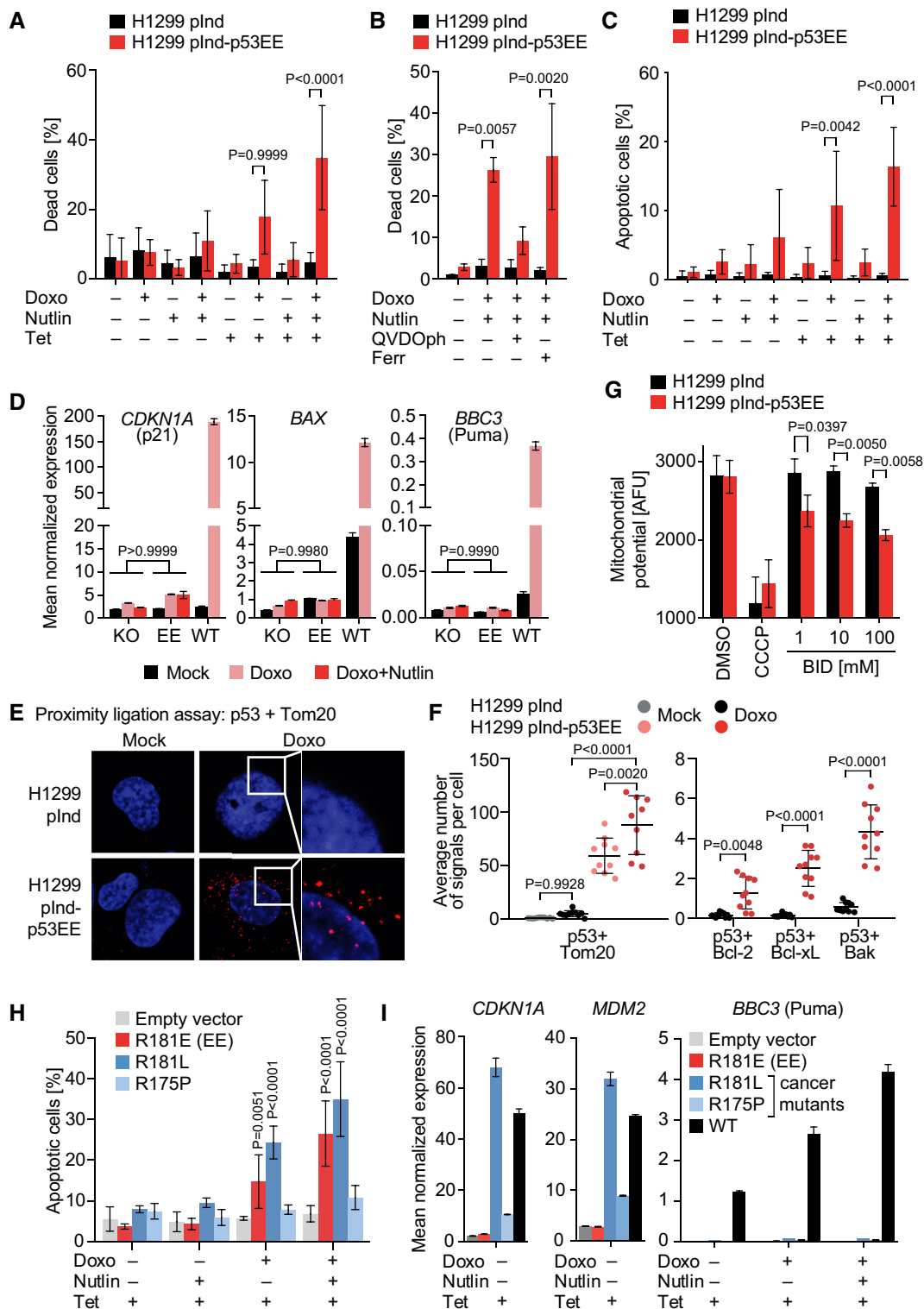


Figure 5.

Figure 5. Residual apoptotic activities of mutant p53 in human cancer cells.

- A, B Cell death measured by flow cytometry using propidium iodide exclusion in human lung adenocarcinoma H1299 cells with Tet-inducible expression of human p53EE. Cells with overexpression of human p53EE mutant display a trend of increased cell death after treatment with 0.5 µg/ml Doxo. This effect is enhanced by addition of Nutlin and blocked by the pan-caspase inhibitor QVDOPh, but not the ferroptosis inhibitor ferrostatin-1 (Ferr) as control. (A) $n = 3$; (B) $n = 2$.
- C Apoptosis analysis using annexin V staining in cells from (A). $n = 3$.
- D mRNA expression analysis (RT-qPCR) of p53 target genes following treatment with 0.5 µg/ml Doxo ± 10 µM Nutlin. KO, Tet-induced H1299-plnd cells; EE, Tet-induced H1299-plnd-p53EE cells; WT, H460 cells. mRNA expression was normalized to β-actin; $n = 3$.
- E Proximity ligation assay for p53 with Tom20 in indicated untreated (Mock) or Doxo-treated (0.1 µg/ml, 24 h) H1299 cells following Tet induction. Shown are representative cells with PLA signals (red) counterstained with DAPI (blue).
- F Quantification of proximity ligation assays for p53EE with Tom20, Bcl-2, Bcl-xL, and Bak in H1299 cells. Doxo treatment (0.1 µg/ml, 24 h) as indicated. Plotted is the average number of PLA signals per cell for 10 fields of view.
- G Mitochondrial membrane potential of control and p53EE-expressing H1299 cells in the absence and presence of increasing concentrations of BID BH3 peptide. Treatment with the mitochondrial depolarizer CCCP is shown as a positive control; $n = 3$.
- H Apoptosis measured by flow cytometry using annexin V in H1299 cells with Tet-inducible expression of the indicated human p53 mutants; $n = 3$.
- I mRNA expression analysis (RT-qPCR) of p53 target genes normalized to β-actin; $n = 3$.

Data information: All data are shown as mean ± SD. Significance was tested by 2-way ANOVA with Sidak's multiple comparisons test. Source data are available online for this figure.

(Fig 6D). Likewise, in a model of acute myeloid leukemia induced by co-expression of the AML1/ETO9a (AE9) fusion oncoprotein and oncogenic Nras^{G12D} (Nras) (Zuber *et al*, 2009), we observed fast malignant transformation of p53^{EE/EE} hematopoietic stem cells (HSCs) and disease progression. Recipient mice transplanted with AE9+Nras-transduced p53^{EE/EE} or p53^{-/-} HSCs succumbed to AML with indistinguishably short latency and significantly earlier than mice transplanted with AE9+Nras-transduced p53^{+/+} HSCs (Fig 6E). Notably, distinct from heterogenous p53EE stabilization in spontaneous tumors (Figs 6C and EV5), p53EE was highly accumulated in all lymphomas from Eµ-Myc;p53^{EE/+} mice and in all AE9+Nras;p53^{EE/EE} AML samples (Fig 6F and G). As stabilization of mutant p53 involves protection from Mdm2-mediated degradation (Terzian *et al*, 2008), the uniform p53EE accumulation might be explained by the exceptionally strong oncogenic signaling through enforced expression of Myc and mutant Nras which inhibits Mdm2 via p19Arf (Zindy *et al*, 1998).

Taken together, these data show that p53EE is inadequate to counteract spontaneous and oncogene-induced tumorigenesis in mice, proving DNA binding cooperativity to be absolutely essential for tumor suppression by p53 even in the presence of residual apoptotic functions.

p53EE confers survival benefit under chemotherapy

The lack of detectable tumor suppressor activity implies that the residual apoptotic activities are not effectively counter-selected during tumorigenesis and can be retained by cancer mutants—the R181L cooperativity mutant being one example (Fig 5H). In fact, p53EE was even constitutively stabilized in various tumor types arising in p53^{EE/EE} mice (Fig 6), indicating escape from Mdm2-mediated degradation. We therefore explored whether this accumulation of p53EE suffices to sensitize tumor cells to cytotoxic stress and provide a therapeutic window for tumor treatment. First, we investigated whether p53EE influences the response of Eµ-Myc lymphoma cells to mafosfamide (MAF), a cyclophosphamide (CTX) analogue active *in vitro*. We established lymphoma cell lines from Eµ-Myc mice with different p53 genotypes (p53^{+/+}, p53^{+/-}, and p53^{+/EE}). Lymphomas from p53^{+/EE} mice (and p53^{+/-} mice) showed the expected loss of the wild-type allele and strongly expressed p53EE as described above (Fig 6F). In comparison with

the rapid and strong response of p53^{+/+} lymphoma cells to MAF treatment, induction of apoptosis started in p53EE cells only after 6 h and gradually increased up to significantly elevated levels of 60–70% at 24 h, whereas p53-null lymphoma cells showed no response (Fig 7A). To test whether the increased sensitivity of p53EE lymphoma cells is directly p53EE-mediated, the lymphoma cells were transduced with a Tet-inducible, red fluorescence protein (RFP)-coupled shRNA to knockdown p53EE expression. RFP-positive, i.e., p53 shRNA-expressing, lymphoma cells became significantly enriched under MAF treatment in a dose-dependent manner, identifying the enhanced cytotoxic response of p53EE lymphoma cells as directly p53EE-mediated (Fig 7B). In support of a non-transcriptional mechanism, the cytotoxic response was not preceded by an upregulation of p53 target genes (Fig 7C).

Next, we transplanted primary lymphomas into syngeneic recipients. After lymphomas became palpable in the peripheral lymph nodes, each cohort was divided into two groups—one was subjected to a single injection of 300 mg/kg CTX, and the second was left untreated (Fig 7D). Independent of p53 genotype, the disease progressed rapidly with similar kinetics in untreated control mice, whereas all treated animals responded well to CTX therapy and went into clinical remission. In line with previous studies (Schmitt *et al*, 1999, 2002b), p53^{-/-} lymphomas rapidly relapsed in all mice, which resulted in a very modest median survival benefit of 19 days. In contrast, all mice transplanted with p53^{+/+} lymphomas remained in complete remission during the whole period of observation (90–180 days after treatment). Importantly, the chemotherapy was also effective for treatment of p53EE lymphoma, provided a median survival benefit of 30 days, and—even more compelling—yielded a complete tumor-free remission in 36% of animals (Fig 7D and E). To monitor the therapy response quantitatively, we measured residual disease in the spleen with a sensitive qPCR copy number assay for the Eµ-Myc transgene of moribund lymphoma mice and non-transgenic littermates as positive and negative controls, respectively (Fig 7F). Tumor load in mice with p53^{+/+} lymphoma decreased by > 3 orders of magnitude within 24 h after treatment and dropped below the detection limit by 7 days, consistent with the uniform long-term clinical remission in this cohort. In line with the delayed apoptotic response of p53EE lymphoma cells *in vitro* (Fig 7A), we observed only a slight, but significant, decline in tumor load at 24 h in p53EE compared to p53^{-/-} lymphoma

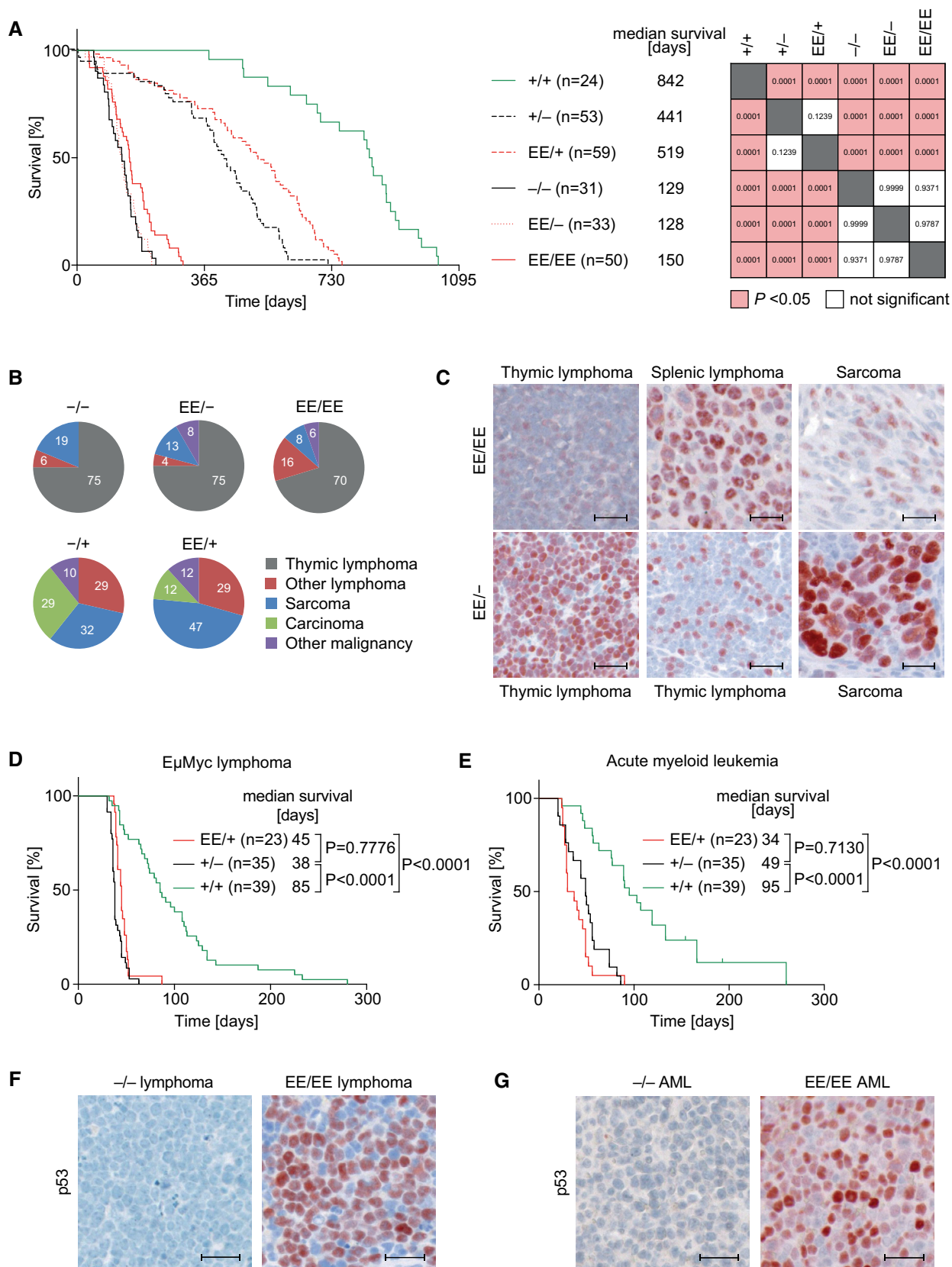


Figure 6.

Figure 6. p53EE fails to suppress tumor development.

- A Kaplan–Meier survival plots for mice with indicated genotypes, number of mice, and median survival. *Right panel*, analysis of survival differences using the log-rank (Mantel–Cox) test.
- B Spectra of malignant tumors found in mice with indicated genotypes ($p53^{-/-}$ $n = 16$; $p53^{EE/-}$ $n = 24$; $p53^{EE/EE}$ $n = 37$; $p53^{+/-}$ $n = 28$; $p53^{EE/+}$ $n = 17$).
- C p53 immunohistochemistry (IHC) in representative spontaneous tumors; scale bars 25 μm .
- D Kaplan–Meier survival plots for $\text{E}\mu\text{-Myc}$ transgenic mice with different p53 genotype.
- E Kaplan–Meier survival plots for wild-type recipient mice transplanted with AML1/ETO9a + Nras^{G12D}-transduced fetal liver cells (5 donors/genotype).
- F, G p53 IHC for representative samples from (D) and (E) illustrates constitutive stabilization of p53EE in cancer cells; scale bars 25 μm .

Data information: Survival differences were analyzed using the log-rank (Mantel–Cox) test. Multiple survival curves were compared by ordinary ANOVA with Tukey's multiple comparisons test.

mice. By 7 days, however, tumor cells had become undetectable in 3 of 5 p53EE lymphoma mice, indicating molecular remission, whereas p53^{-/-} lymphoma cells remained detectable in all animals of the p53^{-/-} group.

To validate in a second independent model that p53EE enhances the chemotherapy response *in vivo*, we transplanted syngeneic recipient mice with AE9/Nras-driven acute myeloid leukemia cells with different p53 genotypes and monitored disease progression by bioluminescence imaging (Fig 7G). p53^{+/+} leukemia cells responded well to a standard chemotherapy protocol with cytarabine (AraC) combined with doxorubicin, which yielded a significant survival benefit (Fig 7G and H). p53^{-/-} leukemia rapidly killed the transplanted animals irrespective of therapy. In striking contrast, chemotherapy controlled progression of p53^{EE/EE} leukemia remarkably well, which translated into a significantly improved survival (Fig 7G and H).

Discussion

Our results obtained with the R178E cooperativity mutation in different mouse cancer models illustrate that a p53 mutant can be as inefficient as a p53 knock-out allele in preventing tumor development and yet retain residual apoptotic activity. Taken together, this indicates that residual apoptotic p53 functions on their own are unable to counteract tumorigenesis, are therefore not efficiently counter-selected, and can be retained by mutant p53 during tumor evolution. Importantly, these residual cytotoxic activities can be triggered by chemotherapeutics to induce a survival benefit, especially when mutant p53 is constitutively or pharmacologically stabilized. Superior chemotherapy responses in p53-mutated versus p53-deficient tumors challenge the current view that a p53 missense mutation invariably signals a worse prognosis than a gene deletion.

p53WT is capable of inducing cell death through multiple pathways including apoptosis, necrosis, and ferroptosis. The cytotoxic activity of p53EE is apoptotic in nature as shown by caspase cleavage (Figs 3E and 4F and H), phosphatidylserine externalization (Figs 4A and 5C and H), and blockage by caspase inhibitors, but not ferroptosis inhibitors (Fig 5B). p53WT induces apoptosis by transcriptional upregulation of pro-apoptotic target genes such as PUMA, NOXA, and BAX in combination with non-transcriptional mechanisms mediated through protein–protein interactions with Bcl-2 family members, which lowers the threshold for engaging the mitochondrial apoptosis pathway (Mihara *et al*, 2003; Chipuk *et al*, 2004; Leu *et al*, 2004; Le Pen *et al*, 2016). The lack of detectable DNA binding and target gene regulation by p53EE suggested that its pro-apoptotic activity relies primarily on the non-transcriptional pathway, and we demonstrate that p53EE efficiently localizes to the

mitochondria (Figs 4I and 5E and F), interacts with Bcl-2 family members (Fig 5F), and primes cells to mitochondrial depolarization by BH3 peptides (Fig 5G). In addition, we provide evidence that p53EE, similar to other p53 mutants, interferes with Nrf2 transcriptional activity, which is critical not only for ROS defense, but also for the respiratory function of mitochondria, their biogenesis, and integrity (Dinkova-Kostova & Abramov, 2015). It is therefore tempting to speculate that direct activities of p53 at the mitochondria and indirect effects through Nrf2-inhibition synergistically prime the mitochondria and lower the apoptotic threshold. Nevertheless, we cannot formally exclude that p53EE under conditions of maximal stimulation induces pro-apoptotic target genes to a degree that is below our detection limit. As embryonic development is very sensitive to deregulated p53 activity, residual transcriptional activity of p53EE could in principle explain the $Trp53^{EE/EE};Mdm2^{-/-}$ embryonic lethality. And indeed, it was shown that a single hypomorphic $Trp53^{neo}$ allele ($Trp53^{neo/-}$) that shows ~7% activity is compatible with $Mdm2^{-/-}$ embryonic development, whereas $Trp53^{neo/neo}$ homozygosity, yielding ~16% activity, already triggers embryonic lethality (Wang *et al*, 2011). However, deregulated p53 can cause embryonic lethality by multiple pathways including apoptosis, ferroptosis, or cell growth arrest (Jiang *et al*, 2015; Moyer *et al*, 2017). Whether $Trp53^{neo/neo};Mdm2^{-/-}$ embryos die by apoptosis was not reported. In general, low p53 levels or reduced p53 DNA binding cooperativity primarily activates homeostatic survival functions, while only strongly elevated and prolonged expression levels shift the cellular response to apoptosis (Chen *et al*, 1996; Vousden & Lu, 2002; Vousden & Lane, 2007; Schlereth *et al*, 2013; Timofeev *et al*, 2013). This is mechanistically explained by higher affinity and torsionally more flexible p53 response elements in target genes regulating, for example, cell proliferation (Murray-Zmijewski *et al*, 2008; Riley *et al*, 2008; Schlereth *et al*, 2010b, 2013; Jordan *et al*, 2012) and a higher target gene expression threshold for triggering apoptosis (Kracikova *et al*, 2013). If p53EE regains residual transcriptional activity upon massive stimulation, it would be difficult to envision why this resulted in apoptosis instead of cell cycle arrest (Figs 3–5). Last but not least, the charge inversion associated with the arginine to glutamic acid substitution in p53EE might affect protein–protein interactions that are responsible for its pro-apoptotic activity. However, the same pro-apoptotic activity is seen for the charge-neutralizing R181L mutation (Fig 5H), excluding the negatively charged glutamic acid residue as the underlying cause. Altogether, we therefore favor the hypothesis that p53EE triggers apoptosis primarily through non-transcriptional mechanisms.

From a clinical perspective, it will be interesting to investigate which p53 mutants in cancer patients display residual apoptotic activity, as p53EE is not a naturally occurring mutation. Since

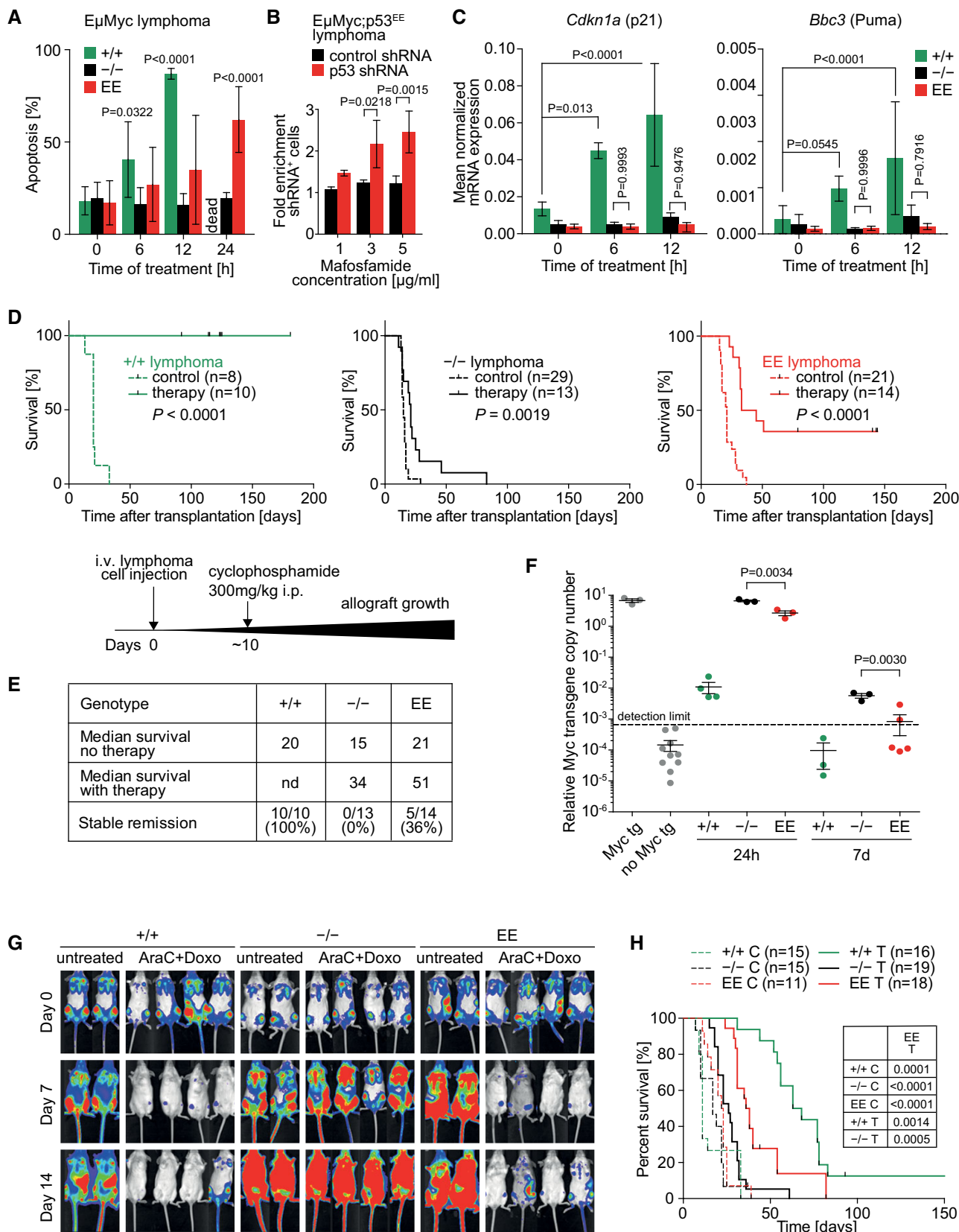


Figure 7.

Figure 7. p53EE confers survival benefit under chemotherapy.

- A Apoptosis in Eμ-Myc lymphoma cells of indicated genotype was measured by flow cytometry (FITC-VAD-FMK staining) at indicated time points after treatment with 3 μg/ml MAF. Significance was calculated versus untreated. $n \geq 5$.
- B Enrichment of p53 shRNA-expressing Eμ-Myc;p53^{EE} lymphoma cells under MAF treatment. Non-silencing control shRNA served as control. $n = 3$.
- C mRNA expression of p53 target genes was measured relative to β-actin by RT-qPCR following treatment of Eμ-Myc lymphoma cells of indicated genotype with 3 μg/ml MAF. $n \geq 3$.
- D, E Kaplan–Meier survival plots for cyclophosphamide-treated versus untreated control mice transplanted with Eμ-Myc lymphoma cells of indicated genotype at day 0. Treatment started ~10 days later when peripheral lymph nodes became palpable. The time course of the experiment is illustrated in a scheme. (E) Summary of data from (D). Survival differences were analyzed using the log-rank (Mantel–Cox) test.
- F Residual disease in the spleen of mice from (D) was quantified 24 h and 7 days after therapy using a quantitative PCR assays with primers specific to the Eμ-Myc transgene (present only in lymphoma cells). Shown is the copy number of the Eμ-Myc transgene relative to a control locus present in all cells. Untreated Eμ-Myc mice (Myc tg) were used as positive control. Non-transgenic mice (no Myc tg) served as negative controls to define the detection limit. Significance was tested by *t*-test (two-sided, unpaired).
- G Representative bioluminescence imaging (BLI) pictures of mice transplanted with AE9+Nras AML cells. Day 0 indicates the start of combination therapy with cytarabine (AraC) + doxorubicin (Doxo).
- H Kaplan–Meier survival plots for animals from (G). Statistical significance of differences calculated by log-rank (Mantel–Cox) test between treated Eμ-Myc;p53^{EE/EE} AML and all other groups is indicated in the table. C, untreated control; T, therapy (AraC+Doxo).

Data information: All data are shown as mean ± SD. Significance was tested by 2-way ANOVA with Sidak's multiple comparisons test unless indicated otherwise.

protein–protein interactions with Bcl-2 family members that account for non-transcriptional apoptosis by p53^{WT} (Mihara *et al*, 2003; Chipuk *et al*, 2004; Leu *et al*, 2004; Le Pen *et al*, 2016) are disrupted by many cancer-derived p53 mutations, such mutations are believed to be “dual hits” which simultaneously inactivate both DNA binding-dependent and non-transcriptional mechanisms of p53-triggered apoptosis (Mihara *et al*, 2003; Tomita *et al*, 2006). However, this has only been shown for a small subset of mainly hot-spot mutants and cannot be directly extrapolated to the entire, functionally and structurally highly diverse, spectrum of > 2,000 distinct p53 mutations observed in cancer patients. The p53^{EE} mutant provides evidence that transcriptional and non-transcriptional apoptotic functions can be genetically separated. Remarkably, the selective loss of p53 DNA binding in the presence of intact non-transcriptional apoptotic activity is just as efficient to promote tumorigenesis as the complete loss of p53 (Fig 6A, D and E), suggesting that the non-transcriptional activity of p53 is insufficient to prevent tumor development on its own. Of note, this does not exclude a supportive role of mitochondrial p53 functions for transcription-dependent apoptosis and is compatible with the model of mitochondrial priming by p53 that sensitizes to p53-induced target genes encoding the BH3-only proteins Puma and Noxa (Chipuk *et al*, 2005; Le Pen *et al*, 2016).

While the most common hot-spot mutants are thermodynamically destabilized and therefore structurally denatured, many non-hot-spot mutants retain the ability to regulate some *bona fide* p53 target genes like p21 (Ludwig *et al*, 1996; Rowan *et al*, 1996; Campomenosi *et al*, 2001). The ability to bind p53 response elements in target promoters implies sufficient structural stability to engage also in p53^{WT}-like protein–protein interactions. We therefore anticipated that non-transcriptional apoptotic activities are retained primarily among non-hot-spot mutants, especially those with only a partial loss of DNA binding activity (Campomenosi *et al*, 2001). Several cooperativity mutants that together account for an estimated 34,000 cancer cases per year (Leroy *et al*, 2014) have selectively lost the ability to transactivate pro-apoptotic target genes (Ludwig *et al*, 1996; Schlereth *et al*, 2010a). Here, we have examined the R181L mutant that has been identified as both a somatic and germline mutation in cancer patients. Consistent with previous reports that R181L has a selective apoptosis defect (Ludwig *et al*, 1996; Schlereth *et al*, 2010a), we failed to detect apoptosis upon R181L overexpression (Fig 5H). However, just like with p53^{EE}, genotoxic doxorubicin treatment

revealed substantial pro-apoptotic activity, supporting the concept that a tumorigenic p53 mutant like R181L can retain residual apoptotic functions and support chemotherapy responses.

Intriguingly, the R175P mutant, which resembles the R181L mutant in its selective loss of pro-apoptotic target gene regulation (Ludwig *et al*, 1996; Rowan *et al*, 1996; Liu *et al*, 2004), failed to enhance apoptosis under identical conditions of doxorubicin treatment (Fig 5H). A possible explanation is that R175 is crucial for the structural integrity of the L2-L3 loop which interacts not only with the minor groove of DNA response elements but also with Bcl-2 family members (Cho *et al*, 1994; Bullock *et al*, 2000; Mihara *et al*, 2003; Tomita *et al*, 2006; Hagn *et al*, 2010). In contrast, R181 is solvent-exposed and R181 mutations do not affect the DBD 3D structure (Dehner *et al*, 2005). It is therefore tempting to speculate that in particular, cooperativity mutants of the H1 helix, which interfere with DNA binding but do not affect the interaction interface with DNA and Bcl-2 family members, have retained non-transcriptional apoptotic activity. A more detailed systematic analysis of the more than 2,000 different cancer mutants is needed to validate this hypothesis and possibly reveal further cancer mutants with a similar phenotype.

Recent studies have revealed that tumors can be addicted to pro-survival GOF activities of mutant p53 and respond to mutant p53 depletion with tumor regression (Alexandrova *et al*, 2015). Mutant p53-destabilizing drugs, such as the Hsp90 inhibitor ganetespib, are therefore considered a promising approach for treatment of p53-mutated tumors, and a first clinical trial combining chemotherapy with ganetespib for p53-mutated ovarian cancer patients has been initiated (Alexandrova *et al*, 2015; Bykov *et al*, 2018; Sabapathy & Lane, 2018). However, mouse models for the R246S (equivalent to human R249S) and humanized G245S mutants have shown that p53 mutations can be highly tumorigenic without exhibiting appreciable GOF activity (Lee *et al*, 2012; Hanel *et al*, 2013). The p53^{EE} mutant does not significantly decrease the latency of tumor development or enhance the incidence of metastatic tumors compared to p53 knock-out mice (Fig 6A; Appendix Tables S1 and S2). There was a trend for increased incidence of non-lymphoid tumors in homozygous p53^{EE} mice, but this was not statistically significant (Fig 6B), leading us to conclude that p53^{EE} does not exhibit the strong GOF activities observed for some hot-spot mutants. When tumors are not dependent on a mutant p53 GOF, its destabilization is expected to be therapeutically ineffective. More importantly, however, our data

imply that a combination of chemotherapy with mutant p53 destabilizing drugs could even turn out counterproductive or dangerous when chemotherapy-sensitizing effects are abolished by removal of the p53 mutant. In support of this, degradation of p53EE by ganetespib did not result in tumor cell death by itself and effectively counteracted the pro-apoptotic effect of combined doxorubicin and Nutlin treatment (Fig 4H).

Instead, our data suggest that tumors which contain a p53 mutant with residual apoptotic activity might require the opposite strategy. Chemotherapy responses of p53EE cells were enhanced in combination with Nutlin-3a or other Mdm2 inhibitors (Fig 4D and E). Enforced overexpression of the human p53EE (R181E) or the cancer mutant R181L strongly sensitized human lung cancer cells to chemotherapy-induced apoptosis, and this was further boosted by Nutlin-3a (Fig 5H). Similarly, lymphoma and leukemia cells with massive constitutive stabilization of p53EE displayed superior chemotherapy responses to p53-deficient tumor cells resulting in improved animal survival (Fig 7). Mutant p53-stabilizing therapies with Mdm2 inhibitors might therefore support chemotherapeutics to trigger the residual cytotoxic activities that have not been efficiently counter-selected during tumorigenesis. In fact, the first clinical studies with Mdm2 inhibitors have observed clinical responses also in a few patients with p53 mutations (Andreiff *et al*, 2016). Even though Mdm2 inhibitors were originally designed for patients with wild-type p53 tumors, they might eventually offer therapeutic benefit also for some p53-mutated cancer patients. Of course, a caveat to the treatment with mutant p53 stabilizing compounds is that pro-metastatic or pro-survival GOF activities might be boosted. The most promising therapy strategy for p53-mutated tumor patients will therefore strongly depend on the functional properties of the p53 mutant. Although it remains to be seen, which and how many p53 mutants have retained apoptotic activity during tumor evolution, our data call for more comprehensive investigations into the functional diversity of p53 mutations to make p53 mutation status more useful for clinical decision making.

Materials and Methods

Animals

For generation of the $Trp53^{LSL-R178E}$ knock-in mouse, we used the targeting vector for the $Trp53^{LSL-R172H}$ mouse, which was kindly provided by Tyler Jacks (Olive *et al*, 2004). The vector was modified by QuikChange Multi Site-Directed Mutagenesis (Stratagene) to carry only the mutation GCG->CTC in exon 5 of $Trp53$, resulting in a Arg->Glu substitution at codon 178 (Fig EV1A). The complete targeting vector was verified by Sanger sequencing. The linearized targeting vector was transfected by electroporation of 129/SvEv (129) embryonic stem cells. After selection with G418 antibiotic, surviving clones were expanded for PCR analysis to identify recombinant ES clones and verify the presence of the R178E mutation by Sanger sequencing. ES cell clones were further validated by Southern blot for correct 5' and 3' homologous recombination using *SspI* digest in combination with the 3' probe and *XbaI* digest with the 5' probe (Fig EV1B). A correctly targeted ES cell clone was microinjected into C57BL/6 blastocysts. Resulting chimeras with a high percentage agouti coat color were mated to wild-type 129/SvEv

mice to generate F1 heterozygous offspring. Tail DNA was analyzed as described below from pups with agouti coat color (Fig EV1C and D). Additional mutations were excluded by sequencing of all exons and exon-intron boundaries in the $Trp53$ gene. ES cell cloning, blastocyst injection, and breeding of chimeras for germline transmission were done at inGenious Targeting Laboratory (Stony Brook, USA). Knock-in mice were kept on a pure 129Sv background.

In 129S/Sv- $Trp53^{LSL-R178E}$ mice, expression of the $Trp53$ gene is blocked by a transcriptional stop cassette, flanked by loxP sites (lox-stop-lox, LSL). The homozygous $Trp53^{LSL-R178E/LSL-R178E}$ mice lack p53 protein expression. $Trp53^{LSL-R178E/LSL-R178E}$ mice, and embryonic fibroblasts isolated from these mice, were used as isogenic p53-null ($Trp53^{-/-}$) controls in all experiments. For generation of knock-in mice expressing the p53EE mutant protein, we crossed heterozygous $Trp53^{+/LSL-R178E}$ mice with Prm-Cre transgenic animals (129S/Sv-Tg (Prm-cre)580g/J; Jackson Laboratory). In double transgenic males, the Prm1-Cre allele mediates excision of the LSL cassette in the male germline. These males were used for breeding with wild-type 129/Sv females to obtain constitutively recombined $Trp53^{+/R178E}$ mice, which were then intercrossed to generate homozygous knock-in and wild-type $Trp53^{+/+}$ (control) animals. In aging cohorts, mice were monitored on the daily basis and sacrificed when they reached objective criteria for a humane endpoint that were defined before the onset of the experiment.

To study lethality of $Mdm2$ knock-out, we used heterozygous $Mdm2^{\Delta7-9}$ ($Mdm2 <tm1.2Mep>$) mice that lack exons 7–9. These mice were obtained from the NCI Mouse Repository (Frederick, USA) and crossed with $Trp53^{EE/EE}$ homozygotes to obtain double heterozygous $Trp53^{+/EE};Mdm2^{+/Δ7-9}$ animals for intercrossing. Genotypes of mice, isolated embryos, and embryonic tissues were identified by PCR. Primer sequences are listed in Table EV1.

All mouse experiments were performed in accordance with the German Animal Welfare Act (Deutsches Tierschutzgesetz) and were approved by the local authorities.

Murine lymphoma model

For generation of Burkitt-like B-cell lymphoma, heterozygous females with different p53 genotypes were crossed to transgenic B6.Cg-Tg(IghMyc)22Bri/J males (Jackson Laboratory; Adams *et al*, 1985). Primary lymphomas were obtained from Eμ-Myc mice with $p53^{+/+}$, $p53^{+/-}$, and $p53^{+/EE}$ genotypes, and 500,000 cells were transplanted into syngeneic recipients via tail vein as described in the literature (Schmitt *et al*, 2002a). After lymphomas became palpable as enlarged peripheral lymph nodes, mice were separated into two groups—one group was treated with a single intraperitoneal dose of 300 mg/kg cyclophosphamide (Cell Pharm, Hannover, Germany), and another group was left untreated. Samples were collected 6 h, 24 h, and 7 days after therapy. In both groups, mice were monitored on the daily basis for up to a maximum of 4 months and sacrificed when they reached objective criteria for a humane endpoint that were defined before the onset of the experiment.

Murine acute myeloid leukemia (AML) model

Primary AML with different p53 genotypes was generated as described (Zuber *et al*, 2009). In brief, fetal liver cells were isolated from $p53^{+/+}$, $p53^{-/-}$, and $p53^{EE/EE}$ embryos at E14–16. Retroviral

plasmids encoding the AML1/ETO9a fusion oncogene (co-expressed with GFP) and NRas^{G12D} oncogene (co-expressed with firefly luciferase) were kindly provided by J. Zuber (Zuber *et al*, 2009). Recombinant retroviruses were packaged in Platinum-E cells (Cell Biolabs). After four rounds of infection with the two retroviral vectors mixed 1:1, transfection efficiency was analyzed by flow cytometry. 24–48 h after last infection, 1 million cells were transplanted intravenously into lethally irradiated (7 Gy) 129X1/SvJ albino recipients. F1 hybrids from breeding 129X1/SvJ/albino X C57B6/albino mice were used as secondary recipients for chemotherapy. After primary recipients developed advanced leukemia with accumulation of malignant myeloid progenitors in bone marrow and infiltration of extramedullary tissues such as spleen, AML cells were isolated, immunophenotyped, and transplanted into sublethally irradiated (3.5 Gy) secondary recipients. Disease development was monitored by bioluminescence imaging (BLI). BLI was performed using an IVIS 100 Imaging System (Xenogen) under isoflurane anesthesia, 5 min after intraperitoneal injection of 200 μ l D-luciferin (15 mg/ml in PBS, BioVision). After first detection of clear signal in bones and initial spleen infiltration, mice were separated into control and therapy groups and the latter was subjected to a standard chemotherapy protocol containing cytarabine (Cell Pharm, Hannover, Germany) and doxorubicin (Cell Pharm, Hannover, Germany): 3 days of cytarabine 100 mg/kg + doxorubicin 3 mg/kg intraperitoneally, followed by 2 days of cytarabine only. Mice under therapy were provided with drinking water containing 120 mg/l ciprofloxacin (Bayer) and 20 g/l glucose (Sigma). Therapy response was monitored by BLI. Mice were monitored on the daily basis and sacrificed when they reached objective criteria for a humane endpoint that were defined before the onset of the experiment.

Cell culture and gene transfer

Human lung cancer cell lines (H1299, H460) were obtained from the American Tissue Collection Center (ATCC) and authenticated by short tandem repeat analysis at the Leibniz Institute DSMZ—German Collection of Microorganisms and Cell Cultures, Braunschweig, Germany. Cells were maintained in high-glucose Dulbecco's modified Eagle's medium (DMEM) supplemented with 10% fetal bovine serum (FBS, Sigma-Aldrich), 100 U/ml penicillin, 100 μ g/ml streptomycin (Life Technologies), and 1 μ g/ml amphotericin B (Sigma) at 37°C with 5% CO₂. Primary MEFs were isolated from E12.5–13.5 mouse embryos and amplified under low oxygen conditions (3% O₂); their gender is not available. E μ -Myc lymphoma cell lines were maintained in B-cell medium: 1:1 mixture of DMEM and Iscove's modified Dulbecco's medium (IMDM) supplemented with 20% FBS, 100 U/ml penicillin/streptomycin, 50 μ M 2-mercaptoethanol, and 1 ng/ml mIL-7 (ImmunoTools). Cells were cultured on a feeder layer of 30 Gy-irradiated NIH 3T3 cells. Nutlin-3a (Sigma) was used at 10 μ M, RG7112 (MedChemExpress) at 5 μ M, RG7388 (MedChemExpress) at 8 μ M, MI773 (Selleckchem) at 10 μ M, and Mafosfamide (Santa Cruz) at 1–5 μ g/ml as indicated. Hydrogen peroxide (Sigma) was used at 50–800 μ M.

Plasmids and gene transfer

Transfections and viral infections were performed as described (Timofeev *et al*, 2013). For production of lentiviruses, helper

plasmids pMD2.g (Addgene plasmid #12259) and psPAX2 (Addgene plasmid #12260) were used. For Tet-inducible gene knockdown with shRNAs, we used the retroviral vector TtRMPVIR (Addgene plasmid #27995), and for Tet-inducible gene expression, we used the lentiviral vector pInducer20 (Addgene plasmid #44012). For expression of mutant p53, the cDNA for murine or human p53 was cloned into pInducer20 using the Gateway[®] System (Invitrogen). MEFs were immortalized by retroviral transduction with pMSCVhygro-E1A.12S or pMSCVneo-E1A.12S (Timofeev *et al*, 2013). For studies on Ras-induced senescence, MEFs were transduced with MSCVhygro-HRas^{G12V} (Timofeev *et al*, 2013).

CRISPR-Cas9 gene editing

For the generation of p53 knock-out cells using CRISPR-Cas9 gene editing, oligos encoding sgRNAs targeting the mouse *Trp53* gene or GFP as a control were annealed and cloned by Golden Gate cloning into Bsmbl-digested lentiCRISPR vector (Addgene plasmid #49535). The presence of indels in the targeted *Trp53* gene locus was confirmed by T7 endonuclease assay. In brief, infected cells were collected, genomic DNA was isolated, and the fragment of interest was PCR-amplified using primers flanking the predicted CRISPR-Cas9 cleavage site. The PCR product was purified using the QIAquick PCR Purification Kit (Qiagen), DNA was denatured, reannealed in 1 \times NEB2 buffer (NEB), digested with 5 U T7 endonuclease I (NEB) for 20 min at 37°C, and analyzed on a 2% agarose gel. Knock-out of p53 in the pool of cells was confirmed by p53 immunofluorescence staining, Sanger sequencing of the targeted *Trp53* region, and InDel analysis using the TIDE algorithm (Brinkman *et al*, 2014). sgRNA and primer sequences are listed in Table EV1.

Cell viability and proliferation assays

Viability of cells after irradiation or drug treatment was assessed using CellTiter-Glo Luminescent Cell Viability Assay (Promega) as described (Timofeev *et al*, 2013). For quantitative real-time monitoring of cell proliferation, we performed automated time-lapse microscopy using the IncuCyte S3 (Essen BioScience). Cells were seeded in triplicates on 96-well plates to reach a starting confluence of 10–30% after 24 h. Following treatment with Nutlin \pm doxorubicin, the plates were imaged for 48 h with a time interval of 2 h. Confluence was calculated using the instrument's IncuCyte Zoom 2017A software. For assessment of long-term proliferative capacity of primary MEFs (Fig EV4A), we used a modified 3T3 protocol: 200,000 cells from passage 1–2 were plated to each well of a 6-well plate. Every 3 days, cells were harvested and counted and 200,000 cells were replated. When the total number of cells was lower than 200,000, all cells were replated. Population doubling was calculated as the log₂ of the ratio N_{px+1}/N_{px} , where N_{px} is the total number of cells at passage X. For proliferation assay with CRISPR-Cas9-edited MEFs (Fig EV3E) and for proliferation at normal (21%) and low (3%) oxygen conditions (Fig EV3H), 500,000 cells were replated every 3 days on 10-cm cell culture dishes. Under these conditions, proliferation of p53^{EE/EE} MEFs declined more rapidly than in Fig EV4A and eventually resulted in deterioration of cell cultures.

Cellular fractionation and western blotting

For immunoblotting, cells were lysed in RIPA buffer (0.1% SDS, 50 mM Tris-HCl at pH 7.4, 150 mM NaCl, 1 mM EDTA, 1% Na-deoxycholate) supplemented with protease inhibitor cocktail (Roche). To prepare nuclear and cytosolic fractions, cells were collected and resuspended in 2–3 volumes of Buffer A (10 mM HEPES pH 7.9, 10 mM KCl, 0.1 mM EDTA, 0.1 mM EGTA, 1 mM β -mercaptoethanol) supplemented with protease inhibitors, and incubated for 10 min on ice before adding 10% NP-40 to a final concentration of 0.25%. Cells were passed through a 27-G needle 5–10 times using a 1-ml syringe. Nuclei were pelleted by centrifugation (500 \times g, 10 min). The cytoplasmic fraction was collected and re-centrifuged for 10–15 min. Nuclear fractions were washed three times in 5–10 volumes of Buffer A and pelleted by centrifugation. Nuclei were lysed with 1–2 volumes of Buffer C (20 mM HEPES pH 7.9, 400 mM NaCl, 1 mM EDTA, 1 mM EGTA, 1 mM β -mercaptoethanol) and soluble fraction collected by centrifugation (10,000 \times g, 10 min). Mitochondrial fractions were isolated using Mitochondria Isolation Kit for Cultured Cells (Thermo Scientific) as described by the manufacturer. For Western blotting, 20–50 μ g of total protein was resolved on 4–12% NuPAGE polyacrylamide gels (Invitrogen). After wet transfer to Hybond P nitrocellulose membrane (GE Healthcare), antigens were detected using the following antibodies: anti-cleaved caspase-3 (#9661, Cell Signaling, 1:500), anti-p53 (NCL-p53-505, Leica Microsystems, 1:2,000), anti-MDM2 (SMP14, #sc-965, Santa Cruz Biotechnology [SC], 1:200), anti-PCNA (PC10, #sc-56, 1:1,000), anti-Bak (A8B4, Abcam, 1:250), anti-Tom20 (FL-145, #sc-11415, 1:100), anti-cleaved PARP (#9541, Cell Signaling, 1:500), anti-cleaved Lamin A small subunit (#3035, Cell Signaling, 1:500), anti-H-Ras (C-20, #sc-520, Santa Cruz Biotechnology, 1:100), anti-E1A (M-73, #sc-25, Santa Cruz Biotechnology, 1:500), and anti- β -actin (AC-15, #ab6276, Abcam, 1:10,000). Detection was performed with secondary anti-mouse or anti-rabbit IgG-HRP (GE Healthcare, 1:5,000) and SuperSignal ECL Kit (Thermo Fisher).

Immunohistochemistry and immunofluorescence

For histology and immunohistochemistry (IHC), formalin-fixed samples were embedded in paraffin and 5- μ m sections were mounted to glass slides and processed as described (Timofeev *et al*, 2013). Apoptosis was detected using the DeadEnd™ Colorimetric TUNEL System (Promega) or antibodies against cleaved caspase-3 (#9661, Cell Signaling, 1:100). Other antibodies used for IHC were anti-p53 (NCL-p53-505, Leica Microsystems, 1:1,000) and anti-BrdU (BU1/75(ICR1), #OBT0030G, 1:100).

Proximity ligation assays

In situ interactions were detected by the proximity ligation assay kit Duolink (DPLA probe anti-rabbit minus, DPLA probe anti-mouse plus (Sigma-Aldrich, St. Louis, MO, USA); Detection Kit Red, Sigma-Aldrich). The DPLA probe anti-rabbit minus binds to the p53 antibody, whereas the DPLA probe anti-mouse plus binds to the antibody against the probable interaction partner, respectively. The Duolink proximity ligation assay secondary antibodies generate only a signal when the two DPLA probes have been bound, which only takes place if both proteins are closer than 40 nm, indicating their interaction. Paraformaldehyde-fixed FFPE sections were pre-

incubated with blocking agent for 1 h. After washing in PBS for 10 min, primary antibodies were applied to the samples. Incubation was done for 1 h at 37°C in a pre-heated humidity chamber. Slides were washed three times in PBS for 10 min. DPLA probes detecting rabbit or mouse antibodies were diluted in the blocking agent in a concentration of 1:5 and applied to the slides followed by incubation for 1 h in a pre-heated humidity chamber at 37°C. Unbound DPLA probes were removed by washing two times in PBS for 5 min. The samples were incubated with the ligation solution consisting of Duolink Ligation stock (1:5) and Duolink Ligase (1:40) diluted in high-purity water for 30 min at 37°C. After ligation, the Duolink Amplification and Detection stock, diluted 1:5 by the addition of polymerase (1:80), was applied to the slides for 100 min. Afterward, the slides were incubated with DAPI for the identification of nuclei. After the final washing steps, the slides were dried and coverslips were applied. Quantification was done with the Duolink Image Tool v1.0.1.2 (Olink Bioscience, Uppsala, Sweden). The signal threshold was adjusted to 100 and the pixel size for spot detection to 5 pixels for each picture.

Flow cytometry

For flow cytometry analysis, an Accuri C6 Flow Cytometer (BD Biosciences) was used. Labeling of S-phase cells with BrdU and processing for FACS were done as described (Timofeev *et al*, 2013) using anti-BrdU Alexa Fluor 488 antibodies (BD Biosciences #347580). For analysis of apoptosis, annexin V-APC (MabTag) and CaspGLOW Staining Kit (BioVision) were used according to manufacturer's protocols. Cell cycle profiles and viability of cells were assessed using staining with propidium iodide (PI) in permeable and non-permeable conditions as described earlier (Timofeev *et al*, 2013). To analyze mitochondrial ROS levels, cells were stained for 15 min on plates with 3 μ M MitoSOX free radical sensor (Thermo Fisher) in HBSS buffer (Sigma), collected with trypsin, washed with PBS, and analyzed by flow cytometry.

μ -Myc:p53^{EE} lymphoma cells were transduced with TtRMPVIR retroviral vectors (Zuber *et al*, 2011) expressing a p53-targeting (shp53.814, Dickins *et al*, 2005) or non-silencing control shRNA coupled to RFP. Knockdown of p53 was induced with 1 μ g/ml doxycycline. After 48 h of doxycycline pre-treatment, cells were treated with 1–5 μ g/ml mafosfamide (Santa Cruz) for 24 h, washed, and left to recover for 48 h. Enrichment of RFP-expressing cells, i.e., cells efficiently expressing shRNA, in treated versus untreated cultures was analyzed with flow cytometry.

Metabolism analysis

Mitochondrial metabolism was assessed using the Seahorse XF Cell Mito Stress Test Kit (Agilent) on the Seahorse XFe96 instrument according to manufacturer's protocols. Cells were treated for 24 h with 0.5 μ g/ml doxycycline to induce p53 expression. A total of 20,000 cells were plated in 96-well XF cell culture microplates and let to adhere for 5 h before measurements were performed. Data were analyzed using MS Excel templates provided by the manufacturer.

Electrophoretic mobility shift assays

Electrophoretic mobility shift assays (EMSAs) were performed in 20 μ l reaction volume containing 20 mM HEPES (pH 7.8), 0.5 mM

EDTA (pH 8.0), 6 mM MgCl₂, 60 mM KCl, 0.008% Nonidet P-40, 100 ng anti-p53 antibody (Pab421), 1 mM DTT, 120 ng salmon sperm DNA, 1 μ l glycerol, 20,000 cpm of [³²P]-labeled double-stranded oligonucleotide, and either 5 μ l of *in vitro* translated protein or 5 μ g of nuclear extracts from Nutlin-treated MEFs. After 30 min incubation at room temperature, reaction mixtures were subjected to electrophoresis on a 3.5% native polyacrylamide gel (37.5:1 acrylamide/bisacrylamide) in a Tris-borate-EDTA buffer at 125 V for 90 min at room temperature. 10 pmoles of competitor were added to control the specificity of DNA binding. For supershift analysis, 1 μ g of anti-p53 antibody (FL393, Santa Cruz) was added. DNA–protein complexes were revealed with X-ray films (Kodak).

Chromatin immunoprecipitation

Primary MEFs were treated for 16 h with 10 μ M Nutlin or 0.1% DMSO as control. Cells were fixed on plates with 0.88% paraformaldehyde (PFA) for 10 min at room temperature and quenched by adding glycine to a final concentration of 54 mM for 5 min. Cells were washed twice with ice-cold PBS and scraped off the plate with PBS supplemented with proteinase inhibitors (Roche). Cell pellets were lysed in SDS lysis buffer (1% SDS, 10 mM EDTA, 50 mM Tris–HCl pH 8.1) supplemented with protease inhibitors (2 \times 10⁷ cells/ml lysis buffer) and sonicated using the Bioruptor[®] Sonication System (Diagenode) to obtain 300–1,000 bp DNA fragments. The shearing efficiency was controlled using agarose gel electrophoresis. After centrifugation (10,000 g, 10 min, 20°C), 100 μ l sheared chromatin was diluted 1:10 with dilution buffer (0.01% SDS, 1.1% Triton X-100, 1.2 mM EDTA, 16.7 mM Tris–HCl pH 8.1, 167 mM NaCl) and pre-cleared for 1 h with 50 μ l Protein G Sepharose (50% slurry in 20% ethanol) beads (GE Healthcare) at 4°C. The p53 protein was immunoprecipitated overnight at 4°C with 2.5 μ g anti-p53 antibody (FL393, Santa Cruz), and normal rabbit IgG (Santa Cruz) was used as the control. The protein complexes were pulled down for 4 h at 4°C with 50 μ l Protein G Sepharose beads. Beads were washed with Low Salt Immune Complex Wash Buffer (0.1% SDS, 1% Triton X-100, 2 mM EDTA, 20 mM Tris–HCl pH 8.1, 150 mM NaCl), then with High Salt Immune Complex Wash Buffer (0.1% SDS, 1% Triton X-100, 2 mM EDTA, 20 mM Tris–HCl pH 8.1, 500 mM NaCl), with LiCl Immune Complex Wash Buffer (0.25 M LiCl, 1% IGEPAL-CA630, 1% deoxycholic acid (sodium salt), 2 mM EDTA, 10 mM Tris–HCl pH 8.1), and finally twice with TE (10 mM Tris–HCl pH 8.1, 1 mM EDTA). Protein/DNA crosslinks were eluted twice for 15 min at 20°C in 100 μ l elution buffer (0.1 M NaHCO₃, 1% SDS). 1% input stored at –20°C was treated in the same way. Crosslinking was reverted upon overnight incubation at 65°C in elution buffer supplemented with 200 mM NaCl followed by RNase A digestion at 37°C for 30 min, addition of 40 mM Tris–HCl pH 6.5 and 10 mM EDTA, proteinase K digestion for 2 h at 55°C, and inactivation of proteinase K at 99°C for 10 min. DNA was purified using the QIAquick PCR Purification Kit (Qiagen), and DNA concentration was measured with the Qubit dsDNA HS reagent (Molecular Probes).

ChIP-seq and RNA-seq

ChIP-seq libraries were prepared from purified ChIP DNA with the MicroPlex Library Preparation Kit (Diagenode) according to the manufacturer's instructions. For RNA-seq, RNA quality was

assessed using the Experion RNA StdSens Analysis Kit (Bio-Rad). RNA-seq libraries were prepared from total RNA using the TruSeq Stranded mRNA LT Kit (Illumina) according to the manufacturer's instructions. Quality of sequencing libraries (for ChIP-seq and RNA-seq) was controlled on a Bioanalyzer 2100 using the Agilent High Sensitivity DNA Kit (Agilent). Pooled sequencing libraries were quantified with digital PCR (QuantStudio 3D, Thermo Fisher) and sequenced on the HiSeq 1500 platform (Illumina) in rapid-run mode with 50 base single reads.

ChIP-seq data analysis

Reads were aligned to the *Mus musculus* genome retrieved from Ensembl revision 79 (mm10) with Bowtie 2.0.0-beta7 using the default parameter settings (Langmead & Salzberg, 2012). Lanes were deduplicated to a single duplicate read, keeping only these effective reads for further analysis. Peak calling was performed individually for each sample using a mixed input as background using MACS 1.4.Orc2 with default parameters for all samples (Zhang *et al*, 2008). To reduce the amount of false positives, peaks were filtered to those peaks showing a strong enrichment over background, i.e., peaks with a minimum of 50 effective foreground reads, not more than 50 effective reads in background, and showing at least a threefold increase in the normalized read counts compared to background. To enable comparison between the samples, tag counts were calculated and normalized to one million mapped reads (tags per million, TPM). The foreground–background ratio used to filter reported peaks was calculated on basis of TPMs in foreground versus TPMs in background. To compare samples, filtered ChIP-seq peaks from the Nutlin-treated p53^{+/+} sample were taken as the basis. Of these 472 peaks, we removed 4 peaks that overlap with non-specific peaks in Nutlin-treated p53^{-/-} MEFs, yielding 468 p53WT peaks. 2,000 bp spanning regions around all of these 468 peak regions were centered to the summit of the p53^{+/+} Nutlin signal (TPM). To allow comparability of the lanes, TPMs were plotted as heatmap for all lanes, and the maximum value was fixed to the 95th percentile of the p53^{+/+} Nutlin signal. To obtain a list of target genes, we annotated the gene with the closest corresponding transcription start site to each peak. Hypergeometric enrichment was performed using Fisher's exact test, based on MSigDB gene sets as reference and our target genes as query.

Motif identification: For *de novo* binding motif search, peaks from Nutlin-treated p53^{+/+} MEFs (filtered as stated above) were trimmed to 150 bp (peak middle \pm 75 bp). These 468 regions were used for analysis with MEME-ChIP (version 4.12.0) using the default parameters (Machanick & Bailey, 2011). To identify motifs of known binding sites, CentriMo (version 4.12.0) analysis was performed on the same 150 bp regions, using the JASPAR CORE 5 (vertebrates) and UniPROBE (retrieved August 2011) databases as reference (Berger *et al*, 2006; Bailey & Machanick, 2012; Mathelier *et al*, 2014).

RNA-seq data analysis

Reads were aligned to the *Mus musculus* genome retrieved from Ensembl revision 79 (mm10) with STAR 2.4. Tag counts were calculated and normalized to one million mapped exonic reads and gene length (FPKM). To generate the set of expressed genes, only genes with a minimum read count of 50 and a minimum FPKM of 0.3 were

kept. DESeq2 (version 1.8.2) was used to determine differentially expressed genes (Berger *et al*, 2006). Genes with a greater than twofold change according to DESeq2 analysis and a maximum FDR of 0.05 were considered as regulated. Gene set enrichment analysis (GSEA) was performed using Molecular Signatures Database (MSigDB) gene sets and GSEA2 software (version 2.1.0) from the Broad Institute (West *et al*, 2005; Liberzon *et al*, 2011, 2015). FPKM values of genes from the indicated gene sets were z-transformed and plotted as heatmaps.

PCR and real-time PCR

For PCR genotyping, tail tips or tissues were lysed overnight at 55°C in PBNB buffer (10 mM Tris–HCl pH 8.3, 50 mM KCl, 2.5 mM MgCl₂, 0.45% NP-40, 0.45% Tween-20) supplemented with 8 U/ml proteinase K (AppliChem) and afterward inactivated at 95°C for 10 min. For LOH and residual disease detection in Eμ-Myc lymphoma samples, crude lysates were prepared as above and 50 ng of genomic DNA purified with peqGOLD Tissue DNA Mini Kit (PeqLab) was used as template for qPCR with primers specific for the EμMyc transgene and a control locus for normalization.

For reverse transcription–quantitative PCR (RT–qPCR), RNA was isolated from cells or tissue samples using the RNeasy Mini Kit (Qiagen) and cDNA was generated with the SuperScript VILO cDNA Synthesis Kit (Invitrogen). Gene expression was analyzed on a LightCycler 480 (Roche) using the Absolute QPCR SYBR Green Mix (Thermo Scientific). Data were evaluated by the $\Delta\Delta C_t$ method with β -actin as a housekeeping gene for normalization.

For mtDNA content analysis, genomic DNA was analyzed by quantitative PCR for the mitochondrial genes *mt-Nd4*, *mt-Co1*, *mt-Cyb*, and *mt-Nd2*, and Ct values were normalized to the nuclear gene *Trp53*.

Primer sequences are provided in Table EV1.

Statistical analyses

Statistical differences between experimental groups analyzed at different time points or under different treatment conditions were calculated using one- or two-way ANOVA test, while correcting for multiple comparisons using Sidak's multiple comparisons test. A significance level of $P < 0.05$ was used throughout the study. Kaplan–Meier curves representing survival analyses were compared by the log-rank (Mantel–Cox) test. Multiple survival Kaplan–Meier curves were compared by ordinary ANOVA with Tukey's multiple comparisons test. Statistical analyses were performed using the Prism software package (GraphPad).

Data availability

The datasets produced in this study are available in the following databases:

- RNA-seq data: EBI ArrayExpress E-MTAB-6774
- ChIP-seq data: EBI ArrayExpress E-MTAB-6793

Expanded View for this article is available online.

Acknowledgements

We thank Ute Moll, Yinon Ben-Neriah, and members of the laboratory for helpful discussion and advice; and Tyler Jacks and Johannes Zuber for providing plasmids. We acknowledge Sigrid Bischofsberger, Angelika Filmer, Alexandra Schneider, Antje Grzeschiczek, Angela Mühlhling, Johanna Grass, Björn Geissert, and trainee Mikhail Moskalenko for excellent technical assistance; the Cell Metabolism Core Facility (Wolfgang Meissner) for performing Seahorse assays; and the Irradiation Core Facility (Rita Engenhardt-Cabillic) for providing access to the X-RAD 320iX platform. This work was supported by grants from the Deutsche Forschungsgemeinschaft (DFG) (DFG STI 182/7-1; TI 1028/2-1), Deutsche Krebshilfe (# 111250, 111444, 70112623), Deutsche José Carreras Leukämie Stiftung e.V. (DJCLS R 13/08, 09 R/2018), Bundesministerium für Bildung und Forschung (BMBF 031L0063), and German Center for Lung Research (DZL).

Author contributions

Conducting experiments: OT, BK, JS, MW, JN, SM, AN, EP, UW, AB, and KK; conceptual input and supervision: OT, BK, SE, SG, and TS; data analysis: OT, BK, MM, BL, UW, and TS; and project design and writing: OT and TS.

Conflict of interest

The authors declare that they have no conflict of interest.

References

- Abbas HA, Maccio DR, Coskun S, Jackson JG, Hazen AL, Sills TM, You MJ, Hirschi KK, Lozano G (2010) Mdm2 is required for survival of hematopoietic stem cells/progenitors via dampening of ROS-induced p53 activity. *Cell Stem Cell* 7: 606–617
- Adams JM, Harris AW, Pinkert CA, Corcoran LM, Alexander WS, Cory S, Palminter RD, Brinster RL (1985) The c-myc oncogene driven by immunoglobulin enhancers induces lymphoid malignancy in transgenic mice. *Nature* 318: 533–538
- Alexandrova EM, Yallowitz AR, Li D, Xu S, Schulz R, Proia DA, Lozano G, Dobbelstein M, Moll UM (2015) Improving survival by exploiting tumour dependence on stabilized mutant p53 for treatment. *Nature* 523: 352–356
- Andreoff M, Kelly KR, Yee K, Assouline S, Strair R, Popplewell L, Bowen D, Martinelli G, Drummond MW, Vyas P *et al* (2016) Results of the phase I trial of RG7112, a small-molecule MDM2 antagonist in leukemia. *Clin Cancer Res* 22: 868–876
- Bailey TL, Machanick P (2012) Inferring direct DNA binding from ChIP-seq. *Nucleic Acids Res* 40: e128
- Berger MF, Philippakis AA, Qureshi AM, He FS, Estep PW III, Bulyk ML (2006) Compact, universal DNA microarrays to comprehensively determine transcription-factor binding site specificities. *Nat Biotechnol* 24: 1429–1435
- Biegging KT, Mello SS, Attardi LD (2014) Unravelling mechanisms of p53-mediated tumour suppression. *Nat Rev Cancer* 14: 359–370
- Brady CA, Jiang D, Mello SS, Johnson TM, Jarvis LA, Kozak MM, Kenzelmann Broz D, Basak S, Park EJ, McLaughlin ME *et al* (2011) Distinct p53 transcriptional programs dictate acute DNA-damage responses and tumor suppression. *Cell* 145: 571–583
- Brinkman EK, Chen T, Amendola M, van Steensel B (2014) Easy quantitative assessment of genome editing by sequence trace decomposition. *Nucleic Acids Res* 42: e168
- Bullock AN, Henckel J, Fersht AR (2000) Quantitative analysis of residual folding and DNA binding in mutant p53 core domain: definition of mutant states for rescue in cancer therapy. *Oncogene* 19: 1245–1256

- Bullock AN, Fersht AR (2001) Rescuing the function of mutant p53. *Nat Rev Cancer* 1: 68–76
- Bykov VJN, Eriksson SE, Bianchi J, Wiman KG (2018) Targeting mutant p53 for efficient cancer therapy. *Nat Rev Cancer* 18: 89–102
- Campomenosi P, Monti P, Aprile A, Abbondandolo A, Frebourg T, Gold B, Crook T, Inga A, Resnick MA, Iggo R et al (2001) p53 mutants can often transactivate promoters containing a p21 but not Bax or PIG3 responsive elements. *Oncogene* 20: 3573–3579
- Chavez-Reyes A, Parant JM, Amelse LL, de Oca Luna RM, Korsmeyer SJ, Lozano G (2003) Switching mechanisms of cell death in mdm2- and mdm4-null mice by deletion of p53 downstream targets. *Cancer Res* 63: 8664–8669
- Chen X, Ko LJ, Jayaraman L, Prives C (1996) p53 levels, functional domains, and DNA damage determine the extent of the apoptotic response of tumor cells. *Genes Dev* 10: 2438–2451
- Chipuk JE, Kuwana T, Bouchier-Hayes L, Droin NM, Newmeyer DD, Schuler M, Green DR (2004) Direct activation of Bax by p53 mediates mitochondrial membrane permeabilization and apoptosis. *Science* 303: 1010–1014
- Chipuk JE, Bouchier-Hayes L, Kuwana T, Newmeyer DD, Green DR (2005) PUMA couples the nuclear and cytoplasmic proapoptotic function of p53. *Science* 309: 1732–1735
- Cho Y, Gorina S, Jeffrey PD, Pavletich NP (1994) Crystal structure of a p53 tumor suppressor-DNA complex: understanding tumorigenic mutations. *Science* 265: 346–355
- Dehner A, Klein C, Hansen S, Muller L, Buchner J, Schwaiger M, Kessler H (2005) Cooperative binding of p53 to DNA: regulation by protein-protein interactions through a double salt bridge. *Angew Chem Int Ed Engl* 44: 5247–5251
- Dickins RA, Hemann MT, Zilfou JT, Simpson DR, Ibarra I, Hannon GJ, Lowe SW (2005) Probing tumor phenotypes using stable and regulated synthetic microRNA precursors. *Nat Genet* 37: 1289–1295
- Dinkova-Kostova AT, Abramov AY (2015) The emerging role of Nrf2 in mitochondrial function. *Free Radic Biol Med* 88: 179–188
- Frebourg T, Kassel J, Lam KT, Gryka MA, Barbier N, Andersen TI, Borresen AL, Friend SH (1992) Germ-line mutations of the p53 tumor suppressor gene in patients with high risk for cancer inactivate the p53 protein. *Proc Natl Acad Sci U S A* 89: 6413–6417
- Freed-Pastor WA, Prives C (2012) Mutant p53: one name, many proteins. *Genes Dev* 26: 1268–1286
- Hagn F, Klein C, Demmer O, Marchenko N, Vaseva A, Moll UM, Kessler H (2010) BclxL changes conformation upon binding to wild-type but not mutant p53 DNA binding domain. *J Biol Chem* 285: 3439–3450
- Hamard PJ, Barthelery N, Hogstad B, Mungamuri SK, Tonnessen CA, Carvajal LA, Senturk E, Gillespie V, Aaronson SA, Merad M et al (2013) The C terminus of p53 regulates gene expression by multiple mechanisms in a target- and tissue-specific manner *in vivo*. *Genes Dev* 27: 1868–1885
- Hanel W, Marchenko N, Xu S, Yu SX, Weng W, Moll U (2013) Two hot spot mutant p53 mouse models display differential gain of function in tumorigenesis. *Cell Death Differ* 20: 898–909
- Huang J, Yang J, Maity B, Mayuzumi D, Fisher RA (2011) Regulator of G protein signaling 6 mediates doxorubicin-induced ATM and p53 activation by a reactive oxygen species-dependent mechanism. *Cancer Res* 71: 6310–6319
- Jiang L, Kon N, Li T, Wang SJ, Su T, Hibshoosh H, Baer R, Gu W (2015) Ferroptosis as a p53-mediated activity during tumour suppression. *Nature* 520: 57–62
- Jones SN, Roe AE, Donehower LA, Bradley A (1995) Rescue of embryonic lethality in Mdm2-deficient mice by absence of p53. *Nature* 378: 206–208
- Jordan JJ, Menendez D, Sharav J, Beno I, Rosenthal K, Resnick MA, Haran TE (2012) Low-level p53 expression changes transactivation rules and reveals superactivating sequences. *Proc Natl Acad Sci USA* 109: 14387–14392
- Kato S, Han SY, Liu W, Otsuka K, Shibata H, Kanamaru R, Ishioka C (2003) Understanding the function-structure and function-mutation relationships of p53 tumor suppressor protein by high-resolution missense mutation analysis. *Proc Natl Acad Sci USA* 100: 8424–8429
- Kim MP, Lozano G (2018) Mutant p53 partners in crime. *Cell Death Differ* 25: 161–168
- Kitayner M, Rozenberg H, Rohs R, Suad O, Rabinovich D, Honig B, Shakked Z (2010) Diversity in DNA recognition by p53 revealed by crystal structures with Hoogsteen base pairs. *Nat Struct Mol Biol* 17: 423–429
- Klein C, Planker E, Diercks T, Kessler H, Kunkele KP, Lang K, Hansen S, Schwaiger M (2001) NMR spectroscopy reveals the solution dimerization interface of p53 core domains bound to their consensus DNA. *J Biol Chem* 276: 49020–49027
- Kracikova M, Akiri G, George A, Sachidanandam R, Aaronson SA (2013) A threshold mechanism mediates p53 cell fate decision between growth arrest and apoptosis. *Cell Death Differ* 20: 576–588
- Lang GA, Iwakuma T, Suh YA, Liu G, Rao VA, Parant JM, Valentin-Vega YA, Terzian T, Caldwell LC, Strong LC et al (2004) Gain of function of a p53 hot spot mutation in a mouse model of Li-Fraumeni syndrome. *Cell* 119: 861–872
- Langmead B, Salzberg SL (2012) Fast gapped-read alignment with Bowtie 2. *Nat Methods* 9: 357–359
- Le Pen J, Laurent M, Sarosiek K, Vuillier C, Gautier F, Montessuit S, Martinou JC, Letai A, Braun F, Juin PP (2016) Constitutive p53 heightens mitochondrial apoptotic priming and favors cell death induction by BH3 mimetic inhibitors of BCL-xL. *Cell Death Dis* 7: e2083
- Lee MK, Teoh WW, Phang BH, Tong WM, Wang ZQ, Sabapathy K (2012) Cell-type, dose, and mutation-type specificity dictate mutant p53 functions *in vivo*. *Cancer Cell* 22: 751–764
- Leroy B, Anderson M, Soussi T (2014) TP53 mutations in human cancer: database reassessment and prospects for the next decade. *Hum Mutat* 35: 672–688
- Leu JI, Dumont P, Hafey M, Murphy ME, George DL (2004) Mitochondrial p53 activates Bak and causes disruption of a Bak-Mcl1 complex. *Nat Cell Biol* 6: 443–450
- Li D, Marchenko ND, Schulz R, Fischer V, Velasco-Hernandez T, Talos F, Moll UM (2011) Functional inactivation of endogenous MDM2 and CHIP by HSP90 causes aberrant stabilization of mutant p53 in human cancer cells. *Mol Cancer Res* 9: 577–588
- Li T, Kon N, Jiang L, Tan M, Ludwig T, Zhao Y, Baer R, Gu W (2012) Tumor suppression in the absence of p53-mediated cell-cycle arrest, apoptosis, and senescence. *Cell* 149: 1269–1283
- Liberzon A, Subramanian A, Pinchback R, Thorvaldsdottir H, Tamayo P, Mesirov JP (2011) Molecular signatures database (MSigDB) 3.0. *Bioinformatics* 27: 1739–1740
- Liberzon A, Birger C, Thorvaldsdottir H, Ghandi M, Mesirov JP, Tamayo P (2015) The Molecular Signatures Database (MSigDB) hallmark gene set collection. *Cell Syst* 1: 417–425
- Liu G, Parant JM, Lang G, Chau P, Chavez-Reyes A, El-Naggar AK, Multani A, Chang S, Lozano G (2004) Chromosome stability, in the absence of apoptosis, is critical for suppression of tumorigenesis in Trp53 mutant mice. *Dev Genet* 36: 63–68
- Liu DS, Duong CP, Haupt S, Montgomery KG, House CM, Azar WJ, Pearson HB, Fisher OM, Read M, Guerra GR et al (2017) Inhibiting the system xC(-)/glutathione axis selectively targets cancers with mutant-p53 accumulation. *Nat Commun* 8: 14844

- Ludwig RL, Bates S, Vousden KH (1996) Differential activation of target cellular promoters by p53 mutants with impaired apoptotic function. *Mol Cell Biol* 16: 4952–4960
- Machanick P, Bailey TL (2011) MEME-ChIP: motif analysis of large DNA datasets. *Bioinformatics* 27: 1696–1697
- Mathelier A, Zhao X, Zhang AW, Parcy F, Worsley-Hunt R, Arenillas DJ, Buchman S, Chen CY, Chou A, Ienasescu H et al (2014) JASPAR 2014: an extensively expanded and updated open-access database of transcription factor binding profiles. *Nucleic Acids Res* 42: D142–D147
- Mello SS, Attardi LD (2018) Deciphering p53 signaling in tumor suppression. *Curr Opin Cell Biol* 51: 65–72
- Merkel O, Taylor N, Prutsch N, Staber PB, Moriggl R, Turner SD, Kenner L (2017) When the guardian sleeps: reactivation of the p53 pathway in cancer. *Mutat Res* 773: 1–13
- Mihara M, Erster S, Zaika A, Petrenko O, Chittenden T, Pancoska P, Moll UM (2003) p53 has a direct apoptogenic role at the mitochondria. *Mol Cell* 11: 577–590
- Montero J, Sarosiek KA, DeAngelo JD, Maertens O, Ryan J, Ercan D, Piao H, Horowitz NS, Berkowitz RS, Matulonis U et al (2015) Drug-induced death signaling strategy rapidly predicts cancer response to chemotherapy. *Cell* 160: 977–989
- Montes de Oca Luna R, Luna R, Wagner DS, Lozano G (1995) Rescue of early embryonic lethality in Mdm2-deficient mice by deletion of P53. *Nature* 378: 203–206
- Moyer SM, Larsson CA, Lozano G (2017) Mdm proteins: critical regulators of embryogenesis and homeostasis. *J Mol Cell Biol* 9: 16–25
- Muller PA, Vousden KH (2014) Mutant p53 in cancer: new functions and therapeutic opportunities. *Cancer Cell* 25: 304–317
- Murray-Zmijewski F, Slee EA, Lu X (2008) A complex barcode underlies the heterogeneous response of p53 to stress. *Nat Rev Mol Cell Biol* 9: 702–712
- Olive KP, Tuveson DA, Ruhe ZC, Yin B, Willis NA, Bronson RT, Crowley D, Jacks T (2004) Mutant p53 gain of function in two mouse models of Li-Fraumeni syndrome. *Cell* 119: 847–860
- Pietsch EC, Perchiniak E, Canutescu AA, Wang G, Dunbrack RL, Murphy ME (2008) Oligomerization of BAK by p53 utilizes conserved residues of the p53 DNA binding domain. *J Biol Chem* 283: 21294–21304
- Riley T, Sontag E, Chen P, Levine A (2008) Transcriptional control of human p53-regulated genes. *Nat Rev Mol Cell Biol* 9: 402–412
- Riscal R, Schrepfer E, Arena G, Cisse MY, Bellvert F, Heuillet M, Rambow F, Bonneil E, Sabourdy F, Vincent C et al (2016) Chromatin-bound MDM2 regulates serine metabolism and redox homeostasis independently of p53. *Mol Cell* 62: 890–902
- Robles AI, Jen J, Harris CC (2016) Clinical outcomes of TP53 mutations in cancers. *Cold Spring Harb Perspect Med* 6: a026294
- Rowan S, Ludwig RL, Haupt Y, Bates S, Lu X, Oren M, Vousden KH (1996) Specific loss of apoptotic but not cell-cycle arrest function in a human tumor derived p53 mutant. *EMBO J* 15: 827–838
- Sabapathy K, Lane DP (2018) Therapeutic targeting of p53: all mutants are equal, but some mutants are more equal than others. *Nat Rev Clin Oncol* 15: 13–30
- Schlereth K, Beinoraviciute-Kellner R, Zeitlinger MK, Bretz AC, Sauer M, Charles JP, Vogiatzi F, Leich E, Samans B, Eilers M et al (2010a) DNA binding cooperativity of p53 modulates the decision between cell-cycle arrest and apoptosis. *Mol Cell* 38: 356–368
- Schlereth K, Charles JP, Bretz AC, Stiewe T (2010b) Life or death: p53-induced apoptosis requires DNA binding cooperativity. *Cell Cycle* 9: 4068–4076
- Schlereth K, Heyl C, Krampitz AM, Mernberger M, Finkernagel F, Scharfe M, Jarek M, Leich E, Rosenwald A, Stiewe T (2013) Characterization of the p53 cistrome–DNA binding cooperativity dissects p53's tumor suppressor functions. *PLoS Genet* 9: e1003726
- Schmitt CA, McCurrach ME, de Stanchina E, Wallace-Brodeur RR, Lowe SW (1999) INK4a/ARF mutations accelerate lymphomagenesis and promote chemoresistance by disabling p53. *Genes Dev* 13: 2670–2677
- Schmitt CA, Fridman JS, Yang M, Baranov E, Hoffman RM, Lowe SW (2002a) Dissecting p53 tumor suppressor functions *in vivo*. *Cancer Cell* 1: 289–298
- Schmitt CA, Fridman JS, Yang M, Lee S, Baranov E, Hoffman RM, Lowe SW (2002b) A senescence program controlled by p53 and p16INK4a contributes to the outcome of cancer therapy. *Cell* 109: 335–346
- Simeonova I, Jaber S, Draskovic I, Bardot B, Fang M, Bouarich-Bourimi R, Lejour V, Charbonnier L, Soudais C, Bourdon JC et al (2013) Mutant mice lacking the p53 C-terminal domain model telomere syndromes. *Cell Rep* 3: 2046–2058
- Slee EA, Benassi B, Goldin R, Zhong S, Ratnayaka I, Blandino G, Lu X (2010) Phosphorylation of Ser312 contributes to tumor suppression by p53 *in vivo*. *Proc Natl Acad Sci USA* 107: 19479–19484
- Sluss HK, Armata H, Gallant J, Jones SN (2004) Phosphorylation of Serine 18 Regulates Distinct p53 Functions in Mice. *Mol Cell Biol* 24: 976–984
- Stiewe T, Haran TE (2018) How mutations shape p53 interactions with the genome to promote tumorigenesis and drug resistance. *Drug Resist Updates* 38: 27–43
- Terzian T, Suh YA, Iwakuma T, Post SM, Neumann M, Lang GA, Van Pelt CS, Lozano G (2008) The inherent instability of mutant p53 is alleviated by Mdm2 or p16INK4a loss. *Genes Dev* 22: 1337–1344
- Timofeev O, Schlereth K, Wanzel M, Braun A, Nieswandt B, Pagenstecher A, Rosenwald A, Elsassner HP, Stiewe T (2013) p53 DNA binding cooperativity is essential for apoptosis and tumor suppression *in vivo*. *Cell Rep* 3: 1512–1525
- Toledo F, Krummel KA, Lee CJ, Liu CW, Rodewald LW, Tang M, Wahl GM (2006) A mouse p53 mutant lacking the proline-rich domain rescues Mdm4 deficiency and provides insight into the Mdm2-Mdm4-p53 regulatory network. *Cancer Cell* 9: 273–285
- Tomita Y, Marchenko N, Erster S, Nemajerova A, Dehner A, Klein C, Pan H, Kessler H, Pancoska P, Moll UM (2006) WT p53, but not tumor-derived mutants, bind to Bcl2 via the DNA binding domain and induce mitochondrial permeabilization. *J Biol Chem* 281: 8600–8606
- Trachootham D, Alexandre J, Huang P (2009) Targeting cancer cells by ROS-mediated mechanisms: a radical therapeutic approach? *Nat Rev Drug Discov* 8: 579–591
- Vousden KH, Lu X (2002) Live or let die: the cell's response to p53. *Nat Rev Cancer* 2: 594–604
- Vousden KH, Lane DP (2007) p53 in health and disease. *Nat Rev Mol Cell Biol* 8: 275–283
- Walerych D, Lisek K, Sommaggio R, Piazza S, Ciani Y, Dalla E, Rajkowska K, Gaweda-Walerych K, Ingallina E, Tonelli C et al (2016) Proteasome machinery is instrumental in a common gain-of-function program of the p53 missense mutants in cancer. *Nat Cell Biol* 18: 897–909
- Wang Y, Suh YA, Fuller MY, Jackson JG, Xiong S, Terzian T, Quintas-Cardama A, Bankson JA, El-Naggar AK, Lozano G (2011) Restoring expression of wild-type p53 suppresses tumor growth but does not cause tumor regression in mice with a p53 missense mutation. *J Clin Invest* 121: 893–904
- West RB, Nuyten DS, Subramanian S, Nielsen TO, Corless CL, Rubin BP, Montgomery K, Zhu S, Patel R, Hernandez-Boussard T et al (2005) Determination of stromal signatures in breast carcinoma. *PLoS Biol* 3: e187

Zhang Y, Liu T, Meyer CA, Eeckhoute J, Johnson DS, Bernstein BE, Nusbaum C, Myers RM, Brown M, Li W et al (2008) Model-based analysis of ChIP-Seq (MACS). *Genome Biol* 9: R137

Zindy F, Eischen CM, Randle DH, Kamijo T, Cleveland JL, Sherr CJ, Rousset MF (1998) Myc signaling via the ARF tumor suppressor regulates p53-dependent apoptosis and immortalization. *Genes Dev* 12: 2424–2433

Zuber J, Radtke I, Pardee TS, Zhao Z, Rappaport AR, Luo W, McCurrach ME, Yang MM, Dolan ME, Kogan SC et al (2009) Mouse models of human AML accurately predict chemotherapy response. *Genes Dev* 23: 877–889

Zuber J, McJunkin K, Fellmann C, Dow LE, Taylor MJ, Hannon GJ, Lowe SW (2011) Toolkit for evaluating genes required for proliferation and survival using tetracycline-regulated RNAi. *Nat Biotechnol* 29: 79–83



License: This is an open access article under the terms of the Creative Commons Attribution 4.0 License, which permits use, distribution and reproduction in any medium, provided the original work is properly cited.

Expanded View Figures

Figure EV1. Generation and characterization of the *Trp53*^{R178E} knock-in mouse.

- A *Trp53* targeting strategy. Asterisk indicates the R178E (EE) point mutation in exon 5; LSL, lox-stop-lox cassette.
- B Southern blot, showing integration of the construct in a correctly targeted 129/SvEv embryonic stem cell clone. Genomic DNA was digested with *SspI* and hybridized with the 3' probe shown in (A). LSL-EE denotes the targeted allele carrying a lox-stop-lox (LSL) cassette and R178E (EE) mutation. The 10.3 kb *SspI* fragment corresponds to the wild-type and the 8.4 kb fragment to the targeted allele.
- C Sanger sequencing of a *Trp53* exon 5-6 PCR amplicon confirms the presence of the Arg->Glu mutation in a tiptail biopsy from a heterozygous founder mouse.
- D PCR used for genotyping of mouse biopsies and cells. Asterisk indicates unspecific PCR product.
- E Electrophoretic mobility shift assay (EMSA) performed with a radiolabeled oligonucleotide containing a p53 consensus binding site incubated with *in vitro* translated full-length p53 protein (IVT p53WT, left) or nuclear extracts from primary MEFs with indicated p53 genotypes treated with 10 μ M Nutlin o/n (right). For supershift analysis, anti-p53 antibody (FL-393, Santa Cruz) was added; asterisks denote disrupted and shifted bands, respectively. Arrowhead, specific p53-DNA complex. ret lys—reticulocyte lysate; specific comp—non-radiolabeled consensus binding site oligonucleotide as competitor; scrambled comp—non-radiolabeled sequence-scrambled competitor oligonucleotide; ns—non-specific.
- F Venn diagram illustrating number and overlap of peaks called in the p53 ChIP-seq datasets from Nutlin-treated MEFs of indicated genotypes. Only peaks present in p53^{+/+}—but not in p53^{-/-} MEFs—were considered p53-specific.
- G Hypergeometric enrichment showing that genes in the vicinity of p53 ChIP-seq peaks from Nutlin-treated p53^{+/+} MEFs are significantly enriched for p53-related gene sets from the Molecular Signatures Database (MSigDB). Shown is the $-\log_{10}$ of the *P* value adjusted for multiple comparisons using Benjamini–Hochberg correction.
- H Nutlin-regulated gene expression in primary MEFs of indicated p53 genotypes. Scatter plot shows the log₂-fold change of the 1,000 top-regulated genes. Box and whiskers indicate the interquartile range and 5–95 percentiles, respectively. Significance was tested by ordinary ANOVA with Sidak's multiple comparisons test.
- I p53EE fails to regulate non-canonical tumor-suppressive target genes identified by transcriptional profiling of transactivation domain mutant mice (Brady *et al*, 2011). Shown are the z-transformed RNA expression values (FPKM).

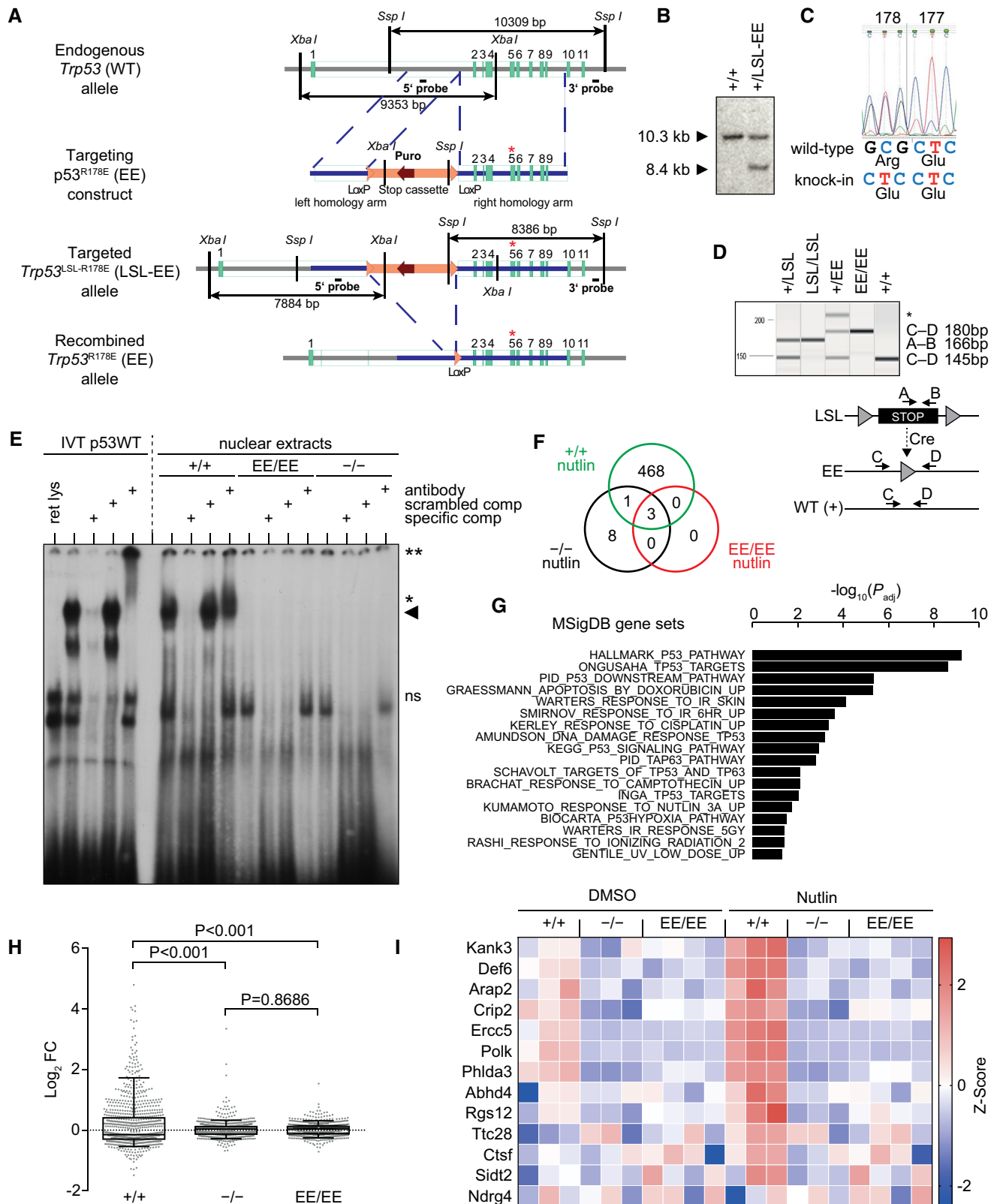


Figure EV1.

Figure EV2. Cells and tissues from p53EE mice show deficiency in cell cycle arrest, senescence, and apoptosis.

- A Oncogenic HRas^{G12V} was overexpressed in primary MEFs, and cells were stained for senescence-associated β -galactosidase (SA β -gal) to detect oncogene-induced senescence (positive cells are marked with arrowheads). Western blots show expression of H-Ras and β -actin as loading control.
- B Senescence caused by cell culture stress was assessed in primary MEFs at passage 8 by SA β -gal staining (arrowheads).
- C *Left*, 3D structure of the double salt bridge formed between the H1 helices of two adjacent p53WT monomers. Residues glutamate 177 (177E) and arginine 178 (178R) are labeled. *Right*, schematic illustration of interactions between the two H1 helices of p53 molecules with wild-type and mutated Glu177 and Arg178.
- D Primary thymocytes were isolated from mice with indicated genotypes and irradiated *ex vivo* with 6 Gy X-ray. Cellular survival at indicated time points was analyzed using CellTiter-Glo assay (Promega). Note, homozygous EE and homozygous RR mutant thymocytes are apoptosis-deficient, while compound EE/RR mutant thymocytes are sensitive to irradiation. Data are shown as mean \pm SD.
- E Apoptosis (detected by IHC staining of cleaved caspase-3) in thymus of control or irradiated mice (6 Gy X-ray) after 6 h. Note massive apoptosis in both p53^{+/+} and p53^{EE/RR} mice.
- F The absence of p53EE expression in small intestine of unstressed mice and accumulation at indicated time points after irradiation. p53^{+/+} are shown for comparison.
- G Dynamics of apoptosis (TUNEL staining) in small intestine at indicated time points after whole-body irradiation (6 Gy X-ray). Arrowheads mark TUNEL-positive apoptotic cells.
- H Cell proliferation in samples from (G) as detected by immunohistochemical staining for BrdU incorporation.

Data information: All scale bars denote 50 μ m.

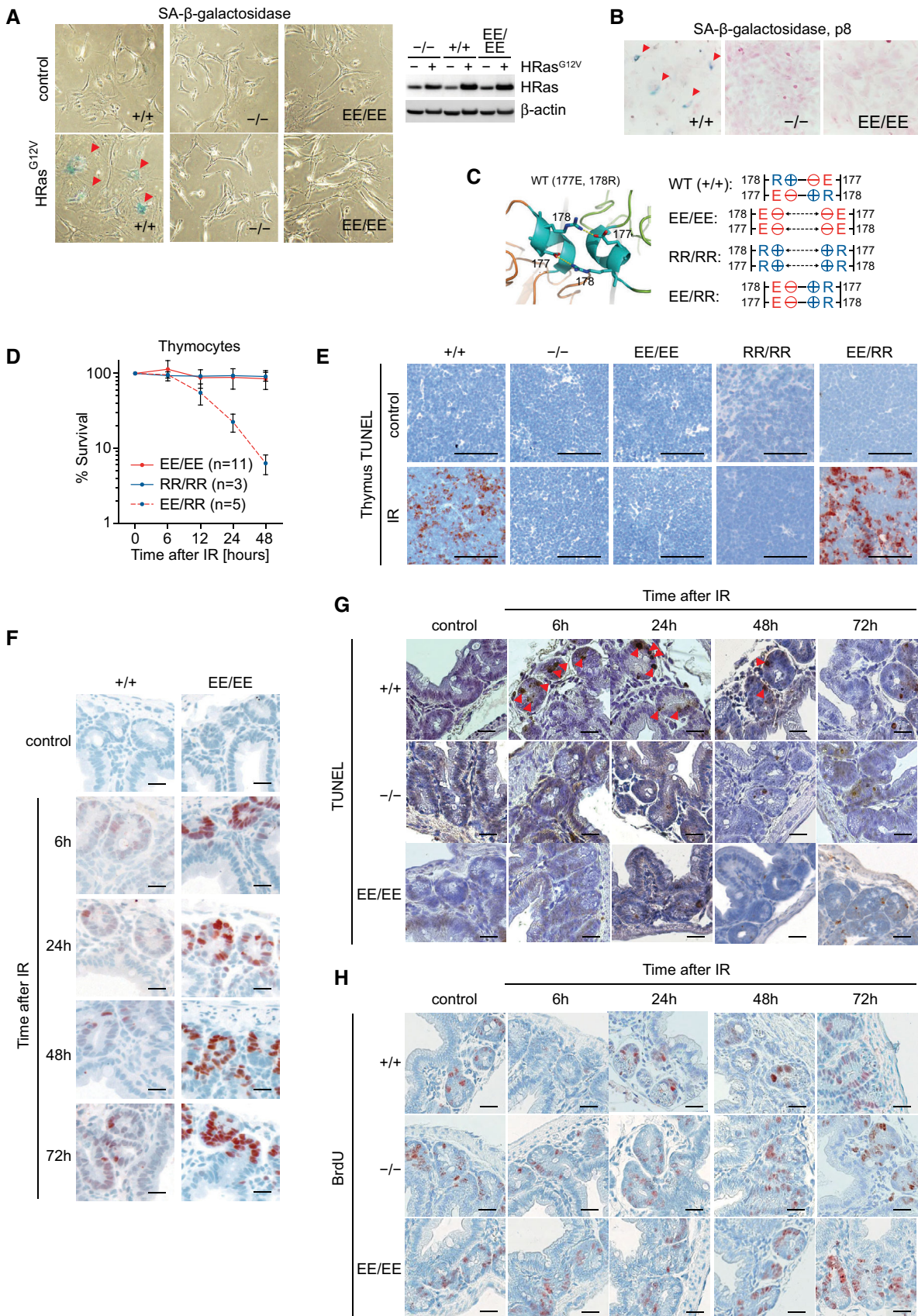


Figure EV2.

Figure EV3. Constitutive p53EE stabilization triggers ROS-dependent senescence.

- A Long-term proliferation assay for freshly isolated primary MEFs with the genotypes $p53^{-/-}$ ($n = 3$), $p53^{+/+}$ ($n = 3$), and $p53^{EE/EE}$ ($n = 6$).
- B SA- β -galactosidase staining of MEFs from (A) at passage 16. Red arrowheads indicate senescent cells positive for SA- β -galactosidase.
- C Western blot of MEFs with indicated genotypes at early (p3) and late passages ($p53^{+/+}$ p7, $p53^{-/-}$, and $p53^{EE/EE}$ p17). Asterisk marks a spontaneously immortalized $p53^{EE/EE}$ cell line, which has lost p53 expression. s.e., short exposure; l.e., long exposure.
- D mRNA expression analysis (RT-qPCR) of MEF cultures from (C). mRNA expression was normalized to β -actin.
- E Long-term proliferation assay with primary $p53^{-/-}$ and $p53^{EE/EE}$ MEFs transduced with two different CRISPR/Cas9 nucleases targeting *Trp53* or GFP (control). Shown is the passage number after gene editing.
- F Mitochondrial ROS in primary MEFs from late passages measured by flow cytometry with MitoSOX red dye. EE*, spontaneously immortalized $p53^{EE/EE}$ cell culture with loss of p53 expression.
- G mRNA expression analysis (RT-qPCR) of early and late passage MEFs cultured in low (3%) oxygen; $n = 4$. mRNA expression was normalized to β -actin.
- H Long-term proliferation of primary $p53^{-/-}$ and $p53^{EE/EE}$ MEFs cultured from frozen stocks in normal high (21%) versus low (3%) oxygen. Shown is the number of passages after revitalization of MEFs frozen at passage 2–4. $n = 4$.
- I Oxygen consumption rate (OCR) assessed with Seahorse XF Cell Mito Stress Test Kit. pInd20-p53EE, Tet-induced p53EE expression in *Trp53^{-/-};Mdm2^{-/-}* MEFs. Control, Tet-treated *Trp53^{-/-};Mdm2^{-/-}* MEFs. Time points of treatment with oligomycin, FCCP, and rotenone+antimycin A are indicated with arrows. Statistical significance was tested with multiple two-sided *t*-tests in combination with the false discovery rate approach. FDR *q*-values < 0.05 are considered significant ($n = 8$).
- J Mitochondrial DNA (mtDNA) content of indicated MEFs determined by qPCR and normalized to early passage $p53^{+/+}$ MEFs and nuclear DNA (nuDNA). $p53^{+/+}$ early, $n = 3$; $p53^{+/+}$ late, $n = 4$; $p53^{-/-}$ early, $n = 1$; $p53^{-/-}$ late, $n = 1$; $p53^{EE/EE}$ early, $n = 3$; $p53^{EE/EE}$ late, $n = 6$.
- K mRNA expression analysis (RT-qPCR) of $p53^{-/-}$ and $p53^{EE/EE}$ MEF cultures for indicated Nrf2 target genes. mRNA expression was normalized to β -actin; $n = 3$.
- L *Hmox1* mRNA expression analysis (RT-qPCR) of $p53^{-/-}$ and $p53^{EE/EE}$ MEF cultures treated for 4 h with 0, 50, 100, 200, 400, and 800 μ M H_2O_2 . mRNA expression was normalized to β -actin; $n = 3$.

Data information: All data are shown as mean \pm SD. Significance was tested by 2-way ANOVA with Sidak's multiple comparisons test unless indicated otherwise.

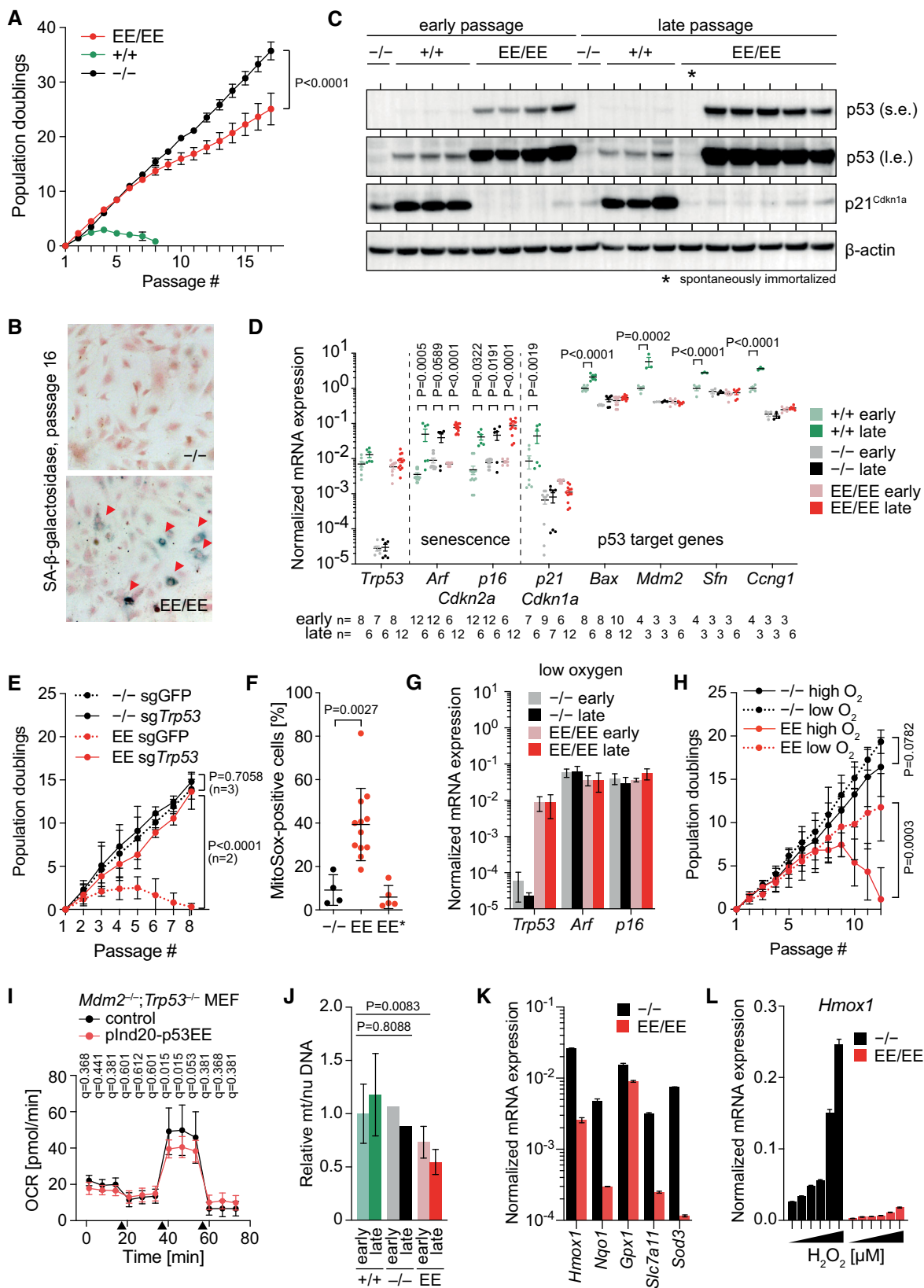


Figure EV3.

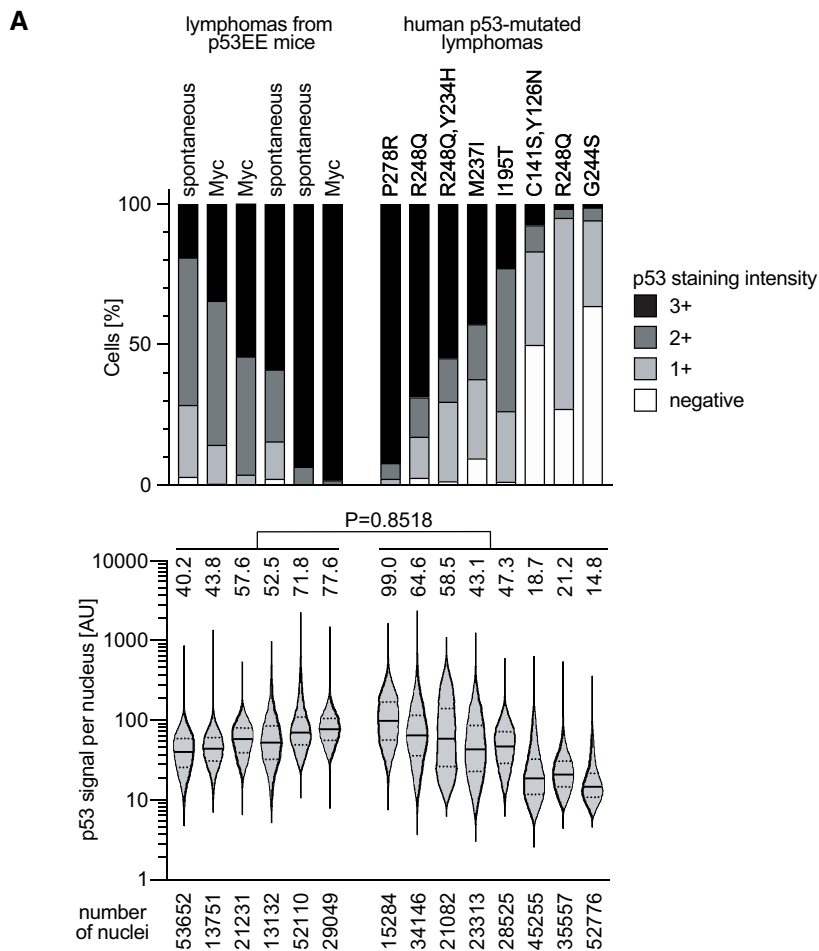
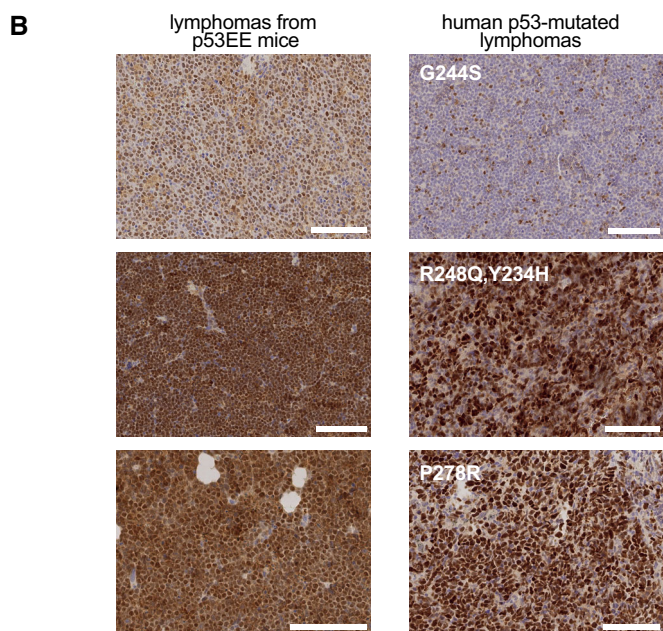


Figure EV4. Mutant p53 expression in p53EE lymphomas compared to human cancer samples.

Spontaneous lymphomas from p53EE mice and human lymphomas with the indicated p53 mutations were stained for p53 using FL-393 antibody (which has comparable affinity for human and murine p53). p53 staining intensity was quantified by automated image analysis.

A Top: Percentage of cells with indicated staining intensity scores for each sample. Bottom: Distribution and mean of cellular staining intensities for each sample. Violin plots were generated with the GraphPad Prism 8 default algorithm (high smoothing) and indicate the median and quartiles with solid and dotted lines, respectively. ns, no significant difference of the mean staining intensity between the two groups of murine and human lymphomas (Mann-Whitney test; unpaired, non-parametric, two-tailed).

B Exemplary images. The analysis demonstrates that p53EE expression in murine lymphomas is within the range for mutant p53 expression in human lymphomas. Scale bar: 100 μ m.



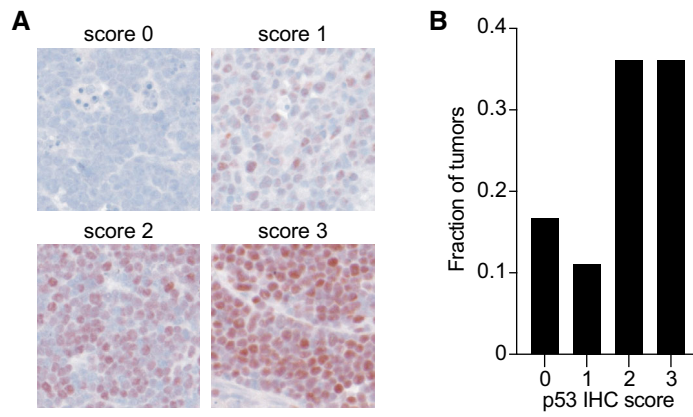


Figure EV5. p53^{EE/EE} expression in tumors from p53^{EE/EE} mice.

- A p53 immunohistochemistry images of spontaneous thymic lymphomas from p53^{EE/EE} mice representative of p53 immunostaining scores 0–3.
- B Fraction of p53^{EE/EE} mouse tumors with indicated p53 immunostaining scores.